Washington State
Department of Ecology
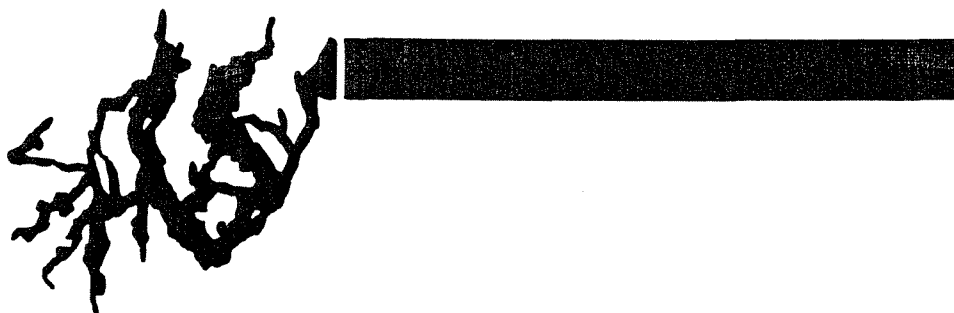
Southern Puget Sound
Water Quality Assessment
Study

COMPREHENSIVE
CIRCULATION AND
WATER QUALITY STUDY
AT BUDD INLET

URS Company

SOUTHERN PUGET SOUND WATER QUALITY ASSESSMENT STUDY

FINAL REPORT

COMPREHENSIVE CIRCULATION

AND

WATER QUALITY STUDY OF BUDD INLET

FOR

WASHINGTON STATE DEPARTMENT OF ECOLOGY

By

URS Corporation

July 31, 1986

PREFACE

South Puget Sound is unique in its beneficial uses, water quality, and circulation. Our detailed knowledge of the factors controlling water quality is somewhat limited because most historical work has occurred in the central basin. The lack of data along with developmental pressures prompted the Southern Puget Sound Water Quality Assessment. Three reports were developed to provide a technical basis for making informed planning decisions concerning environmental protection. The first established general guidelines for siting wastewater discharges in consideration of dilution potential and beneficial uses. The second report expanded our knowledge of circulation and flushing. This third and final report specifically addresses anthropogenic pollutant loads, water quality, and circulation in Budd Inlet.

Collectively, these reports greatly expand our understanding and knowledge of interactions in the South Sound area. They provide a solid foundation from which others may expand.

Lynn R. Singleton, Project Manager
Southern Puget Sound Water Quality Assessment
Washington State Department of Ecology

TABLE OF CONTENTS

FIGURES

FIGURES (cont.)

FIGURES (cont.)

FIGURES (cont.)

FIGURES (cont.)

FIGURES (cont.)

FIGURES (cont.)

TABLES

x

ACKNOWLEDGEMENTS

Jeff Cox	Southern Sound Current Meter Deployment/Recovery
Bob Hamilton	Southern Sound Current Meter Deployment/Recovery
Dr. Curt Ebbesmeyer	Field Logistics, Current Meter Analysis

Horton Dennis & Associates Inc.

Alan Meyers	Source Survey, Tide Gauge

Fisheries Research Institute

Dr. Alan Duvall	Sediment Oxygen Demand Survey
Ron Citterman	Sediment Oxygen Demand Survey

Entranco Engineers

Dr. Andrea Copping	C-14 Primary Productivity

Geo-Ocean Horizons Inc.

Roberta Rice	Field Sampling, Sample Processing

AB Consultants

Ann Bailey	Field Sampling, Source Survey, Sample Processing

Raven Systems & Research

John Dermody	Southern Sound Current Meter Recovery

Thurston County Health District

Mary Lou Taylor	Source Survey
Sara Cassatt	Source Survey

J. E. Edinger Associates, Inc.

Edward M. Buchak	Modeling

Washington State Department of Ecology

Joy Michaud	Field Support

EXECUTIVE SUMMARY

A number of fish kills and water quality violations reported in Budd Inlet over the past fifteen years have raised concerns among regulatory agencies and with the general public regarding chronic water quality problems in the Inlet. The major problem identified in the Inlet was low dissolved oxygen levels in the water column. Algal blooms and their subsequent decline and decay have been suggested as the major cause of the oxygen depletion in the inner Inlet. The overall goal of this study was to identify the cause of the low dissolved oxygen concentrations which occur in the late summer and early fall and, if the causes are controllable, identify what measures might be implemented to resolve the problem.

A number of interrelated studies were conducted to satisfy the goals of the project:

1.   Two short-term intensive synoptic water quality and current meter studies of Budd Inlet during September, 1984 and May, 1985.

2.   Five point source surveys were conducted over a one year time period to measure the contribution of seven major sources of algal nutrients, BOD, dissolved oxygen and fecal coliform bacteria to Budd Inlet.

3.   Two detailed point and non-point bacteriological surveys in April, 1985 and September, 1985.

4.   A study of the sediment oxygen demand and benthic nutrient flux at two sites in the Inlet during May, 1985.

5.   A study of the nutrient and dissolved oxygen budgets for May, 1985 using a two-dimensional box model.

6.   Development of a comprehensive dynamic circulation and water quality model for Budd Inlet.

The major observations, conclusions and recommendations of this
study are contained in Chapter 5 of the text. What follows is a summary of
the major findings most closely related to the overall goal of determining
the causes and remedies of the low dissolved oxygen problem in Budd Inlet.
For the purpose of discussion, the Inlet was divided into three longitudinal
sections. The inner Inlet is defined as being south of Priest Point, with
the central Inlet lying north of Priest Point and south of Gull Harbor. The
outer Inlet is defined as the area north of Gull Harbor to the mouth of the
Inlet which lies between Dover Point and Cooper Point.

Circulation

The results of this study indicate that estuarine circulation and
vertical mixing play key roles in controlling the dispersion and transport
of material throughout Budd Inlet. The Inlet is a stratified, partially
mixed estuary, with an outward flow of surface water and an inward flow of
subsurface water. These flows represent the net estuarine circulation which
are relatively small in comparison to the large, oscillatory tidal flow.
Vertical mixing is generated by the strong tidal flows as the Inlet shoals
from the mouth to the head.

Current meter measurements from Budd Inlet provide an overall picture
of the tidal currents within the Inlet. This general picture suggests that
there is a substantial amount of flow from east to west as well as eddy-like
flow in the central portion of the Inlet during most tidal periods. During
strong ebb and floods, however, flows are generally north and south. The
east to west flow was very pronounced during and following the strong
west-southwest winds in the September, 1984 survey. On weak ebbs a
clockwise circulation was noted in the inner Inlet south of Priest Point,
while flows near the mouth of the Inlet were nearly north and south on the
ebb and flood tides with a short period of rotation in between.

These results suggest that the eddy-like and cross-channel currents
in the inner and central Inlet would tend to retard the flushing, and
therefore decrease the overall dilution potential in these areas. In

addition, estuarine circulation would carry material which was mixed into the lower layers back into the Inlet.

Flushing and Dilution

Modeling results indicate that the flushing efficiency of Budd Inlet south of Priest Point is low. It is not significantly affected by high or low flow conditions of freshwater entering the Inlet. The surface waters of the outer Inlet, near the mouth, are very efficiently flushed regardless of flow conditions, while the central Inlet is more efficiently flushed during high flow conditions. Modeling results suggest that recycling of Budd Inlet water at the mouth results in a minor decrease in flushing efficiency.

Dilution and dispersion modeling showed the influence of estuarine circulation in transporting subsurface material toward the head of the Inlet. Upon reaching the head of the Inlet, some of the material appeared to become detained due to vertical cirulation. A computer model analysis of Budd Inlet indicates that a wastewater discharge at a constant flow rate of 24 million gallons per day (mgd) would receive 5 times more dilution at the outer Inlet than the inner Inlet. This is because of the much greater flushing efficiency at the outer Inlet. It would also receive 3 times more dilution at the central Inlet than at the inner Inlet.

Limiting Nutrient and Algal Blooms

Study results show that during the growing season in Budd Inlet when bloom conditions prevail, algal growth is nutrient limited. Analysis of historical data and data from the two intensive surveys described in this report indicates that nitrogen is the growth limiting nutrient in Budd Inlet. During spring blooms, which are initiated and sustained by a series of clear days, diatoms predominate showing a preference for the ammonium form of dissolved nitrogen. The magnitude of these blooms is limited by the supply of nutrients. Results of the study further indicate that in the late summer and early fall, dinoflagellate blooms are sustained by nutrient inputs and by poorer tidal mixing and clear, calm days that promote a stable water column.

Point Source Surveys

The major sanitary wastewater contributor to Budd Inlet is the Lacey, Olympia, Tumwater, Thurston County (LOTT) wastewater treatment plant. The results of the five source surveys indicate that the LOTT treatment plant contributes about 75 percent of the nitrate, 95 percent of the nitrite, and 95 percent of the ammonium from the measured sources. Capitol Lake contributes between 60 and 80 percent of the BOD loading to Budd Inlet and 90 percent of the dissolved oxygen.

The major sources of fecal coliform bacteria to the Inlet were Moxlie Creek, Capitol Lake, and the LOTT treatment plant. The relative contribution of each major source varies between source surveys with the dominant source ranging from 60 to 90 percent of the total loading for any one survey. Moxlie Creek was found to be the major source of fecal coliforms during the detailed bacteriological surveys. The majority of the bacterial loading from Moxlie Creek appears to be introduced into the lower reaches of the creek.

Sediment Oxygen Demand and Nutrient Flux

Modeling results indicate that more than 90 percent of the sediment oxygen demand (SOD) is related to algal production in the water column, and less than 10 percent is derived directly from BOD point sources such as Capitol Lake or LOTT. Measured SOD in the inner Inlet was higher than in the central Inlet, a finding consistent with modeling results. Ammonium release from the sediments, the result of the oxidation and remineralization of recently deposited organic matter, was related to the SOD at the central Inlet site, and followed the same trend as seen in other coastal marine estuaries and bays. Ammonium release was not observed at the inner Inlet site. This was attributed to increased irrigation and nitrification, resulting from increased burrowing and mixing by benthic animals near the LOTT wastewater outfall.

Because sediment oxygen demand is linked to algal production in the water column, it is included in the dynamic modeling. Modeling results suggest that a 30 to 50 percent increase in algal production causes a 10 to 15 percent increase in SOD in the inner Inlet and only slight increases in the central and outer Inlet. Since the benthic release of ammonium is related to the sediment oxygen demand, an increase in algal production also produces a similar increase in ammonium release from the sediments.

Nutrient Budgets

A two-dimensional box model for Budd Inlet was developed to evaluate the nutrient budget for May and to aid in calibrating the more complex dynamic model. The budget revealed that the major sources of nitrogenous nutrients to Budd Inlet are Puget Sound, LOTT, and benthic release, each contributing approximately 60, 20 and 20 percent respectively. The budget for the surface layer (upper 3 meters) indicates that LOTT supplies about 50 percent and vertical mixing of Puget Sound water supplies about 50 percent of the total inorganic nitrogen (TIN) to the surface.

Nutrient contribution divided into ammonium and nitrate + nitrite (NO_3/NO_2) is as follows:

Nutrient Contribution
to Budd Inlet

	Total Inlet			Surface Waters		
	Ammonium	NO_3/NO_2	TIN	Ammonium	NO_3/NO_2	TIN
Puget Sound	20%	92%	63%	20%	78%	51%
LOTT	36%	8%	19%	80%	11%	49%
Sediments	44%	-	18%	--	--	

Dynamic Modeling of the Dissolved Oxygen System

The calibrated dynamic model for May showed that spring diatom blooms are initiated and sustained by periods of clear, calm weather, and are enhanced by at least 30 percent in the inner portions of Budd Inlet by the current nutrient loadings from the LOTT treatment plant. Predicted bottom water dissolved oxygen results for the inner Inlet from the May model runs show increased oxygen levels with increased algal production in the water column even though the sediment oxygen demand is greater. This is due to horizontal and vertical mixing and transport which transfer photosynthetically produced oxygen to the bottom water of the inner Inlet faster than it can be consumed by the sediment oxygen demand. This was confirmed by the field data which showed supersaturated dissolved oxygen concentrations throughout the water column. This suggests that the death and decay of algal blooms is probably not the main cause of the low dissolved oxygen in the bottom water.

Computer modeling and analysis of the intensive survey data from September, 1984, suggest that the high respiration rates of dinoflagellates, coupled with the daily vertical migration of the dinoflagellates, were the probable cause of the low dissolved oxygen conditions in the bottom waters. In effect, the dinoflagellates are acting as a biological "pump" taking oxygen out of the bottom water at night and producing it in the surface water during the day. When this pump, which is related to the vertical migration rate, is stronger than the vertical mixing, large vertical gradients of oxygen concentration are produced resulting in' supersatured surface waters and highly depleted bottom waters.

Athough dinoflagellate blooms are common in Budd Inlet in the late summer and early fall, other conditions which exist at this time, such as decreased flushing, lower Puget Sound dissolved oxygen concentrations, and higher SOD rates, compound the low dissolved oxygen problem. However, these conditions alone, without the migration and respiration of dinoflagellates, cannot account for the observed oxygen gradients.

Based on available data, it would appear that the severity of the dissolved oxygen depletion is related to the magnitude and duration of the dinoflagellate bloom. Analysis of the modeling results and the existing data also suggests that the dinoflagellate blooms have the potential of being enhanced at least as much as the diatom blooms by the addition of nutrients from the LOTT treatment plant in the inner Inlet. Therefore, even though the oxygen depletion cannot be quantitatively predicted at this time, the evidence strongly suggests that a reduction in nutrient addition will result in a reduction the magnitude of the dinoflagellate bloom, and consequently a reduction in the magnitude of the oxygen depletion.

LOTT Alternative Discharge Configurations

Computer simulations were made using alternative discharge configurations based on estimated average dry weather flow (ADWF) conditions for the year 2010 of 24 mgd, and the design capacity average dry weather flow (ADWF) of 16 mgd. The results of the simulations indicate that, next to complete discharge elimination, nutrient removal is the next best solution to substantially reduce algal blooms. All scenarios without nutrient removal, regardless of placement within the Inlet, show a 30 to 50 percent increase in the strength of the algal bloom for the year 2010 ADWF scenario relative to the no-discharge scenario for the inner portions of the Inlet. The magnitude of this increase in strength of the bloom is related to the placement of the outfall within the Inlet, with the inner Inlet placement showing the greatest increase.

Under the recommendations of WDOE, we believe an algal bloom enhancement of 10 percent or less as the result of nutrient addition from the LOTT treatment plant is acceptable. The following recommendations would achieve this acceptable level which would minimize the potential magnitude of oxygen depletion in the late summer and early fall due to dinoflagellate blooms in Budd Inlet.

o   For the <u>present</u> <u>outfall</u> <u>location</u>, maintain the permitted flow rate
    of 16.3 mgd (AWWF) and establish nutrient removal of at least
    90 percent using best available technology. This could be
    accomplished on a seasonal basis from April through October.

o   For <u>any</u> <u>outfall</u> <u>location</u> within the Inlet or any increase in
    permitted flow up to 22 mgd (AWWF), establish nutrient removal of
    at least 90 percent using best available technology. This could
    be accomplished on a seasonal basis from April through October.

CHAPTER 1.   INTRODUCTION

1.1   INTRODUCTION

Budd Inlet is one of seven major inlets in Southern Puget Sound which is traditionally defined as that part of the Puget Sound Basin which lies southwest of The Narrows (Figure 1.1).   It is the largest inlet (by volume) west of Dana Passage and the southernmost inlet in Puget Sound.   Budd Inlet also has the largest tributary of any of the inlets in Southern Puget Sound; the Deschutes River which flows through Capitol Lake before reaching the Inlet at its head.

The Inlet serves as a commercial shipping lane for the Port of Olympia, the main seaport for the city of Olympia and the surrounding South Sound communities.   The waters of Budd Inlet are used for fishing, boating and other recreational activities.   The aesthetic appeal of the Inlet also provides a pleasant environment for the residents of the area and a backdrop for the state capitol in Olympia.   Concerns have been raised over water quality problems which diminish its value as a resource.   These concerns have been amplified in recent years in light of the rapid population growth and developement in the area.

A number of fish kills and water quality violations have been reported over the past fifteen years for the inner section of Budd Inlet near its head at Capitol Lake.   The number of fish kills reported relative to other areas of the state has indicated a persistent water quality problem which has been associated with low dissolved oxygen levels.   Algal blooms in the late summer and early fall, and their subsequent decline and decay, have been implicated as the major cause of the oxygen depletion in the inner inlet.
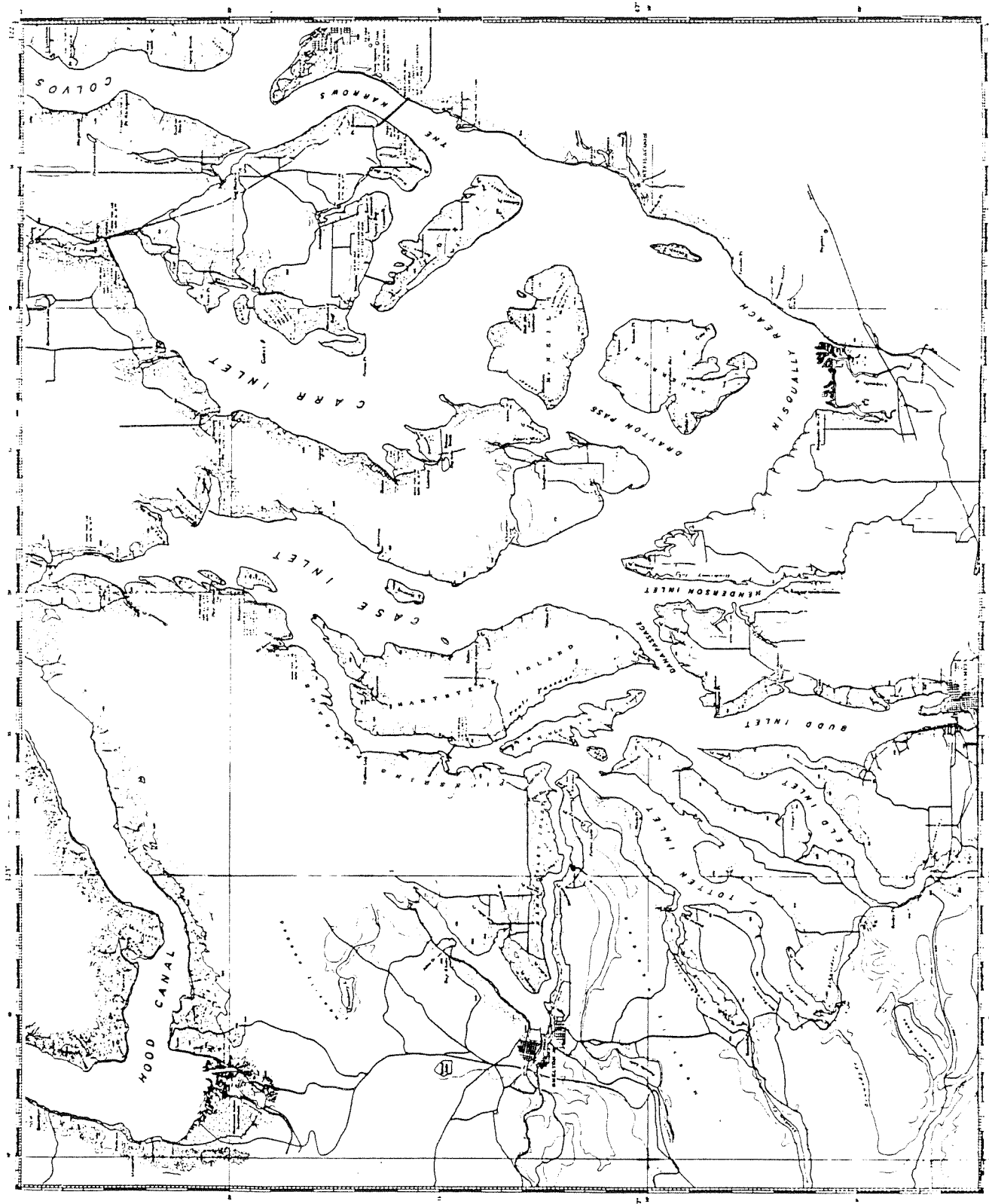
Figure 1.1 Budd Inlet and Southern Puget Sound.

1.2 PURPOSE

The purpose of this study was to identify the cause of low dissolved oxygen concentrations which are known to occur within Budd Inlet. This would be accomplished by developing a water quality model. Consideration would be given to the seasonal and spatial variations in source loading and circulation and would include other critical environmental parameters such as winds and tides. The study included two intensive field surveys within the inlet and a five month source survey investigation.

1.3 SCOPE

A dynamic water quality computer model was included to aid in interpreting and evaluating the complex interactions involved in controlling the distribution and concentration of dissolved oxygen within the inlet. The model was used to evaluate the effects of existing and proposed discharge configurations for the LOTT secondary wastewater treatment facility on dissolved oxygen concentrations within the inlet. The model was also used to determine flushing efficiencies for various points within Budd Inlet and to estimate dilution and dispersion.

CHAPTER 2 MATERIALS AND METHODS

2.1 SEPTEMBER AND MAY INTENSIVE SURVEYS:
WATER QUALITY AND CURRENT MEASUREMENTS

Introduction

The purpose of the Budd Inlet intensive surveys was to collect synoptic water quality and current data in Budd Inlet. These data were used to develop, calibrate, and verify a dissolved oxygen/circulation computer model of Budd Inlet.

Sampling Program

The Budd Inlet intensive surveys involved two sampling periods. The first survey was conducted during the week of September 18th, 1984. Two complete 25 hour tidal cycles were sampled. The second survey was conducted during the week of May 20th, 1985, and covered one complete 25 hour tidal cycle.

Eight sampling stations were established in Budd Inlet for the collection of water quality and current meter/CTD (conductivity, temperature, depth) data. Stations were located to adequately represent the Inlet and to satisfy the requirements of the dynamic model. The stations (Figure 2.1) were positioned with sextant fixes and marked with anchored and lighted vinyl floats.

Survey vessels included a 22 foot SeaRay and 18 foot Olympic. Each survey boat was equipped with hand operated winches capable of handling the load of the 5 liter Niskin water sampler or the Aanderaa RCM4 current meter.

Cooper Point

Dofflemeyer Point

● 1   ● 2

Gull Harbor

Tykle Cove

● 3   ▲   ● 4

Butler Cove

● 5

Priest Point

● 6   Ellis Cove

◆

● 7   ● 8

● WATER QUALITY / CURRENT METER

◆ SOD LANDER SITE # 1
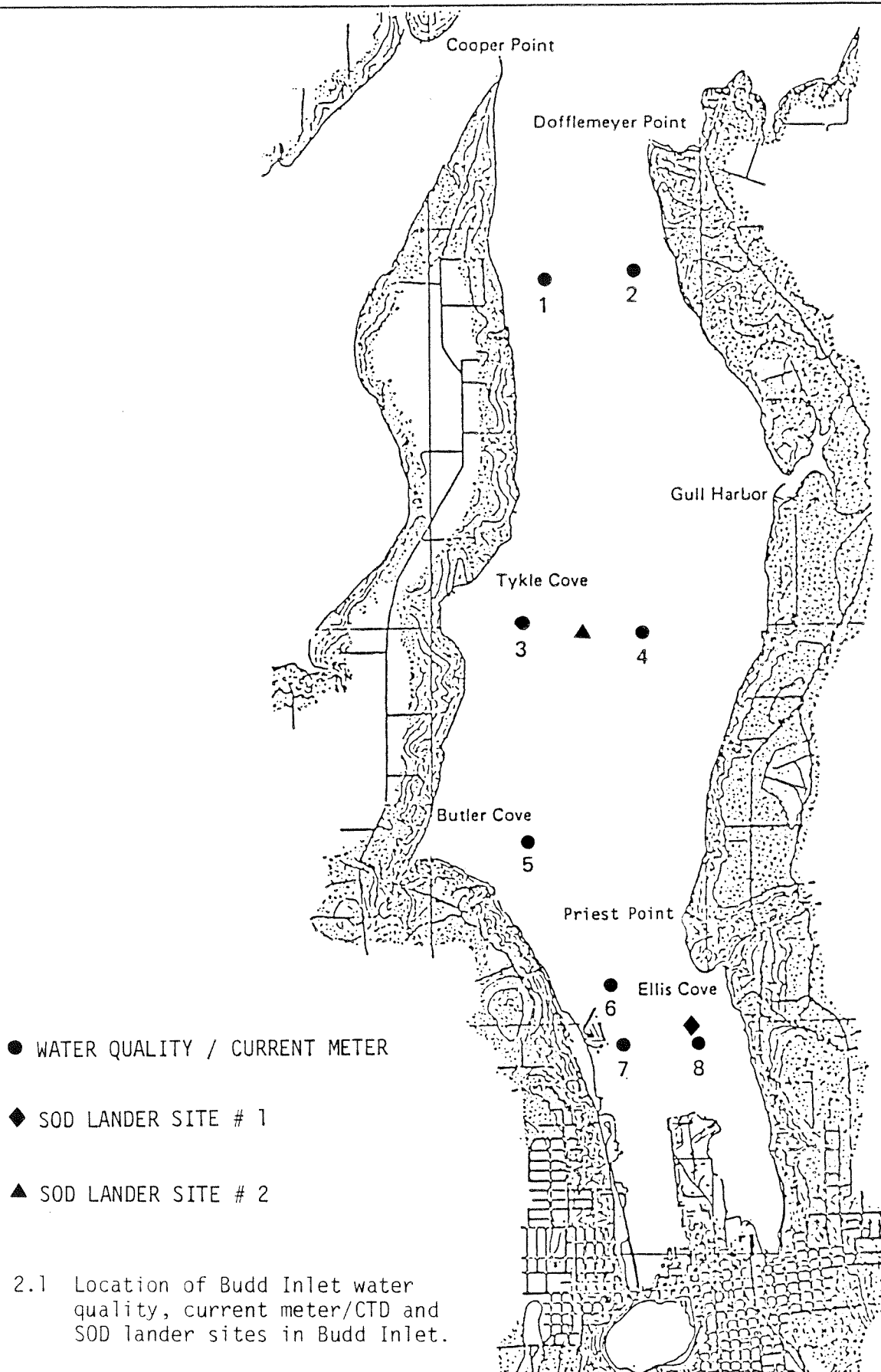
▲ SOD LANDER SITE # 2

Figure 2.1   Location of Budd Inlet water
quality, current meter/CTD and
SOD lander sites in Budd Inlet.

During the September 1984 survey, water quality stations were sampled at four hour intervals; current meter/CTD stations were sampled every two hours. The overall station and tidal cycle coverage is depicted in Figure 2.2.

During the May 1985 survey, all data were collected every two hours by skipping selected stations and locating the water quality and current meter/CTD crews on a single research vessel. The overall station and tidal cycle coverage for May is depicted in Figure 2.3.

Water Quality Sampling

Water quality samples were collected with a 5 liter Niskin bottle for dissolved oxygen, algal nutrients (PO4-P, SIO2-Si, NO3-N, NO2-N, NH3-N, Total N, Total P), chlorophyll a, pheopigments and BOD-5. BOD-5 samples were collected at 4 depths at station 1 only. During the May intensive survey, BOD samples were collected at this station every other circuit. A phytoplankton archive sample was collected at the second depth at each station during the September survey only. One percent light levels were obtained using a submarine photometer, and ambient readings were also taken during the May survey. Secchi disk readings were taken at all stations during both surveys. Wind velocity and direction were logged hourly in the September survey, and at each station occupation during the May cruise. The wind data were collected with a hand held anemometer, or a Dwyer wind gauge.

During the September survey, water quality samples were collected at stations 1, 3, 4, 5, 7 and 8 (Figure 2.4). Four depths were sampled at station 1 (0.5m, 8m, 15m, and 2m off the bottom) and three depths were sampled at the other stations (0.5m, 1.5m, and 1m off bottom). Each sampling circuit was accomplished within four hours to adequately cover the two full tidal cycles. Additional sampling was conducted to provide additional data where necessary.

WATER QUALITY TIDAL CYCLE COVERAGE
BY STATION, SEPTEMBER 1984
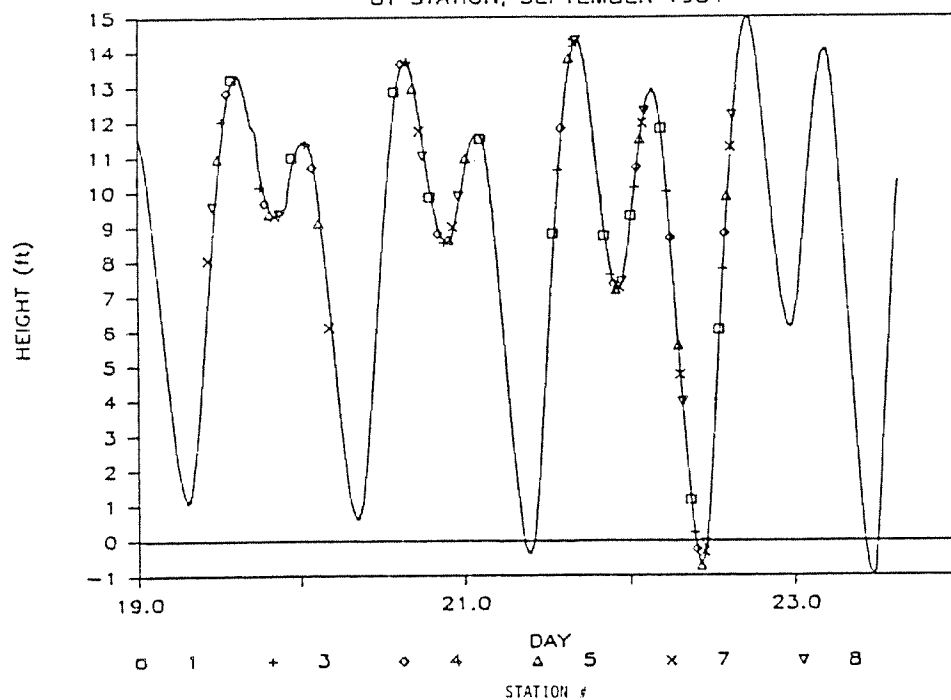
CURRENTS/CTD TIDAL CYCLE COVERAGE
BY STATION, SEPTEMBER 1984
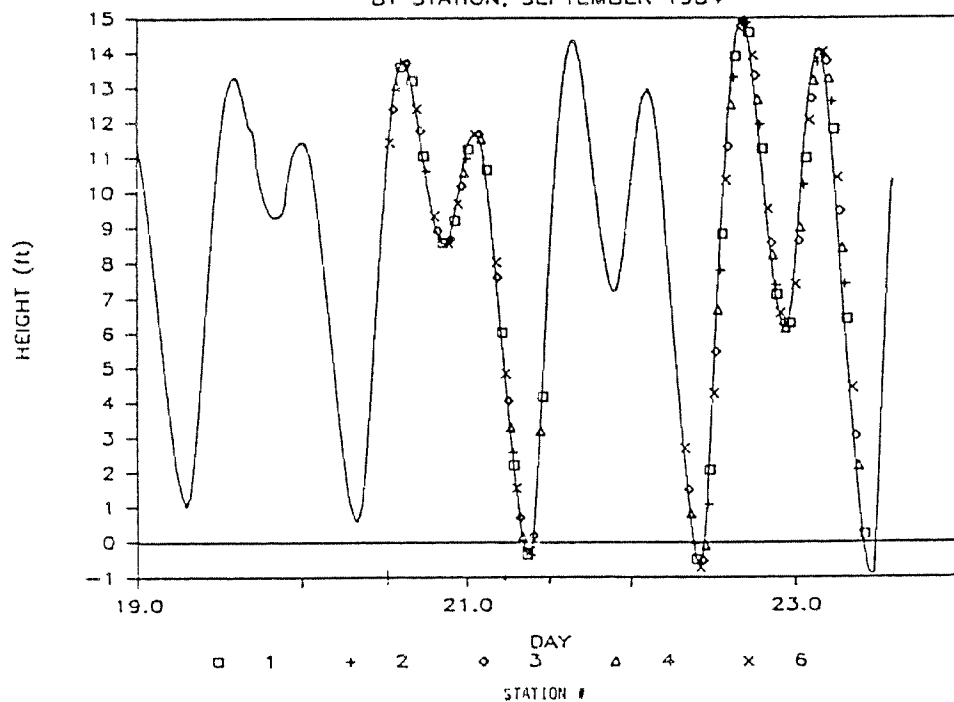
Figure 2.2 Water quality and current meter/CTD measurements related to the tidal cycle during the September 1984 intensive survey.

WATER QUALITY/CURRENT METER STATIONS
May OCCUPATIONS ON TIDAL CYCLE
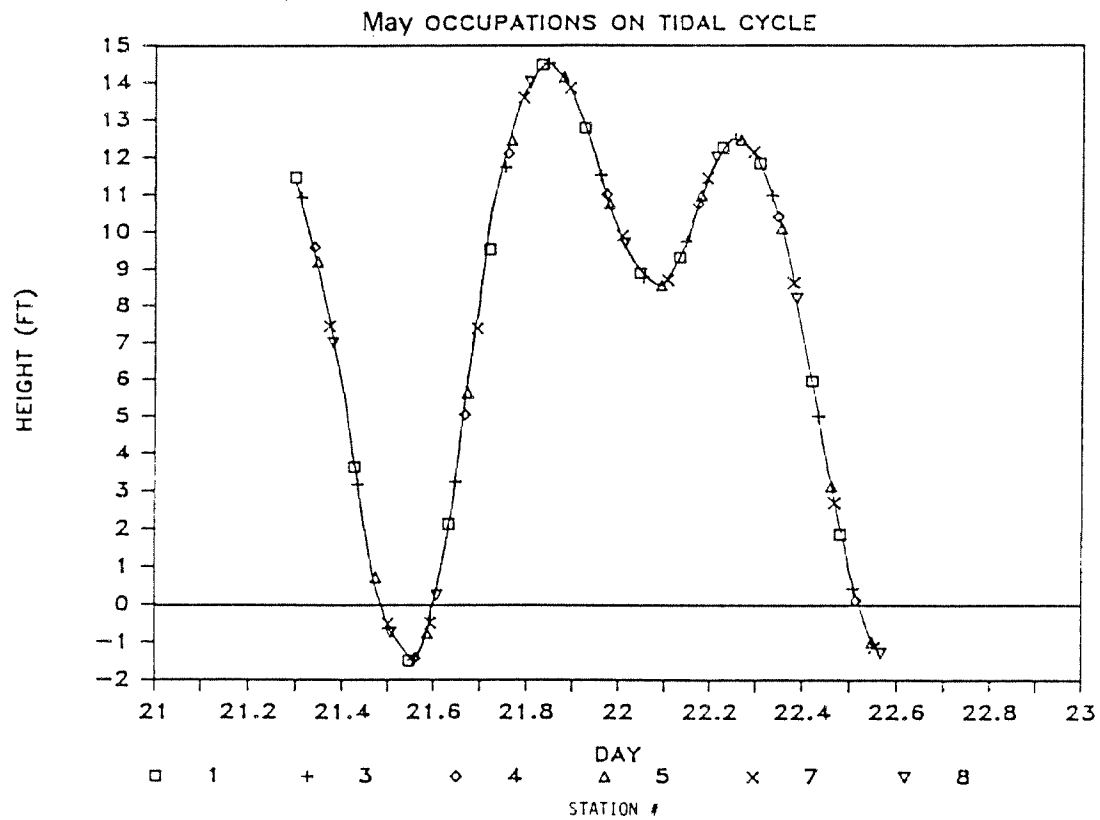
Figure 2.3   Water quality and current meter/CTD measurements related to tidal cycle during the May 1985 intensive survey.
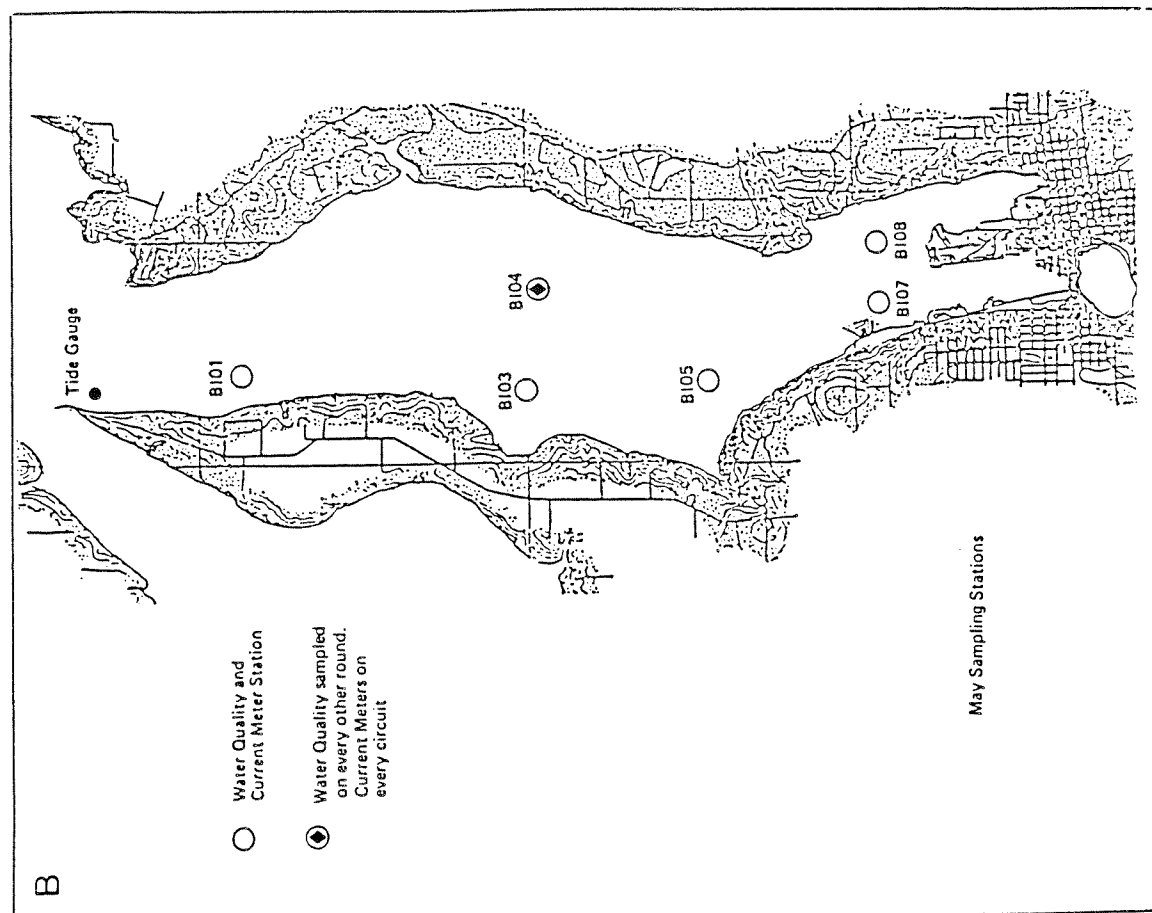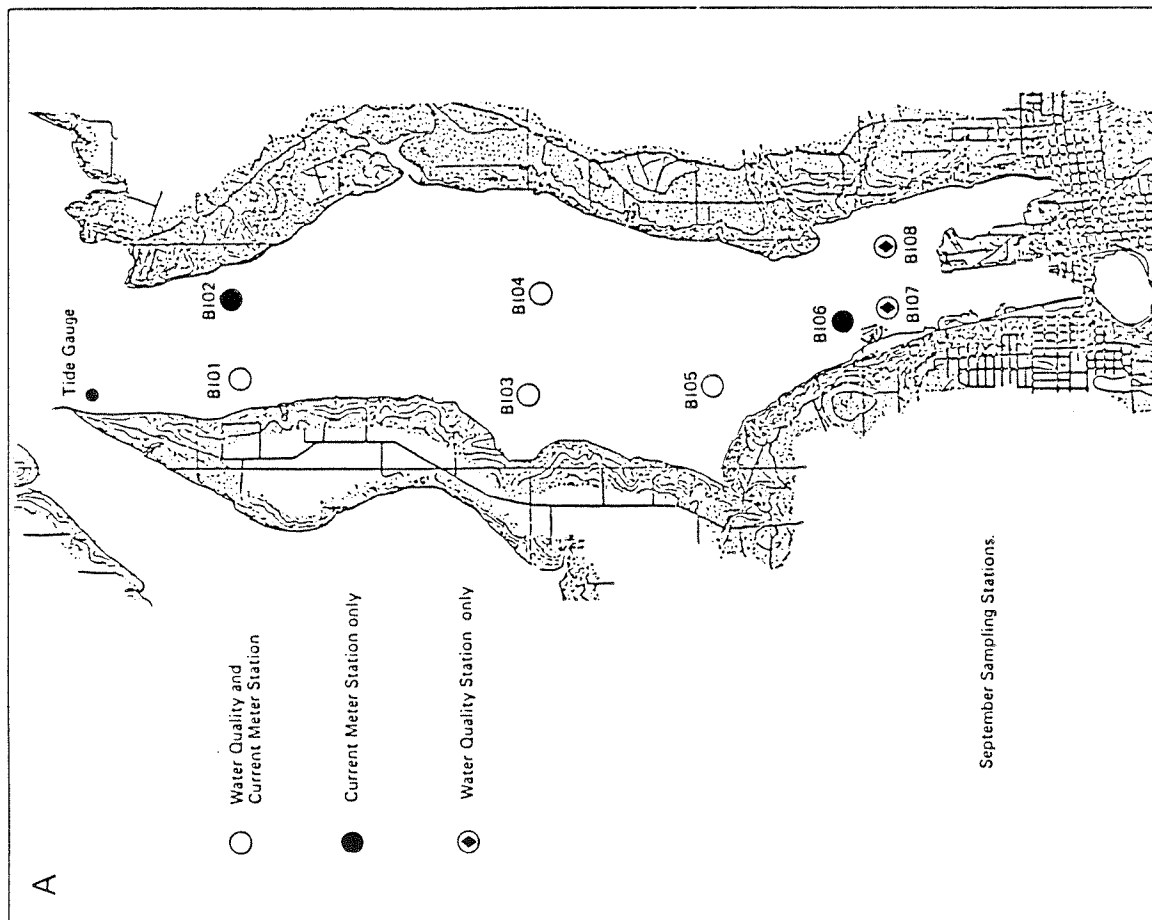
Figure 2.4   Water quality and current meter/CTD stations sampled during (A) September 1984 and (B) May 1985.

During the May survey, water quality data were collected at stations
1, 3, 4, 5, 7 and 8 (Figure 2.4). Each station was sampled at four depths
except stations 7 and 8 where three depths were used. Station 4 was
occupied on every other circuit. To account for the change in water depths
over the tide cycle, a reference table was developed to allow sampling
crews to occupy the predetermined depths given the total water depth at the
time of sampling.

Sample Processing

The dissolved oxygen samples were drawn into a 250mL Carpenter bottle,
and treated with 1mL each of $MnCl_2$ and NaOH/NaI. The sample was then
shaken and placed in a dark container and later fixed with 1mL of H_2SO_4 in
the field. The dissolved oxygen samples were stored in a cool, dark
environment until they were transported to the lab for analyses. Water
samples for algal nutrients, chlorophyll a, and pheopigments were
collected in cured 1000 mL polybottles which were rinsed twice with the
water sample before filling. The polybottles were stored in ice chests
aboard the survey boat until transfer to the field laboratory. Samples for
total N and total P were collected in pre-washed 60 mL polybottles. The
BOD-5 samples were collected in sterile 1000 mL polybottles provided by
Lauck's Testing Laboratories of Seattle.

The algal nutrient, pheopigment and chlorophyll a samples collected in
the field were processed in the field lab immediately at the end of each
collection round. The filtration apparatus consisted of two inline vacuum
pumps connected to a suction flask for the algal nutrients and a
multi-funnel system for chlorophyll a samples. Each sample filtered was
subsampled from the 1000mL polybottle. The chlorophyll a and pheopigments
subsamples were collected in 140mL polybottles which were immediately
inverted on the inline suction system. The sample was drawn through a .42
micron glass fiber Gelman GFC filter. Each filtered sample was stored in a
pre-labeled envelope and placed in cold storage. Nutrient samples were
filtered through glass fiber filters to remove detritus and algal. The

glass fiber filters were washed in 10% HCL, then rewashed in deionized distilled water before use. Each sample was immediately frozen in a 3/4 filled 60mL polybottle.

During the September survey, processed samples were stored in ice chests with dry ice until transfer to a local storage freezer. During the May survey, a 14 cubic foot freezer was used for sample storage. At the completion of the survey, the freezer was transported by truck to the receiving labs.

Water Quality Analysis

Dissolved oxygen, salinity, and nutrient samples were analyzed at the Routine Chemistry Laboratory located at the University of Washington's Department of Oceanography. D.O. samples were analyzed by the modified Winkler method. Nutrients were analyzed by standard autoanalyzer colorimetric procedures using a Technicon AutoAnalyzer II (Whitledge, 1981). Salinity samples were processed using the Autosal 8400A inductive salinometer calibrated with Standard sea water. Chlorophyll a readings were obtained using the Fluorometric Method (Strickland and Parsons, 1972). BOD-5 samples were analyzed by Laucks Testing Labs in Seattle, Washington, following Standard Methods (APAH 1976).

Physical Oceanographic Studies

On the day before and after each intensive field study a detailed surface salinity and temperature survey was conducted in Budd Inlet. Eighteen to 22 stations were occupied and locations established by sextant fixes. An Aanderaa RCM4 current meter was used to collect conductivity and temperature at a depth of 1.0 meter. The data maps created from these surveys aided in the interpretation of current patterns.

During the intensive surveys, current speed and direction and temperature and salinity were collected with the Aanderaa RCM4 current

meter with a deck readout unit. During the September 1984 survey, stations
1, 2, 3, 4, and 6 were occupied. Data were collected at three depth ranges
with two one-minute averages at each depth. A sampling circuit of two
hours was maintained over two entire 25 hour tidal cycles. During the May
1985 survey, stations 1, 3, 4, 5, 7 and 8 were occupied. Data were
collected in a similar fashion and a two hour circuit was maintained.

Tide Gauge Deployment and Retrieval

Tidal data for the Budd Inlet Model were collected using a Sea-Data
TDR-2A tide gauge which recorded temperature and pressure (depth) data
every 10 minutes. The tide gauge was positioned in 6 meters of water 400
feet offshore from a temporary benchmark south of Cooper Point. The
correct tidal height to apply to the recording tide gauge was obtained with
a surveyor's level and measuring the water level height in relation to the
temporary bench mark at the exact time of deployment. Upon recovery of the
tide gauge, the data on magnetic cassette tape was sent to Sea-Data where
the data was encoded on 9-track tape for analysis by URS.

2.2 SOURCE SURVEY

Introduction

The purpose of the source survey was to identify and characterize the
major sources of BOD, fecal coliform bacteria and algal nutrients to Budd
Inlet.

Location of Source Stations

Stations were selected after interviews with personnel from the
Washington State Department of Ecology, Thurston County Health District,
LOTT Sewage Treatment Facility and City of Olympia. The eleven sites
ultimately selected for source sampling presented in Figure 2.5.
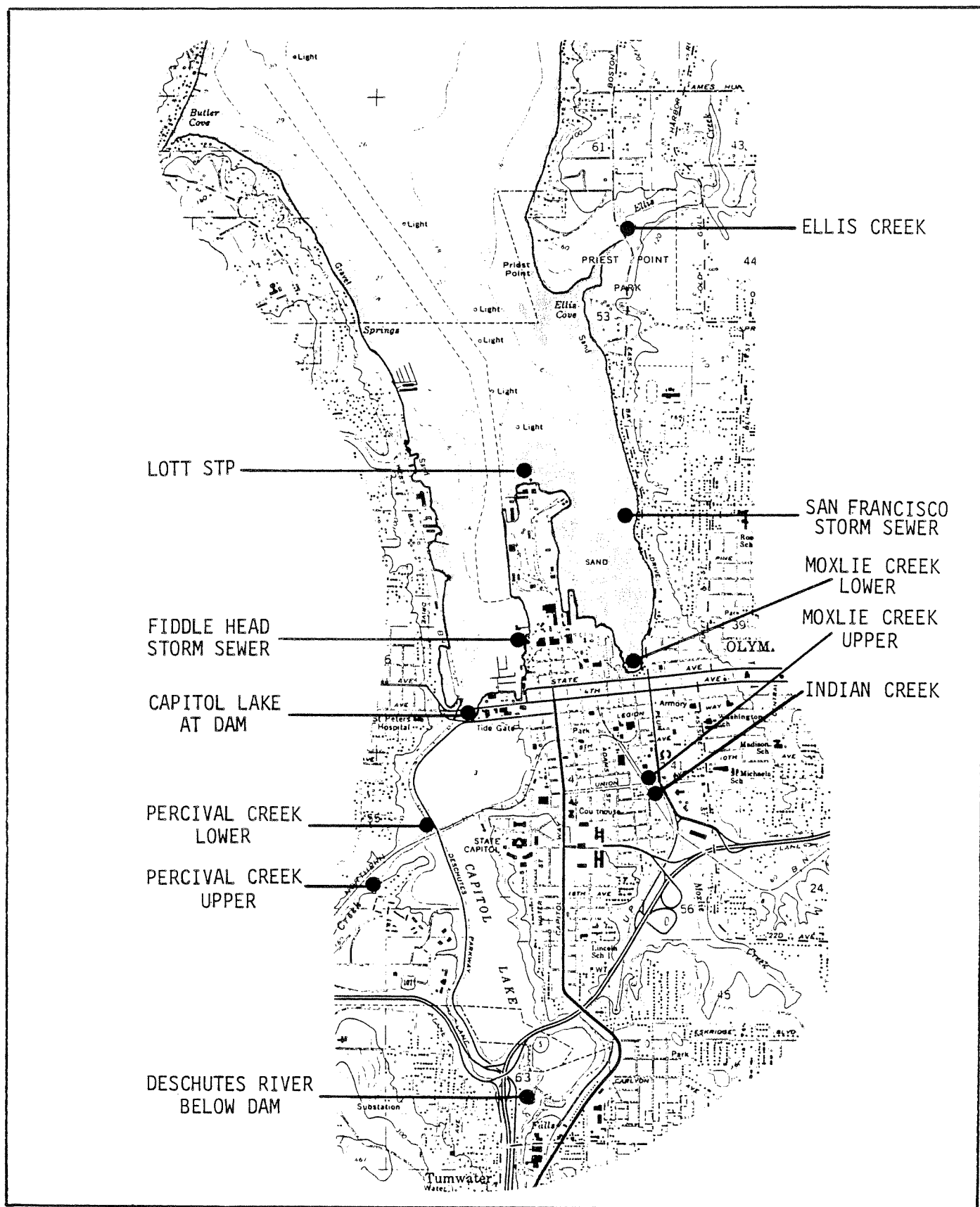
Figure 2.5 Location of Source Survey sampling stations in and around
Budd Inlet: September 1984 to September 1985.

Description of Sources Sampled

The source sampling locations were as follows:

LOTT Sewage Treatment Plant Final discharge effluent from the chlorine contact tank.

Capitol Lake at Dam Northern end of Capitol Lake about 20 feet southeast of the fish ladder entrance to the dam.

Percival Creek, Upper Reach 400 feet upstream of the mouth of Percival Creek in a channel at the base of a steep cliff.

Percival Creek, Lower Reach In Capitol Lake just west of the Deschutes Parkway at the northwest corner of a bridge opposite the mouth of Percival Creek.

Deschutes River, Below Falls 300 feet downstream from Tumwater Falls on the left bank about 500 feet upstream from the historical park.

Ellis Creek 35 feet upstream of the entrance to a 42 inch concrete culvert on the north side of East Bay Drive.

Moxlie Creek, Lower At entrance to Budd Inlet through an 84-inch diameter concrete storm sewer.

Moxlie Creek, Upper 100 feet southwest of the intersection of Plum and Union Streets.

Indian Creek   Just above intersection point of Indian and
                                Moxlie Creeks.

San Francisco Storm Sewer   Within a manhole approximately fifteen feet
                                east of the curb on the east side of the
                                street opposite a house numbered
                                1349 East Bay Drive.

Fiddle Head Storm Sewer   A manhole located at the north end of
                                Columbia Street at a point approximately
                                100 feet northwest of the Fiddle Head
                                Marina Building.

Other Sources

Three private sewage treatment plants discharge into Budd Inlet.
Tamoshan STP and Beverly Beach STP are located near the mouth of the inlet,
north of Gull Harbor. Seashore Villa STP is located just south of Gull
Harbor, across the inlet from Big Tykle Cove. Discharge monitoring reports
for 1983 indicate that Tamoshan discharged an yearly average of 0.018 mgd
(0.028 cfs) and loaded 3.0 lbs/day Total N and 0.8 lbs/day Total P to Budd
Inlet. Beverly Beach averaged .003 mgd (0.005 cfs) with Total N loadings
of 0.5 lbs/day and Total P loadings of 0.13 lbs/day. Seashore Villa
averaged 0.015 mgd (0.023 cfs) and loaded 2.5 lbs/day Total N and 0.6 lbs/day
Total P (Kendra and Determan, 1985). Given the location, discharge rates
and nutrient loadings of these private plants, it was decided not to
include them in the source survey of Budd Inlet. The three private plants
were considered during the Budd Inlet Bacteriological Survey which
encompassed point and non-point sources from Boston Harbor to the head of
Budd Inlet. These data are presented in Section 3.6, Bacteriological
Survey of Budd Inlet.

Source Sampling

Five source surveys were conducted on September 19-21, 1984 and on
February 24, April 11, May 21, and June 19, 1985. Samples were collected

at each source station for algal nutrients, BOD-5, fecal coliform and dissolved oxygen. Measurements for flow rate and water temperature were taken whenever possible.

Water samples from the LOTT STP were obtained from a 24-hour composite or by a grab sample. All other samples were grab samples. All nutrient samples collected, except the February 1984 survey, were filtered before analysis.

Flow Measurement

Flow rates and water temperature were measured whenever possible at each source. Low flows (0.1 to 5.0 cfs) were measured with a Pygmy current meter; flow velocities for flow rates above 5.0 cfs were measured with a Price Current Meter. Flows at Capitol Lake were calculated as the sum of the flows from the Deschutes River (USGS gaging station) and Percival Creek (upper reach), since both enter Capitol Lake at its southern end and drain into Budd Inlet through the Capitol Lake Dam. Flows at LOTT were obtained from the support staff whenever a sample was collected. Water temperature was measured with an Americal SP Laboratory Thermometer and recorded to 0.1 degree.

2.3 BACTERIOLOGICAL SURVEY

Station Location/Sample Collection

Two bacteriological surveys were conducted, the first on April 9, 15 and 17, 1985, and the second on September 10 and 11, 1985 (Figure 2.6). Flow measurements were calculated in three ways depending upon the source: timing flow into a calibrated container; utilizing a current meter; or by measuring the width and depth of the source and timing a floating object from one fixed point to another as it moved downstream.

Figure 2.6 Location of Bacteriological Survey sampling stations
along the shoreline of Budd Inlet:
April 1985 and September 1985.

Laboratory Analysis

Laboratory analysis of the collected fecal coliform samples was provided by the Thurston County Health District in Olympia, Washington. The samples collected from sewage treatment plants were analyzed using the A1 modified Most Probable Number Method (MPN). The remainder of the samples were analyzed using the Membrane Filter (MF) method.

2.4 PRIMARY PRODUCTIVITY STUDIES

Primary productivity was measured using the C-14 uptake rate method. The procedures followed can be found in Parsons et al. (1984). Samples were collected at Stations 3 and 5 (Figure 2.1) at four to five depths within the photic layer and incubated at Station 1 during the September survey. This was necessary due to the very dense algal populations at Station 3 and 5 at the time the productivity samples were taken. This lowered the one percent light level to about 3 meters at station 5 which would have made it difficult to determine productivity versus depth for these stations. The one percent light level at Station 1 of 13 meters facilitated the determination versus depth. Primary productivity samples during the May survey were incubated at the actual station location.

2.5 SEDIMENT OXYGEN DEMAND STUDY

Sampling and Equipment

Studies were conducted to measure the sediment oxygen demand present in Budd Inlet. Station locations are depicted in Figure 2.1. Benthic flux measurements were made with an aluminum frame tripod (Figure 2.7) which was lowered to the sediment surface and moored to a free floating buoy during operation. Within the tripod is mounted a "tray" which moves up and down on four verticle guide rods located on the corners. Attached to the bottom of the tray are two stainless steel box cores (412 cm^2 each). The stainless steel lids for the box cores are mounted on hinged "arms" fixed
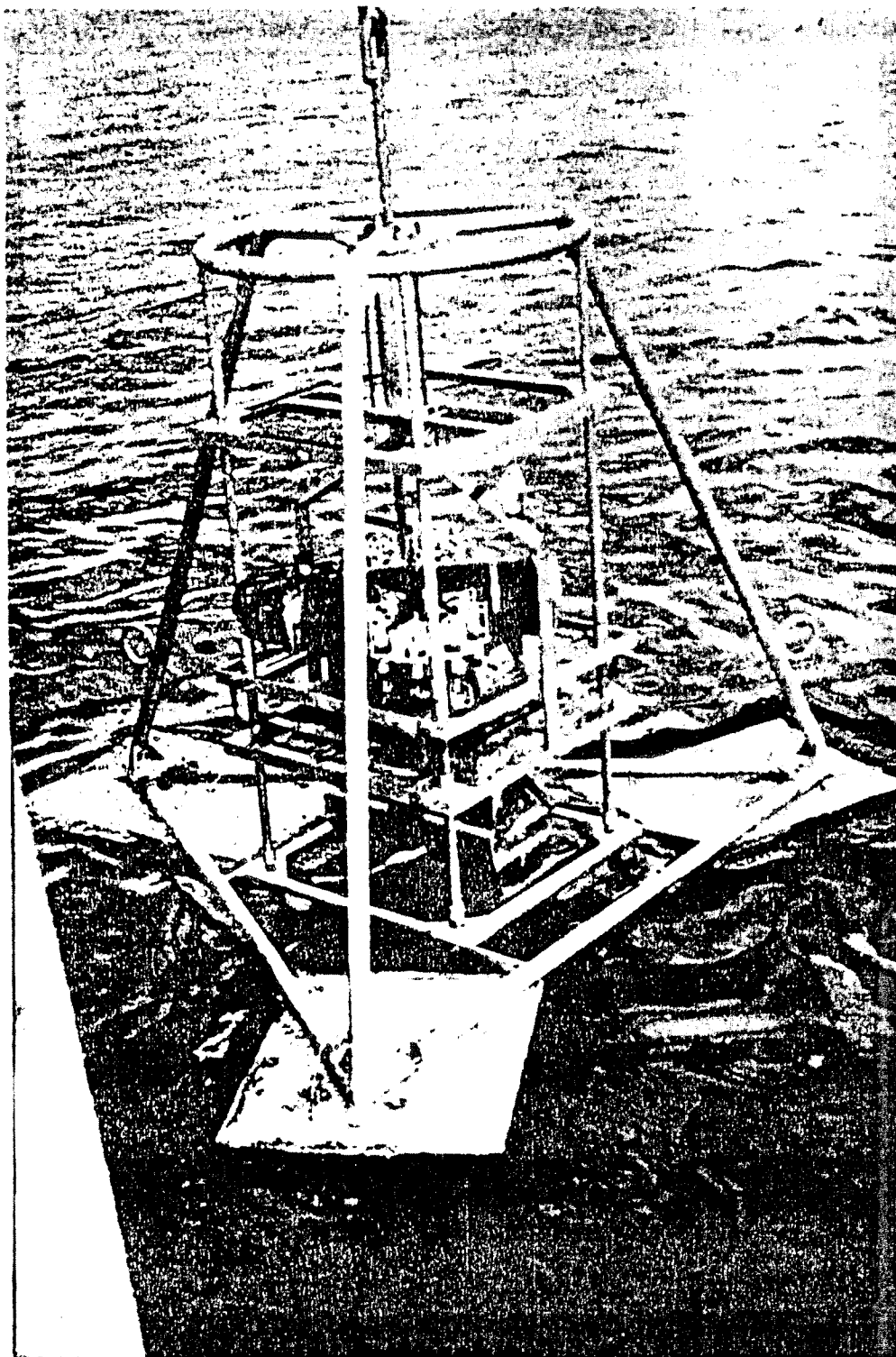
Figure 2.7 The Lander used to measure the flux of solutes
between the sediments and the overlying water.

2-16

to the tray top. Inserted into each lid is a magnetically coupled, solid state stirring motor. Also mounted on each box core are eight spring actuated 50 mL plastic syringe samplers used to take sequential samples of the overlying water in the box cores. All sampling events were controlled by an electronics package consisting of the stirring motor electronics, a rechargable battery pack and a multi-event programmable timer. Sampling operations were accomplished by using electric "dissolving link" releases.

In the cocked positon (ready for deployment), the movable tray was in the up position so that the box cores were above the base of the tripod and were open at both the top and bottom. After the tripod was set on the bottom, a period of time was allowed to elapse before the box cores penetrated the sediments. The elapsed time was generally 0.5 to 1.5 hour, depending upon the overall deployment time. Lead weights drove the box cores into the sediments and the rate of penetration was controlled by a hydraulically damped dashpot. Penetration depth was regulated by adjustable stops. Overlying water volumes for typical deployments ranged from 2.5 to 5.0 liters.

Eight sequential samples were drawn from the water overlying the box cores by the spring-actuated syringes. Water withdrawn over the cores was replaced with bottom water. In this study, the first sample was drawn 10 minutes after closure and subsequent samples were drawn at 2 hour intervals. Injection of tritiated water took place between the first and second syringes sampling events. After all samples were taken, a final release closed the box core shovels.

Upon retrieval, the arms containing the box core lids and syringe samplers were removed and the cores were visually checked for disturbance of surface sediments. The depth of overlying water was then measured and the box core sediments were subcored using a 10 cm diameter core tube. Subcores were subsequently sectioned (0.5 cm intervals in the upper 2 cm and 1.0 cm intervals below) and the pore water separated from the bulk sediment by centrifugation.

All samples were analyzed within six hours of tripod retrieval. Prior to analysis, samples were stored at 2 degrees C. Silicate, phosphate, nitrate, nitrite and ammonium were determined by standard auto analyzer techniques (Whitledge, 1981).

The dissolved oxygen from the gas sampling loops was separated on molecular sieve 5A column at 60 degrees C with helium carrier flow of 60 mL/minute. The thermal detector was operated at 25 degrees C for maximum sensitivity. All values were corrected for distilled water dilution.

2.6 SOUTH SOUND CURRENT METER ARRAY STUDY

The Southern Puget Sound current study was conducted to provide informaton on current refluxing in the area of Dana Passage. Three current meter arrays were deployed in Southern Puget Sound on April 16, 1985 and recovered on June 24 and 25, 1985. The sites selected correspond to historical current meter stations (Collias, 1970) and the same historical data station numbers were used to identify the current meter arrays. The three locations were Station 438 near Dougall Point in Pickering Passage, Station 450 over an old dredge spoil site in Dana Passage, and Station 452 in Dana Passage north of Dover Point (Figure 2.8). Array deployment dates, locations, depths and methods are summarized in the Circulation and Flushing in South Puget Sound report (URS, 1986).

2.7 COMPUTER MODELS

Two-Dimensional Box Model

The two-dimensional box model is a steady state model utilizing salt balance (salinity measurements) in estimating horizontal and vertical advection and vertical diffusion rates. These are then used in analyzing fluxes and budgets of water quality constituents. Modeling methodology was taken from Pritchard (1969) and Officer (1981). An extensive discussion of box modeling methods, calibration/verification and results is presented in Section 4.1, Box Modeling.

N

Sta. 438

Carr Inlet

Case Inlet

Pickering Passage

Oakland Bay

Hale Passage

Fox Island

The Narrows

Harstene Island

Hammersly Inlet

Shelton

McNeil Island

Squaxin

Sta. 450

Balch Passage

Totten Inlet

Sta. 452

Diana Passage

Drayton Pass

Anderson Island

Eld Inlet

Dover Pt.

Henderson Inlet

Nisqually Reach

Budd Inlet

Dofflemeyer Pt.

OLYMPIA

0 1 2 3 4 5 6
miles

■ = Current meter locations

Figure 2.8 Current meter locations.

Generalized, Longitudinal Vertical Hydrodynamic (GLVHT) Model

The GLVHT model was developed by J. Edinger Associates and adapted to dynamically model the Budd Inlet dissolved oxygen system. GLVHT is a fortran program incorporating the implicit finite-difference solution of the momentum, continuity, transport and state equations in the longitudinal, vertical and time dimensions. Transport equations include heat, salinity and water quality constituents which are specified for each application to address the overall problems being considered. The program was developed to assist in the analysis of water quality problems in rivers, lakes, reservoirs, estuaries and coastal waterbodies where density induced flows are important and lateral homogeneity can be assumed. GLVHT may be applied to both open and closed boundary conditions and to cases where the waterbody is branched. For use in the GLVHT dynamic model, Budd Inlet is divided into longitudinal segments of length Δx (759 meters) and vertical layers of thickness Δz (3 meters). The width of each cell thus formed is then taken as the area at that particular elevation divided by the Δx. Therefore, an average width is used such that the sum of each individual cell's area and volume reproduce the waterbody's elevation-area-volume curves. A complete discussion of GLVHT methods, calibration/verification and results is presented in Section 4.2, Dynamic Modeling.

2.8 DATA MANAGEMENT

A number of computer systems were utilized to store data, manage data, generate graphs and drive the Budd Inlet Dynamic Model.
Most of the data entry and storage was performed upon IBM-PC and Compaq microcomputers utilizing hard-disk mass storage devices. Database and graphic software utilized by these machines included Lotus 123 by Lotus Development Corporation, DisplayWrite 2 by IBM Software, Inc. and Contur by In-Situ, Inc. Contur was especially useful in generating the contour plots of Budd Inlet presented in the Appendices.

CHAPTER 3. DATA ANALYSIS AND RESULTS

This chapter presents the results and analysis of the major data collection efforts of this study. Included are an analysis of historical data related to determining the limiting nutrient in Budd Inlet; the results of two intensive water quality and current meter surveys in Budd Inlet; an analysis of flushing and circulation patterns outside of Budd Inlet; the results of five point source surveys and two detailed bacteriological surveys; and a sediment oxygen demand and benthic flux survey. These interrelated studies provide an integrated data set necessary to calibrate the dynamic water quality model and to understand the dissolved oxygen system in Budd Inlet. This integrated data set has been used to diagnose and interpret the historical data.

3.1 DETERMINING THE LIMITING NUTRIENT IN BUDD INLET

Background

Historically, the "Redfield ratio" (Redfield, 1958) has been used to assign a limiting role to major phytoplankton nutrients in marine waters. The ratio is based on the observation that the atomic ratio of nitrogen to phosphorus (N:P) in both phytoplankton and the nutrient-rich waters below the thermocline is approximately 15:1. However, in more recent investigations where the phytoplankton have been analyzed independently from the surrounding detritus, it has been shown that the N:P ratio ranges from 5:1 to 15:1 and that the Redfield ratio is attained only when the maximum growth is approached (McCarthy, 1980).

In laboratory experiments with phytoplankton cultures, the amount of P per cell can be reduced farther below the maximum cellular content than can N before growth rates become reduced (Goldman and McCarthy, 1978). Other experiments with N and P-limited marine phytoplankton cultures have shown

with very few exceptions that nitrogen is the agent responsible for nutrient limitation. Therefore, at present, the view of marine biologists and oceanographers is that nitrogen, not phosphorus, is the limiting nutrient in coastal waters.

In determining which of the major nitrogen species accounts for the majority of the nitrogen uptake (NO_3^-, NO_2^-, NH_4^+), Dugdale and Goering (1967) observed that ammonium in coastal and nearshore waters accounted for about 60 percent of the inorganic nitrogen used by phytoplankton. More recent studies and reviews have thoroughly documented (see, for example, McCarthy et al., 1977; Paasche and Kristiansen, 1982) that nitrate uptake is diminished in the presence of ammonium. Paasche and Kristiansen (1982) found that the maximum uptake rate of nitrate approached that of ammonium only for very low ammonium concentrations (<5ug-N/L). The maximum uptake rate for nitrate relative to that for ammonium decreases exponentially with increasing ammonium concentrations up to about 40 ug-N/L ammonium, with a small and constant uptake rate at higher concentrations (Figure 3.1). This relationship was found to be insensitive to the specific composition of the phytoplankton.

It should be noted that these results are based on phytoplankton populations containing diatoms. Other researchers (Epply and Harrison, 1975) have shown that for dinoflagellates, nitrate uptake is not inhibited by the presence of ammonium. Consequently, phytoplankton composition can be an important factor in determining the preference for nitrogenous nutrients.

In determining the limiting nutrient in Budd Inlet, the trend in concentration ratios of N:P within the Inlet were examined. As the N:P ratio approached 5:1, nitrogen limitation was indicated, especially as nitrogen values approach zero and phosphorus is present in substantial amounts.
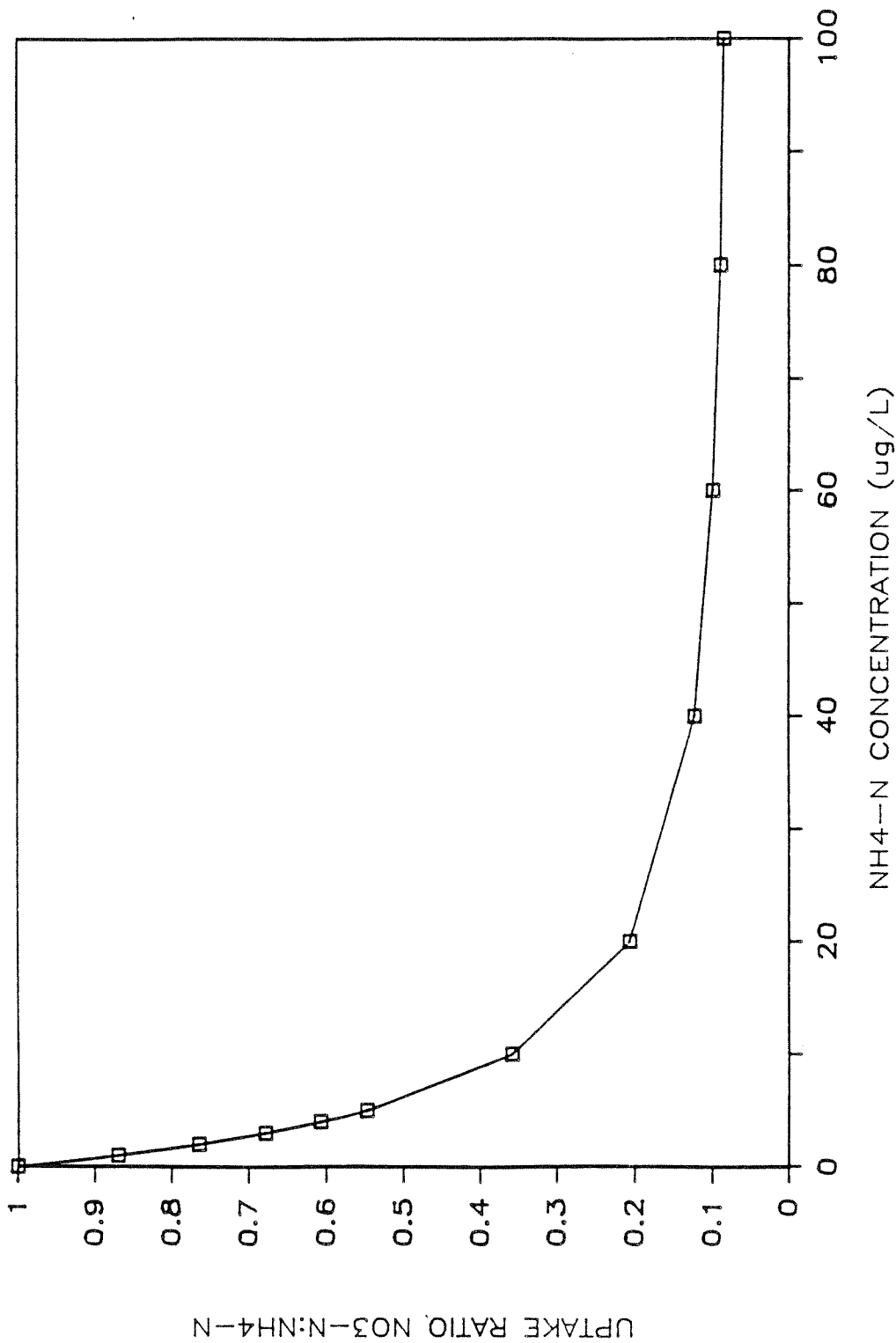
Figure 3.1 Ammonium inhibition factor, Rn, expressed as the ratio of the maximum uptake rate of NO3-N:NO4-N, given as a function of ammonium concentration. Source: Paasche and Kristiansen (1982).

Budd Inlet Analysis

The historical data from Budd Inlet used in this analysis are from WDOE's ambient water quality network (stations BUD002 and BUD005) and from a 1977 WDOE Study of Budd Inlet (Kruger, 1979; stations 510, 522, 532, 542, 562, and 592). The recent water quality measurements from the May and September intensive surveys are also used in the analysis. The station locations are shown in Figure 3.2.

Figure 3.3 shows the seasonal trends of N:P from Kruger's report throughout the Inlet for 1977 in the surface waters. A number of observations can be made from this data. First, N:P ratios in the winter are similar throughout the Inlet (between 10:1 and 15:1), and do not indicate nitrogen limitation. Second, there is a peak in N:P ratios in March except for stations 592 and 532. This was due to low phosphorus concentrations which may be the result of a change in loading or possibly uptake by phytoplankton, which will be discussed later. Third, there is a drop in N:P ratios in April to between 5:1 and 10:1, except for the mouth of the Inlet (station 592). Finally, all inner Inlet stations fall below a ratio of 5:1 during July, August, and September, suggesting nitrogen limitation during these months. Figures 3.4, 3.5, and 3.6 show the trends in surface concentrations of nitrate, ammonium, and phosphorus, respectively, throughout the Inlet for 1977.

Figures 3.4 and 3.5 would seem to indicate nitrate assimilation at higher ammonium concentrations, perhaps due to the loadings from the LOTT treatment plant exceeding the algal uptake and/or the H_2SO_4 used in preserving the non-filtered samples releasing labile NH_4^+ from algal cells. Measured values of ammonium were much lower than the WDOE data both in May and in September in the surface water, which suggests that ammonium is released from algal cells and possibly from other living and non-living organic material during preservation of the non-filtered samples. Figures 3.7A and 3.7B illustrate the first point showing the advection of low ammonium and nitrate water into the Inlet on the flood tide (Figure 3.7A) and the advection of high ammonium water out of the inner
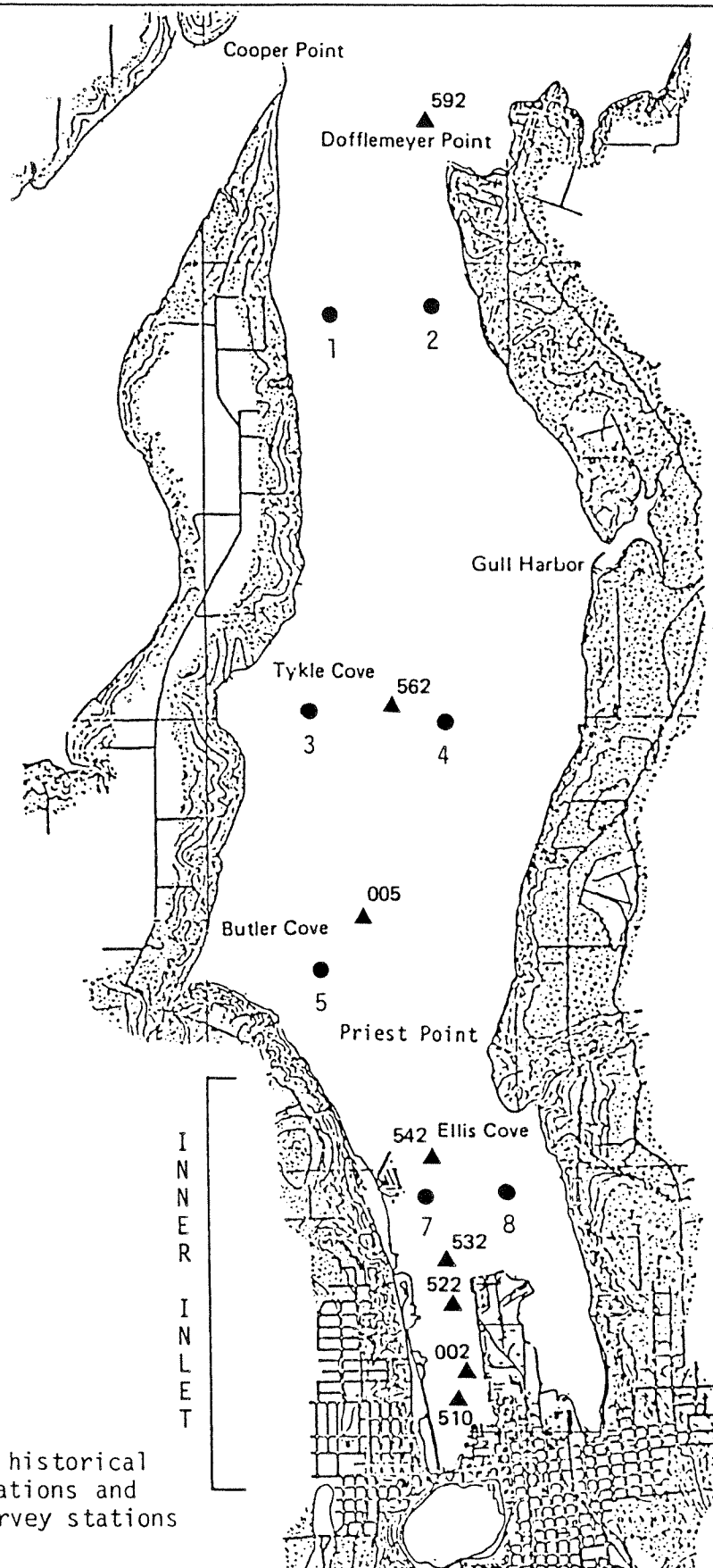
Figure 3.2   Location of WDOE historical
              water quality stations and
              URS intensive survey stations
              in Budd Inlet.

Figure 3.3 Seasonal trends in N:P ratios for 1977.

Figure 3.4 Seasonal trends in nitrate concentrations for 1977.

INORGANIC NH3-N AT SURFACE

SEASONAL TRENDS FOR 1977
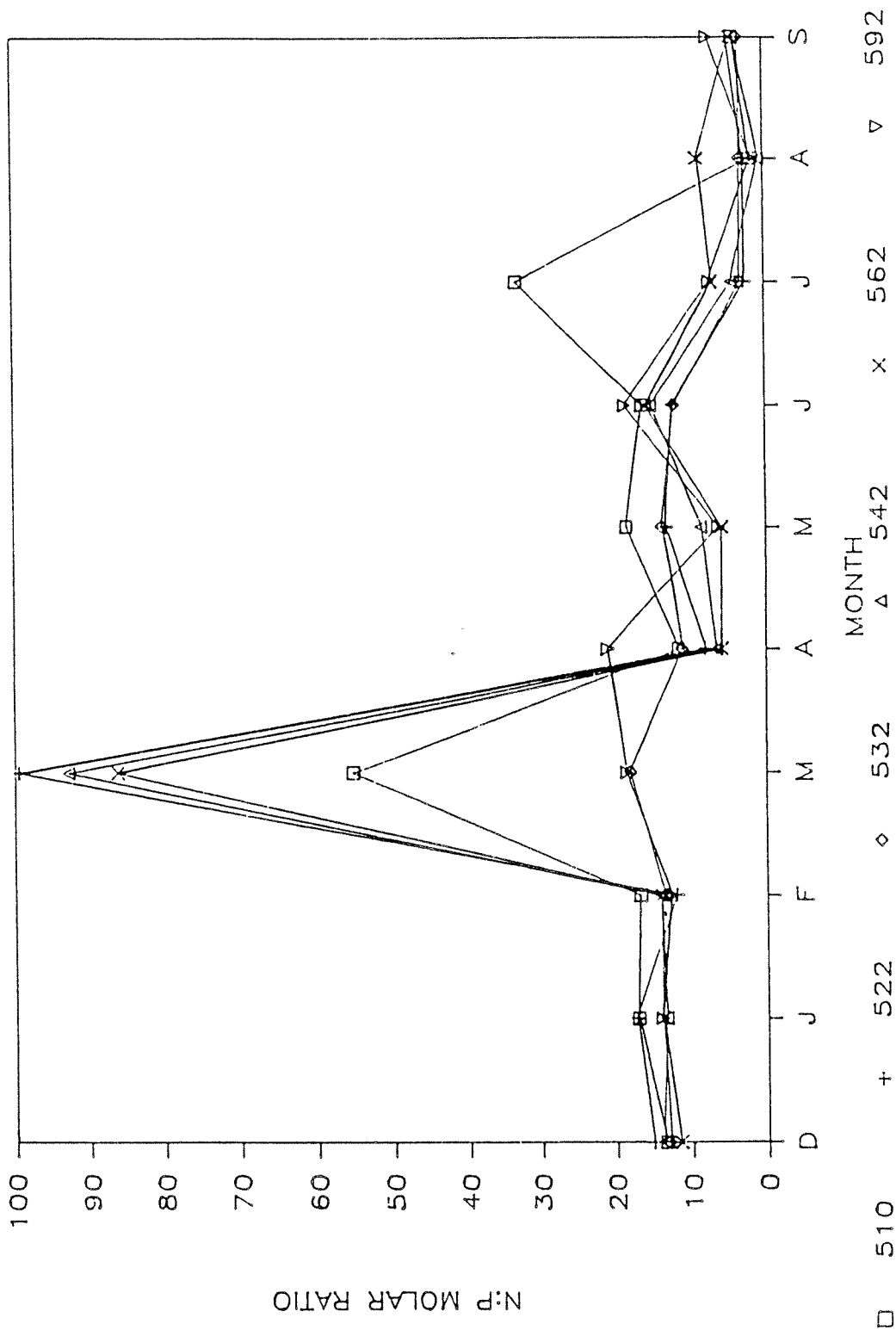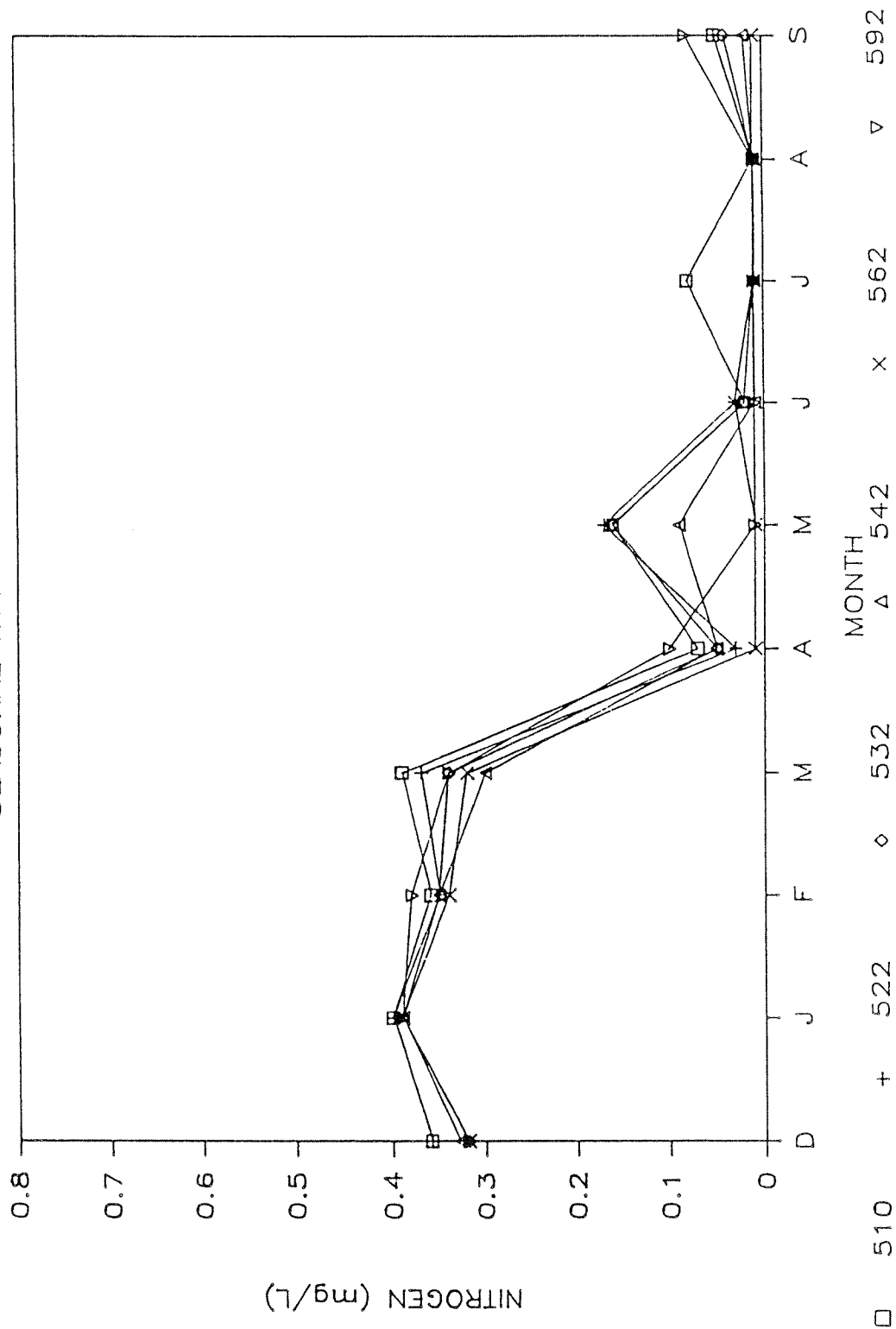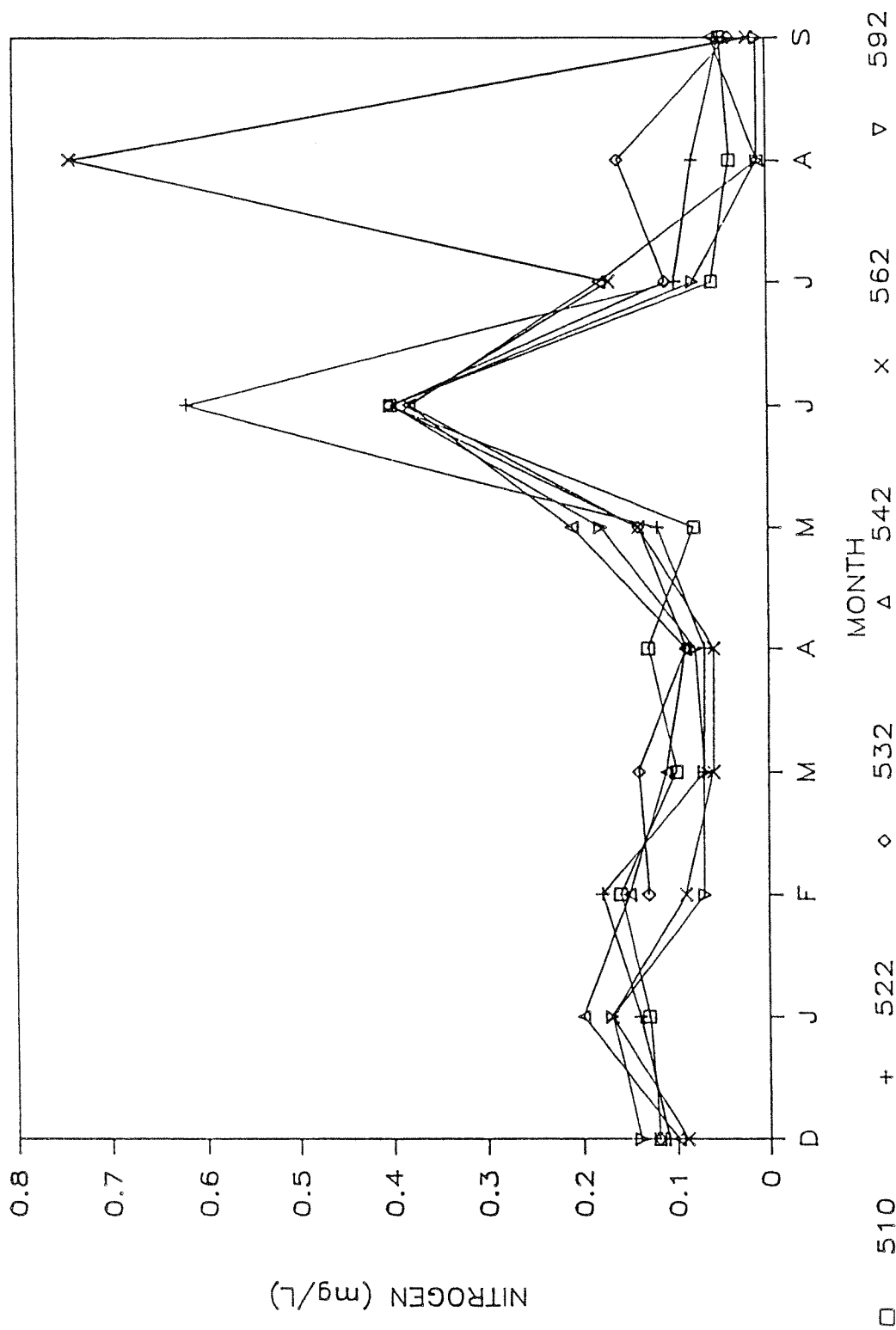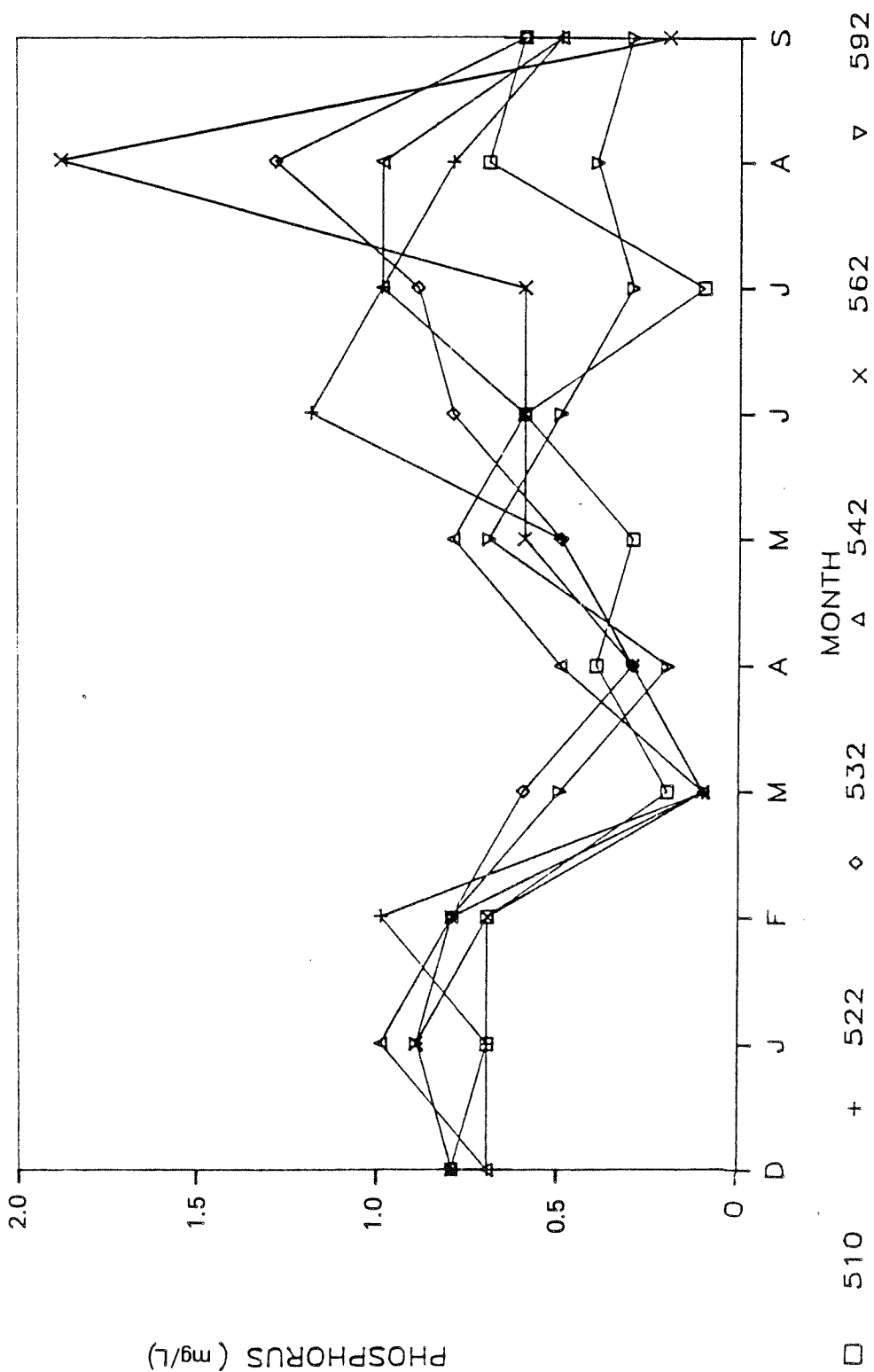
HISTORICAL STATION NUMBER (KRUGER, 1979)
510, 522, 532 AND 542 ARE INNER STATIONS

□ 510   + 522   ◇ 532   △ 542   × 562   ▽ 592

Figure 3.5 Seasonal trends in ammonium concentrations for 1977.

Figure 3.6 Seasonal trends in phosphorus concentrations for 1977.
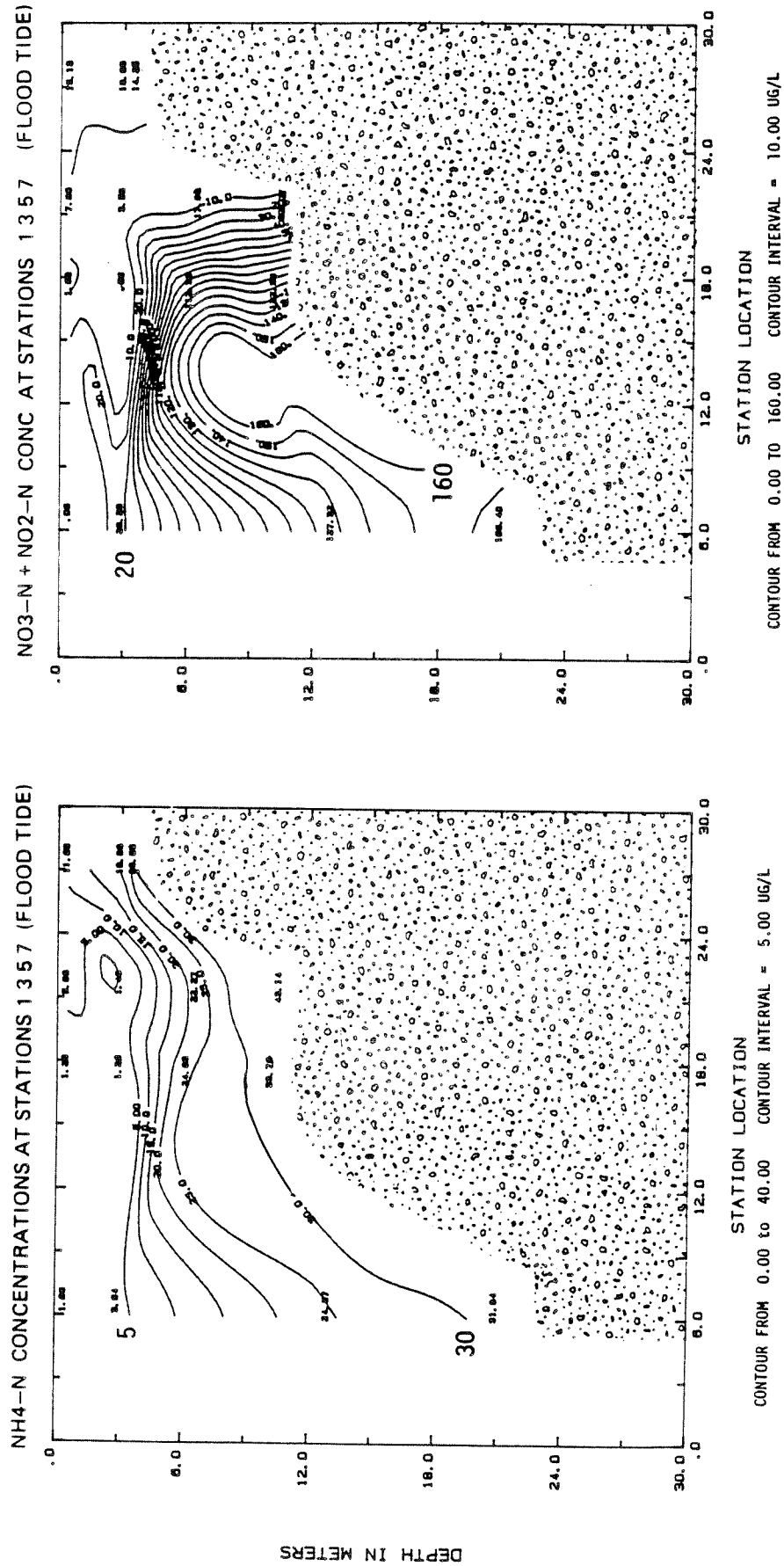
Figure 3.7A Ammonium and nitrate + nitrite concentrations in ug/L at URS intensive survey station 1,3,5 and 7 during flood tide.
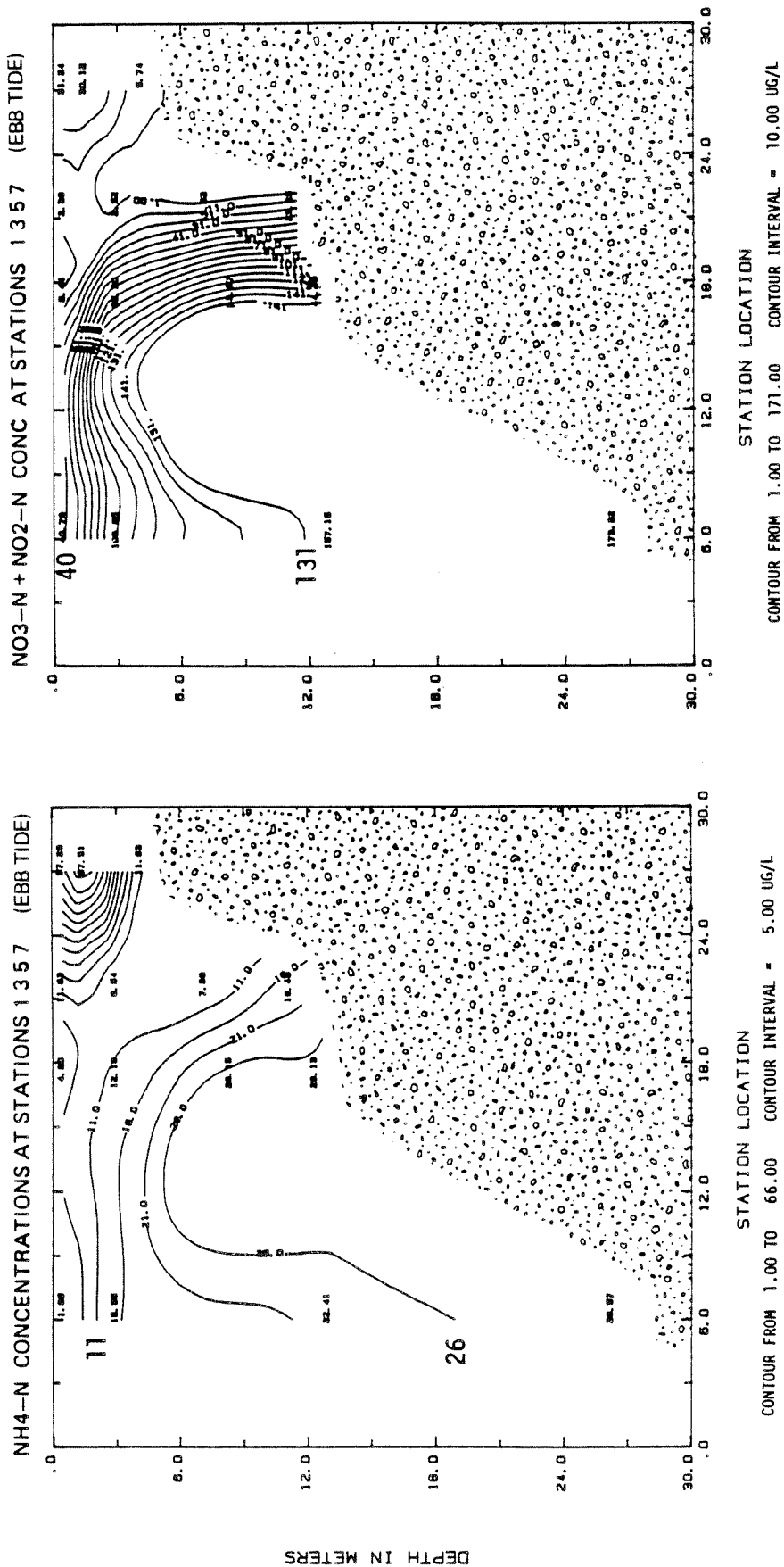
Figure 3.7B Ammonium and nitrate + nitrite concentrations in ug/L at URS intensive survey station 1,3,5 and 7 during ebb tide.

Inlet during ebb tide (Figure 3.7B). Therefore, water high in ammonium is advected into water low in nitrate. The uptake of ammonium by the phytoplankton cannot keep up with this input and consequently high ammonium values are observed along with low nitrate values, especially in the inner Inlet.

The trend toward nitrogen limitation is seen in the 1981-83 data from WDOE's water quality station BUD002 and BUD005 (Figures 3.8 and 3.9). This includes data before and after the upgrade to secondary treatment by the LOTT plant which occurred in August 1982. Phosphorus is always available at both stations; nitrogen was depleted during June 1981 and August 1983 at station BUD005. Ammonium was very low on several occasions and all nitrogen was depleted at times.

Figure 3.10 shows the N:P ratios in the surface water for WDOE stations BUD002 and BUD005 for 1981 through 1983. Station BUD005 shows that concentration ratios fall below 5:1 during the spring and summer months, while station BUD002 falls below 5:1 only during the summer except for 1982 when it remained above 5:1. Station 510 in 1977 (Figure 3.3) also shows higher N:P ratios from April through July which may be related to the fact that both stations 510 and 002 are located near the Capitol Lake discharge (see Figure 3.2).

The N:P ratios at the surface during the URS September 1984 and May 1985 intensive surveys are shown in Figure 3.11 and 3.12, respectively. The ratios for September all fall below 5:1 while the ratios for May are generally below 5:1 with the exception of station 1 during high tide and one value at station 7 near the LOTT outfall.

Figures 3.13 and 3.14 show the modeled algal primary production as a function of ammonium concentration (or nitrate for low ammonium concentrations) using the measured productivity for September 1984 and May 1985. These figures graphically illustrate the functional relationship between the nitrogenous nutrients and algal productivity. It can be seen that inorganic nitrogen controls or limits growth at levels below about 30-40 ug/L. Above this level, growth rate is less sensitive to ambient
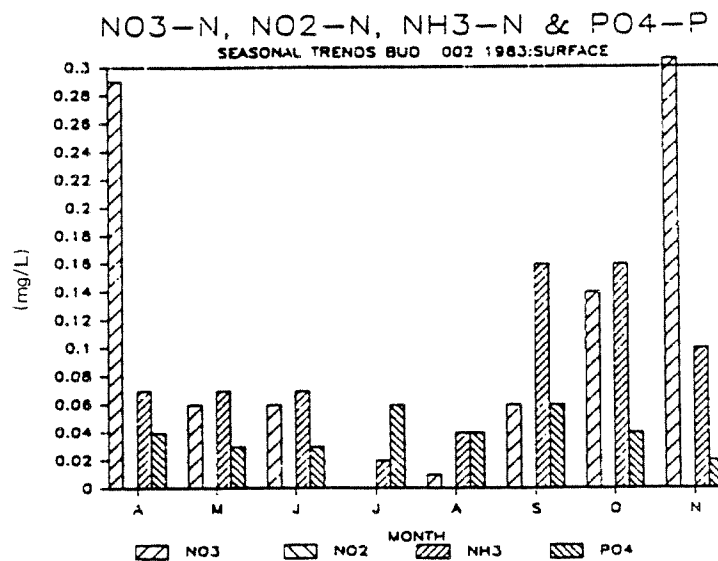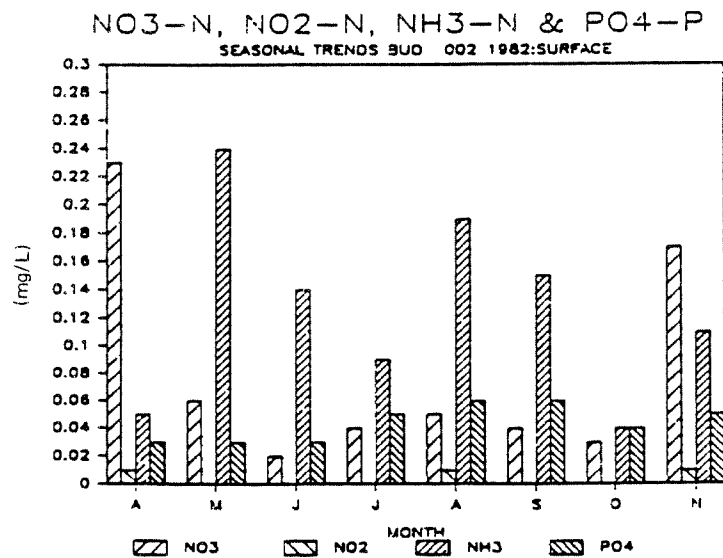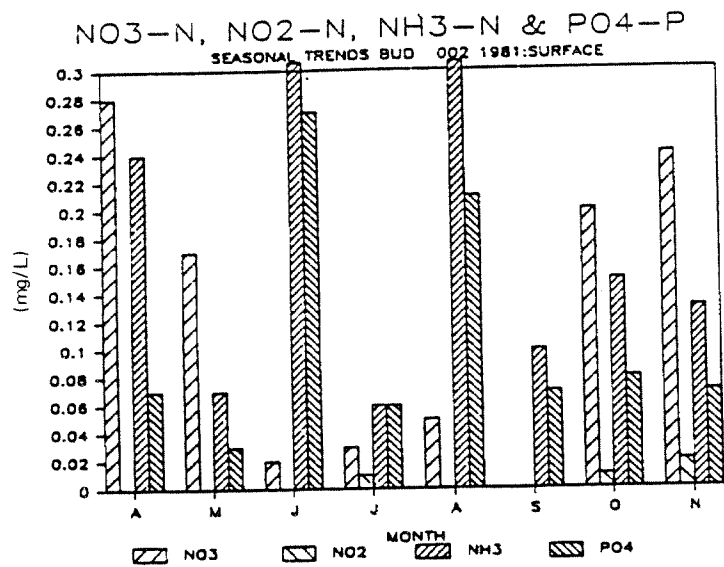
Figure 3.8 Seasonal trends in nitrate, nitrite, ammonium and
phosphorus concentrations at WDOE station BUD002 (1981-1983)

NO3—N, NO2—N, NH3—N & PO4—P
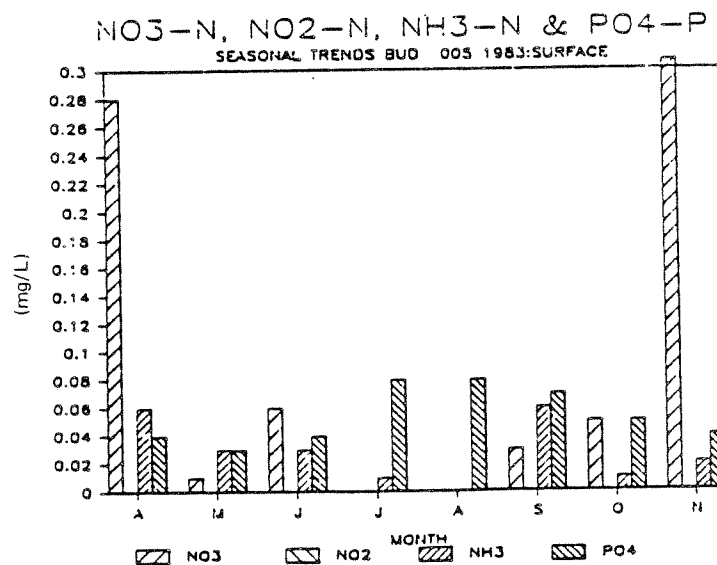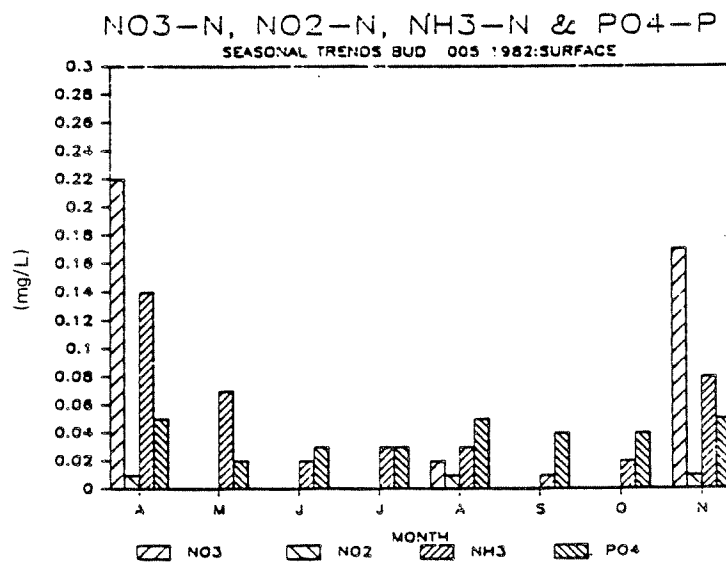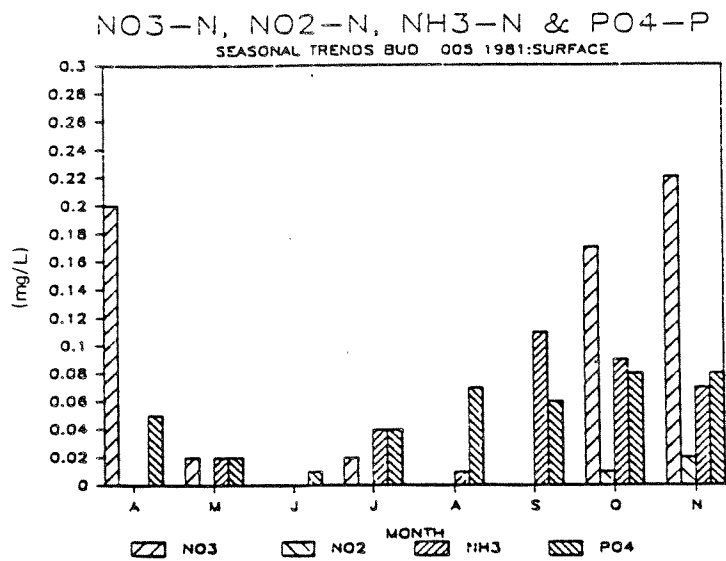
Figure 3.9 Seasonal trends in nitrate, nitrite, ammonium and phosphorus concentrations at WDOE station BUD005 (1981-1983)

3-14
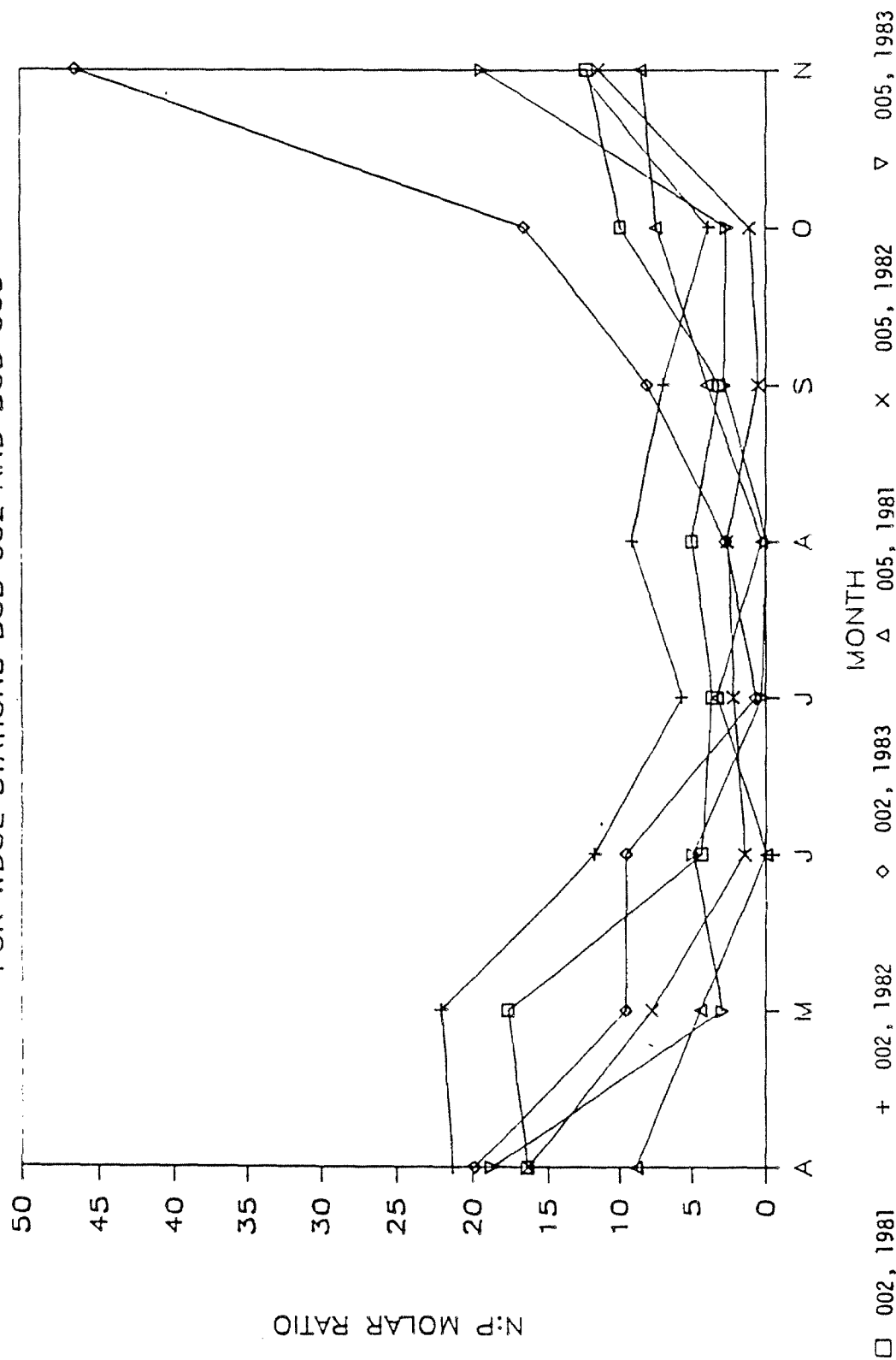
Figure 3.10 Total inorganic nitrogen:phosphorus molar ratios for surface
waters at WDOE stations BUD002 and BUD005 from 1981 to 1983.

Figure 3.11 Total inorganic nitrogen:phosphorus molar ratios for surface waters at URS intensive survey stations 1,3,4,5,7 and 8 for September 1984.

N:P MOLAR RATIO IN BUDD INLET

MAY 1985, 0.5 METER DEPTH
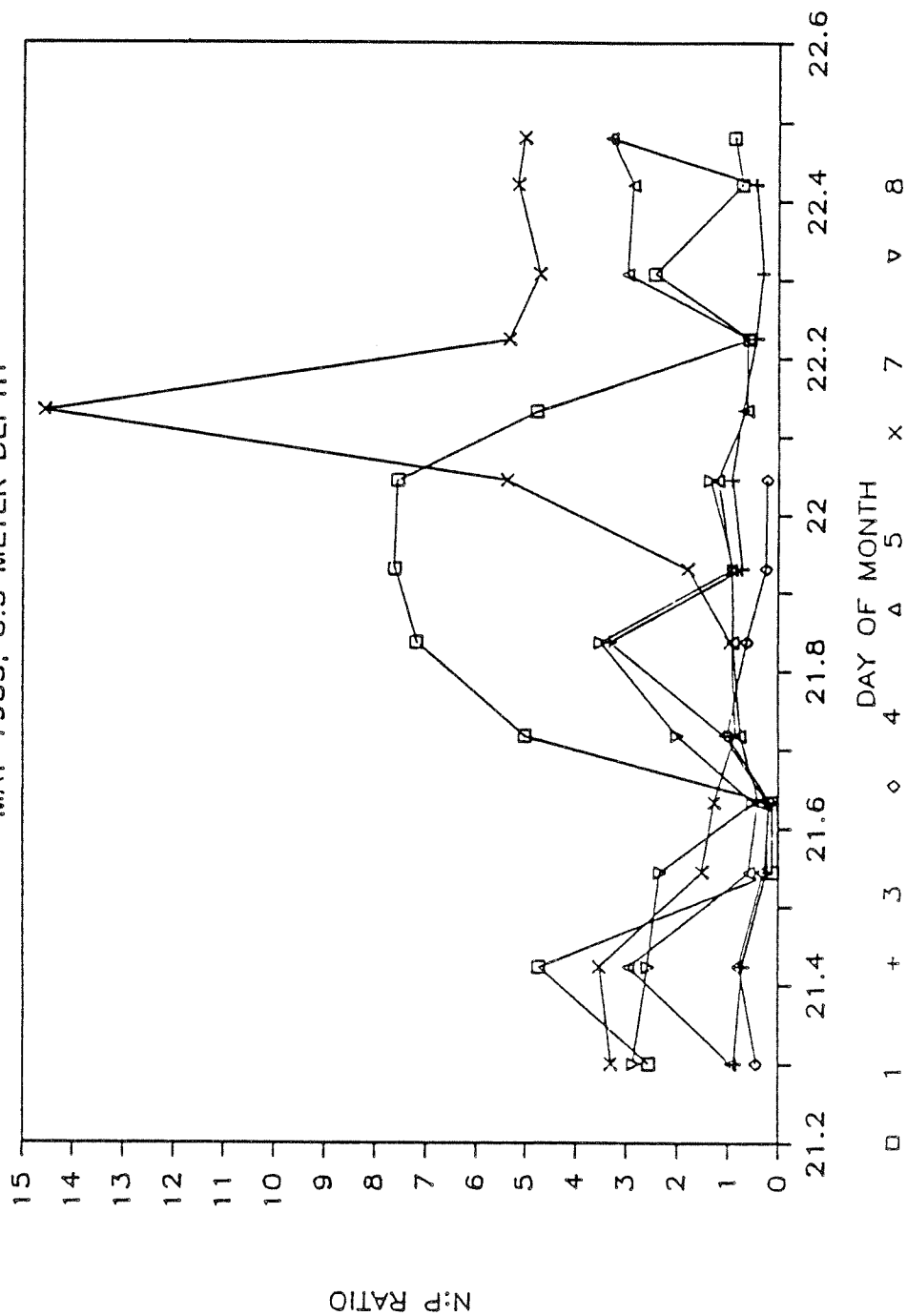
URS INTENSIVE SURVEY STATION NUMBER

□	+	◇	△	×	▽	□
1	3	5	4	7	8	

Figure 3.12 Total inorganic nitrogen:phosphorus molar ratios for surface waters at URS intensive survey stations 1,3,4,5,7 and 8 for May 1985.

Algal Primary Production

as a function of NH4 in the upper 2–3 m

NH4–N (ug/L)
+   Sta 5 Sept '84

Production (mg C/m^2/day)
(Thousands)
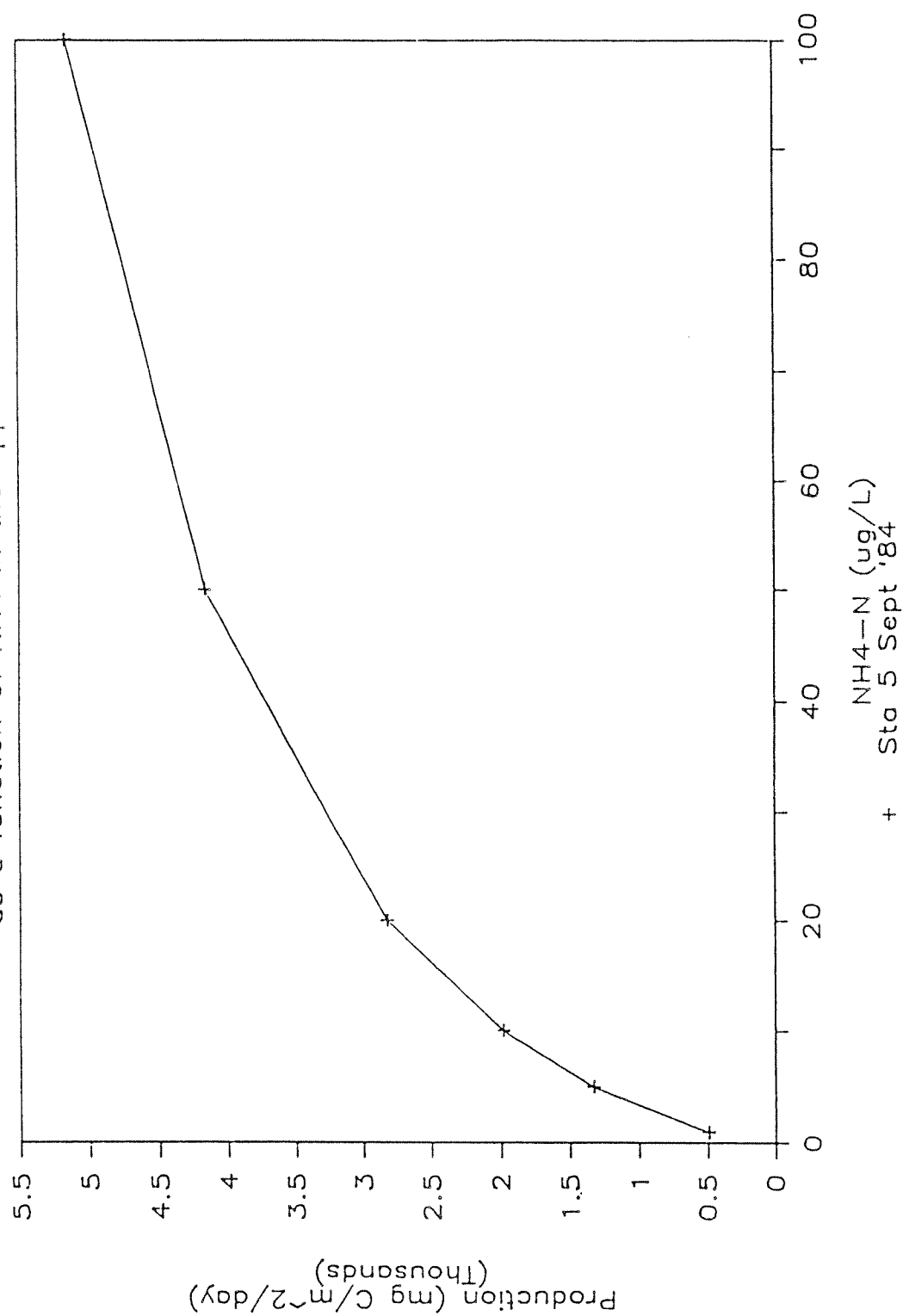
Figure 3.13   Algal primary productivity as a function of ammonium:
URS station 5, September 1984.

Algal Primary Production
as a function of NH4 in the upper 2–3 m

Production (mg C/m^2/day)

NH4-N (ug/L)

□ Sta 3 May '85   + Sta 5 May '85
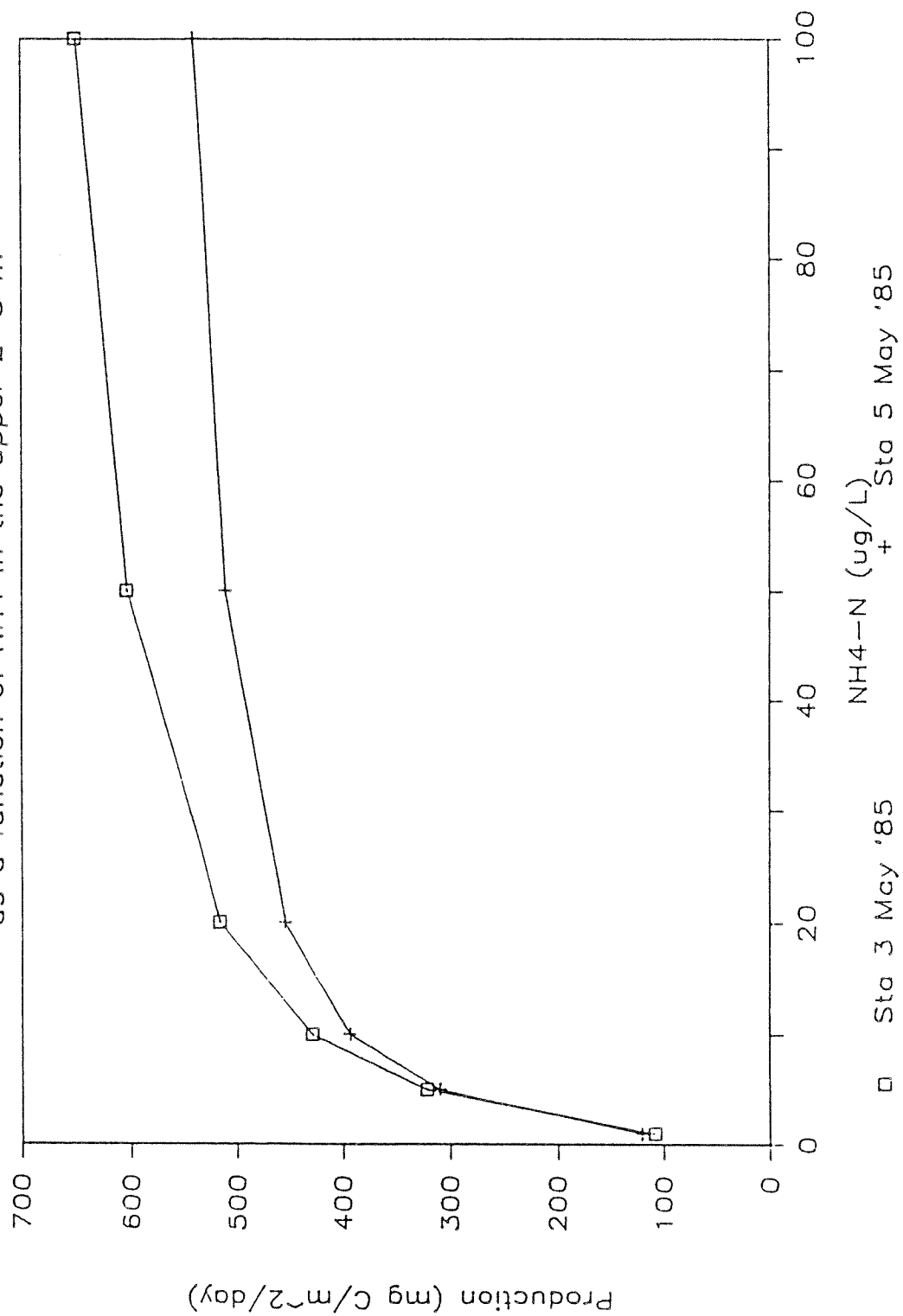
Figure 3.14 Algal primary productivity as a function of ammonium:
URS stations 3 and 5, May 1985.

inorganic nitrogen concentration. Consequently, either ammonium or nitrate at concentrations from 5-40 ug-N/L will limit production, while nitrate will limit production only for ammonium values less than about 5 ug-N/L.

Summary

Both the historical and intensive survey data indicate that nitrogen is the limiting nutrient in Budd Inlet during the spring, summer and early fall. Nitrogen limits production at levels below about 40 ug/L. Above this level, algal growth is less sensitive to the nutrient concentration. For diatom populations, ammonium is preferred to a substantial degree over nitrate at ammonium levels above about 5 ug/L. Below this level nitrate is utilized on a par with ammonium. The inner Inlet has an excess of ammonium due to the input from the LOTT treatment plant. In the outer Inlet, both nitrate and ammonium levels are low and their relative concentrations are controlled by physical processes as well as by algal uptake.

3.2 DISSOLVED OXYGEN AND NUTRIENT LEVELS IN BUDD INLET

In this section the dissolved oxygen and algal nutrient trends observed during the intensive surveys are compared to historical data reported in Westley, et al. (1973) and Kruger (1979). Data tables summarizing the two surveys are presented in Data Appendices 1.1 (September 1984) and 1.2 (May 1985). Contour plots referred to in this section are presented in Data Appendices 1.3 (Comparison of the Surveys), 1.4 (September 1984 contours) and 1.5 (May 1985 contours). The reader is referenced to the Data Appendices for a more detailed graphical presentation of the following narrative summary.

September 1984 Survey

The general trends in dissolved oxygen concentrations in Budd Inlet during the September intensive survey showed episodes of extremely high near surface dissolved oxygen concentrations (18 to 20 mg/L) coupled with

low near bottom values (<5 mg/L) at the head and mid Inlet stations
(Table 3.1). This stratified condition existed until about 1400 hours on
September 20th when a storm delivering strong south-westerly winds produced
vertical mixing and horizontal transport destroying the vertical
stratification. The effects of the storm on dissolved oxygen
concentrations were most dramatic from Station 3 south to the head of the
Inlet. This can be seen in contour plots of dissolved oxygen over time at
Stations 5 (west-side) and 4 (east-side), shown in Figures 3.15 and 3.16
respectively. At approximately 1400 hours (Time=20.6) on September 20th,
the storm event began, and by about 1700 hours (Time=20.7) the vertical
stratification had broken down, resulting in relatively uniform dissolved
oxygen concentrations of about 5-6 mg/L throughout the water column at
Station 5. Station 4, located "downwind" of 5, maintained the stratified
condition longer, but eventually also became mixed vertically. By about
1200 hours on the 21st, the entire Inlet was fairly well vertically mixed
with dissolved oxygen concentrations of about 5 to 8 mg/L. At the end of
the September 1984 survey, stratification had not yet returned and high
dissolved oxygen concentrations were not present.

Table 3.1 Average concentrations of dissolved oxygen,
nitrate and ammonium before and after the
storm: September 1984 intensive survey

Dissolved Oxygen (mg/L)

	Station 1		Station 3		Station 5		Station 7	
	Before	After	Before	After	Before	After	Before	After
Near Surface	9	9	13	7	20	7	19	5
Mid-Water	7	7	10	7	7	7	13	6
Near Bottom	7	7	7	7	4	5	11	6

Nitrate (ug-N/L)

	Station 1		Station 3		Station 5		Station 7	
	Before	After	Before	After	Before	After	Before	After
Near Surface	45	50	15	70	0	70	30	60
Mid-Water	125	130	50	120	0	90	12	65
Near Bottom	134	180	100	150	7	150	1	65

Ammonium (ug-N/L)

	Station 1		Station 3		Station 5		Station 7	
	Before	After	Before	After	Before	After	Before	After
Near Surface	8	7	2	20	11	45	100	100
Mid-Water	25	20	20	35	25	50	30	80
Near Bottom	40	25	50	40	60	62	20	100

Historical data from Westley et al. (1973) showed a similar pre-storm dissolved oxygen pattern, with high values occurring in approximately the same areas and at similar concentrations. A storm and mixing event also occurred during the September 12, 1972 survey which resulted in the destruction of the vertical gradients.

Little variation in dissolved oxygen concentrations between flood and ebb tides were observed. Typical values are shown in Table 3.2. This table shows that dissolved oxygen levels are slightly higher during flood tide conditions at Stations 3, 5 and 7 and slightly higher at Station 1 during ebb tide conditions.

Table 3.2 Typical values of dissolved oxygen, nitrate and ammonium observed during the flood and ebb tides of the September 1984 intensive survey

Dissolved Oxygen (mg/L)

	Station 1 Flood	Station 1 Ebb	Station 3 Flood	Station 3 Ebb	Station 5 Flood	Station 5 Ebb	Station 7 Flood	Station 7 Ebb
Near Surface	9	10	7	6	7	6	7	6
Mid-Water	8	9	5	5	6	6	7	6
Near Bottom	7	9	5	5	5	5	5	4

Nitrate (ug/L)

	Station 1 Flood	Station 1 Ebb	Station 3 Flood	Station 3 Ebb	Station 5 Flood	Station 5 Ebb	Station 7 Flood	Station 7 Ebb
Near Surface	2	30	40	65	70	60	55	60
Mid-Water	130	60	55	62	80	75	55	50
Near Bottom	200	170	140	145	150	87	86	70

Ammonium (ug/L)

	Station 1 Flood	Station 1 Ebb	Station 3 Flood	Station 3 Ebb	Station 5 Flood	Station 5 Ebb	Station 7 Flood	Station 7 Ebb
Near Surface	5	3	45	20	75	50	96	90
Mid-Water	20	4	20	20	55	45	90	80
Near Bottom	26	25	25	35	60	45	110	90

In general, high near-surface dissolved oxygen concentrations in Budd Inlet are associated with algal blooms which are dependent upon the presence of algal nutrients, sunlight and the absence of strong winds or other factors that might mix the phytoplankton and the dissolved oxygen throughout the water column. Kruger (1979) described this phenomena, along with the presence of a "red tide" event (dinoflagellate bloom), in the inner Inlet during his sampling survey. A similar "red tide" was noticed during the September 1984 URS survey. Further investigation revealed the bloom to be primarily composed of the dinoflagellates Gymnodinium spp. and Ceratium spp. with Gymnodinium the dominant. The bloom in 1977 was reported to be made up of the dinoflagellate Cerativa fusus and Noctiluca scitallans.

Nitrate-N. The general trend in nitrate concentration and distribution during the September 1984 intensive survey showed that concentrations were generally low near the head of the Inlet and higher near the mouth at mid and near bottom depths. Table 3.1 shows this trend and also the effects of the mixing event on the nitrate concentrations. Again, the most dramatic changes in nitrate concentrations before and after mixing are present in the mid and inner Inlet stations. It also seems apparent that Puget Sound is the dominant source of nitrate to Budd Inlet, since the highest values are present near bottom at Station 1 and gradually decrease toward the head of the Inlet. The behavior of nitrate during flood and ebb tide events is summarized in Table 3.2. The highest nitrate values generally are found during flood tide, providing further evidence that Puget Sound is probably the dominant nitrate source.

Ammonium-N. Generally, the highest values of ammonium in Budd Inlet occurred in the inner Inlet near the LOTT Treatment Plant outfall site, with levels at Station 7 from 90 to 100 ug-N/L near surface (Table 3.1). Table 3.1 shows that ammonium concentrations before and after mixing showed the largest changes from about Station 3 south to the head of the Inlet. Table 3.2 summarizes the distribution of ammonium during ebb and flood tide events and shows that concentrations were generally lower in the surface on the ebb.

DO CONC. OVER TIME. STA. 5. BUDD INLET INTEN..SEPT 84

TIME (DAY OF MONTH + 24 HOUR TIME / 2400.0)

CONTOUR FROM   2.00 TO   21.00   CONTOUR INTERVAL =   1.00 MG/L
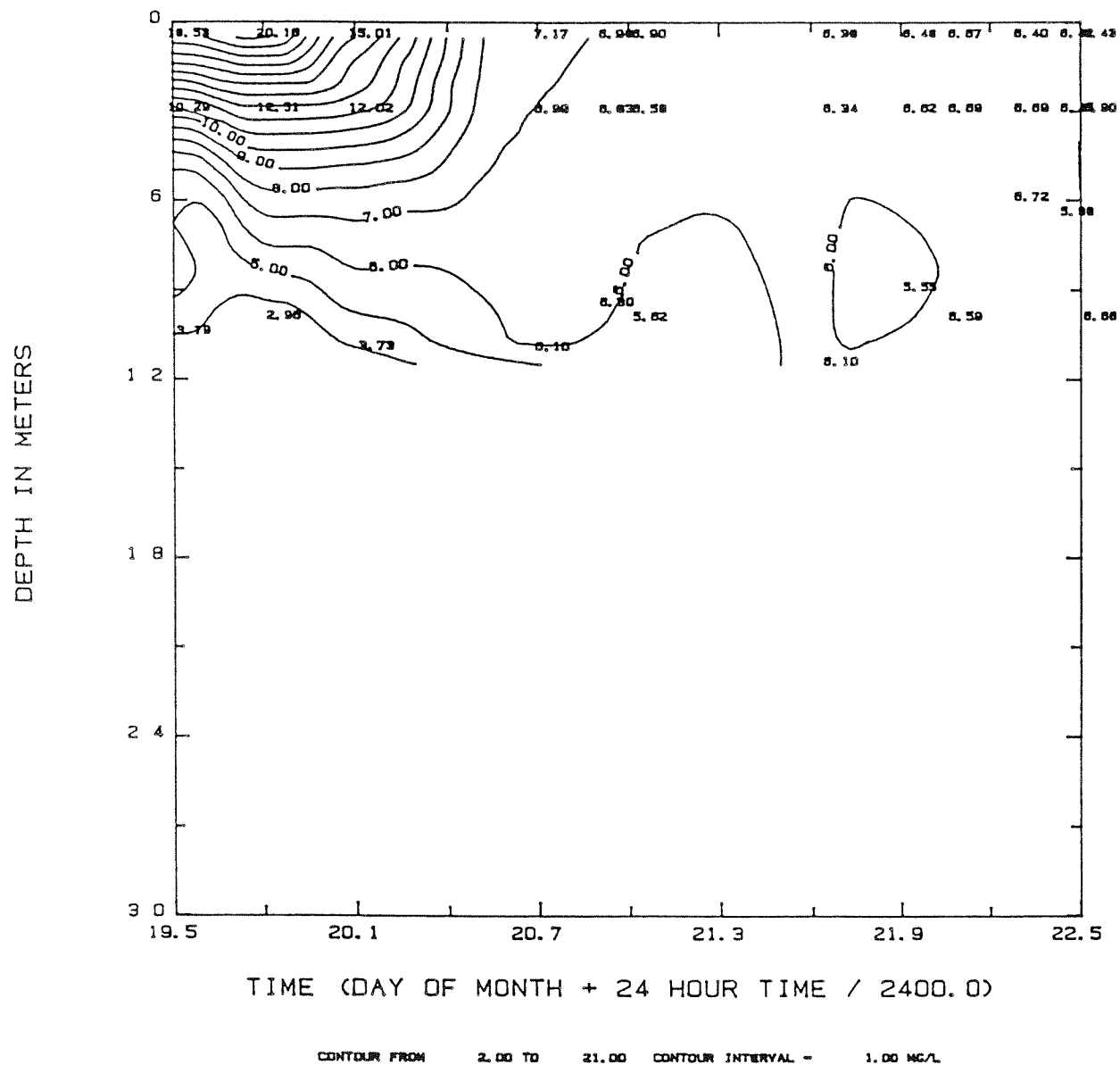
Figure 3.15   Dissolved oxygen concentrations over time at station 5
during the September 1984 intensive survey.

DO CONC. OVER TIME. STA. 4. BUDD INLET INTEN..SEPT 84
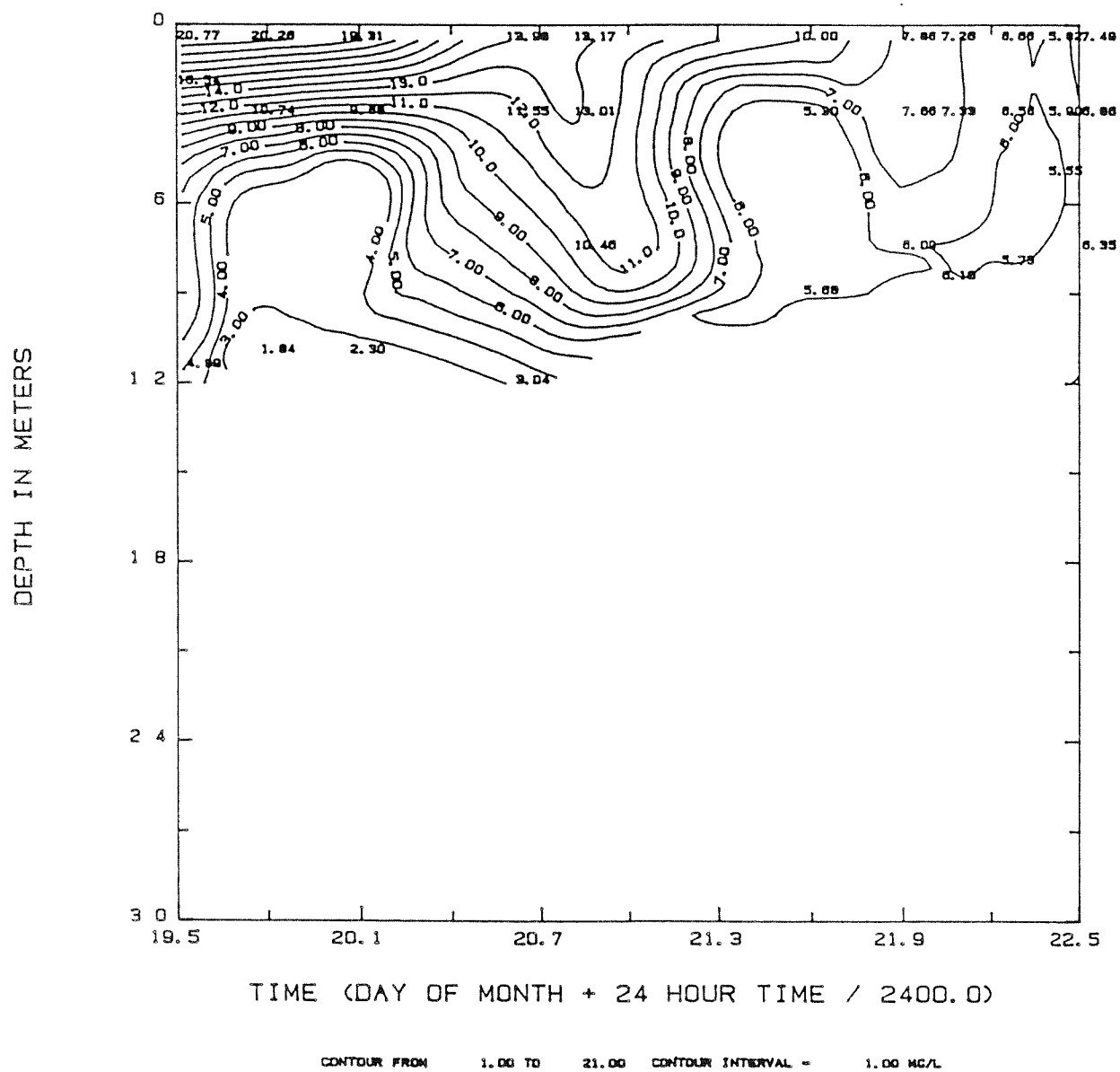
Figure 3.16 Dissolved oxygen concentrations over time at station 4
during the September 1984 intensive survey.

May 1985 Survey

The May 1985 survey was conducted on the 21st and 22nd of the month and covered one complete tidal cycle. No historical data was available for comparison. Since no storm event causing vertical mixing was observed during this survey, dissolved oxygen and algal nutrient concentrations summarized in Table 3.3 are average values over the entire survey for each depth range.

Dissolved Oxygen. Dissolved oxygen concentrations throughout the Inlet ranged from a near surface high of approximately 15 mg/L to a near bottom low of about 9.0 mg/L during this survey. Dissolved oxygen concentrations tended to decrease from the head to the mouth of the Inlet and from the surface to bottom. Average dissolved oxygen concentrations at all stations were relatively consistent throughout the water column.

An algal bloom was again identified during the May 1985 survey, but appeared to be composed of diatoms instead of the dinoflagellates observed during the September, 1984 survey. The extreme differences in surface versus bottom dissolved oxygen levels were not present during this bloom.

Nitrate-N. Nitrate concentrations in Budd Inlet increased with increasing depth at all stations except Station 7 (Table 3.3). The general trend showed an increase from the head of the Inlet north to the mouth, consistent with the September 1984 findings. The overall trends throughout the Inlet were quite similar to the September 1984 data, although the September concentrations were much less at Station 5 before the storm.

Ammonium-N. The highest ammonium concentrations recorded during the May 1985 survey occurred at inner Station 7 in the near surface waters, where concentrations exceeded 800 ug-N/L in some instances. These high concentrations seemed to occur in pulses, indicating they were most probably due to the activities of LOTT STP, which is the primary source of ammonium to Budd Inlet. Table 3.3 presents ammonium values averaged over

Table 3.3   Average concentrations for dissolved
           oxygen, nitrate and ammonium for the
           May 1985 intensive survey

Dissolved Oxygen (mg/L)   Averaged over entire survey

	Station 1	Station 3	Station 5	Station 7
Near Surface	11	13	13	11
Mid-Water	10	13	13	11
Near Bottom	10	10	10	10

Nitrate (ug-N/L)   Averaged over entire survey

	Station 1	Station 3	Station 5	Station 7
Near Surface	50	8.5	6	21
Mid-Water	134	104	15	10
Near Bottom	158	130	30	5.4

Ammonium (ug-N/L)   Averaged over the entire survey

	Station 1	Station 3	Station 5	Station 7
Near Surface	10	4	14	162
Mid-Water	20	20	8	126
Near Bottom	27	27	13	28

the entire study period and shows a general trend of decreasing concentrations from head to mouth with near bottom concentrations of about 27 ug-N/L from Station 3 to the mouth.

Summary

Dissolved Oxygen. The two intensive surveys exhibited a considerable difference in dissolved oxygen concentrations and algal nutrient patterns. The September 1984 survey was conducted during an active dinoflagellate bloom composed of Gymnodinium spp. and Ceratium spp., reflected in near surface dissolved oxygen concentrations exceeding 20 mg/L (250% saturation) and near bottom dissolved oxygen values of less than 3 mg/L (30% saturation). This phenomena was also recorded by Westley et al. (1973). During the May, 1985 intensive survey, a centric diatom bloom was in progress dominated by Chaetoceros sp. (Andrea Copping, personal communication) which created near surface oxygen levels of about 13 mg/L which were over 150% saturation, and near bottom values exceeding 10 mg/L. The September 1984 storm event showed how the Inlet reacted to wind induced vertical mixing and transport, with the destruction of oxygen stratification.

Nitrate-N. Nitrate concentrations at Stations 1 and 3 were quite similar between intensive surveys and changed through the water-column in a similar fashion. At Station 5, however, the September 1984 nitrate concentrations before the storm were much lower than the May 1985 values.

Ammonium-N. Ammonium values at Station 1 showed similar ranges between the September 1984 and May 1985 samplings, with about 9 ug-N/L near surface and 26 to 30 ug-N/L near bottom. At Station 3, the May 1985 surface and near bottom values were significantly less than the September 1984 values, with similar mid-depth values recorded. Station 5 data showed September ammonium concentrations approximately four times greater than May 1985 data at mid and near bottom depths, and over twice as great near surface. May 1985 surface values at Station 7 were much greater

than the September data, with some readings in excess of 800 ug-N/L and an overall May average of 162 ug-N/L versus 100 ug-N/L for September 1984.

3.3 HYDROGRAPHIC AND CURRENT MEASUREMENTS

Within Budd Inlet

Hydrographic Data. Salinity contours representing four tidal phases are presented in Figure 3.17. The contours are of a vertical transect along the axis of the Inlet through stations 1, 3, 5, and 7. Changes in the salinity patterns reflect the flow conditions at various phases of the tide. During a flood tide, the lower salinity water entering Budd Inlet is pushed into the head of the Inlet, and contours become more vertical. As the tide ebbs this water flows out of the Inlet and the contours become more horizontal. As this water is pushed back and retained at the head of the Inlet, mixing of fresh and salt water is reduced.

The contour data show that the Inlet is moderately stratified. Salinities range from about 26.2 o/oo to 29.3 o/oo top to bottom at mid-Inlet stations. At the mouth of the Inlet, stratification is not as pronounced with salinities generally ranging from 27.3 ^{o}/oo at the surface to 29.3 o/oo near the bottom. The greatest changes in salinity values occur in the upper 3 to 4 meters. Below about 4 meters water in the Inlet is relatively homogeneous. Density contours are very similar to those of salinity. In Budd Inlet, as in most of Puget Sound, salinity is the factor primarily controlling density stratification.

Surface salinity maps (Figures 3.18 and 3.19) represent conditions of the September, 1984 and May, 1985 surveys, respectively. Generally, the lower salinity water seems to move along the east side of the Inlet. The prevailing wind direction from the southwest would tend to push the surface water toward the east side of the Inlet. In addition, any effects of Coriolis force would also push water toward the east as it moves northward out of the Inlet. Westley et al. (1973) reported similar results with lower salinity water primarily on the east side of the Inlet.

SALINITY CONC. AT STATIONS 1 3 5 7   (HIGH SLACK)

SALINITY CONC. AT STATIONS 1 3 5 7   (EBB TIDE)

SALINITY CONC. AT STATIONS 1 3 5 7   (LOW SLACK)

SALINITY CONC. AT STATIONS 1 3 5 7   (FLOOD TIDE)

DEPTH IN METERS

STATION LOCATION

CONTOUR FROM 23.00 TO 30.00   CONTOUR INTERVAL = .50

CONTOUR FROM 22.00 TO 30.00   CONTOUR INTERVAL = .50

CONTOUR FROM 25.00 TO 30.00   CONTOUR INTERVAL = .50

CONTOUR FROM 24.00 TO 25.00   CONTOUR INTERVAL = .50

Figure 3.17   Contour plots of salinity during four tidal phases: May 1985.

3-30

Final Survey - 9/23/84
Salinity (o/oo)
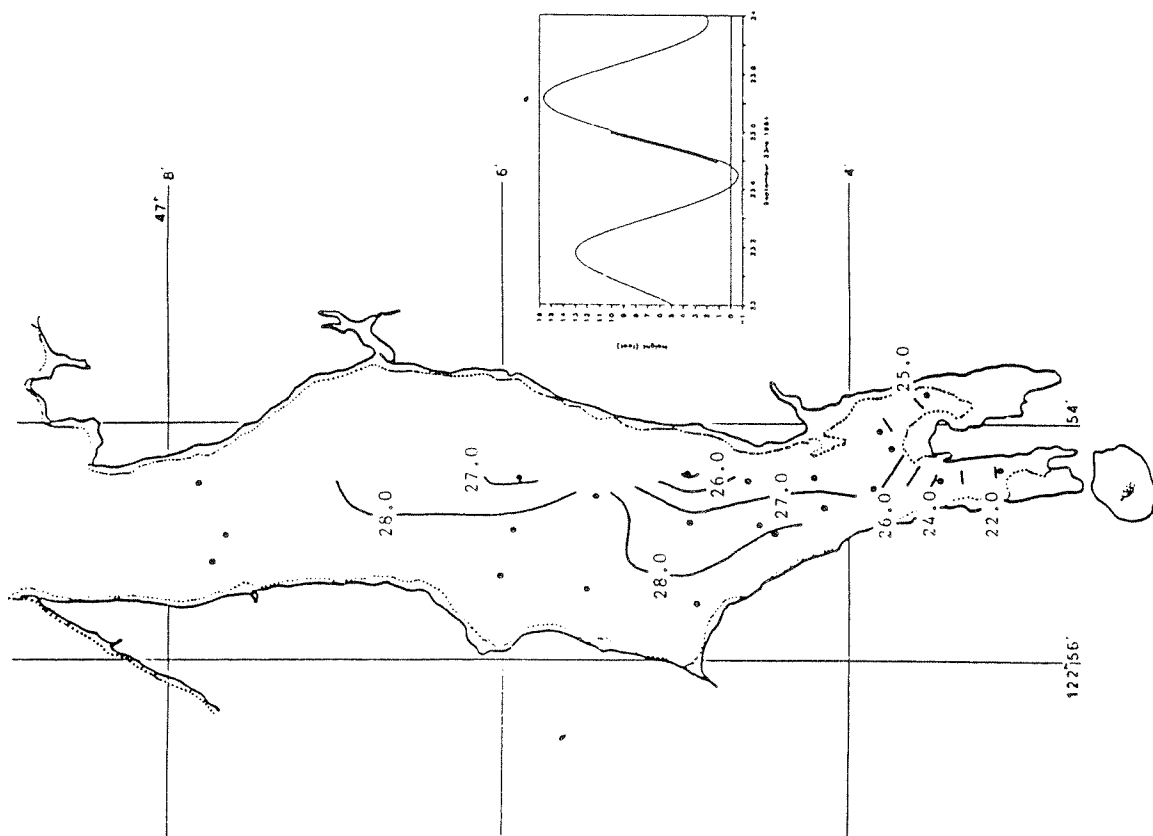
Initial Survey - 9/18/84
Salinity (o/oo)
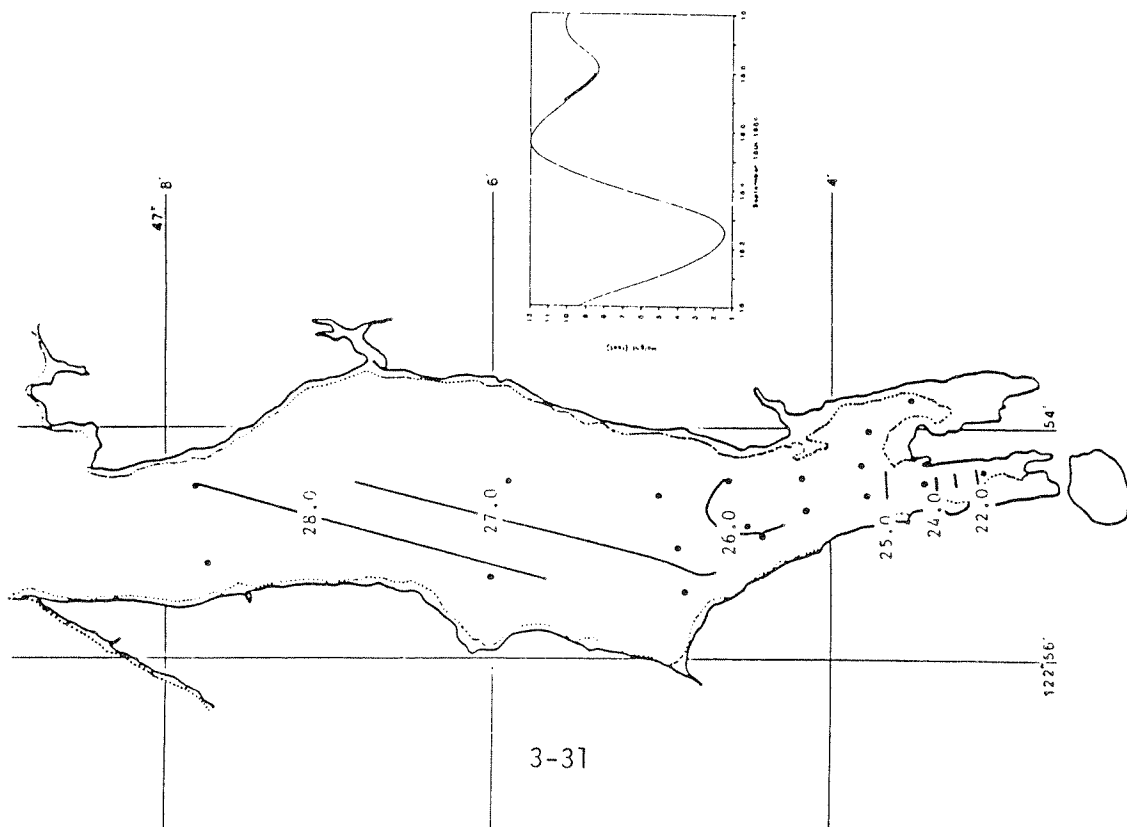
Figure 3.18 Surface salinity, 9/18 and 9/23, 1984.

3-31

Initial Survey – 5/20/85
Salinity (o/oo)
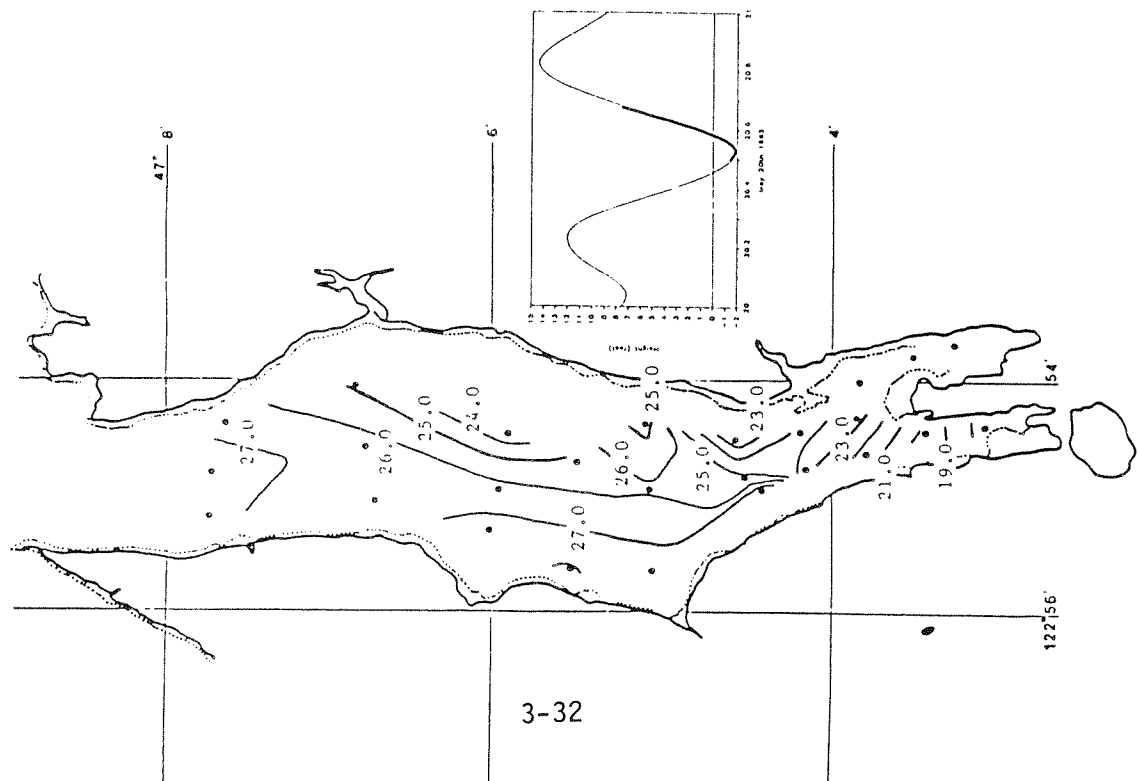
Final Survey – 5/22/85
Salinity (o/oo)
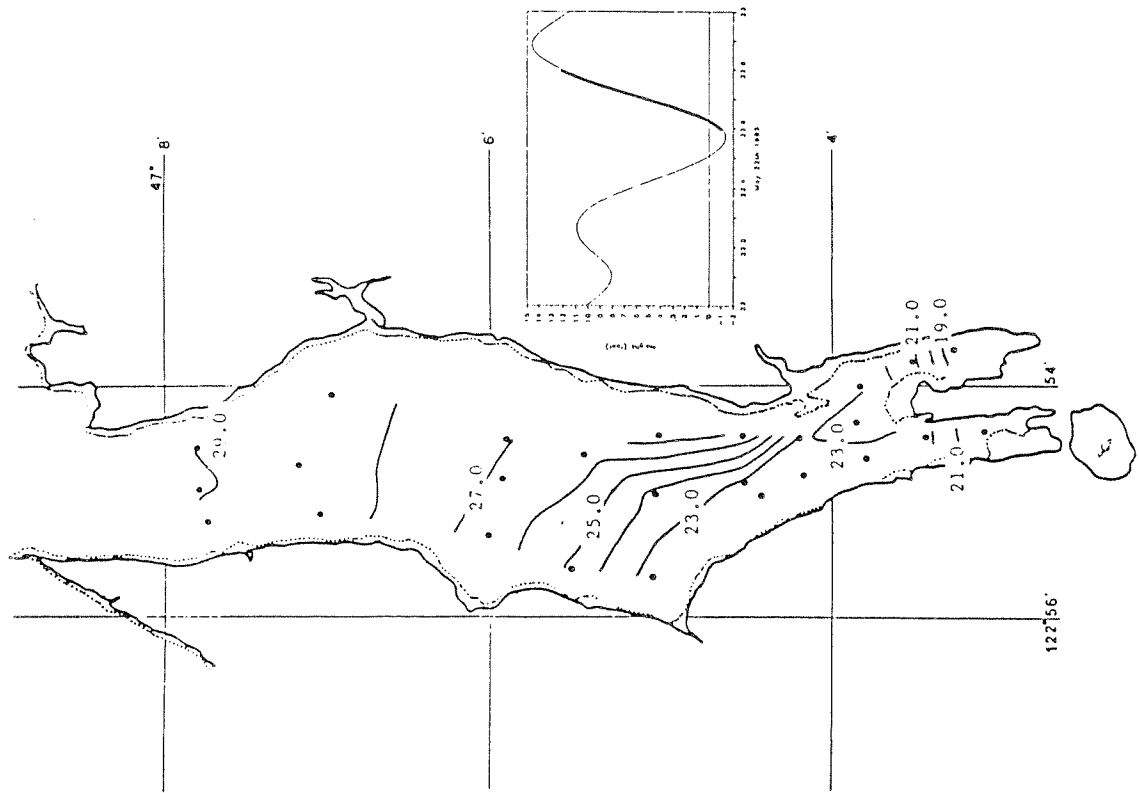
Figure 3.19 Surface salinity, 5/20 and 5/22, 1985.

The surface salinity maps show along-channel and cross-channel variations. Salinity increases from the head to the mouth of the Budd Inlet as the freshwater input from Capital Lake mixes with the seawater. Surface salinities ranged from 17 o/oo to 29 o/oo from the head to the mouth of the Inlet. Cross-channel variations ranged from less than 2 o/oo to 4 o/oo. Cross-channel variations reflect differences in the flow regime of the east and west sides of the Inlet and the effects of winds on the surface water.

Current Data. Figure 3.20 presents the net velocity calculated over one complete tidal day during each of the intensive surveys. The net velocity is the vector average of individual current measurements. One day is a very short time over which to average and obtain a net velocity. Usually at least 28 days should be used to obtain a representative value. While the net velocities calculated may not be completely accurate, they do indicate some aspects of estuarine flow in Budd Inlet. The net flow is generally northward out of the Inlet in the upper few meters with deeper water flowing southward into the Inlet. Net current speeds ranged from less than 2 cm/s to about 13 cm/s. There are several values which indicate eastward or westward flow. Individual measurements show that there are many times when flow is directed across-channel. The uncertainty in individual measurements can lead to a large error in the averaged value when velocities are low or close to the threshold of the current meter, so it is difficult to determine if these are actual flow directions or artifacts of the averaging process.

However, the east to west flow was very pronounced during and following the strong WSW winds in the September 1984 survey. Figure 3.21 shows this sustained cross-channel flow in the surface for four hours on the 22nd, while winds were averaging about 6 knots from the NNE following two days of strong winds from the WSW.
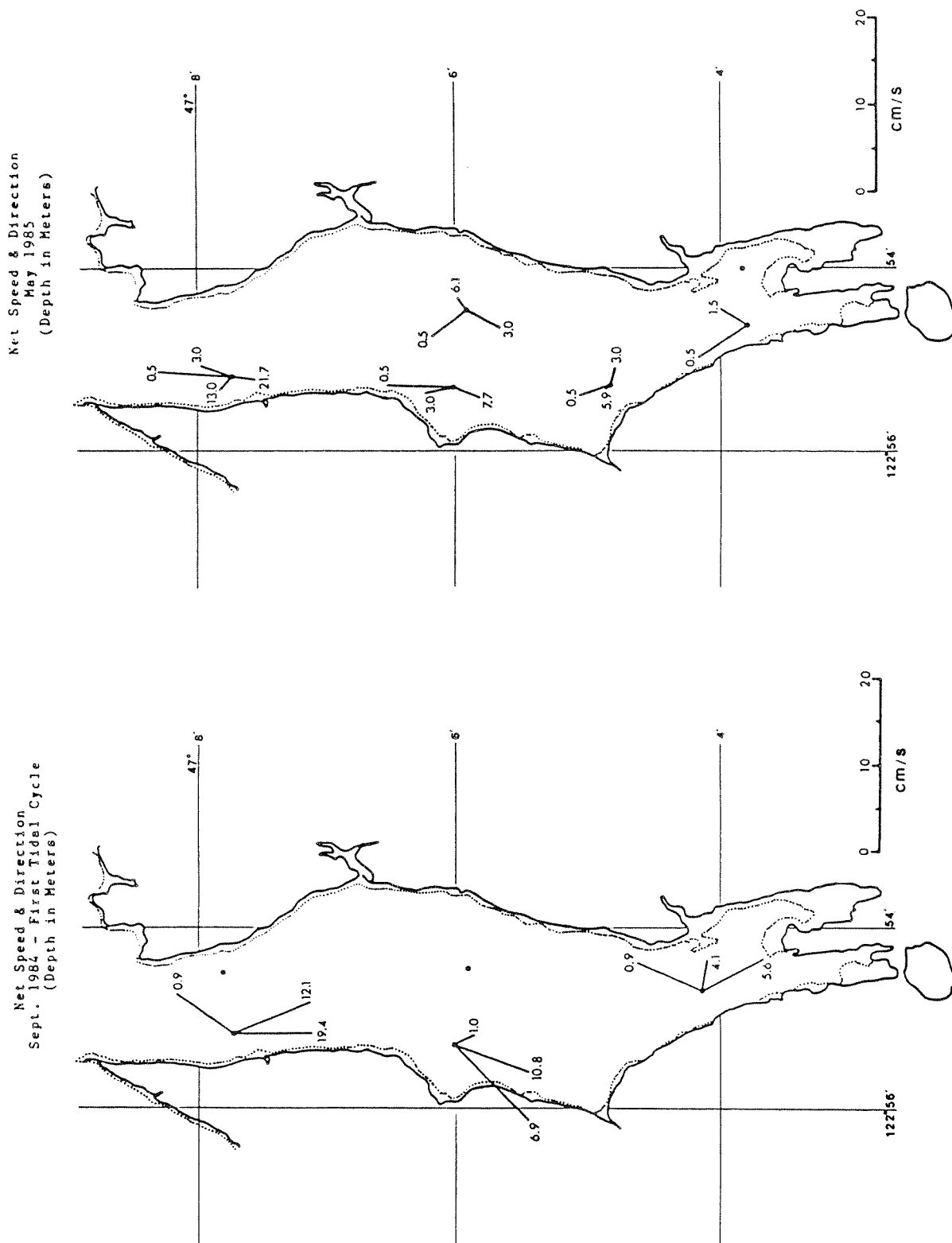
Figure 3.20 Net current velocity measured over one tidal day during the two intensive
surveys. Lines are proportional to speed and point in the direction of the
current. Number indicates depth in meters.
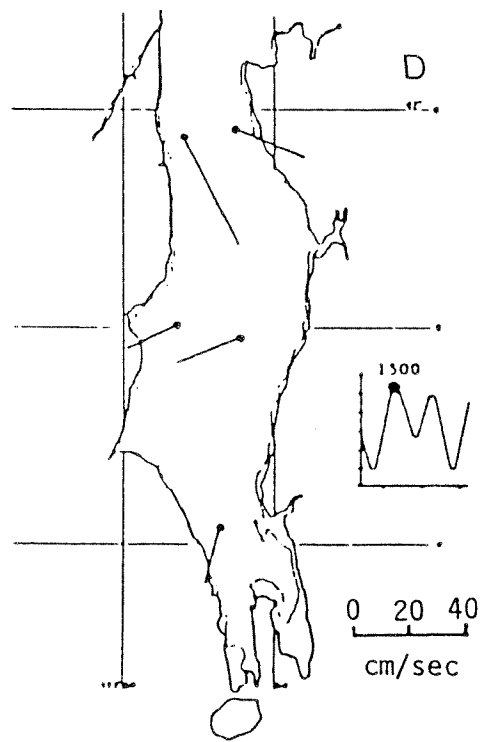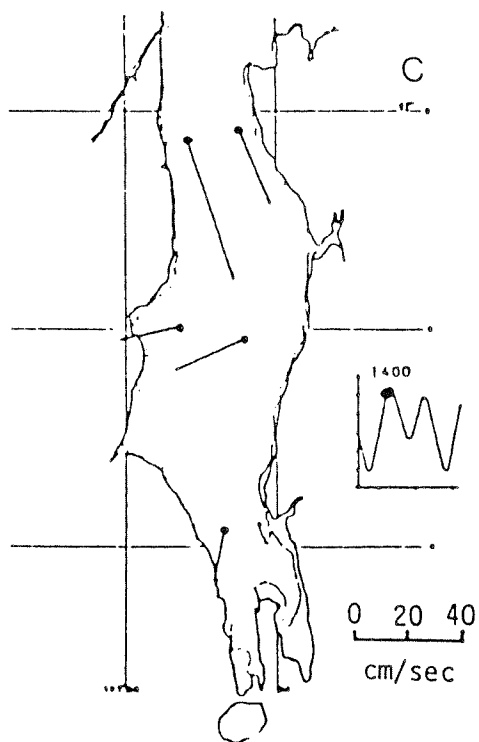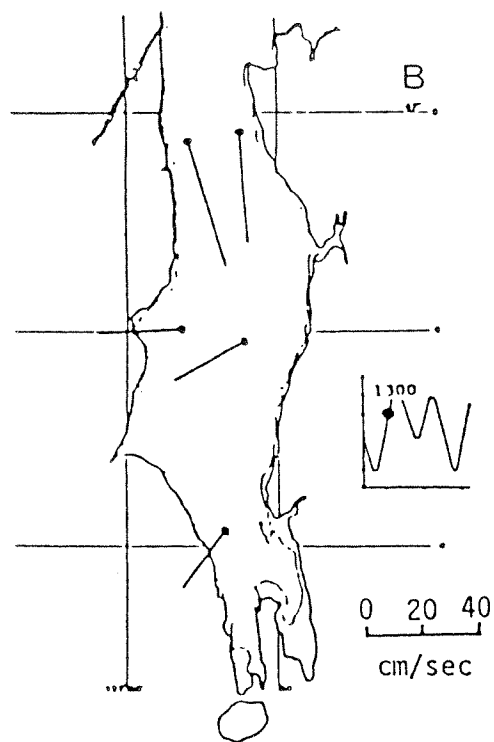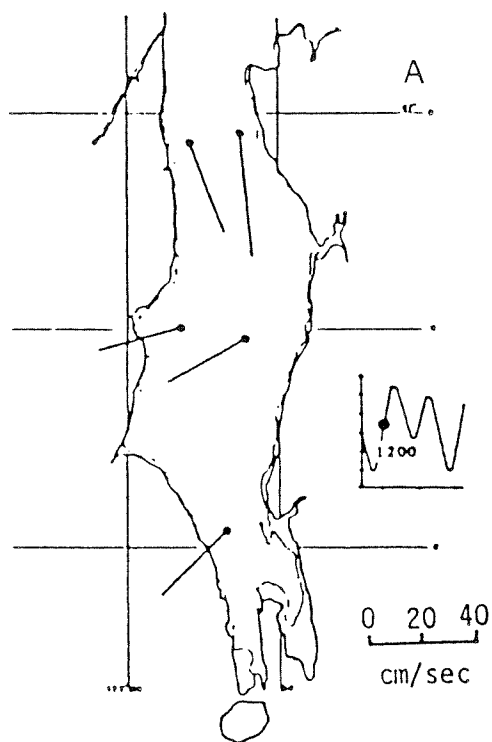
Figure 3.21   Tidal currents measured at the surface for four hours
              showing cross channel circulation during September, 1984.

Current measurements at various tidal phases of the May 1985 survey are shown in Figure 3.22. Figures 3.22(A) through 3.22(F) represent surface values (0.5 m) at six times through the tidal cycle. Figures 3.22 G and H show currents at 3.0 m depth and 5 m off the bottom for the same time period represented in F. The sequence of figures start with conditions during a strong flood tide (Figure 3.22A). Currents are directed southward into the Inlet with speeds in excess of 40 cm/s near the mouth. At high slack tide (Figure 3.22B), speeds have slowed and current directions are turning. During the minor ebb tide that follows (Figure 3.21C), current speeds are close to 30 cm/s near the mouth. During the following minor flood (Figure 3.22D), currents at the mouth remain directed northward, while currents in the interior of the Inlet are directed more easterly and westerly. During this time at 3.0 m depth and at 5 m off the bottom, currents are southerly into the Inlet indicating that the flood tides are stronger at deeper depths. At the start of and through the next major ebb (Figures 3.22E and F), currents are again directed strongly out of the Inlet.

During strong and well established tides, the current profile is quite uniform with depth, and currents are directed into or out of the Inlet approximately parallel with the bottom contours. However, during periods of small tidal range changes and short duration tides, currents can be quite different with depth and show more erratic directions. During these times, currents are often directed across channel and also show eddy-like patterns. For example, on weak ebbs a clockwise circulation was noted in the inner Inlet south of Priest Point in which water from north of East Bay flowed east and water north of West Bay flowed SSW (Figure 3.22C), while the central Inlet showed counter clockwise circulation going from strong ebb to strong flood. These currents enhance lateral mixing and increase the residence time in the Inlet. This will decrease the flushing and overall dilution potential.

Estuarine Circulation. Four types of estuarine circulation have been classified by Pritchard (1956 and 1967) on the basis of salinity gradients, river discharge, tidal exchange, and estuary width and depth. The
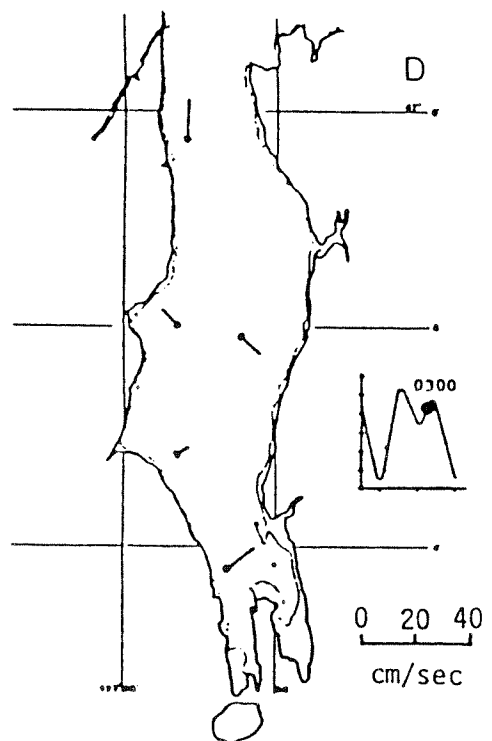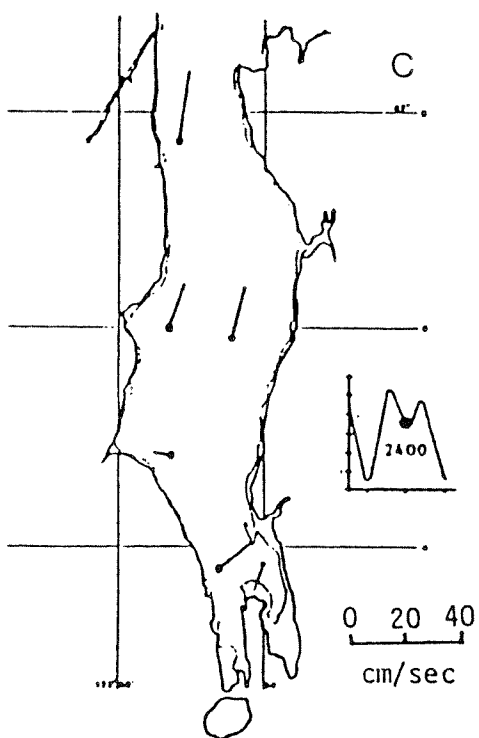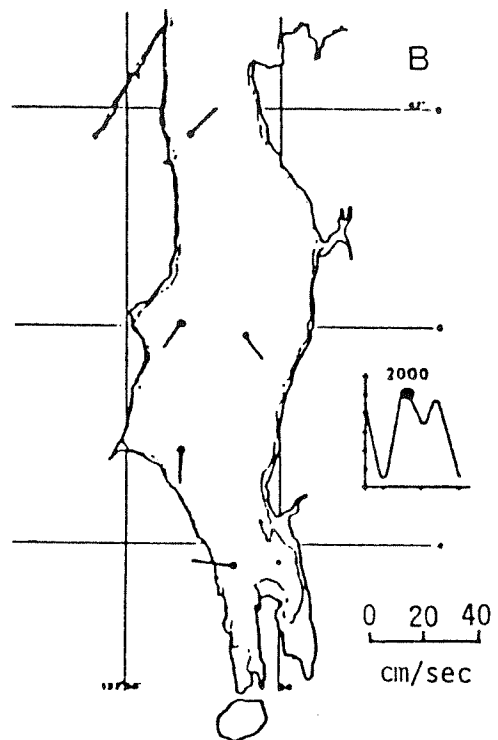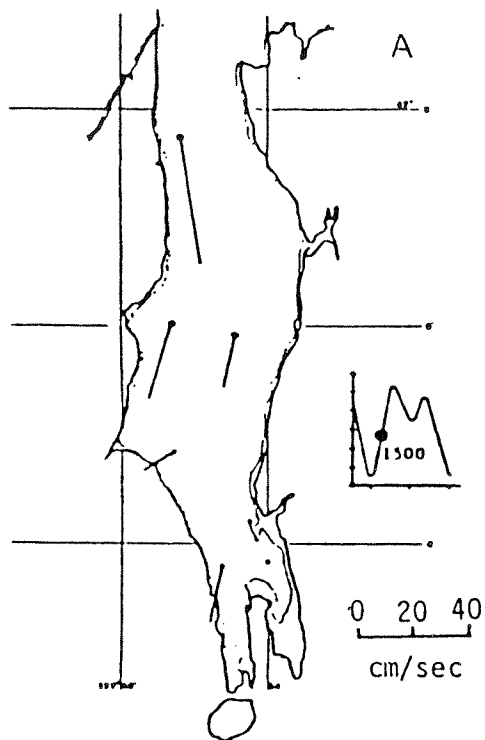
Figure 3.22   Tidal currents measured at several stages of the tidal
cycle during May 1985.
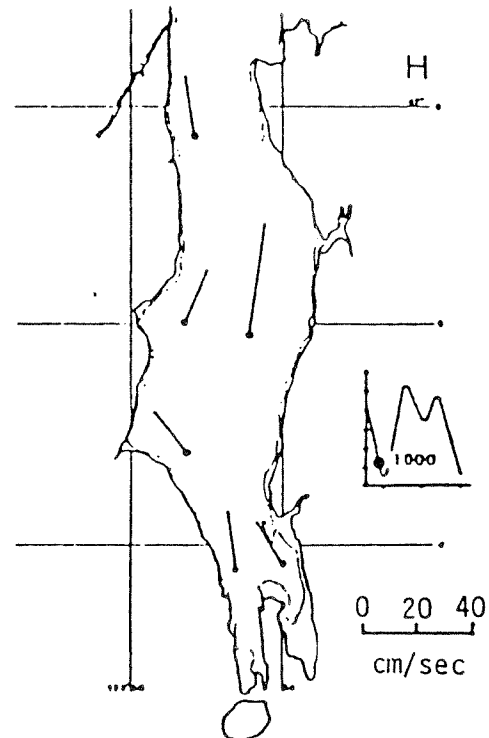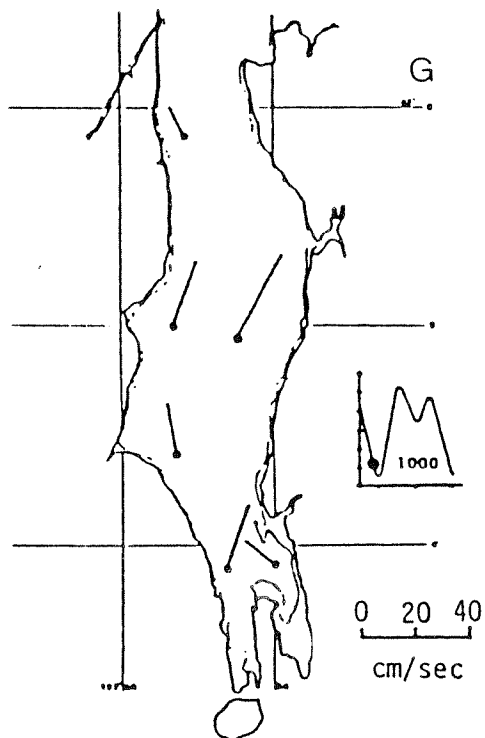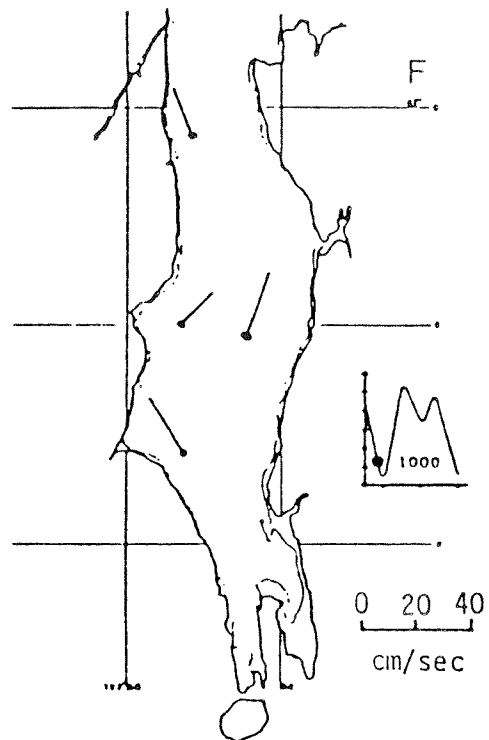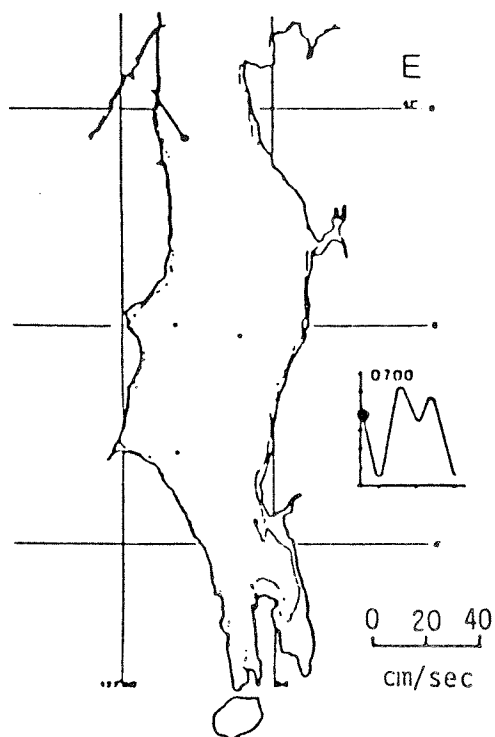
Figure 3.22 Continued

circulation of salt wedge and fjord type estuaries are similar, with saltwater being entrained into the large freshwater outflow. There is little or no mixing of fresh water into the underlying saltwater. In a homogeneous estuary, the tidal flow works against frictional forces exerted by the bottom causing turbulence. This occurs when the freshwater influence is low and the tidal influence is large. Turbulence mixes the freshwater and saltwater and produces a water column that is well-mixed.

Between these two extremes are the partially mixed estuaries where both entrainment and turbulent mixing are important. The salinity of the surface water is increased due to entrainment and mixing so that the more saline surface water flow must increase to discharge a volume of water equal to the river flow. This, in turn, causes an increase in the volume of the compensating landward flow in the deeper saltwater. Consequently, a distinct two-layer flow system is developed.

The salinity profiles in the partially mixed estuary show an increasing surface salinity down the estuary with freshwater only occurring near the head of the estuary (Pritchard, 1956). This is typically what is seen in Budd Inlet (Figures 3.18 and 3.19). Partially mixed estuaries show distinct vertical gradients which are observed in Budd Inlet (Figure 3.17). Budd Inlet is also relatively shallow and wide with an average tidal exchange to river discharge of 350:1 (Kruger, 1979). This places Budd Inlet in the partially mixed category of estuaries, according to Pritchard (1967).

Outside Budd Inlet

One of the objectives of the Southern Puget Sound Water Quality Assessment Study was to describe circulation and flushing throughout Southern Puget Sound. A separate part of the study was directed toward this goal and a report describing these findings was prepared (URS, 1986). Some of the information presented in that report is directly relevant to this investigation of Budd Inlet. The relevant information presented here includes circulation and transport in the area to the north of Budd Inlet and refluxing across Dana Passage.

<u>Available Data</u>. Describing circulation and estimating transport and refluxing depend on measurements of currents and water properties. For the waters west of Dana Passage monthly sampling of water properties was most consistently done during 1957 to 1958 (Olcay, 1959). These measurements were collected in Nansen bottles, and the water properties determined using calibrated instruments or by chemical analysis. The WDOE also collects water property data in this region; however, because winter data were not available, these data were not used.

Current meter measurements were made by several investigators using a variety of instruments. The measurements vary in length, sampling interval, and quality. Cox et al. (1984) have indexed the majority of these measurements and their sources, and also provided net speed and direction of the currents computed over a tidal day (24.84 hrs) and the length of the record.

For this project current meter measurements were collected at the east and west ends of Dana Passage and at the northern end of Pickering Passage. These measurements were made using Aanderaa RCM4 current meters. The meters were attached to subsurface moorings and were left in the water for approximately 90 days. Due to some equipment failure and severe biofouling of the meters some of the data were not useable. Net current speed and direction, mean speed, and variance were calculated over 28 day periods. These data are shown in Table 3.4. Current meter sites and general circulation patterns are shown in Figure 3.23.

Table 3.4 Net current speed and direction of current measurements made in Pickering and Dana Passages

Site No.	Meter Depth (m)	Observation Period (PST)	Mean Speed ($cm\ s^{-1}$)	Net Speed ($cm\ s^{-1}$)	Net Dir. (True)	Variance ($cm^2\ s^{-2}$)
Dana Passage						
450	9	4/17-5/14/1985	20.24	3.08	169	513
	16.5	4/17-5/14/1985	18.30	6.62	224	402
	24	4/17-5/14/1985	17.86	10.75	216	330
	31.5	4/17-5/14/1985	18.00	12.67	214	280
	39	4/17-5/14/1985	17.07	12.70	209	227
452	15	4/17-5/14/1985	25.87	17.81	246	1,090
	24	4/17-5/14/1985		No Data		
	33	4/17-5/14/1985	29.23	21.00	258	1,384
	41	4/17-5/14/1985	28.21	21.60	254	1,365
	50	4/17-5/14/1985	27.41	21.04	255	1,188
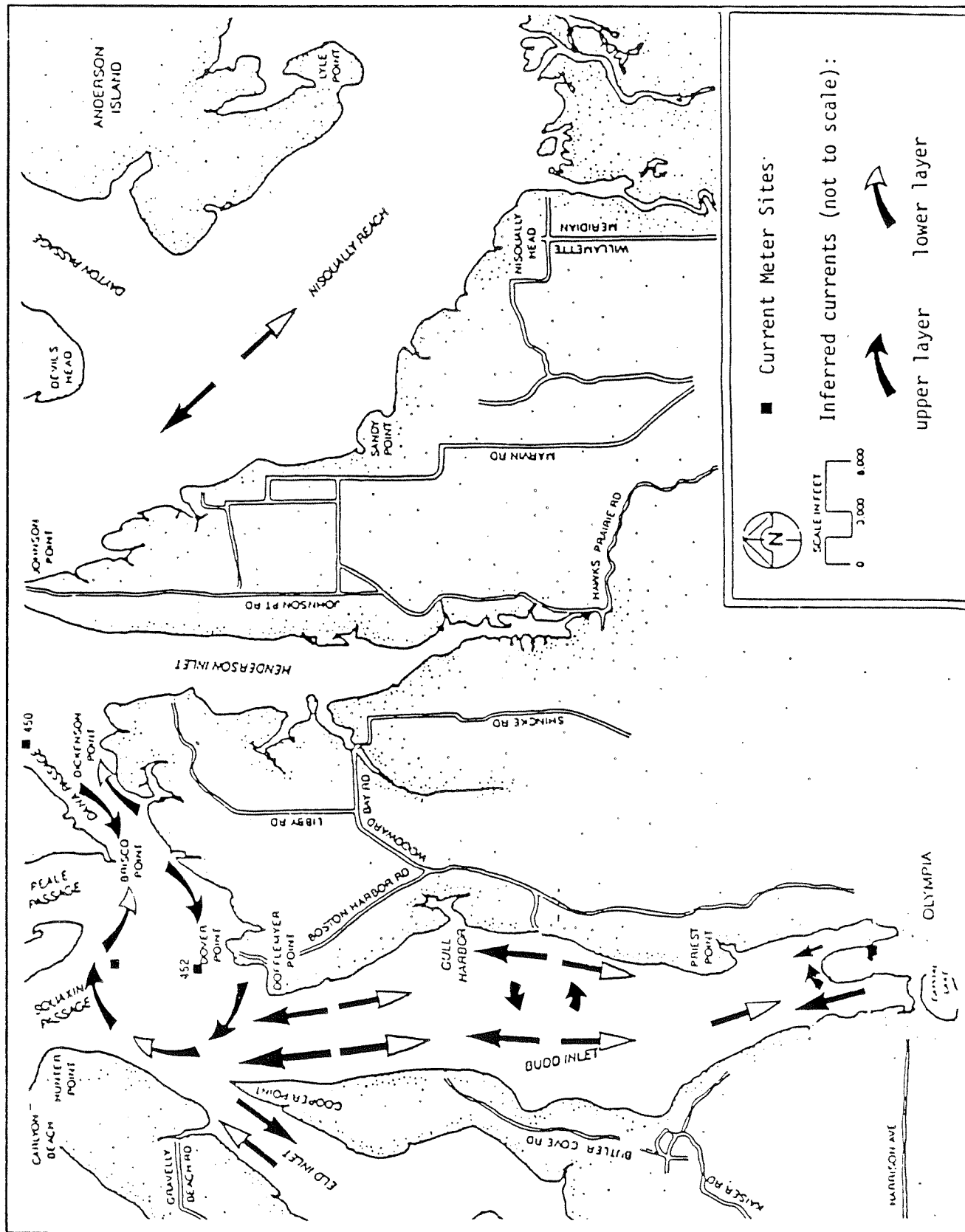
Figure 3.23 Circulation patterns for Budd inlet and approaches.

Circulation. Figure 3.23 presents circulation patterns based on available current meter records. The figure shows a two-layer flow pattern where the flow is seaward near the surface and landward near the bottom. In some areas such as Eld and Totten Inlets, very little or no data exists.

Of particular interest to this study is the clockwise circulation north of Dover and Dofflemeyer points. Directly north of Dover Point the net flow is extremely strong (approximately 20 cm/s), directed westward, and does not appear to reverse near surface. A bit farther north, a 5-day record taken in 1945 at 5 meters depth indicates that a strong flow (approximately 24 cm/s) exists directed eastward. While no data exists at depth there, it is likely that net flow is eastward top to bottom in that area to compensate for the net westward flow farther south. To determine if this feature was real, the 5 days of record at the northern site were compared to 5 days of the shallowest record at the southern site during similar types of tides. At each site the current reaches approximately 2 knots during one tidal phase; it slows during the opposite tidal phase, but does not reverse direction.

This flow pattern was confirmed by visual observation of dye released in the University of Washington's hydraulic model of Puget Sound. The model showed that water exiting Budd Inlet on an ebb tide, moved more strongly out on the west side. This water then moved out across the mouth of Eld Inlet before turning eastward toward the southern tip of Squaxin Island. Much of the water which had just left the Inlet would re-enter on a flood tide. The water would work its way back and forth and around until it reached Dana Passage.

Transport. Transport is the volume of water passing through or out of an area per unit time. Transports were calculated by URS (1986) using current meter measurements and a water and salt balance. Using current meter measurements, the net transport is calculated as the current speed times the cross-sectional area. The accuracy of the transport depends largely on how well currents measured at one site represent the entire

cross-sectional area. The accuracy of transports derived from the water and salt balance depend largely on how representative the salinity values are of each of the water bodies. Using current meter measurements, a transport of 1,200 m^3/s was calculated for Dana Passage. For Budd Inlet, the estimates were 600 m^3/s and 500 m^3/s using the water budget and current measurement methods, respectively. This reasonable comparison lends some confidence to the accuracy of the numbers. However, these estimates should still be used cautiously, considering the limited data base used and the number of assumptions involved.

Refluxing. Refluxing is the return of a portion of the seaward flowing water on the following incoming (landward) tide. The effect of refluxing is increasing the flushing time of a two layer net flow system. Refluxing occurs primarily within mixing zones, the majority of which are relatively shallow constrictions (sills) separating two deeper basins. The flow exiting any layer is divided into two parts when it enters a mixing zone. The part which mixes and returns into the opposite layer of its original source basin is the refluxed portion.

Cokelet and Stewart (1985) describe the theory and method of calculating reflux coefficients. The method which includes balancing water, salt and transport between adjoining basins, yields a refluxing coefficient of 0.62 for Dana Passage.

The majority of water from Budd, Eld, Totten and Hammersley Inlets (approximately 80 to 90 percent) exits through Dana Passage. It is difficult to determine how much of the water from each Inlet is refluxed back into the same Inlet. As a first approximation it was assumed that the refluxing for each Inlet was 0.6. This value may be high because the waters from all the Inlets mix to some degree and are returned to other Inlets. However, observations of the hydraulic model indicate that some of the water is refluxed into the Inlet before it reaches Dana Passage. A minimum value could be derived by assuming that water from Budd, Eld, Totten and Hammersley Inlets completely mix, that 0.6 of the mixture is

refluxed at Dana Passage and that the refluxed portions are redistributed to the Inlet proportional to their transports. According to previous estimates the ratio of Budd Inlet transport to Dana Passage transport is 555 m^3/s to 1215 m^3/s or 0.46. Combined with the reflux coefficient for Dana Passage, this would result in a minimum reflux of 0.3 for Budd Inlet. This would also mean that the rest of the refluxed Budd Inlet water (the other 0.3) is transported into Eld, Totten and Hammersley Inlets.

3.4 PRIMARY PRODUCTIVITY

September, 1984 Results

Samples were collected at Stations 3 and 5 (Figures 2.4 and 3.2) on September 18, 1984. Due to an unusually dense layer of red-brown phytoplankton at Station 5 (later identified at _Gymnodinium_ spp.), the samples from both Stations 3 and 5 were taken to the mooring at Station 1 for the six-hour incubation. Each sample was incubated at the same depth from which it was collected. The sample depths, chlorophyll _a_ and primary productivity data for Stations 3 and 5 are listed in Table 3.5.

Average primary production rates measured in September, 1984 are comparable to those measured in September, 1972 by Westley et al. (1973). For example, the 1972 data averaged about 300 mgC/m^3/day in the central portion of the Inlet. However, the specific production rates, which relate the primary productivity to the amount of chlorophyll _a_ present, were lower in 1972 than those measured at Station 3 in the September, 1985 survey. Peak values in 1972 were less than 50 mg/C/mg Chl _a_/day while a peak value of 112 mgC/mg Chl _a_/day was observed at Station 3. Specific production at Station 5 was lower than at Station 3 possibly due to the less than optimum growing conditions at Station 5 and dense algal populations (the 1 percent light level was 3.5 meters).

Table 3.5 Primary Productivity for September 1984

Station 3

Depth (m)	Chlorophyll a (mg/m^3)	Primary Production (mgC/m^3/day)	Specific Production (mgC/mgChla/day)
0	1.81	203.3	112.32
2	3.14	198.4	63.18
3.5	25.57	422.4	16.52
6	13.01	135.7	10.43

Total Integrated Areal
Production (mgC/m^2/day)   2019.1

Station 5

Depth (m)	Chlorophyll a (mg/m^3)	Primary Production (mgC/m^3/day)	Specific Production (mgC/mgChla/day)
0	7.75	128	16.52
0.5	44.83	1039.2	23.18
2	32.47	481.4	14.83
4.5	38.38	350.5	9.13

Total Integrated Areal
Production (mgC/m^2/day)   2472.1

May 1985 Results

Samples were collected on May 20, 1985 at Stations 3 and 5. During this survey, the samples were incubated at their respective station moorings. The results (Table 3.6) show that the primary productivity, specific production and chlorophyll <u>a</u> levels during the May survey were generally lower at Station 3 than in September, 1984. Station 5 showed lower chlorophyll <u>a</u> and primary production levels in May and about the same specific production as in September, 1984. There is no historical productivity data for May in Budd Inlet.

3.5 SOURCE SURVEY

A total of 11 point sources were sampled during the Budd Inlet Source Survey. A number of these sources flow into the Inlet at common discharge points. Five distinct discharge points to Budd Inlet are listed where algal nutrient, fecal coliform and BOD-5 loadings to Budd Inlet occur:

1. LOTT Regional Sewage Treatment Plant;

2. Moxlie Creek, consisting of:
    Moxlie Creek, Lower Reach
    Moxlie Creek, Upper Reach
    Indian Creek

3. Capitol Lake, consisting of:
    Deschutes River
    Percival Creek, Upper Reach
    Percival Creek, Lower Reach

4. Ellis Creek

5. San Francisco Storm Sewer

Table 3.6 Primary Productivity for May 1985

Station 3

Depth (m)	Chlorophyll a (mg/m^3)	Primary Production (mgC/m^3/day)	Specific Production (mgC/mgChla/day)
0	4.06	113.1	27.86
2	6.12	72.3	11.81
4	3.84	12.6	3.28
7	8.93	13.89	1.56

Total Integrated Areal
Production (mgC/m^2/day)   310.1

Station 5

Depth (m)	Chlorophyll a (mg/m^3)	Primary Production (mgC/m^3/day)	Specific Production (mgC/mgChla/day)
0	3.8	176.1	46.34
2	3.84	77.6	20.21
4	3.58	27.4	7.65
6.5	4.43	6.6	1.49

Total Integrated Areal
Production (mgC/m^2/day)   400.99

The San Francisco storm sewer was initially chosen to be representative of urban runoff in determining loadings to the Inlet. However, the lack of rainfall during the source survey resulted in very low loadings which could not be reasonably extrapolated to represent total urban runoff under more normal wet weather conditions.

Two other sources which discharge into Budd Inlet, Fiddle Head Storm Sewer and Hardel Street Storm Sewer, were not considered active point sources. Hardel Street was sampled only in April, 1985 and did not show sufficient loading to Budd Inlet to warrant its inclusion as an active point source. Fiddle Head was sampled during low tides, the only time it was not completely submerged. This proved to be regrettable, since information supplied late in the study indicated that during extremely high tides, LOTT is unable to discharge through its primary outfall due to unfavorable hydrostatic pressure caused by the high tide. During these times, the LOTT effluent is diverted through the Fiddle Head Storm Sewer Discharge into the West Bay area of Budd Inlet. This was not known until both intensive and all source survey field work was completed. Time and budget did not permit additional field investigations of this discharge.

Total and relative loadings for each water quality parameter from the five discharges during the sampling period from September, 1984 through June, 1985 are shown in Figure 3.24 and Table 3.7. Some general observations are made for the more significant findings.

o   The major contributor of BOD-5 loadings to Budd Inlet was Capitol Lake, accounting for 60 to 80 percent of the loadings over the five sampling periods.

o   The major sources of fecal coliform bacterial loading shifted throughout the study.

o   The variation in source loadings seems to be dependent upon the flow of Capitol Lake and the fecal coliform counts from Moxlie Creek.

ORIGIN OF BOD—5 LOADINGS
Budd Inlet, All Sampling Periods
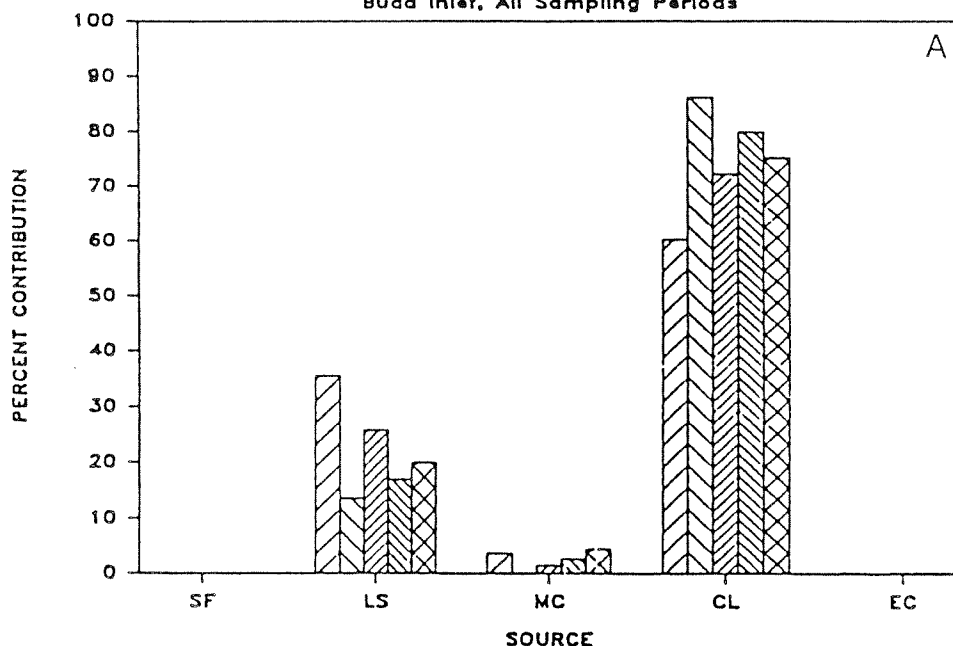
ORIGIN OF F. C. LOADINGS
Budd Inlet, All Sampling Periods
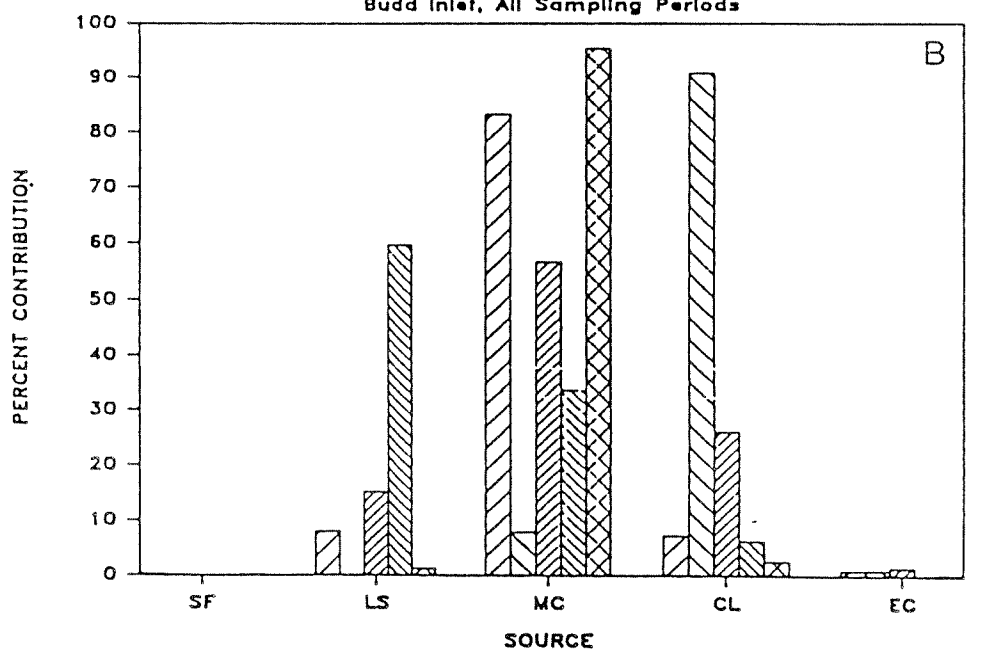
☐☐ 9/84   ☐☐ 2/85   ☐☐ 4/85   ☐☐ 5/85   ☐☐ 6/85

SF = San Fransisco   LS = LOTT STP   MC = Moxlie Creek
CL = Capitol Lake   EC = Ellis Creek

Figure 3.24 BOD-5 (A) and fecal coliform (B) loadings to Budd Inlet.

3-49

Table 3.7   Source loadings to Budd Inlet, for each measured parameter over five sampling periods.

Measured Parameter	Sept. 85	Feb. 85	Apr. 85	May 85	June 85	Mean
BOD-5 (Lbs/Day)	2871	7867	7206	8151	2652	5749
Fecal Coliform (MPN/Day)	5.15×10^{11}	5.53×10^{11}	1.03×10^{11}	9.60×10^{11}	3.38×10^{11}	4.94×10^{11}
PO4-P (Lbs/Day)	384	418	359	557	285	401
SIO4-SI (Lbs/Day)	6115	22365	15050	12209	12902	13728
NO3-N (Lbs/Day)	342	1241	1332	271	116	660
NO2-N (Lbs/Day)	78	115	86	205	92	115
NH3-N (Lbs/Day)	959	1020	825	1321	960	1017
Total N (Lbs/Day)	1223	3987	3286	3461	2303	2852
Total P (Lbs/Day)	339	467	613	551	305	455
Dissolved O2 (Lbs/Day)	NO DATA	NO DATA	17300	17787	14444	16510

o   LOTT Sewage Treatment Plant coliform counts were generally low
     during the study period, except for an instance in May, 1985
     where the MPN /100 mls was 1375.

o   LOTT STP was the dominant source of inorganic phosphorus (PO4-P)
     to Budd Inlet during all sampling periods, accounting from 92 to
     99 percent of the observed phosphorus loadings.

o   Nitrate-nitrogen (NO3-N) contributions to Budd Inlet were
     generally dominated by LOTT STP with relative contributions
     averaging about 60 percent.

o   The dominant source of nitrite-nitrogen (NO2-N) to Budd Inlet was
     the LOTT Sewage Treatment Plant, contributing between 88 to 99
     percent of the total nitrite loadings to the Inlet.

o   The dominant source of ammonium-nitrogen (NH4-N) to Budd Inlet
     was the LOTT Sewage Treatment Plant, contributing 90 to 98
     percent of all the NH3 loadings to the Inlet.

o   Total nitrogen loadings were dominated by LOTT STP during all
     sampling months except February, 1985, when no LOTT data were
     available.

o   Total P contributions to Budd Inlet were dominated by LOTT STP
     during all sampling periods, with a relative contribution of
     between 90 and 95 percent.

o   The major source of dissolved oxygen contributions to Budd Inlet
     were from Capitol Lake, contributing between 89 and 93 percent of
     the source loadings.

ORIGIN OF PO4--P LOADINGS

Budd Inlet, All Sampling Periods

ORIGIN OF SIO4 LOADINGS

Budd Inlet, All Sampling Periods

9/84   2/85   4/85   5/85   6/85
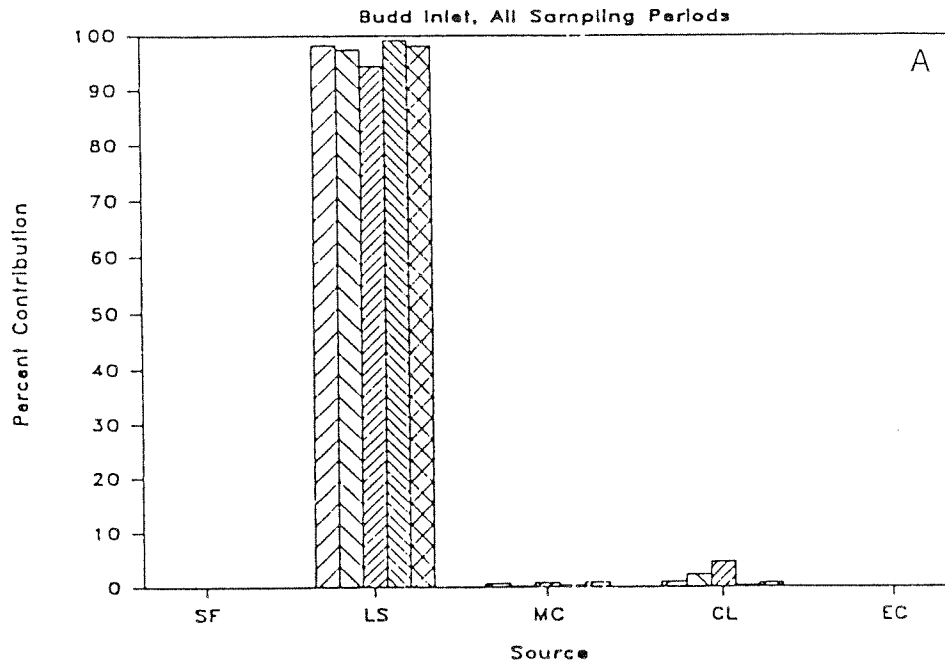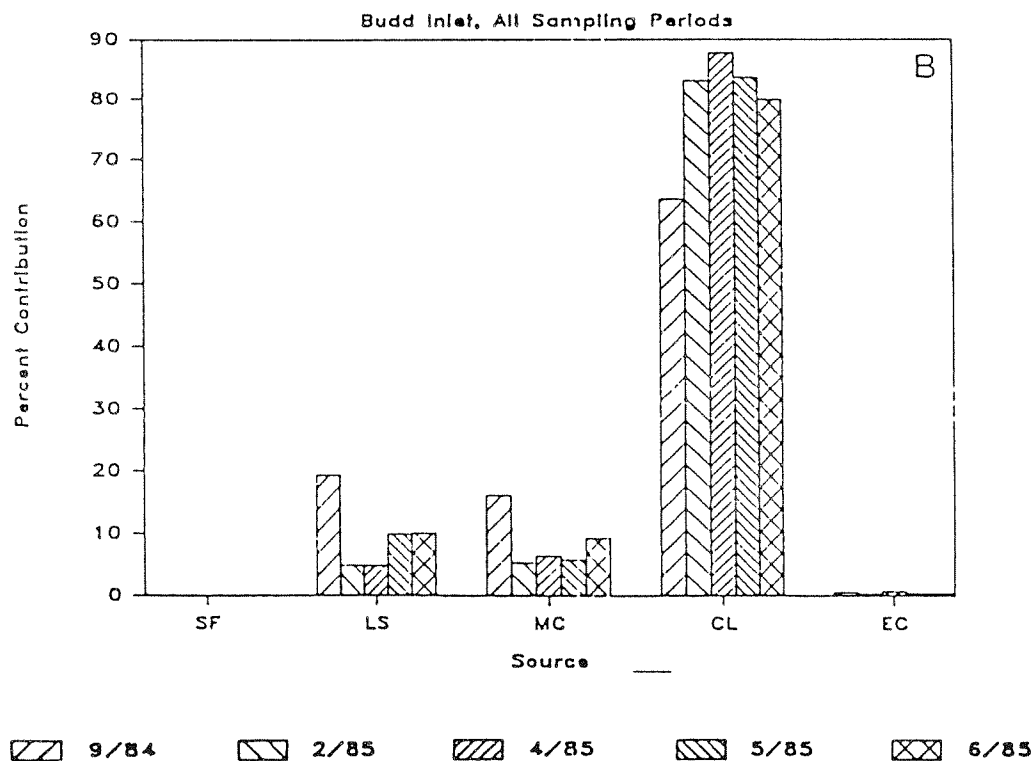
SF = San Francisco   LS = LOTT STP   MC = Moxlie Creek
CL = Capitol Lake   EC = Ellis Creek

Figure 3.25   Phosphate (A) and silicate (B) loadings to Budd Inlet.

ORIGIN OF NO3-N LOADINGS

Budd Inlet, All Sampling Periods

ORIGIN OF NO2-N LOADINGS

Budd Inlet, All Sampling Periods

9/84   2/85   4/85   5/85   6/85

SF = San Fransisco   LS = LOTT STP   MC = Moxlie Creek
CL = Capitol Lake   EC = Ellis Creek
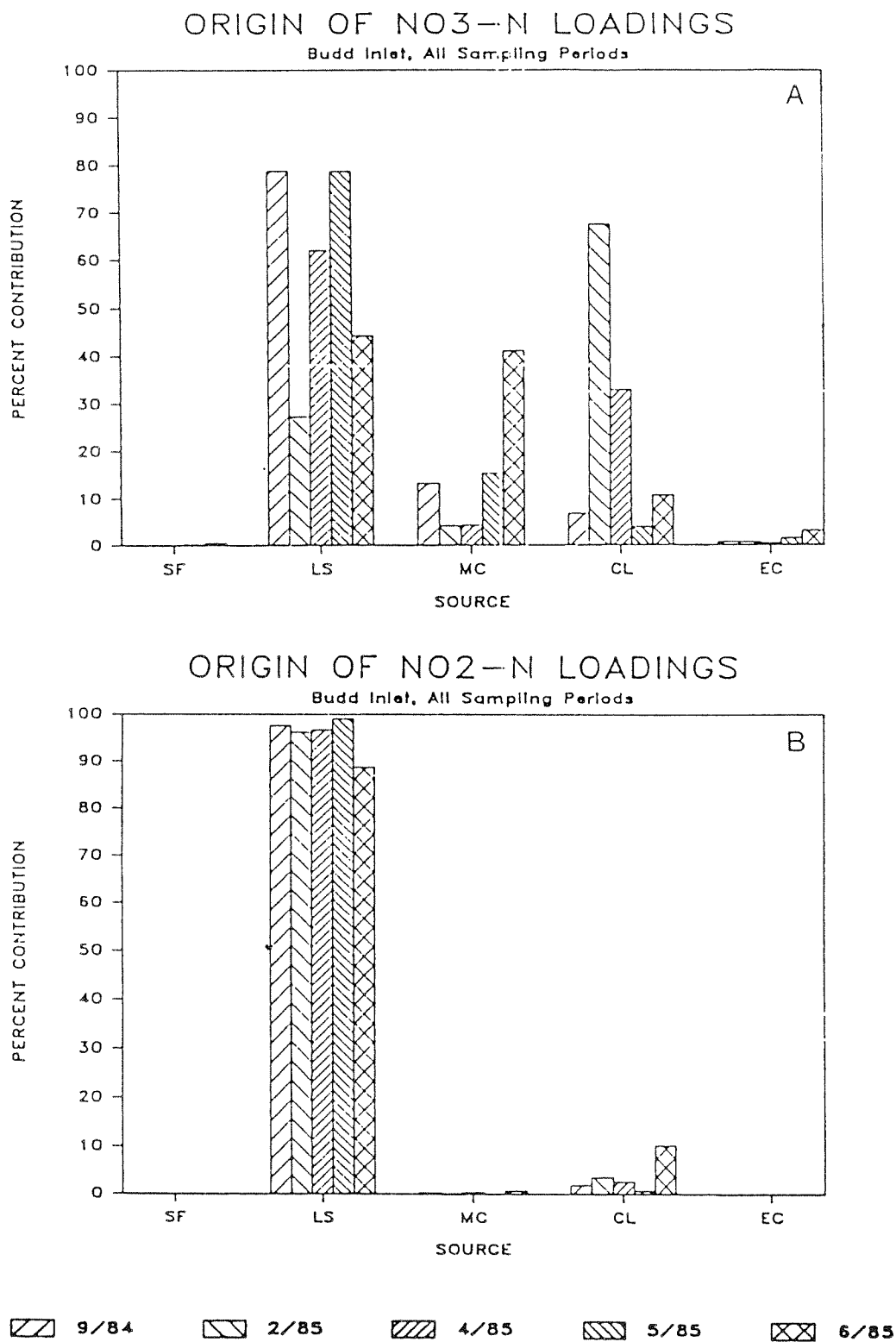
Figure 3.26 Nitrate (A) and nitrite (B) loadings to Budd Inlet.

ORIGIN OF NH3—N LOADINGS
Budd Inlet, All Sampling Periods

A

ORIGIN OF TOTAL N LOADINGS
Budd Inlet, All Sampling Periods

B

9/84   2/85   4/85   5/85   6/85

SF = San Fransisco   LS = LOTT STP   MC = Moxlie Creek
CL = Capitol Lake   EC = Ellis Creek
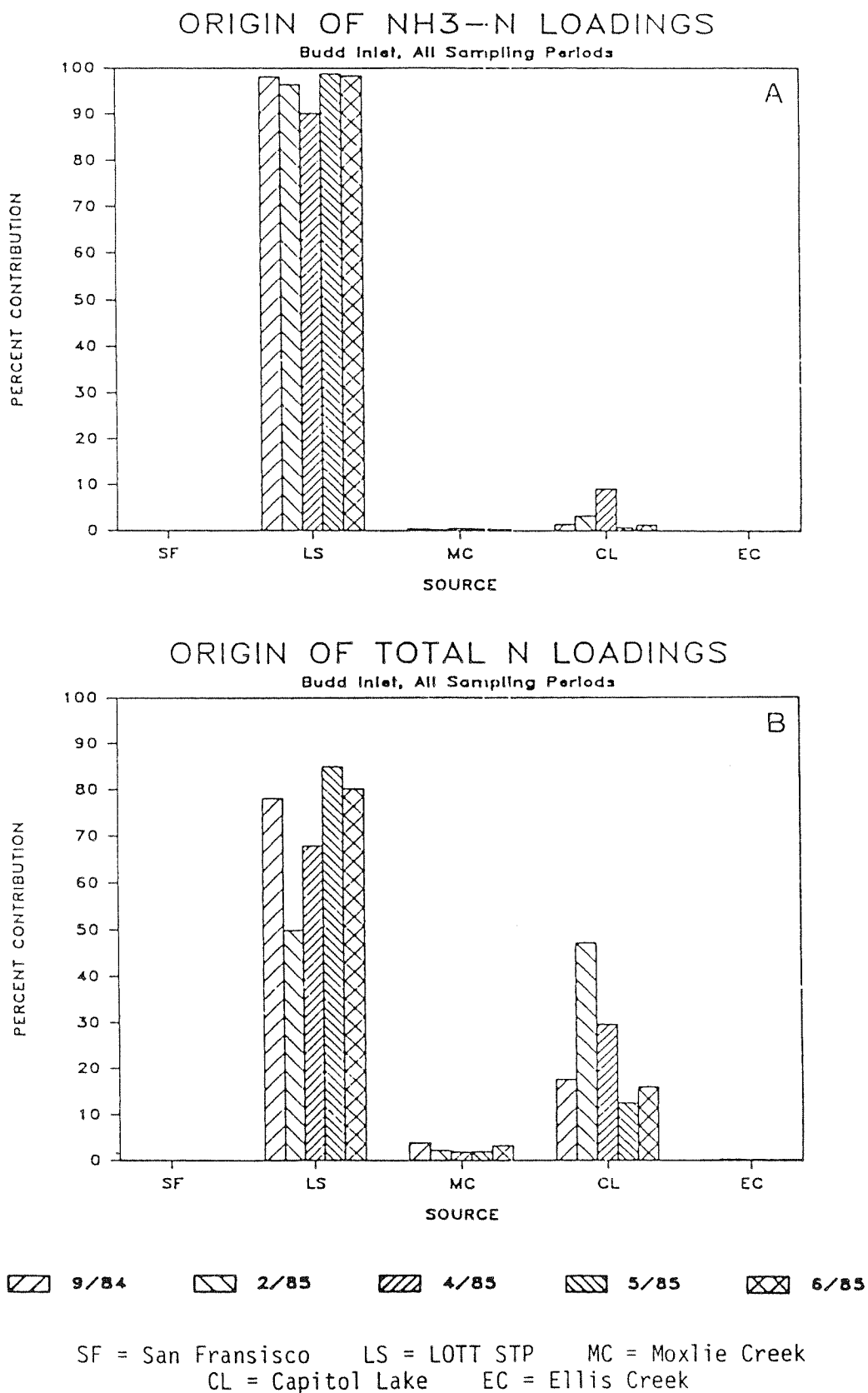
Figure 3.27 Ammonium (A) and total nitrogen (B) loadings to Budd Inlet.

ORIGIN OF TOTAL P LOADINGS
Budd Inlet, All Sampling Periods

ORIGIN OF D.O. LOADINGS
Budd Inlet, All Sampling Periods

9/84   2/85   4/85   5/85   6/85

SF = San Fransisco   LS = LOTT STP   MC = Moxlie Creek
CL = Capitol Lake   EC = Ellis Creek

Figure 3.28   Total phosphorus (A) and dissolved oxygen (B) loadings
to Budd Inlet.

Discussion

    LOTT Regional Sewage Treatment Plant. The LOTT Regional Treatment
Plant is the major point source of phosphate (PO4-P), nitrate (NO3-N),
nitrite (NO2-N), ammonia (NH3-N), Total Nitrogen and Total Phosphorus to
Budd Inlet. (Figures 3.24-3.28, Table 3.8). Rates of discharge ranged
from a low of 9.0 cfs in June, 1985 to a high of 17.5 cfs in May 1985
(Appendix 6). LOTT is also a minor contributor of BOD-5, fecal coliform
and silicate loadings compared with other point sources.

    LOTT normally discharges through an outfall and diffuser system
located just off the peninsula separating East and West Bays in southern
Budd Inlet (Figure 2.5). During periods of high effluent flows and/or high
tide events, a portion of LOTT's effluent must be diverted through the
Fiddle Head storm sewer, located on the eastern shore of West Bay near the
Fiddle Head Marina. Whenever the tide exceeds a critical height, the
pressure head prohibits effluent discharge through the normal diffuser,
resulting in discharge through the lower Fiddle Head system. During a
November 1985 meeting involving LOTT officials, WDOE and URS, it was
speculated that a +12.0 foot tide was probably the critical height. Many
factors influence the amount and duration of the effluent diversion,
including demands on LOTT (inflow) and tidal height.

    Calculating the actual volume of effluent diverted and discharged
through the Fiddle Head storm sewer at any given tidal height is not
possible at this time. However, general discharge trends were examined by
obtaining LOTT's flow data for days corresponding to the two field
intensive surveys. By overlaying the tidal cycles upon the flows, it is
possible to pick out "unfavorable" tidal events (designated here as +12
feet) and estimate the volume of effluent that was discharged at that time
(Figures 3.29 and 3.30). During the five day September period, the
critical +12 foot limit was exceeded six times, with four
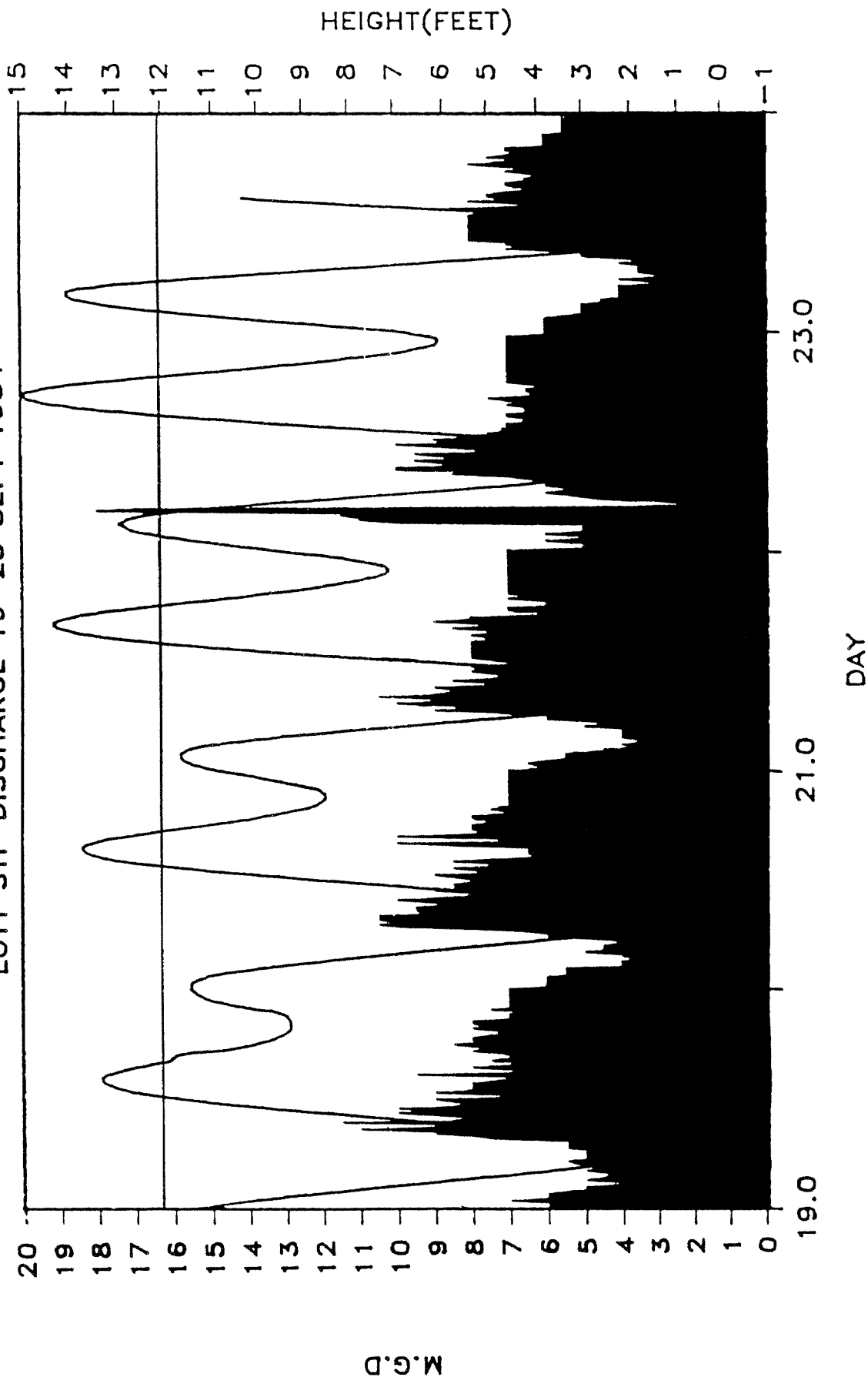
Figure 3.29 LOTT Treatment Plant discharge rates (shaded area) versus tide for the week of September 19, 1984.
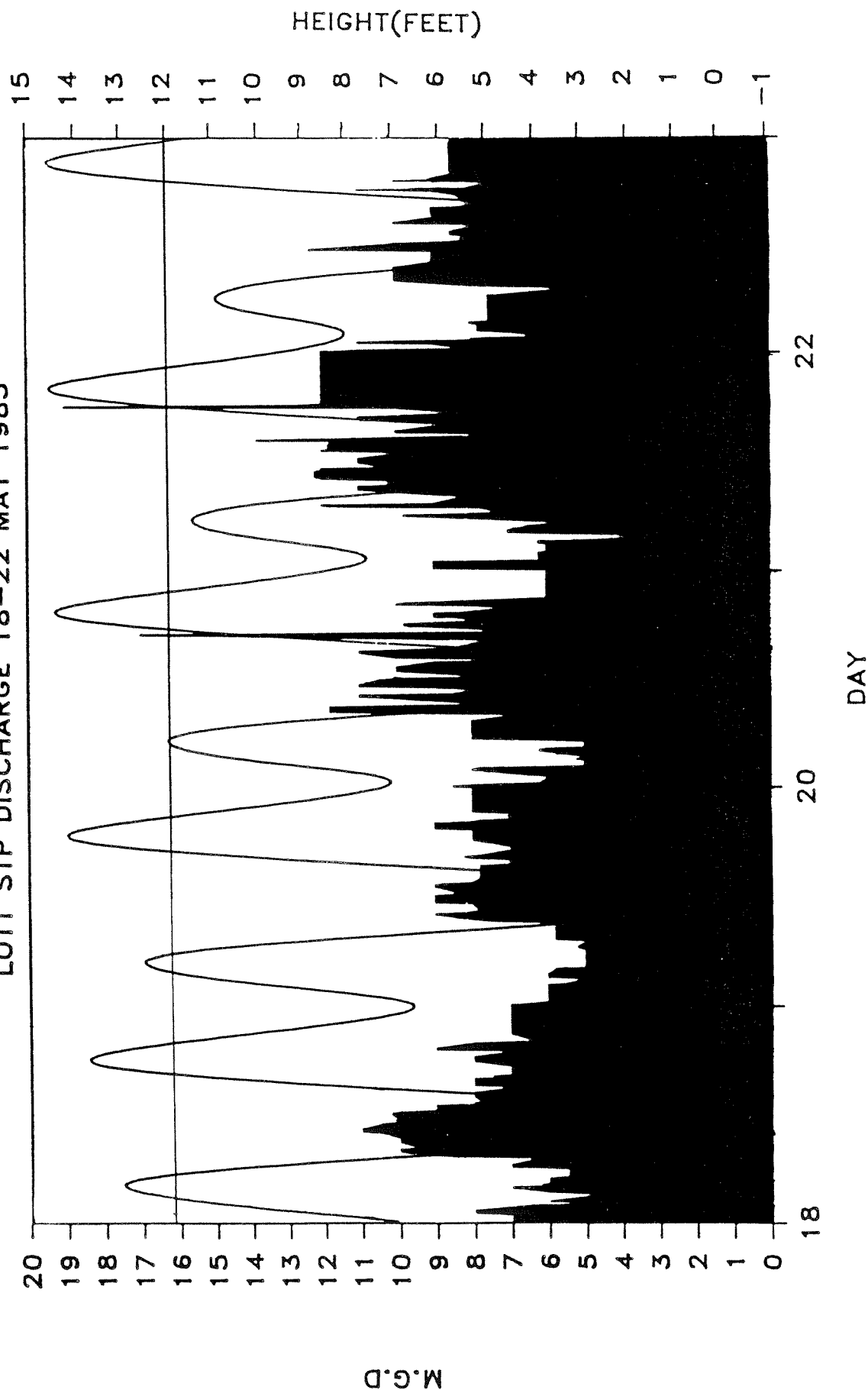
Figure 3.30   LOTT Treatment Plant discharge (shaded area) versus tide for the week
of May 18, 1985.

events corresponding to 7-8 mgd discharges and two events corresponding to 4-6 mgd. The May five day period showed the critical tidal limit exceeded seven times with discharge rates of 9-12 mgd twice, 7-8 mgd three times and 4-6 mgd twice. The worst case scenario would include a high system demand and high tide, since all of these conditions would favor a discharge through Fiddle Head.

Moxlie Creek. The Moxlie Creek point source is composed of sampling stations Moxlie Creek Lower, Moxlie Creek Upper and Indian Creek sampling stations (Figure 2.5). This point source was the dominant contributor of fecal coliform bacteria loading to Budd Inlet during the months of September 1984 and June 1985. Moxlie also contributed approximately 40 percent of the nitrate-nitrogen (NO_3-N) loadings to Budd Inlet during the June 1985 sampling.

Moxlie Creek seems to gain fecal coliform bacteria between its upper reaches (Moxlie Creek, Upper and Indian Creek) and lower discharge into Budd Inlet (Moxlie Creek, Lower). Some of the gain in fecal coliform bacteria to Moxlie Creek may be due to contributions from Indian Creek (Table 3.8). The only sampling information available for Indian Creek was April, 1985. The coliform counts were 1,200 MPN/100 mls for Indian Creek at that time. During the periods when Indian Creek data were not available, a net increase in fecal coliform was observed from upper to lower Moxlie Creek. Other sources of coliform bacteria loading to Moxlie Creek might include broken sewer lines beneath Olympia's streets or malfunctioning storm sewers. Documents supplied by the Thurston County Health District indicate a similar problem with fecal coliform loadings to Moxlie Creek existed in 1975. It is possible the problem was either never completely corrected or has occurred again. Additional data and information concerning fecal coliform loadings to Budd Inlet and Moxlie Creek in particular is provided in Section 3.6, Bacteriological Survey of Budd Inlet.

Table 3.8   Source or sink nature of Moxlie Creek
and its tributaries

	Inputs		Outputs
	Moxlie		Moxlie
	Creek	Indian	Creek
Date	Upper	Creek	Lower
Sampled	(MPN/Day)	(MPN/Day)	(MPN/Day)
9-84	4.69×10^{10}	No Data	2.58×10^{11}
2-85	2.03×10^{10}	No Data	4.45×10^{10}
4-85	2.42×10^{10}	7.04×10^{10}	5.87×10^{10}
5-85	3.43×10^{10}	No Data	3.24×10^{11}
6-85	1.02×10^{11}	No Data	3.23×10^{11}

Capitol Lake. Capitol Lake was responsible for the majority of the BOD-5, Silicate (SIO_4) and dissolved oxygen loadings to Budd Inlet and contributed significantly to the fecal coliform loadings during the February 1985 sampling period. The lake was also a major contributor of nitrate-nitrogen (NO_3-N) to Budd Inlet, especially during the February 1985 and April 1985 surveys (Figures 3.24-3.28, Table 3.8). Capitol Lake modifies the water flowing through it since the water leaving Capitol Lake via the dam at the end of West Bay is significantly different in its water quality than the source water (Deschutes River and Percival Creek), as shown in Table 3.9. This table shows that Capitol Lake acts as a source of BOD-5 and dissolved oxygen most of the year and acts as either a source or sink for algal nutrients depending upon the month or season sampled. The source period corresponds to the winter and early spring months when phytoplankton populations and nutrient uptake are relatively small. At that time, a large percentage of the nutrients entering Capitol Lake from the Deschutes River and Percival Creek are passing through Capitol Lake and entering Budd Inlet. The periods which Capitol Lake acts as a sink occur during the late spring, summer, early fall times when phytoplankton are actively taking up the nutrients from Capitol Lake. Were it not for the natural phytoplankton population growth and nutrient uptake in Capitol Lake during the spring and summer months, a greater amount of algal nutrients would reach Budd Inlet.

Table 3.9   Source or sink nature of Capitol Lake, Washington for each measured parameter over five sampling periods.

	Deschutes River		Percival Creek

Internal Sink (-)

Capitol Lake

Internal Source (+)

Budd Inlet
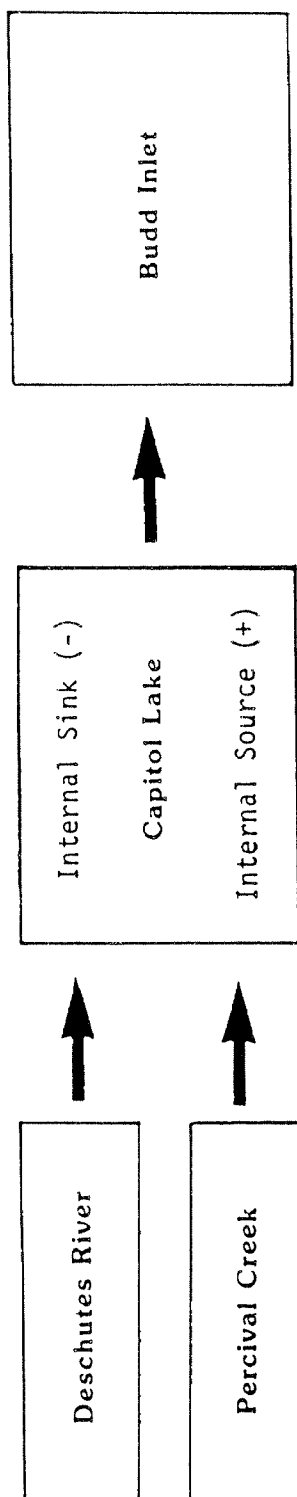
PARAMETER	SEPT 1984		FEB 1985		APRIL 1985		MAY 1985		JUNE 1985	
BOD-5	224.82	source	0.00	data = 0	214.50	source	113.65	slight source	417.12	source
F.Coliform (MPN/Day)	3.84	sink	79.54	sink	20.21	sink	65.22	sink	23.84	sink
PO4-P	37.09	sink	151.74	source	87.57	sink	12.78	sink	13.86	sink
SIO4-SI	83.37	sink	101.95	slight source	104.68	slight source	80.42	sink	97.61	slight sink
NO3-N	11.18	sink	104.37	slight source	92.54	slight sink	2.27	sink	4.27	sink
NO2-N	87.43	sink	129.97	source	146.00	source	79.05	sink	537.29	source
NH3-N	96.71	slight sink	301.78	source	523.03	source	50.03	sink	94.85	slight sink
Total N	97.71	slight sink	107.95	slight source	104.67	slight source	60.62	sink	67.75	sink
Total P	145.97	source	140.75	source	75.53	sink	85.94	sink	84.32	sink
Dissolved O2					97.62	slight sink	127.04	source	134.43	source

Net Gain or Loss
<100 % = Sink
>100 % = Source
(Outputs / Inputs * 100)

During the period of the survey, the flow regime of Deschutes River was at a level close to an average condition (Figure 3.21) and falls somewhere in between the flow regimes of other historical sampling periods, such as Westley et al. (1973) and Kruger (1979).

Ellis Creek. Ellis Creek was not a significant source of algal nutrients, BOD-5, fecal coliform or dissolved oxygen during the study (Figure 3.24, Table 3.8). This is probably due to the lack of runoff during the source surveys and the dominance of the other sources with respect to loading volumes.

San Francisco Storm Sewer. The San Francisco Storm Sewer point source did not contribute significantly to the relative loadings of algal nutrients, fecal coliform bacteria, BOD-5 or dissolved oxygen to Budd Inlet. The explanation for this is probably due again to a lack of rainfall during the survey periods and the large loading volumes from the other sources.

3.6 BACTERIOLOGICAL SURVEYS OF BUDD INLET

Purpose of Study

The purpose of the Budd Inlet Bacteriological Surveys was to quantify and describe the fecal coliform loadings to Budd Inlet, and determine the origin, significance and extent of the loadings. The first of the surveys was conducted in April, 1985. The location of each station is shown in Figure 2.6. The second survey occurred in September, 1985. Fecal coliform samples were analyzed by the Thurston County Health District. The information gained from the two surveys provided an understanding of the sources of bacterial loadings to Budd Inlet.

Analysis

Based upon field descriptions, each station was designated either a point source, non-point source or combination source. A combination

DESCHUTES FLOW

Monthly Averages, C.F.S.
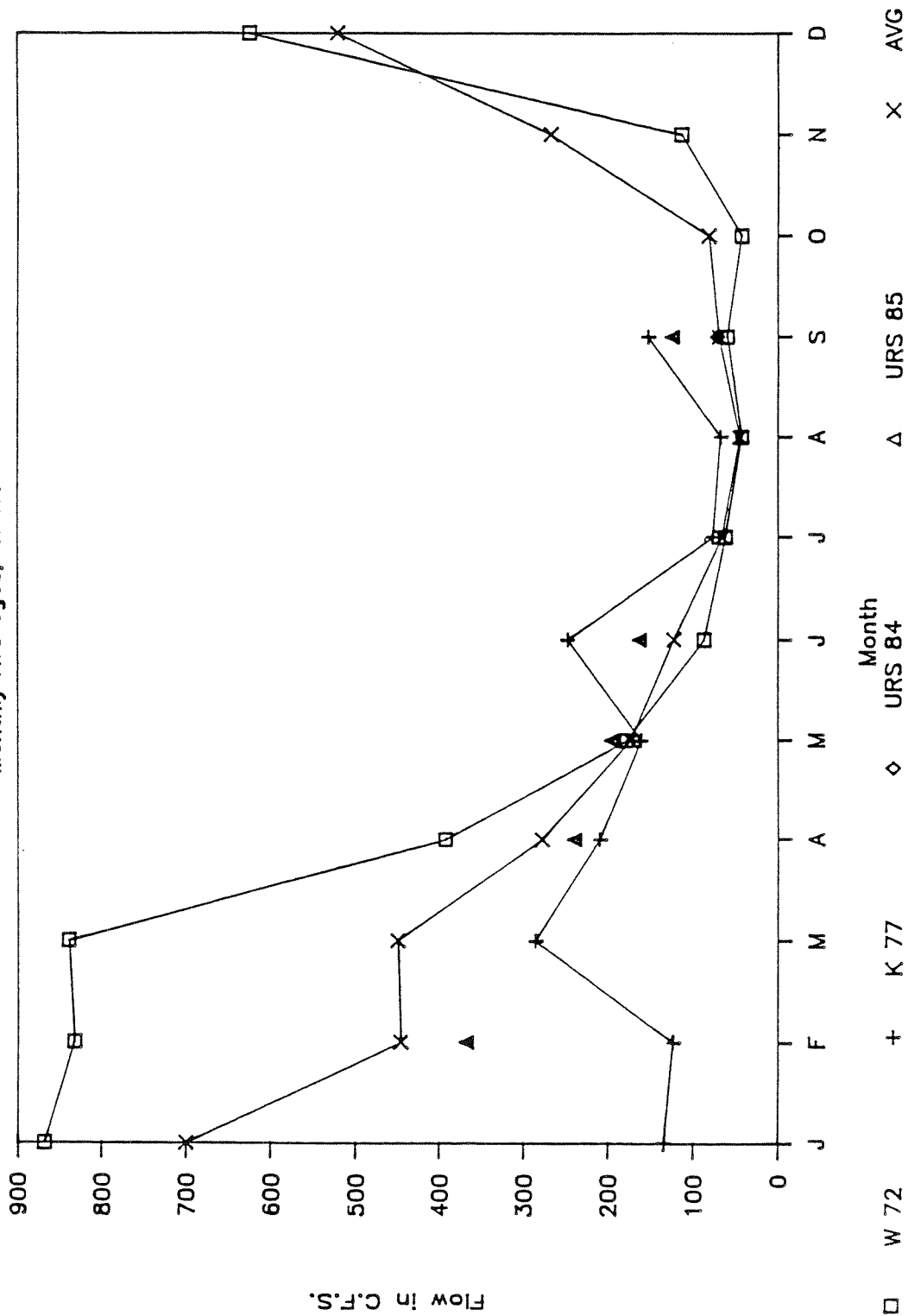
Figure 3.31 Comparison of the Deshutes River flow during three studies.
W 72 = Westley survey, K 77 = Kruger survey, URS = URS surveys
and AVG = average river flow for the years 1970 to 1975.

source is defined here as a non-point source such as a river or stream which is confined to a pipe or culvert. Point sources were further broken down into subcategories based upon the nature of the source. The type of point, non-point and combination sources are shown below:

Point Sources

P1   Sewage Outfall
P2   Chlorinator Discharge
P3   Pipe or Culvert, 4" to 12" in diameter
P4   Pipe or Culvert, larger than 12" in diameter
P5   Storm Sewer Discharge
P6   Industrial Drain Discharge
P7   Dam Spillway (Capitol Lake)

Non-Point Sources

NP1   Creek or Stream Discharge

Combination Sources

P4/NP1   Creek or Stream flowing through a large
         diameter pipe or culvert (e.g., Moxlie Creek)

This classification system enabled a database to be constructed and arranged and interpreted by point, non-point and combination categories (Tables 3.10 and 3.11).

Relative Contributions and Significance of Bacterial Loadings to Budd Inlet From Sources

Point, Non-Point and Combination Sources.   During the April 1985 bacteriological survey, fecal coliform bacteria loading to Budd Inlet was

primarily from combination sources. More than 99 percent of the total coliform bacterial loadings were from combination sources as well. Ninety-four percent of that was due to one source. The discharge of Moxlie Creek into the extreme southeastern end of Budd Inlet at East Bay. A river or creek is generally thought of as a non-point source, but Moxlie flows under the streets of Olympia through an 84 inch pipeline, hence the P4/NP1 designation. The path of the creek through Olympia and the sampling stations along it are shown in Figure 3.33. The upper station was sampled only during source survey field sampling, discussed in Section 3.5. Figure 3.34 presents the fecal coliform MPN/day loadings and percent contribution of fecal coliform bacteria to Budd Inlet at each sampling station during the April 1985 survey. The majority of fecal coliform loading is occurring in the area from Ellis Creek south to the head of the Inlet, with Moxlie Creek, Capitol Lake and LOTT accounting for almost all of the fecal coliform loading. This pattern was repeated during the September survey.

The main difference between the two surveys with respect to point and non-point loadings was that the NP1 non-point sources contributed a greater percentage during the September survey (6.37 percent) than the 0.60 percent contribution recorded in April (Table 3.12). This was due to an increase in coliform loading from Ellis Creek (Station 1H), Station AB7 (a stream on the northwest side of Budd Inlet) and Station AB-16 (a stream near Butler Cove). This increase was probably due to the rain event preceding the September bacteriological survey. A number of sources that were active during the April survey were either completely dry during the September survey or not flowing with enough volume to measure.

Urban Drains. The contributions of fecal coliform loadings from urban drains (subgroup P5) is difficult to assess due to the abnormally dry conditions that occurred during both bacteriological surveys. The rainfall event that preceded the September survey increased the relative contribution of this source up from 0.39 percent in April to 1.31 percent in September (Table 3.12, Figure 3.32). In contrast to this observed

Table 3.10 Fecal coliform bacteria inputs to Budd Inlet: April 1985 Survey.

BUDD INLET BACTERIAL SURVEY, APRIL 9-17, 1985
FECAL COLIFORM INPUTS TO BUDD INLET
SORTED BY POINT OR NONPOINT SUBCATAGORY

Date	Time	Source	Flow (c.f.s.)	Fecal Coliform 100 mls	Loading: F. Colifora Day	% Of Total Loading	Point or Non-point Code	Description of Source Area	Collector
4-9-85	1300	1 H	2.000	75	3.67E+09	0.395	NP1	south of Ellis Creek	A. Meyers
4-9-85	1345	8 4	0.000	8	0.00E+00	0.000	NP1	stream flowing over bluff,100'S. 43	M. Taylor
4-9-85	1355	8 5	0.007	0	0.00E+00	0.000	NP1	stream cascading over bluff	S. Cassatt
4-9-85	1405	8 6	0.050	0	0.00E+00	0.000	NP1	stream w/log bulkhead near br house	M. Taylor
4-9-85	1440	AB 7	0.100	0	0.00E+00	0.000	NP1	small stream, 20° wide	A. Bailey
4-9-85	1650	8 H	0.001	5	1.22E+05	.000	NP1	seepage beneath 9"x20" plank,dstream log yard	A. Meyers
4-9-85	1740	AB 16	2.100	5	2.57E+08	0.028	NP1	stream thru gully at Butler Cove	A. Bailey
4-9-85	1755	AB 14	0.100	370	9.95E+09	0.097	NP1	creek N. of Butler Cove	A. Bailey
4-17-85	1100	*GH-1 (1)(2)	0.170	27.5	1.14E+08	0.012	NP1	Gull Harbor Creek #1 (S. creek)	M. Taylor
4-17-85	1103	*GH-2 (1)(2)	0.186	26.5	1.21E+08	0.013	NP1	Gull Harbor Creek #2 (middle creek)	M. Taylor
4-17-85	1120	*GH-3 (1)(2)	0.495	26.5	3.21E+08	0.035	NP1	Gull Harbor Creek #3 (N. creek)	M. Taylor
4-17-85	1150	9	0.000	1150	0.00E+00	0.000	NP1	small creek 100' N. #8, near logs	M. Taylor
4-17-85	1210	10	0.500	0	0.00E+00	0.000	NP1	bubbling creek 600' N. of #9	M. Taylor
4-17-85	1216	11	0.200	3	1.47E+07	0.002	NP1	small stream near large green house	M. Taylor
4-17-85	1320	16	0.100	85	2.09E+08	0.022	NP1	small stream 100 yds N. DNR	M. Taylor
4-9,4-16	AVERAGE	**LOTT STP	13.905	33	1.12E+10	1.208	P1	secondary sewage treatment plant (~10agd)	P. Zeha
4-9-85	1030	TAMOSHAN	0.028	110	7.53E+07	0.008	P1	secondary sewage treatment plant	V. Berube
4-9-85	1910	Beverly Bch	0.905	2400	2.94E+08	0.032	P1	holding tank at Beverly Beach	A. Bailey
4-9-85	1905	SEASHORE	0.019	23	1.07E+07	0.001	P1	secondary sewage treatment plant (9500gad)	A. Meyers
4-15-85	1530	17	0.000	2400	0.00E+00	0.000	P2	Bryant Chlorinator discharge pipe	M. Taylor
4-9-85	1500	AB 8	0.017	0	0.00E+00	0.000	P3	12" drain in concrete wall	A. Bailey
4-9-85	1430	AB 6	0.004	149	1.45E+07	0.002	P3	12" metal pipe under stairway, house above	A. Bailey
4-9-85	1405	AB 4	0.007	5	8.56E+05	.000	P3	12" concrete pipe at foot of small ravine	A. Bailey
4-9-85	1330	8 2	0.003	0	0.00E+00	0.000	P3	6" black corr. pipe ext. up bluff	M. Taylor
4-9-85	1525	AB 10	0.007	0	0.00E+00	0.000	P3	6" drain in concrete wall	A. Bailey
4-9-85	1420	AB 5	0.006	140	2.05E+07	0.002	P3	3" black pipe	A. Bailey
4-9-85	1312	AB 1	0.099	1020	0.00E+00	0.000	P3	3" black pipe	A. Bailey
4-9-85	1335	AB 2	0.000	0	0.00E+00	0.000	P3	5" and 4" black pipes	A. Bailey
4-9-85	1335	8 3	0.000	0	0.00E+00	0.000	P3	6" black pipe	M. Taylor
4-9-85	1355	AB 3	0.002	0	0.00E+00	0.000	P3	two 6" black pipes draining hillside	A. Bailey
4-9-85	1510	AB 9	0.005	0	0.00E+00	0.000	P3	two 12" drains in concrete wall	A. Bailey
4-9-85	1755	AB 17	0.047	0	0.00E+00	0.000	P3	10" black plastic pipe S. of Butler Cove	A. Bailey
4-17-85	1310	15	0.000	5	0.00E+00	0.000	P3	submerged 6" cement culvert,200'N DNR	M. Taylor
4-17-85	1240	13	0.005	0	0.00E+00	0.000	P3	6" bulkhead culvert from	M. Taylor
4-17-85	1200	9A	0.000	0	0.00E+00	0.000	P3	seep. from well casing, N. Ellis C.	M. Taylor
4-17-85	1145	8	0.010	0	0.00E+00	0.000	P3	4" blk pipe from b-head, house N.EC	M. Taylor
4-17-85	1225	12	0.000	345	0.00E+00	0.000	P3	drain from blk perf pipe from house	M. Taylor

POINT SOURCES: P1 = Sewage outfall   P2 = Chlorinator discharge   P3 = Pipe/Culvert, 4" to 12" diameter
                 P4 = Pipe/Culvert, > 12"   P5 = Storm sewer discharge   P6 = Industrial drain discharge   P7 = Dam spillway

NON-POINT
SOURCES   NP1 = Creek or stream discharge

3-66

Date	Time	Source	Flow (c.f.s.)	Fecal Coliform / 100 mls	Loading: F. Coliform / Day	% Of Total Loading	Point or Non-point Code	Description of Source Area	Collector
4-9-85	1225	# 1	0.005	720	1.06E+08	0.011	P4	B.H. Marina, culvert under cabin	M. Taylor
4-9-85	1545	AB 11	0.008	2400	4.70E+08	0.051	P4	24" concrete pipe 1/2 covered by beach	A. Bailey
4-9-85	1630	AB 12	0.050	0	0.00E+00	0.000	P4	24" concrete pipe on beach	A. Bailey
4-9-85	1655	AB 13	0.080	0	0.00E+00	0.000	P4	30" concrete pipe, front of mobile home	A. Bailey
4-9-85	1725	AB 15	0.034	30	2.49E+07	0.003	P4	24" concrete pipe, 6" metal pipe	A. Bailey
4-17-85	1025	7	0.050	0	0.00E+00	0.000	P4	large culvert on rocky bluff, CNR	M. Taylor
4-17-85	1250	14	0.040	50	4.89E+07	0.005	P4	12" cement culvert from stone bulkhead	M. Taylor
4-9-85	1535	7 H	15.000	2400	8.81E+11	94.777	P4/NP1	Discharge of Moxlie and Indian Creeks (84" pipe)	A. Meyers
4-9-85	1340	2 H	0.800	135	2.64E+09	0.284	P5	storm sewer near Ellis Creek, 36" diameter	A. Meyers
4-9-85	1430	3 H	0.025	20	1.22E+07	0.001	P5	storm sewer, 30", San Fransisco St.	A. Meyers
4-9-85	1440	4 H	0.100	185	4.53E+09	0.049	P5	storm sewer	A. Meyers
4-9-85	1455	5 H	0.100	35	8.56E+07	0.009	P5	storm sewer	A. Meyers
4-9-85	1508	6 H	0.100	110	2.69E+08	0.029	P5	storm sewer	A. Meyers
4-9-85	1712	10 H	0.200	25	1.22E+08	0.013	P5	storm sewer, W. side of W. Bay Drive	A. Meyers
4-9-85	1725	11 H	0.001	15	3.67E+05	.000	P5	storm sewer, S. end of plywood plant	A. Meyers
4-9-85	1735	12 H	0.001	0	0.00E+00	0.000	P5	storm sewer, 15" diameter 4' above ground	A. Meyers
4-16-85	AVERAGE	*HS	0.020	0	0.00E+00	0.000	P5	Hardel Street storm sewer	A. Meyers
4-16-85	AVERAGE	*SF	0.020	2	9.76E+05	.000	P5	San Fransisco Street storm sewer	A. Meyers
4-9-85	1655	9 H	0.050	0	0.00E+00	0.000	P6	sawmill discharge from 36" diameter drain	A. Meyers
4-16-85	AVERAGE	***CLDRPC	276.4	4	2.70E+10	2.911	P7	Capitol Lake at dam fecal coliform counts.	A. Meyers

POINT SOURCES: P1 = Sewage outfall   P2 = Chlorinator discharge   P3 = Pipe/Culvert, 4" to 12" diameter
               P4 = Pipe/Culvert, > 12"   P5 = Storm sewer discharge   P6 = Industrial drain discharge   P7 = Dam spillway
NON-POINT
SOURCES   NP1 = Creek or stream discharge

* indicates average of morning and afternoon values
** indicates average of values: 4-9-85 and 4-16-85.
*** Fecal coliform loadings were determined by multipying
the fecal coliform count at the Capitol Lake Dam by the
collective flows of the Deschutes River and Percival Creek.

Table 3.11 Fecal coliform bacteria inputs to Budd Inlet: September 1985 Survey.

BUDD INLET BACTERIAL SURVEY, SEPTEMBER 10-11, 1985
FECAL COLIFORM INPUTS TO BUDD INLET
SORTED BY POINT OR NONPOINT SUBCATAGORY

Date	Time	Source	Flow (c.f.s.)	Fecal Coliform 100 mls	Loading: F. Coliform Day	% Of Total Loading	Point or Non-point Code	Description of Source Area	Collector
9-10-85	1320	1 H	0.600	1230	1.81E+10	2.220	NP1	mouth of Ellis Creek	A. Meyers
9-10-85	1055	# 5A	0.04	710	6.95E+08	0.085	NP1	Burfoot Creek	S. Cassatt
9-10-85	1025	# 6	0.110	140	3.77E+08	0.046	NP1	stream w/log bulkhead near br house	S. Cassatt
9-10-85	1030	AB 7	0.330	2000	1.61E+10	1.986	NP1	small stream, 20° wide	A. Bailey
9-10-85	1345	AB 16	0.500	800	9.78E+09	1.203	NP1	stream thru gully at Butler Cove	A. Bailey
9-10-85	1320	AB 14	0.360	310	2.73E+09	0.336	NP1	creek N. of Butler Cove	A. Bailey
9-10-85	1215	GH-1	0.000	1000	0.00E+00	0.000	NP1	Gull Harbor Creek #1 (S. creek)	S. Cassatt
9-10-85	1205	GH-2	0.040	25	2.45E+07	0.003	NP1	Gull Harbor Creek #2 (middle creek)	S. Cassatt
9-10-85	1200	GH-3	0.310	520	3.94E+09	0.485	NP1	Gull Harbor Creek #3 (N. creek)	S. Cassatt
9-11-85	1100	# 9	0.000	2000	0.00E+00	0.000	NP1	small creek 100' N. #8, near logs	S. Cassatt
9-11-85	1120	# 10	0.000	400	0.00E+00	0.000	NP1	bubbling creek 600' N. of #9	S. Cassatt
9-10-85	1315	# 16	0.000	920	0.00E+00	0.000	NP1	small stream 100 yds N. DNR	S. Cassatt
9-10-85	1230	CD-6	0.02	50	2.45E+07	0.003	NP1	waterfall from wooded area	A. Bailey
9-10-85	1140	LOTT STP	18.409	0	0.00E+00	0.000	P1	secondary sewage treatment plant (~10mgd)	J. Ward
9-10-85	1200	TAMOSHAN	0.028	23	1.58E+07	0.002	P1	secondary sewage treatment plant	V. Berube
9-10-85	1100	BEVERLY BCH	0.005	23	2.81E+06	.000	P1	holding tank at Beverly Beach	A. Bailey
9-10-85	1010	SEASHORE	0.020	23	1.13E+07	0.001	P1	secondary sewage treatment plant (8500gpd)	A. Meyers
9-10-85	1045	# 2	0.020	0	0.00E+00	0.000	P3	6" black corr. pipe ext. up bluff	S. Cassatt
9-10-85	1115	AB 9	0.050	0	0.00E+00	0.000	P3	two 12" drains in concrete wall	A. Bailey
9-10-85	1405	AB 17	0.025	115	7.03E+07	0.009	P3	10" black plastic pipe S. of Butler Cove	A. Bailey
9-11-85	1055	# 8	0.000	0	0.00E+00	0.000	P3	4" blk pipe from b-head, house N.EC	S. Cassatt
9-11-85	1140	# 12	0.000	2000	0.00E+00	0.000	P3	drain from 6" blk perf pipe from house	S. Cassatt
9-10-85	1102	CD-3	0.100	0	0.00E+00	0.000	P3	6" pipe next to Beverly Beach STP	A. Bailey
9-10-85	1130	# 1	0.010	1000	2.45E+08	0.030	P4	East of B.H. Marina, culvert under cabin	S. Cassatt
9-10-85	1126	# 1A	0.000	2000	0.00E+00	0.000	P4	West of B.H. Marina, culvert drainage	S. Cassatt
9-10-85	1130	AB 11	0.010	1000	2.45E+08	0.030	P4	24" concrete pipe 1/2 covered by beach	A. Bailey
9-10-85	1335	AB 15	0.010	0	0.00E+00	0.000	P4	24" concrete pipe, 6" metal pipe	A. Bailey
9-10-85	1345	# 14	0.040	975	9.54E+08	0.117	P4	12" cement culvert from stone bulkhead	S. Cassatt
9-10-85	1100	7 H	15.000	2000	7.34E+11	90.251	P4/NP1	Discharge of Moxlie and Indian Creeks (84" pi	A. Meyers
9-10-85	1300	2 H	0.400	1000	9.78E+09	1.203	P5	storm sewer near Ellis Creek, 36" diameter	A. Meyers
9-10-85	1208	3 H	0.010	100	2.45E+07	0.003	P5	storm sewer, 30", San Fransisco St.	A. Meyers
9-10-85	1150	5 H	0.040	870	8.51E+08	0.105	P5	storm sewer	A. Meyers
9-10-85	1140	6.5 H	0.02	0	0.00E+00	0.000	P5	storm sewer	A. Meyers
9-10-85	1340	#CLDRPC	125.000	3	1.53E+10	1.880	P7	Capitol Lake at Dam	A. Meyers

POINT SOURCES:
P1 = Sewage outfall   P2 = Chlorinator discharge   P3 = Pipe/Culvert, 4" to 12" diameter
P4 = Pipe/Culvert, > 12"   P5 = Storm sewer dischagre   P6 = Industrial drain discharge   P7 = Dam spillway

NON-POINT SOURCES   NP1 = Creek or stream discharge

3-68

FECAL COLIFORM SOURCES
April 1985 Survey

FECAL COLIFORM SOURCES
September 1985 Survey
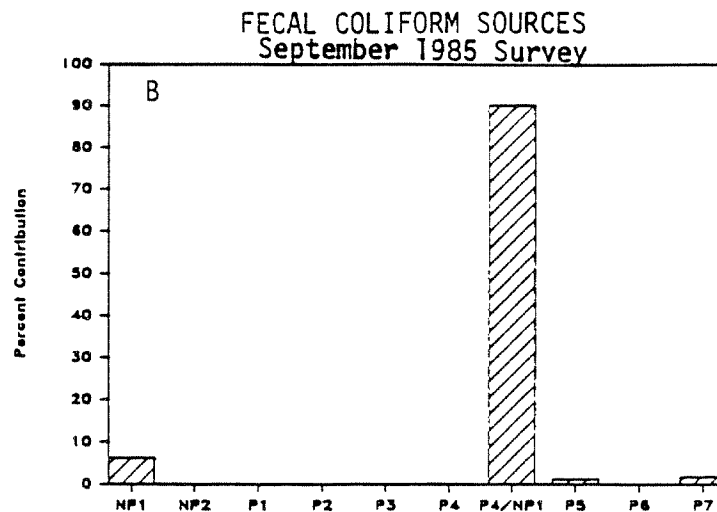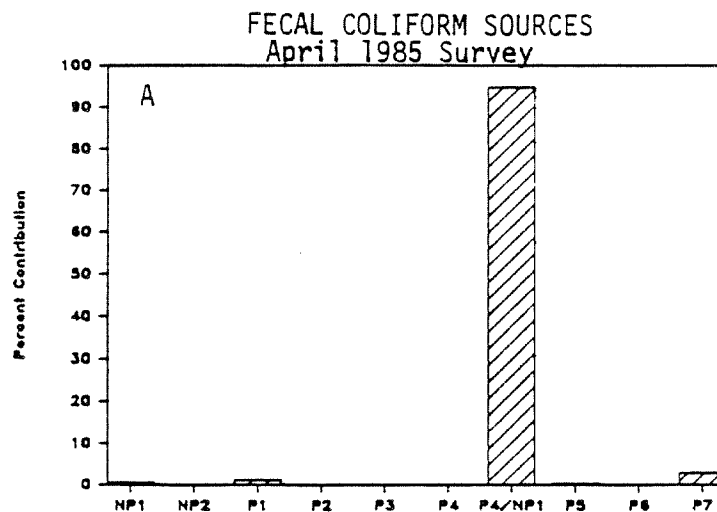
POINT SOURCES

P1 Sewage Outfall   P5 Storm Sewer Discharge
P2 Chlorinator Discharge   P6 Industrial Drain Discharge
P3 Pipe or Culvert 4"-12"   P7 Dam Spillway (Capitol Lake)
P4 Pipe or Culvert 12" +

NON-POINT SOURCES

NP1 Creek or Stream Discharge

COMBINATION SOURCES

P4/NP1 Creek or stream flowing through
        pipe or culvert

Figure 3.32   Percent contribution of non-point, point
              and combination sources to Budd Inlet.
              A = April 1985 Survey, B = September 1985 Survey
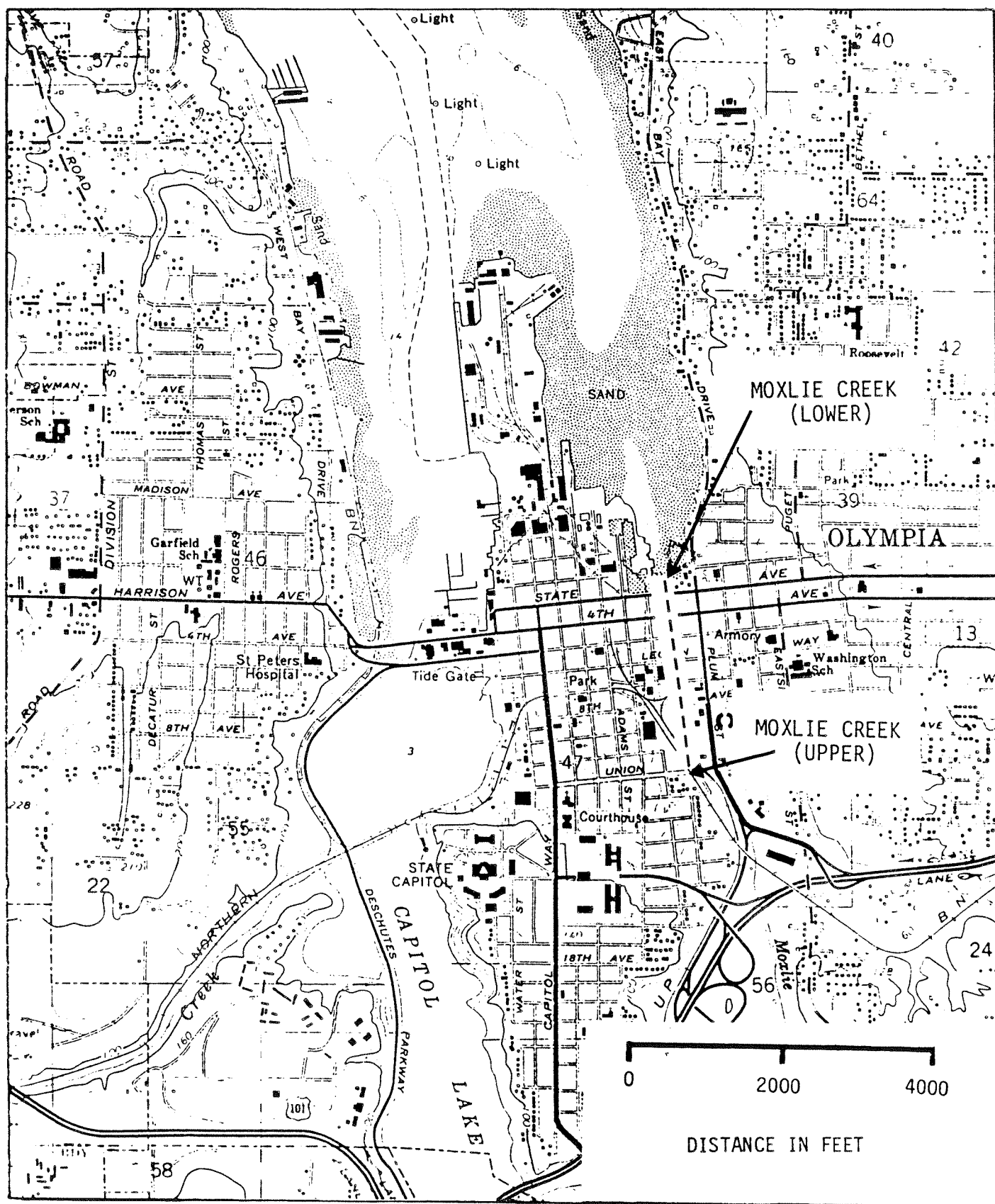
Figure 3.33 Path of Moxlie Creek beneath the streets of Olympia.

Figure 3.34 Fecal coliform loadings in MPN/Day during the April 1985
             Bacteriological Survey. Number in brackets indicates the
3-71   relative percent contribution.
             MPN/Day are expressed in scientific notation.
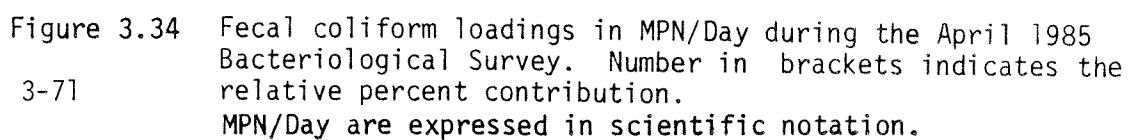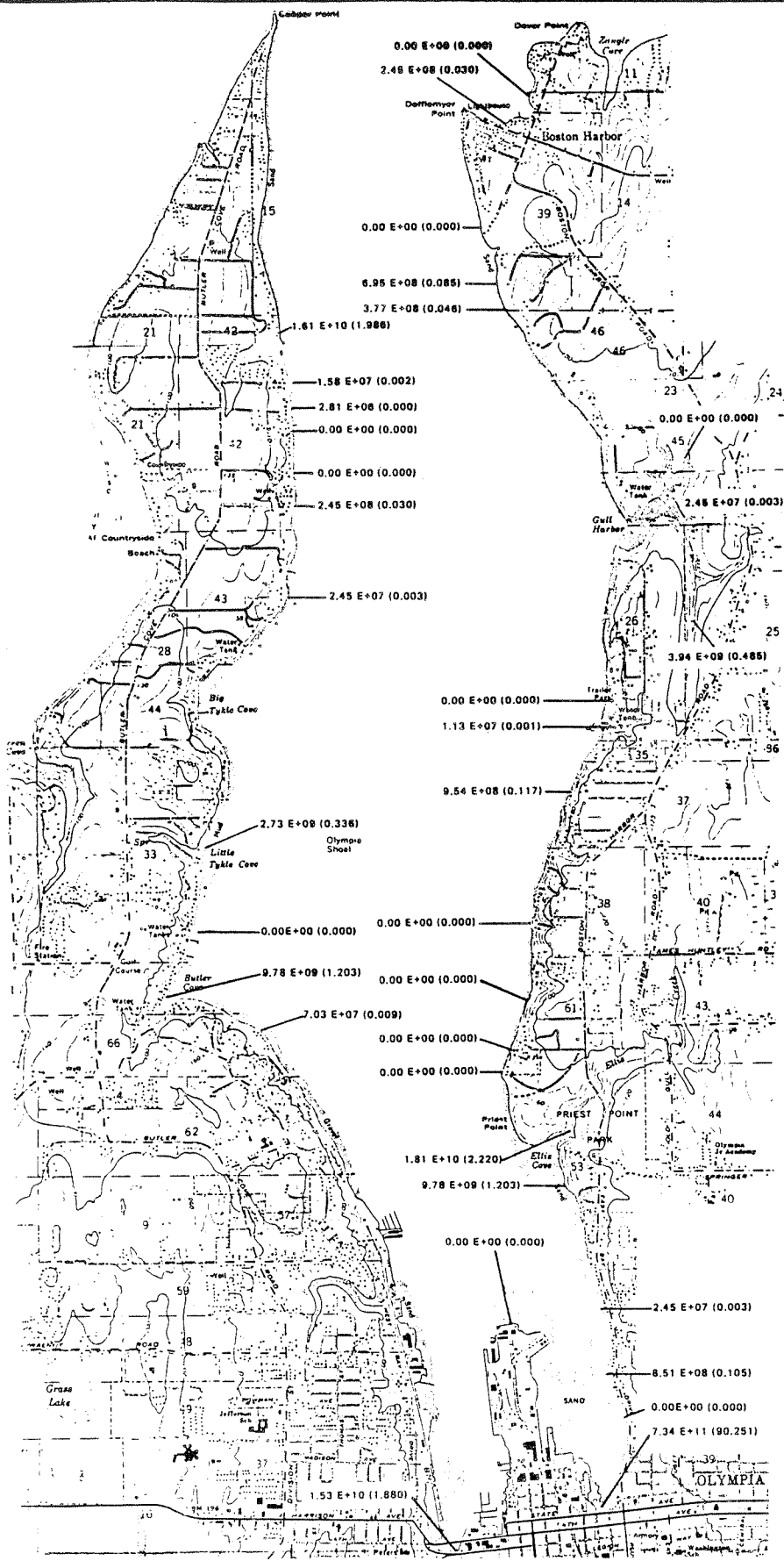
Figure 3.35 Fecal coliform loadings in MPN/Day during the September 1985
Bacteriological Survey. Number in brackets indicates the
3-72 relative percent contribution.
MPN/Day are expressed in scientific notation.

Table 3.12   Percent contribution to Budd Inlet from
point, non-point and combination sources

April 1985 Bacteriological Survey

Total Point Contribution (%)   99.40
Total Non-Point Contribution (%)   0.60

Subgroup	Number of Sources	Description	Percent Contribution[1]
NP1	15	Creek or stream	<1
P1	4	Sewage outfall	1
P2	1	Chlorinator discharge	0
P3	17	Pipe, culvert (4"-12")	0
P4	7	Pipe, culvert (>12")	<1
P4/NP1	1	Creek flowing through pipe	95
P5	10	Storm sewer discharge	<1
P6	1	Industrial drain discharge	0
P7	1	Dam spillway (Capitol Lake)	3

September 1985 Bacteriological Survey

Total Point Contribution (%)   99.40
Total Non-Point Contribution (%)   0.60

Subgroup	Number of Sources	Description	Percent Contribution[1]
NP1	13	Creek or stream	6
P1	4	Sewage outfall	0
P2	0	Chlorinator discharge	0
P3	6	Pipe, culvert (4"-12")	<1
P4	5	Pipe, culvert (>12")	<1
P4/NP1	1	Creek flowing through pipe	90
P5	4	Storm sewer discharge	1
P6	0	Industrial drain discharge	0
P7	1	Dam spillway (Capitol Lake)	2

(1) To nearest whole percent.

percent loading, the Thurston County Health District found that storm
sewers were a significant source of coliform loading to nearby Henderson
and Eld Inlets (Taylor, 1984). That study, however, was long-term and
conducted before the recent dry weather event occurred. Given the response
of the storm sewers in Budd Inlet to a small rain event, it seems
reasonable to assume that, over a typical year, the storm sewers would
contribute a much greater percent of total fecal coliform loading to Budd
Inlet than was observed in this study.

Rural Areas. Creeks and streams draining farmland and rural areas
provide information about rural loadings to Budd Inlet. During the April
survey, 15 NP1 subcategories were sampled. During the September survey, 13
streams and creeks were sampled. Creek and stream loading to Budd Inlet
was less than 1 percent of the total fecal coliform loading during the
April survey, and 6 percent during the September survey, probably in
response to the rain event preceding the survey (Table 3.12, Figure 3.32).

Septic Tank Drainage. Septic tank discharge of coliform bacteria into
Budd Inlet was represented by sampling small culverts and pipes from
surrounding areas not served by local sewage systems. Privately owned and
operated chlorinator systems were also included in this group. These pipes
and culverts generally ran down hillsides to the waters edge, presumably
draining the surrounding land and the septic systems utilized by the
residents of the area. This collection of pipes and culverts was labelled
point source subgroups P2, P3 and P4, depending upon the size of the pipe
or whether a chlorinator was present. None of these point sources was a
significant contributor of fecal coliform bacteria to Budd Inlet. To
accurately assess the behavior of these sources of bacterial loadings, a
field survey during a major storm event would be necessary.

Summary of Fecal Coliform Concentrations in Sources to Budd Inlet.
During the April survey, more than half of the samples contained fecal
coliform concentrations of 0 to 10 MPN/100 mls, with 23 percent in the 11

to 100 MPN/100 mL range and 10.5 percent exceeding 1000 MPN/100mls
(Table 3.13). The September fecal coliform concentrations were higher with
23 percent of the samples in the 0 to 10 MPN/100 mL range and almost 30
percent of the samples exceeding 1000 MPN/100 mls (Table 3.13). This
increase might have been due to the rain event preceding the September
sampling survey. since some runoff probably occurred during the night and
early morning. It is not possible at this time to assess the impact of the
high fecal coliform concentrations upon Budd Inlet, since no offshore
samples were collected.

Table 3.13   Summary of fecal coliform concentrations
from sources to Budd Inlet

April 1985 Survey

Fecal Coliforms (MPN/100 mls)	Number of Samples	Percent of Total Samples
0-10	29	50.9
11-100	13	22.8
101-1000	9	15.8
> 1000	2	3.5
> 2000	4	7.0
Total	57	100.0

September 1985 Survey

Fecal Coliforms (MPN/100 mls)	Number of Samples	Percent of Total Samples
0-10	8	23.5
11-100	6	17.5
101-1000	10	29.5
> 1000	5	14.8
> 2000	5	14.7
Total	34	100.0

Given the high fecal coliform concentrations found in some sources, it seems likely that the Inlet periodically experiences a fecal coliform problem in some areas, especially during periods of heavy rain. The September survey showed that the sources do indeed respond to a rain event (0.61 inches) in that samples exceeding 1000 MPN/100 mls nearly tripled the percentages recorded during the April dry weather sampling (no ppt.).

3.7 SEDIMENT OXYGEN DEMAND STUDY

Results

The two "Lander" sites occupied during the Sediment Oxygen Demand (SOD) Study are shown in Figure 2.1. Lander Site 1 was just north of Station 8 and sampling was conducted on May 21, 1985. Lander 2 was located between Stations 3 and 4 and sampling was conducted on May 22, 1985. The flux of oxygen into the sediments was determined from the change of oxygen concentration over time in the box core flux chambers. The data are shown in Figures 3.36 and 3.37 for Lander Sites 1 and 2, respectively. The systematic difference in oxygen concentrations between box cores A and B over time is in part due to the difference in volume of the flux chambers between the two cores and in part due to the natural variability between cores.

A linear regression analysis was performed on the data to determine the rate of oxygen uptake. This was done for the initial uptake rate which was considered to be the first four hours, and the overall rate for the full twelve hours. These results are shown in Table 3.14.

Table 3.14 Sediment oxygen demand for benthic lander sites 1 and 2 (units: mg O2/m^2/hr)

	Site 1			Site 2	
	Box A	Box B		Box A	Box B
Initial 4 hour	73.4	73.3		41.5	65.8
Regression Coefficient (r^2)	1.00	1.00		0.99	0.98
Overall 12 hours	55.3	57.6		42.2	30.4
Regression Coefficient (r^2)	0.98	0.96		0.99	0.88

OXYGEN CONCENTRATION OVER TIME

Lander #1, Station 8, Box Cores A and B
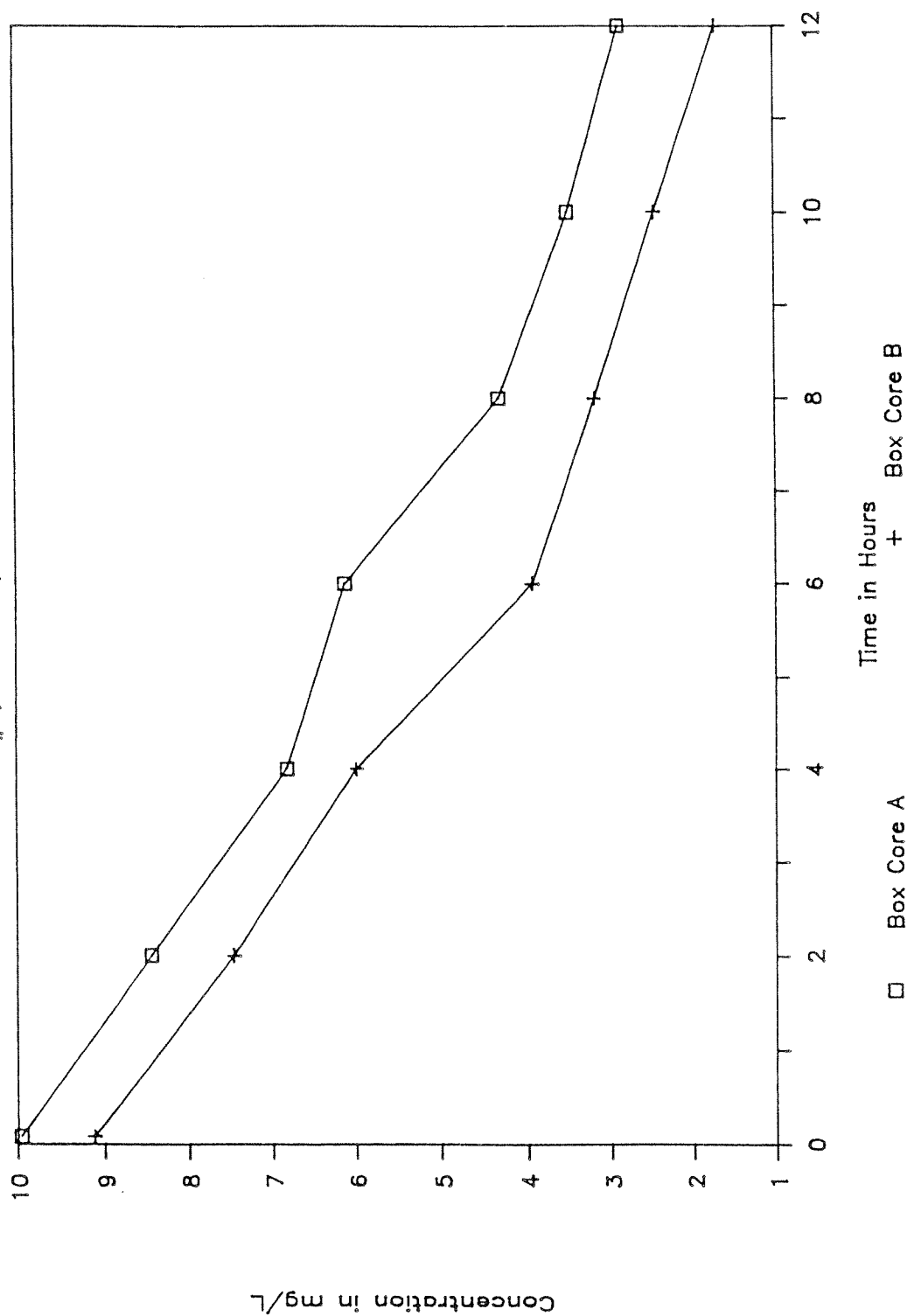
Figure 3.36 Sediment Oxygen Demand Study: oxygen concentration over time, Lander Site #1, box cores A and B.
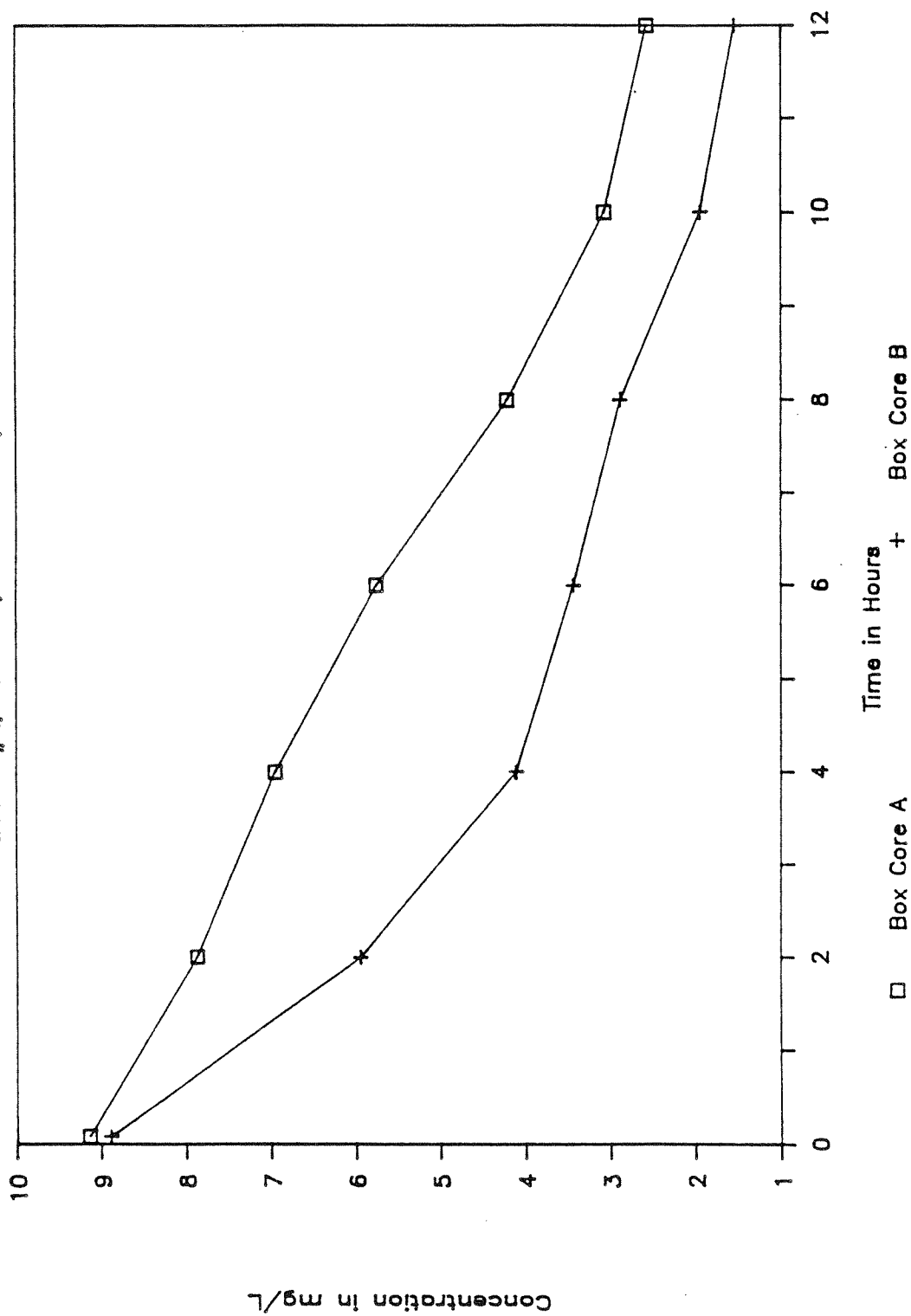
Figure 3.37. Sediment Oxygen Demand Study: oxygen concentration over time, Lander Site #2, box cores A and B.

The oxygen demand was somewhat greater at Site 1 than it was at Site 2 for both the initial rates and the overall rates. The regressions were nearly linear for the first four hours in all instances. All boxes showed a slight decrease in rate after four hours or when the oxygen level dropped below about 5 mg/L. The SOD was consistently greater than measurements made by Pamatmat (1971) in July 1969 which ranged from 22 and 35 mg $O_2/m^2/hr$.

Figure 3.38 shows the increase of ammonium over time from Lander Site 2. The regression analysis of these data are shown in Table 3.15. There was no apparent difference between the initial release rate and the overall rate for Site 2. There was no detectable ammonium release from Site 1 even though there was a large oxygen demand.

Table 3.15 Benthic ammonium flux for benthic lander sites 1 and 2 (units: mg NH4-N/m^2/hr)

	Site 1		Site 2	
	Box A	Box B	Box A	Box B
Initial 4 hours	ND	ND	2.03	1.71
Regression Coefficient (r^2)	--	--	0.94	0.96
Overall 12 hours	ND	ND	2.41	1.53
Regression Coefficient (r^2)	--	--	0.99	0.93

(ND = not detected)

The lack of ammonium release is explained by the very high rate of bioturbation and irrigation of the upper sediments at Site 1 due to the burrowing of benthic animals. This was evident by casual observation of the box cores when they were sampled for their interstitial water. This is consistent with the typically observed pattern of increased numbers of animals along with decreased diversity in the vicinity of wastewater outfalls (Parsons et al., 1984). It can also be seen in a comparison of the pore water concentration profiles from Sites 1 and 2 shown in Figure 3.39. The profiles show very large gradients for ammonium and silica in the upper few centimeters for Site 2 and only a slight gradient

NH4 CONCENTRATION OVER TIME

Lander #2, Sta 3&4, Box Cores A,B

□ Box Core A   +   Box Core B

Time in Hours

Concentration in umoles/L
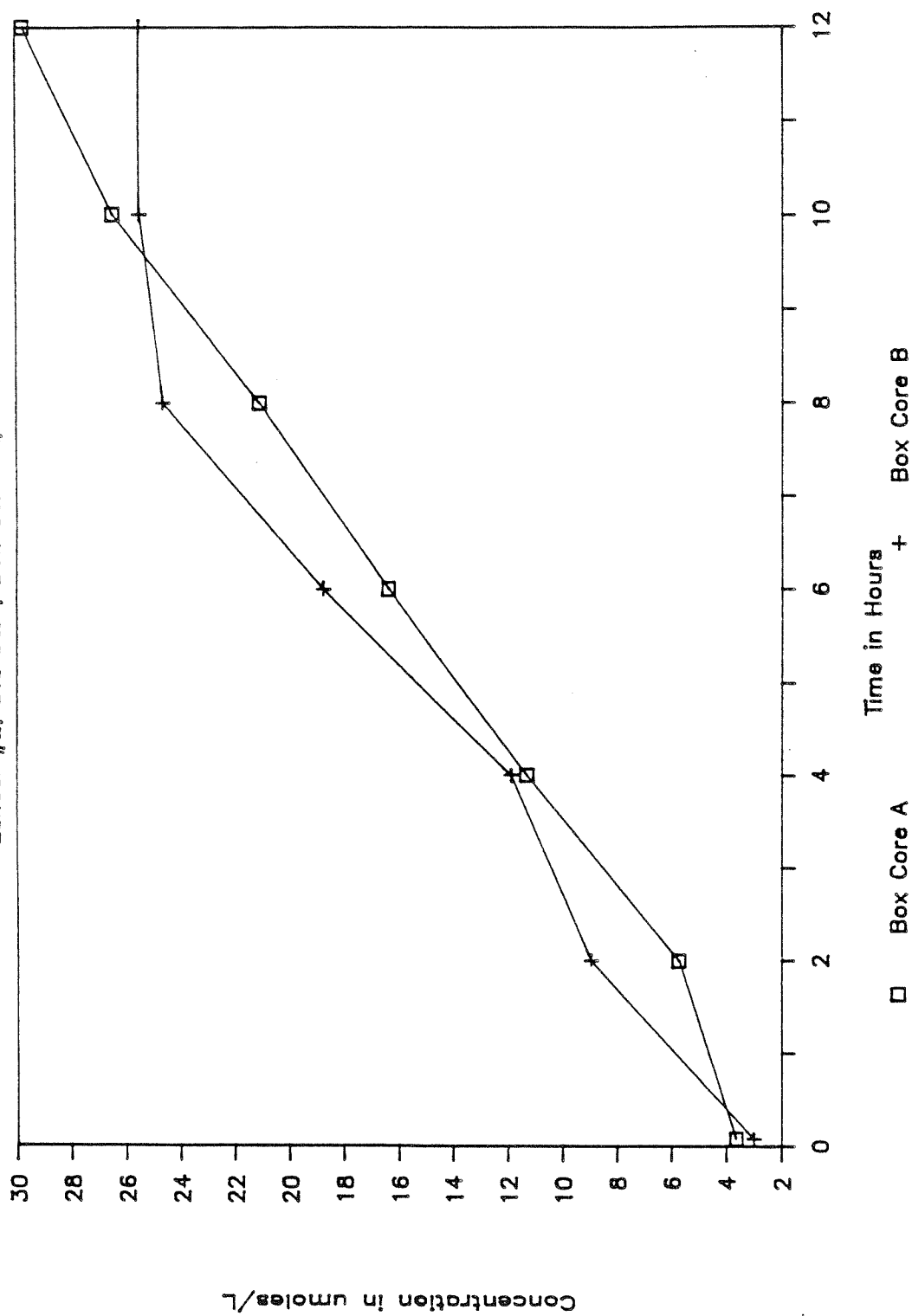
Figure 3.38   Sediment Oxygen Demand Study: ammonium concentrations over time,
Lander site #2, box cores A and B.
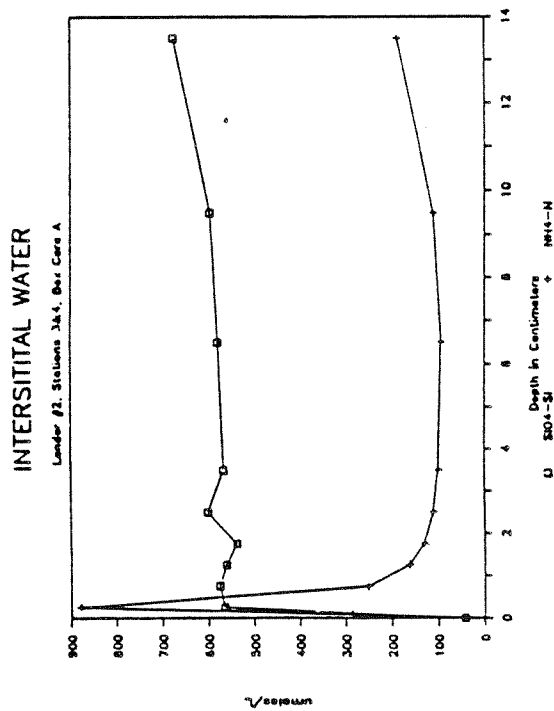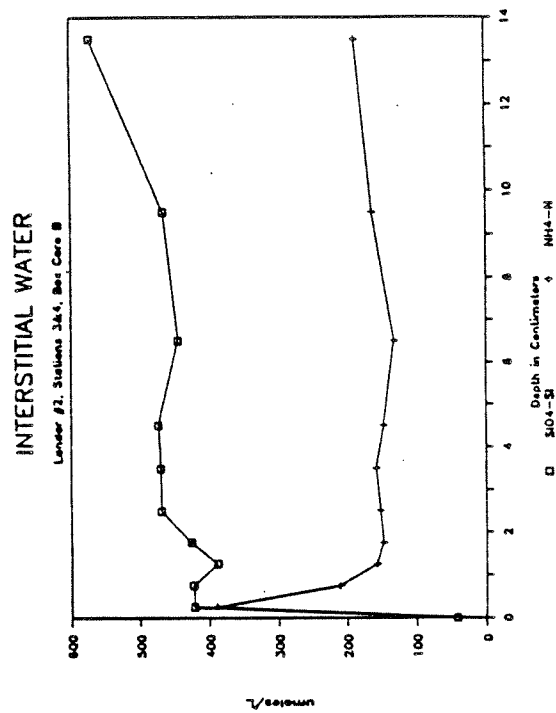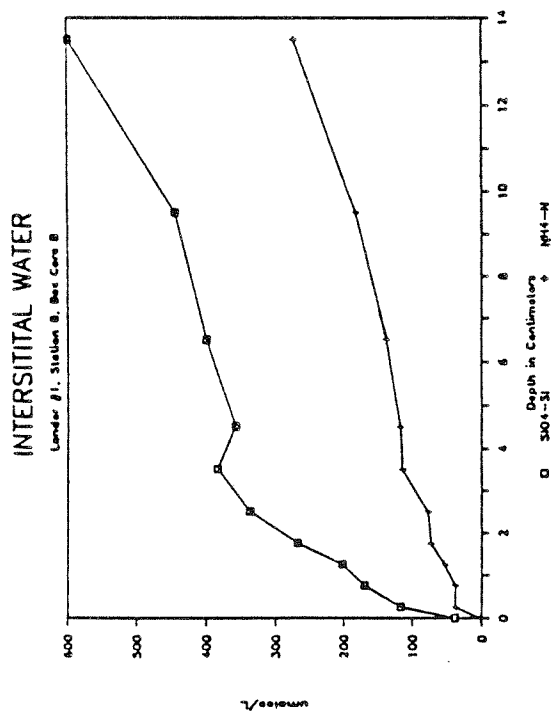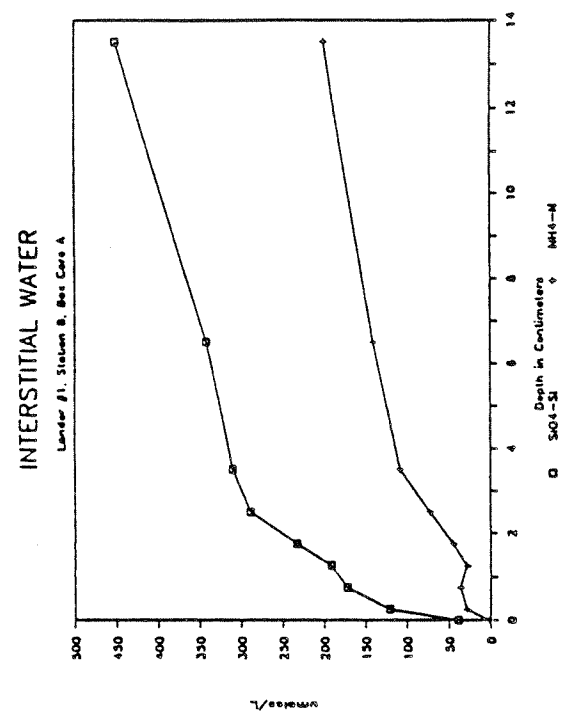
Figure 3.39 Sediment Oxygen Demand Study: ammonium and silica profiles
in interstitial water, Landing sites #1 and #2, box cores A and B.

at Site 1. This is indicative of increased mixing of the upper sediments of Site 1 due to increased animal burrowing. The diffusional flux of ammonium is, therefore, much reduced at Site 1, while the total amount of respiration from benthic animals is greater. In addition, oxygenated bottom water is mixed into the sediments which allows for nitrification of the ammonium before it can be released. A similar finding of large oxygen uptake not accompanied by release of combined nitrogen was found for shallow areas of San Francisco Bay (Hammond et al., 1985).

The results for SOD and ammonium release from Site 2 are compared with results from nine other coastal marine estuaries and bays in Figure 3.40. The other results (from Fisher et al., 1982; Callender and Hammond, 1982) follow the same general trend and yield a good correlation ($R^2 = .75$) between ammonium flux and SOD.

SOD vs. Ammonium Release for Budd Inlet
and other Coastal Marine Systems

$NH4-N = 0.046 \times SOD - 0.11$

$R2 = 0.75$

Ammonium Release (mg-N/m^2/hr)

Sediment Oxygen Demand (mg-O2/m^2/hr)

□ Other Studies   ◇ Budd Inlet (4 hours)   △ Budd Inlet (12 hours)
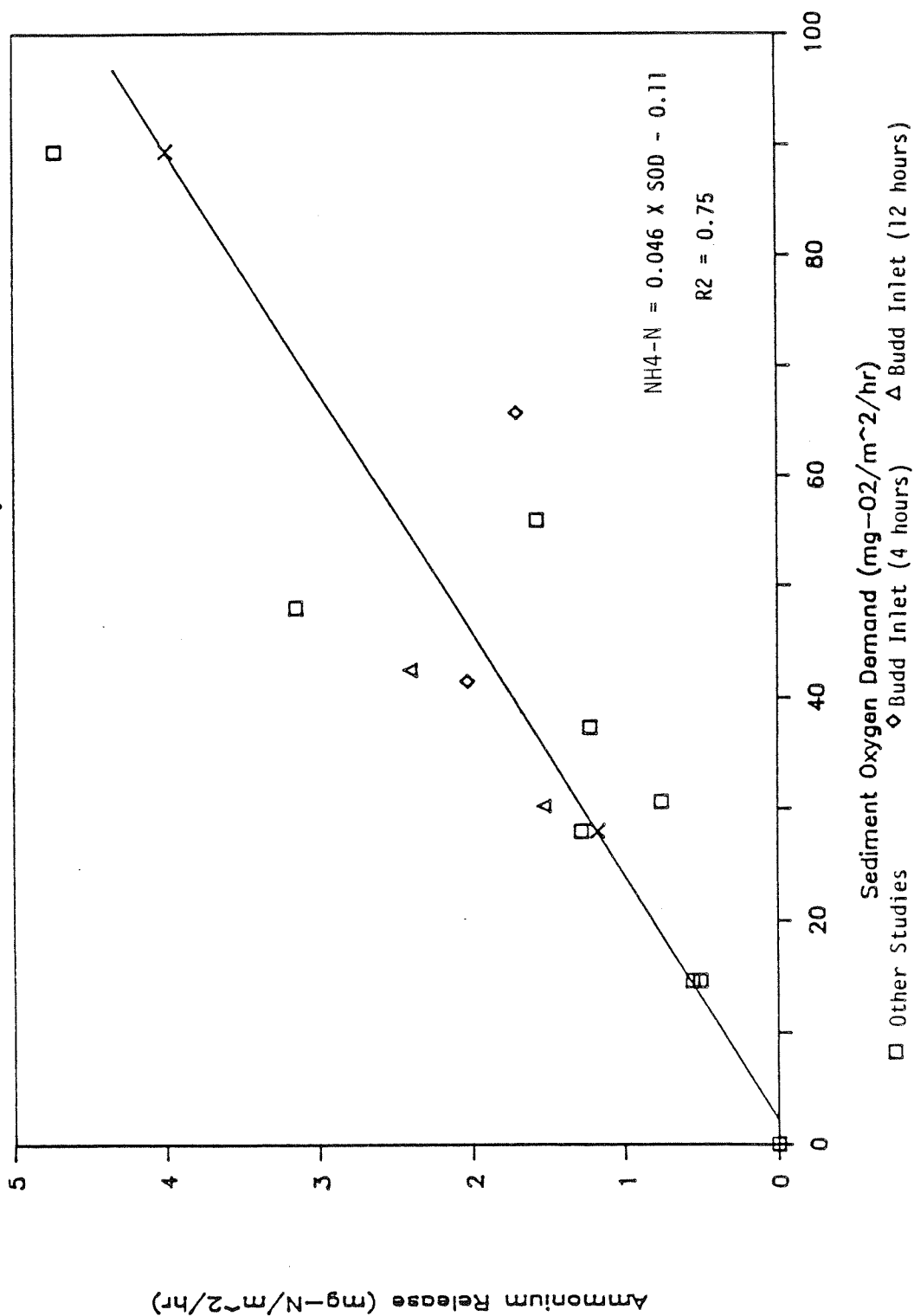
Figure 3.40 Sediment oxygen demand versus ammonium release: Budd Inlet compared with other coastal marine studies.

CHAPTER 4. MODELING DISSOLVED OXYGEN DYNAMICS IN BUDD INLET

4.1 BOX MODELING

Introduction

The two-layered box model is the simplest possible approach to modeling the net steady-state circulation of an estuary. In this approach, the estuary is divided into longitudinal segments or "boxes" with vertical boundaries at lateral transects through the intensive survey stations. Budd Inlet is divided into three segments: the upper Inlet (UB), the central Inlet (CB) and the lower Inlet (LB) (Figure 4.1). Each segment is subdivided into an upper layer and a lower layer with the horizontal boundary near the pycnocline, so that the upper layer contains the net flow moving seaward and the lower layer contains the net flow moving into the estuary.

The advantage of this approach to modeling the circulation is that the transport of nutrients or other water quality parameters within the Inlet can be determined from measurements taken at the survey stations. Assuming steady state, the transport of the parameters into and out of each of the boxes may be used to calculate net sources and sinks for each box. Changes in concentration due to advection or mixing can then be distinguished from changes due to internal and external sources and sinks. This information also aids in developing and calibrating the more complex dynamic model.

Box modeling was conducted on the data collected during the May, 1985 intensive survey. This was done for two reasons. First, SOD and sediment nutrient release were measured as part of the May survey to document this internal source/sink, and second, all physical and chemical measurements
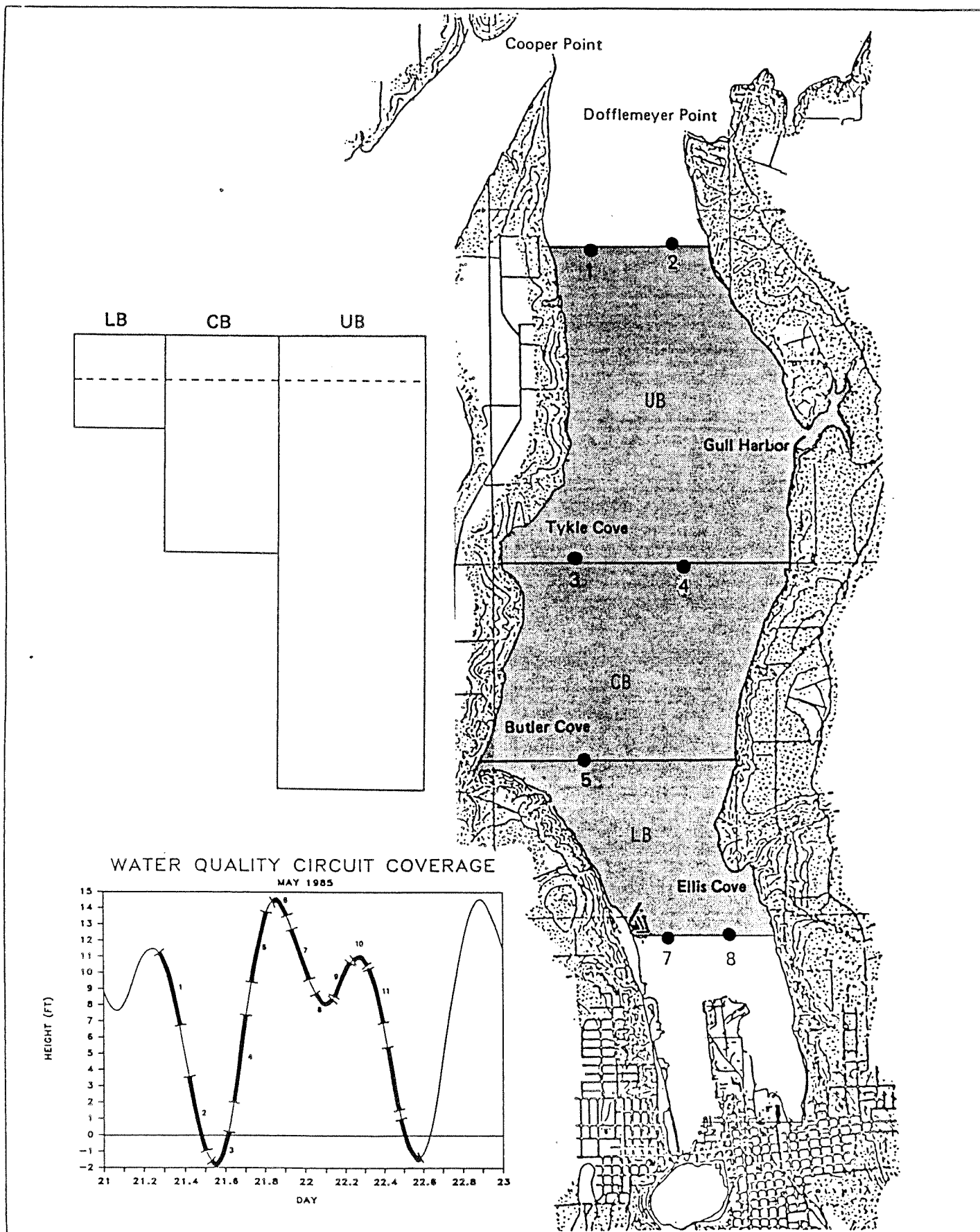
Figure 4.1   Horizontal and vertical boundaries depicted in the box model
of Budd Inlet.   Insert graph shows eleven May 1985 occupations
used in the box modeling.

were made simultaneously during the May survey. The data presented in this section are the average of eleven separate occupations of stations 1,3,4,5 and 7 (Figure 4.1) over a complete tidal cycle. Salinity, water quality and current measurements were averaged between stations 3 and 4 and are described as station 3 in the text.

Model Formulation

The box modeling methodology used was taken from Pritchard (1969) and Officer (1981). The nomenclature and exchange coefficients are shown in Figure 4.2. These include horizontal advection (Q), vertical advection (Q_v) and vertical diffusion (E_v).

There are six equations which define the salt flux and flow continuity across the two vertical boundaries and the halocline, for the upper box m in terms of the six unknown coefficients, Q_{m-1}, Q_m, Q'_m, Q'_{m+1}, Q_{vm} and E_{vm}. These equations are:

$$Q_{m-1} \, S_{m-1} = Q'_m \, S'_m \qquad\qquad (4.1)$$

$$Q_m \, S_m = Q'_{m+1} \, S'_{m+1} \qquad\qquad (4.2)$$

$$Q_{m-1} - Q'_m = R \qquad\qquad (4.3)$$

$$Q_m - Q'_{m+1} = R \qquad\qquad (4.4)$$

$$Q_{m-1} + Q_{vm} = Q_m \qquad\qquad (4.5)$$

$$Q_{m-1} \, S_{m-1} + Q_{vm} \, S'_m + E_{vm} \, S'_m = Q_m \, S_m + E_{vm} \, S_m \qquad\qquad (4.6)$$
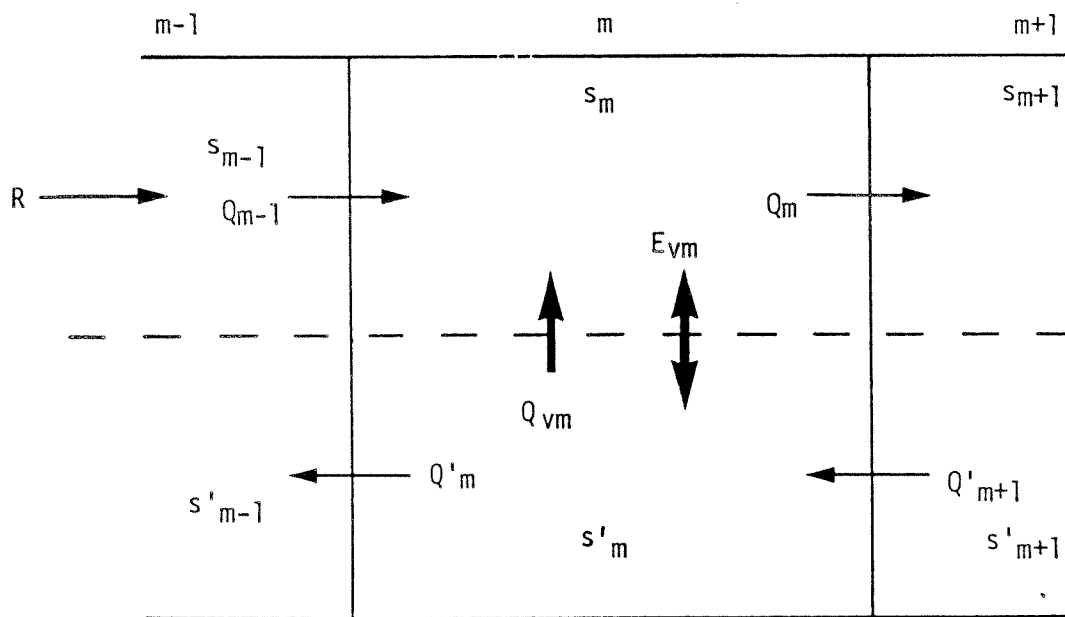
S_m = Salinity in upper layer of segment m.

S'_m = Salinity in lower layer of segment m.

Qm = Volumetric transport from upper layer of segment m.

Q'm = Volumetric transport from lower layer of segment m.

Qvm = Vertical volumetric transport for segment m.

Evm = Vertical diffusive exchange coefficient for segment m.

R = Freshwater Input

Figure 4.2 Nomenclature and exchange coefficients for the two dimentional box model.

Solving equations 4.1 and 4.3 for Q_{m-1} and Q'_m and equations 4.2 and 4.4 for Q_m and Q'_{m+1} yields:

$$Q_{m-1} = S'_m/(S'_m - S_{m-1}) \, R \qquad (4.7)$$

$$Q'_m = S_{m-1}/(S'_m - S_{m-1}) \, R \qquad (4.8)$$

$$Q_m = S'_{m+1}/(S'_{m+1} - S_m) \, R \qquad (4.9)$$

$$Q'_{m+1} = S_m/(S'_{m+1} - S_m) \, R \qquad (4.10)$$

The vertical advective flux is then derived from equation 4.5:

$$Q_{vm} = \frac{S_m S'_m - S_{m-1} S'_{m+1}}{(S'_{m+1} - S_m)(S'_m - S_{m-1})} \, R \qquad (4.11)$$

and the vertical diffusion from equation 4.6:

$$E_{vm} = \frac{S_m (S'_{m+1} - S'_m)}{(S'_m - S_m)(S'_{m+1} - S_m)} \, R \qquad (4.12)$$

The S terms refer to the salinity of each respective box while the term R is the river flow, which, for Budd Inlet, would be the flow from Capitol Lake. The vertical boundaries are taken at lateral transects through the survey stations which divide the Inlet into three segments (Figure 4.1). Each segment is further divided into an upper and lower layer for a total of six "boxes."

The horizontal (Q_m), vertical advective (Q_{vm}), and vertical diffusive (E_{vm}) exchange coefficients for Budd Inlet are computed for each data set and then averaged over the tidal cycle. The nutrient concentrations at the vertical boundaries are averaged for the upper and lower layers and the nutrient flux at each boundary is calculated using the horizontal advection terms. Vertical advection and diffusion of nutrients are calculated from the vertical advective and diffusive exchange coefficients and the average concentration of lower and/or upper layer boxes.

Model Verification

Model assumptions were tested by comparing the net velocities measured by current meters over a tidal cycle in the May survey with the velocities predicted from the box model. The box model velocities are calculated by dividing the volume transport at each vertical boundary by the cross-sectional area of that boundary shown in Table 4.1. This comparison is shown in Figure 4.3 which shows the measured and predicted longitudinal currents at each of the boundaries. There is reasonably good agreement between the predicted average velocites and the measured profiles, keeping in mind that the box model velocities are the average velocity over the whole vertical boundary, while the current meter measurements are at a descrete depth. The net current meter velocities at stations 3, 4 and 5 reflect, in part, the added effect of gyre-like circulation in the central Inlet.

Table 4.1 Volume transports and cross-sectional areas for the May 1985 box model

	Volume Transport (m^3/sec)	Cross-sectional Area (m^2)
Station 7		
Upper	83	4,881
Lower	76	6,069
Station 5		
Upper	174	7,053
Lower	107	14,475
Stations 3 & 4		
Upper	150	8,766
Lower	143	26,035
Station 1		
Upper	174	5,004
Lower	167	23,482

Other more quantitative comparisons such as calculated transports at each boundary from current meter measurements would be difficult to interpret with only two to three measurements at each station. However, measured transports can be computed in the upper three meters from the

4-6
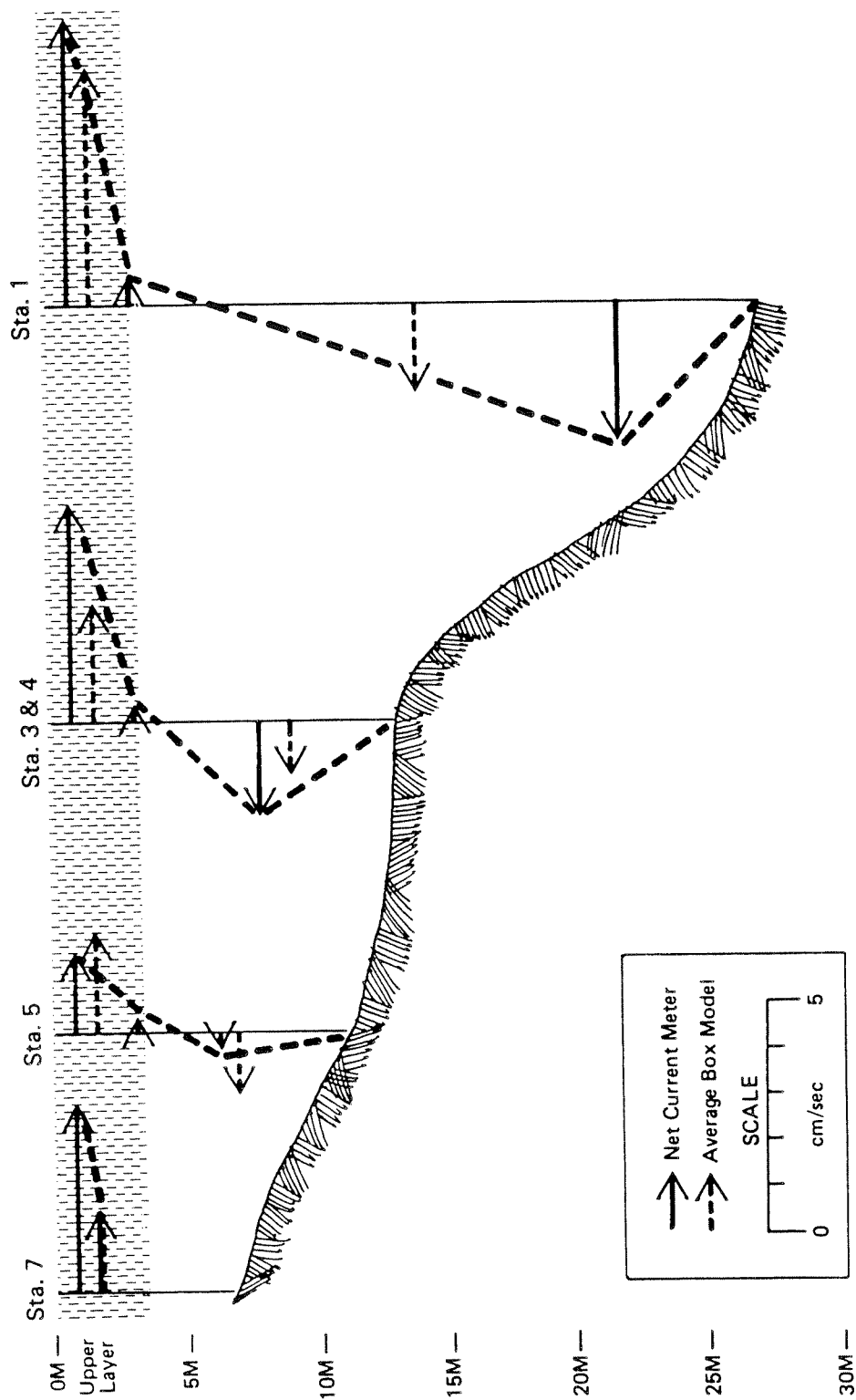
Figure 4.3 Vertical profiles of the measured net velocities at each current meter (solid arrow) and predicted average velocities in the upper and lower layer from the box model (dashed arrows). The dashed line between the net current meter velocities represent a possible current profile in the upper and lower layer for comparison.

current meters, which are generally in agreement to within 25 percent of the predicted values. Based on these comparisons, it was concluded that using the box modeling approach to predict net circulation and transport within the Inlet was appropriate.

Hydrodynamic Residence Time

The hydrodynamic or water residence time is the standard which is used to compare the residence time of other water quality constituents within the Inlet. Residence times for water quality constituents which are less than the water residence time for a given box would indicate a net removal from that box. Conversely, constituent residence times greater than the water residence time indicate a net accumulation.

The hydrodynamic residence time is defined as the average amount of time a parcel of water stays in a given volume of estuary. The residence time T, is given by the expression

$$T = V/Q \qquad (4.13)$$

where Q is the volumetric transport into or out of a given box with a volume, V. This average amount of time is the time it takes for the original volume to be replaced so that only 1/e or about 37 percent of the "original" water remains (Officer, 1981).

Figure 4.4 shows the calculated residence times and volumetric transports for the three box model segments. The time required for a water parcel to travel from the head of the Inlet to the mouth would be about four days, whereas the maximum residence time for a parcel entering the Inlet from Puget Sound would be about 14 days. The average residence time for the Inlet as a whole is about eight days based on the net output and the total volume. It must be kept in mind that these times are for the steady-state net circulation and would represent a maximum for the Inlet. Portions of the Inlet most influenced by the large tidal exchange would have proportionality shorter residence times.

7　　　　　　5　　　　　　3　　　　　　1

83 →　┌─────┐　114 →　┌─────┐　150 →　┌─────┐　174 →
　　　　│1.05 │　　　　│1.11 │　　　　│1.61 │
　　　　└─────┘　　　　└─────┘　　　　└─────┘

　　　　　↑　　　　　　　↑　　　　　　　↑
　　　　　31　　　　　　36　　　　　　25

← 76　　　← 107

┌─────┐
│1.33 │
└─────┘

┌─────┐
│3.04 │　← 143
└─────┘

┌─────┐
│5.67 │　← 167
└─────┘
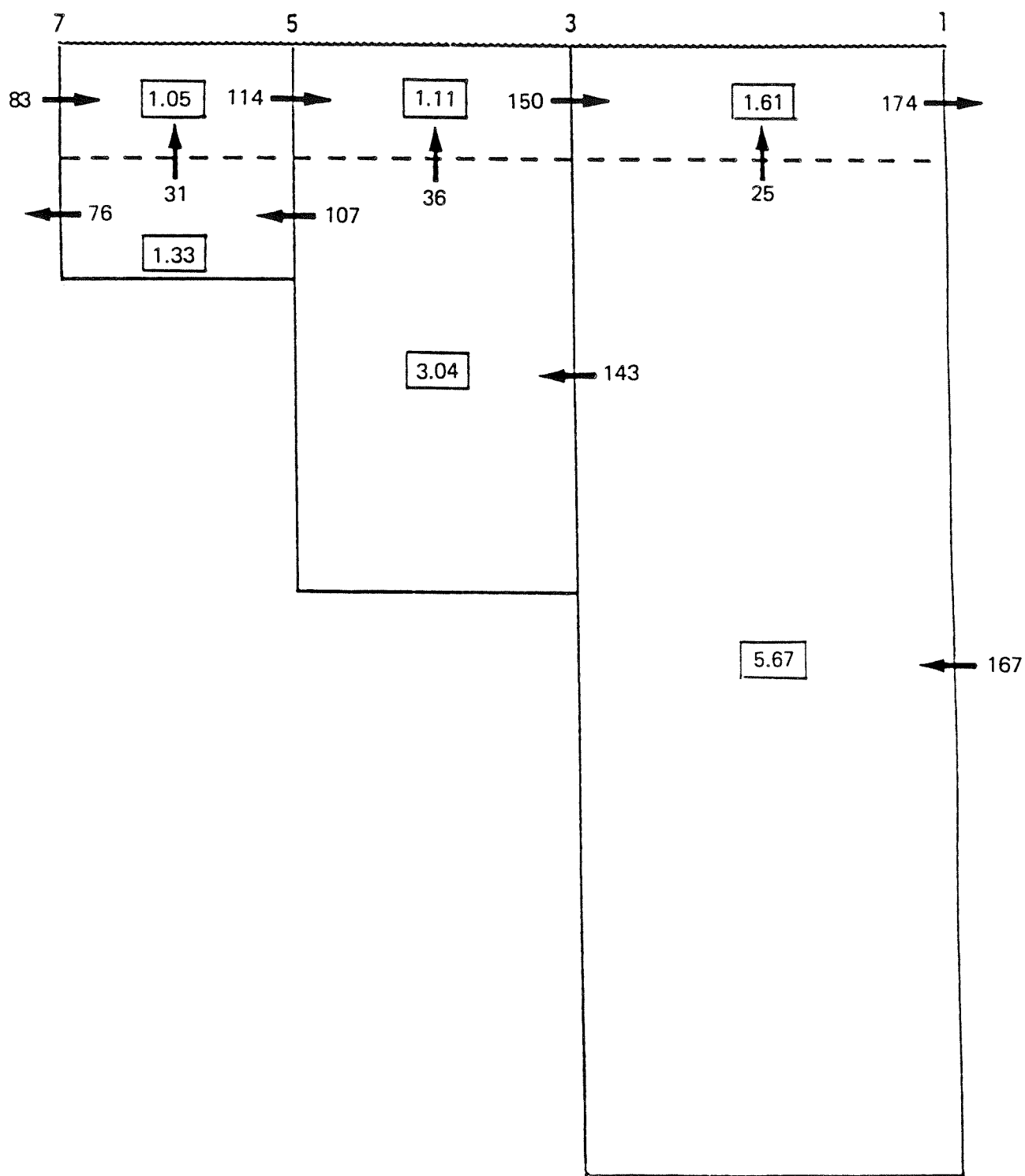
Figure 4.4　Calculated residence time in days (enclosed in boxes)
and volumetric transports (m^3/sec) for the upper and lower
layers of the three box model segments:　May 1985 intensive
survey.

Relative Residence Times

The average fluxes and relative residence times for oxygen, ammonium, and nitrate + nitrate are shown respectively in Figure 4.5. The relative residence time (T_r) is calculated by dividing the residence time of the constituent by the water residence time (Figure 4.4). The residence time (T) of the constituent is taken to be

$$T = Mass/Output \qquad (4.14)$$

where Mass is the average mass of constituent and Output is the output flux. A T_r which is less than one indicates a net sink within the box and/or dilution due to advective input. A T_r greater than one indicates a net source within the box and/or a net accumulation due an external loading into the box.

The relative residence times determined from the box model for ammonium (Figure 4.5) indicate that there is a significant ammonium source in the upper layer of segment LB near the head of the Inlet. The large loading into the left-hand side of the box (2164 lbs ammonium/day) creates about a six fold increase in the ammonium residence time relative to that of the water. This is no doubt due to the LOTT outfall which is by far the major point source of ammonium to the Inlet (see Section 3.5) and is located just south of the station 7 vertical boundary. The other upper layer boxes show a decreasing T_r as the surface layer flows away from the source, with the outer Inlet (UB) upper layer showing a net sink. This decrease is due to the constant uptake by algal production in the upper photic zone, which ranged from the upper 4 to 10 meters.

The major input of ammonium to the upper layer in the outer Inlet between stations 1 and 3 is no longer the advected surface water. Instead this role is shared with the vertical advection and mixing of the deeper water introduced into the Inlet from Puget Sound at the mouth as it shoals approaching station 3. This can be seen in the pattern of the longitudinal contour plots in Figures 4.6 and 4.7 which show the progression from an incoming flood tide to high slack (see Data Appendix 1 for more detail).
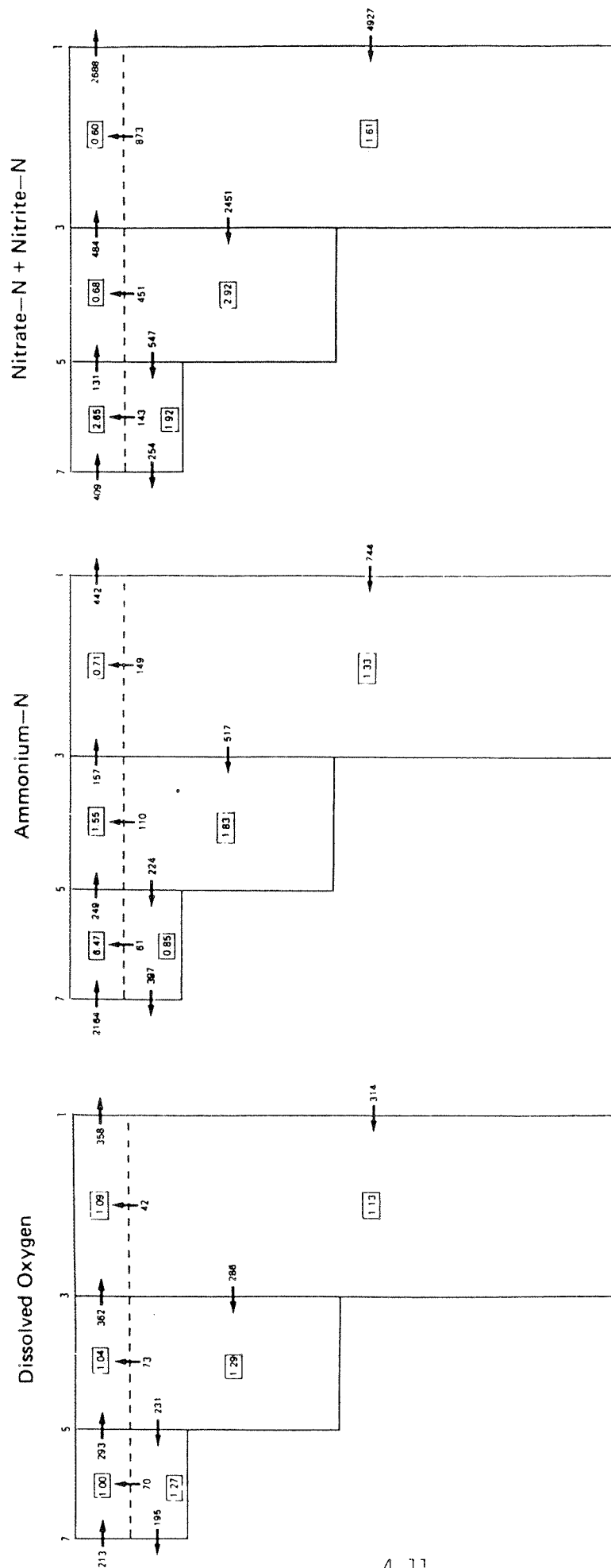
Figure 4.5 Average fluxes(lbs/day except for dissolved oxygen which is 1,000 lbs/day) and relative residence time in days (enclosed in boxes) for dissolved oxygen, ammonium-n and nitrate-n + nitrite-n. The relative residence time is calculated by dividing the residence time of the constituent by the water residence time.

SALINITY CONC. AT STATIONS 1 3 5 7 (HIGH SLACK)

D. O. CONCENTRATION AT STATIONS 1 3 5 7 (HIGH SLACK)

NH4-N CONCENTRATIONS AT STATIONS 1 3 5 7 (HIGH SLACK)

NO3-N + NO2-N CONC. AT STATIONS 1 3 5 7 (HIGH SLACK)
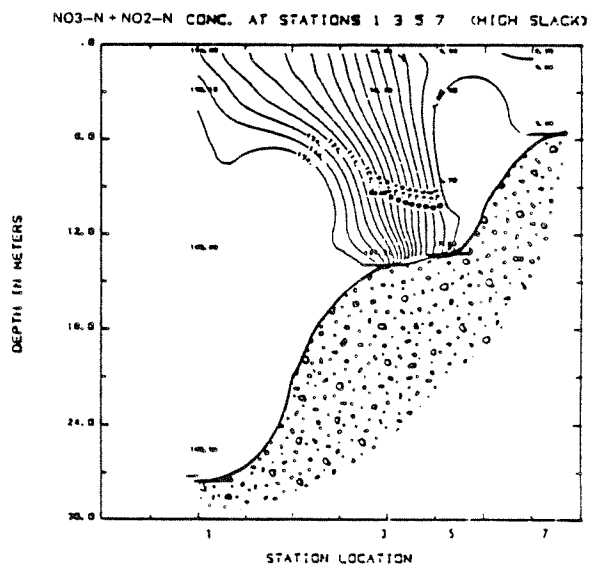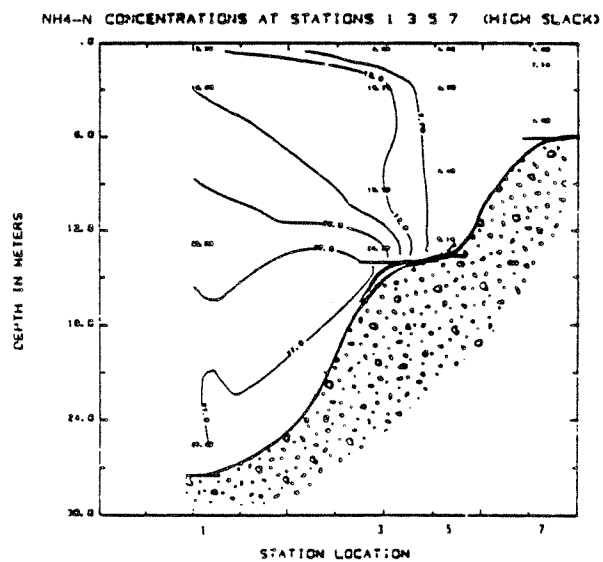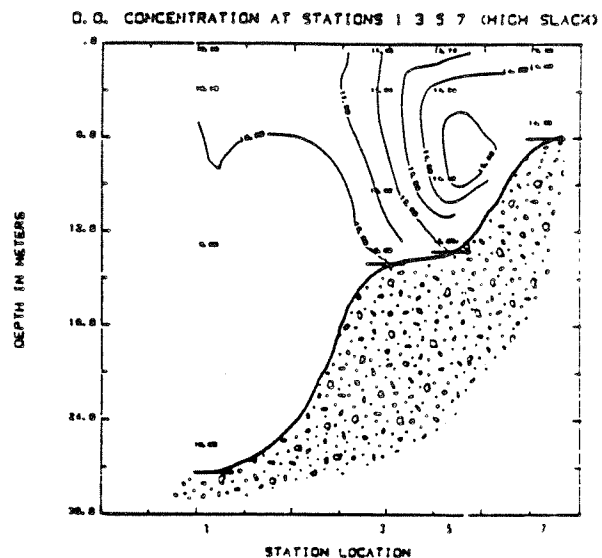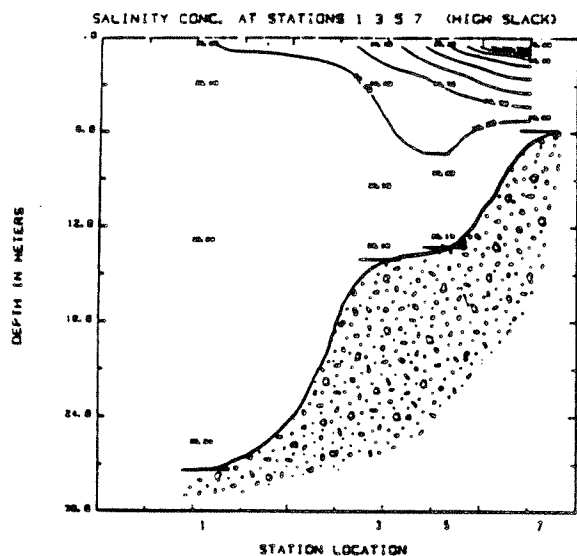
Figure 4.6   Longtitudal contour plot for salinity, dissolved oxygen,
             ammonium-n and nitrate-n + nitrite-n during high slack tide:
             May 1985 Intensive Survey.

4-12

SALINITY CONC. AT STATIONS 1 3 5 7 (FLOOD TIDE)

D. O. CONCENTRATION AT STATIONS 1 3 5 7 (FLOOD TIDE)

NH4-N CONCENTRATIONS AT STATIONS 1 3 5 7 (FLOOD TIDE)

NO3-N + NO2-N CONC. AT STATIONS 1 3 5 7 (FLOOD TIDE)
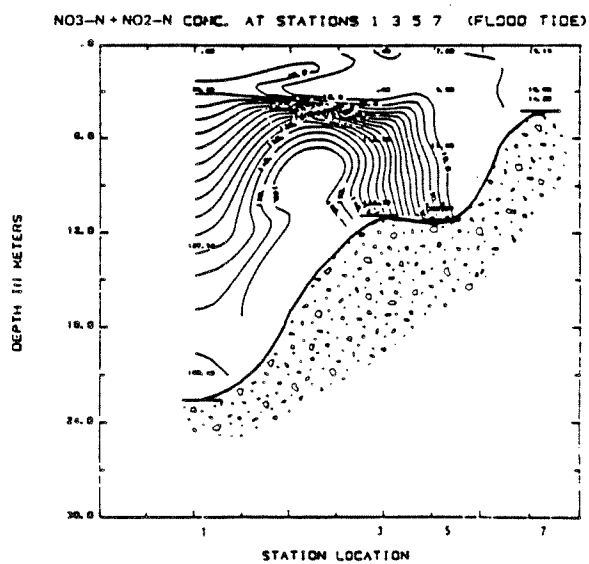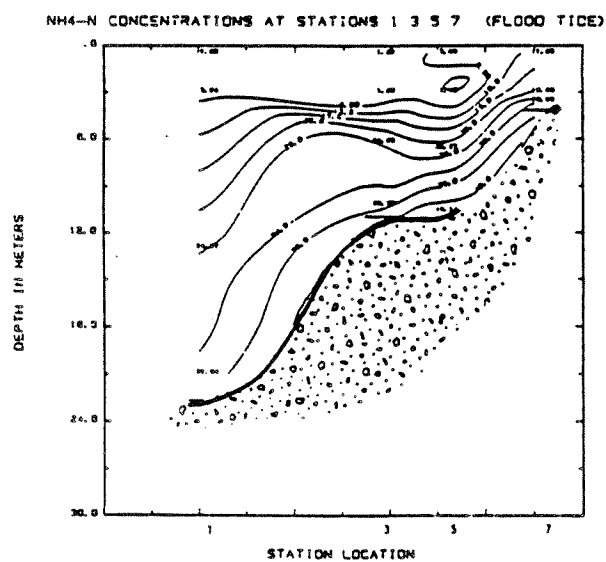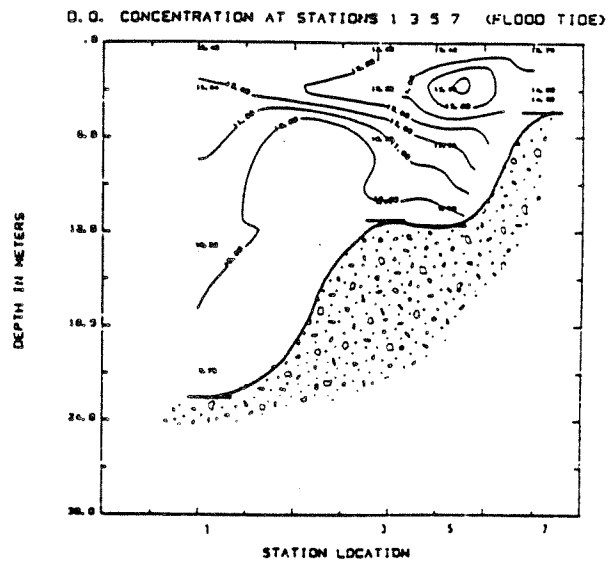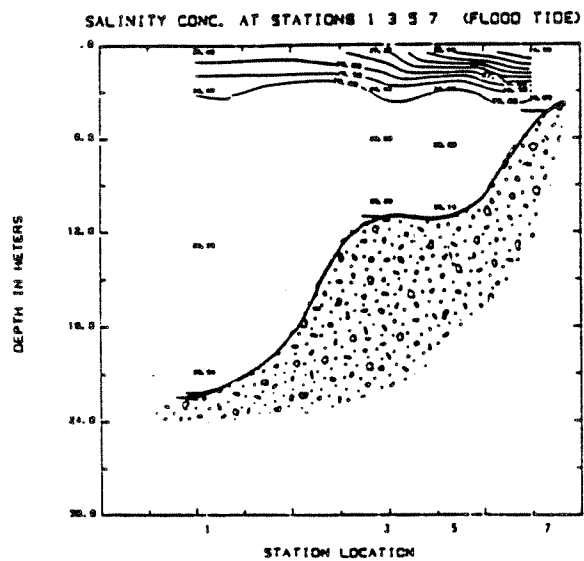
Figure 4.7   Longitudinal contour plot for salinity, dissolved oxygen, ammonium-n and nitrate-n + nitrite-n during flood tide: May 1985 Intensive Survey.

The bottom layer segments show a possible net source in the central segment and a net sink in the lower segment. The bottom layer of the lower segment is always within the photic zone so that the net sink is probably due to algal production. The bottom layer T_r of the middle segment (CB) indicates a net source which could be due to benthic release of ammonium associated with the decay of organic matter in the sediments. The bottom layer of the outer segment (UB) may show a net source.

The relative residence times for nitrate + nitrite show a similar pattern to those of ammonium (Figure 4.5). The upper layer in the lower segment (LB) shows a net source due to the nearby outfall, although the T_r is not as great as was seen for ammonium. The central and outer upper layer segments show a net sink due to algal production. The most significant input flux to these upper layer segments is by vertical advection and mixing. This is evidenced in the longitudinal contour plots (Figures 4.6 and 4.7). The bottom layer segments show the same pattern of T_r as was seen for ammonium. The net source indicated for the bottom layer of the central segment may be due in part to nitrification.

Figure 4.5 shows the relative residence times for dissolved oxygen. Most layers indicate a net source due to algal production. The source could not be due to reaeration since the surface waters are all supersaturated, so that the net transfer of oxygen will be from the surface into the atmosphere. The major flux of oxygen to the upper layers is due to the down-estuary surface flow. The vertical advection and mixing is less important than for the nitrogen species since oxygen is much less stratified.

Nutrient and Dissolved Oxygen Budgets

Nutrients. The nutrient budget is developed from the fluxes shown in Figure 4.5 along with measurements of primary productivity (Section 3.4), SOD/benthic release (Section 3.7) and source loadings (Section 3.5) made during the May survey. Simple ratios of N/Chl a (10) and C/Chl a (112) were

used (see section 4.2) to convert the primary productivity results from the value of 0.4 gC/m^2/day to .09 gN/m^2/day. Surface areas in the LB, CB and UB segments were used to convert the benthic release, areal productivity and gas exchange rate data into lbs/day. Table 4.2 shows the nutrient budget for the Inlet as a whole. The sources and sinks are classified as either internal or external for ammonium, nitrate + nitrite and Total Inorganic N, which is the sum of the nitrogen species. The numbers in parentheses next to the fluxes are the percentage of the total source or sink represented by that flux.

The total Inlet budget (Table 4.2) indicates that Puget Sound supplies 21 percent of the ammonium and 92 percent of the nitrate+nitrite to the Inlet and 63 percent of the total inorganic nitrogen. LOTT supplies about 36 percent of the ammonium and 8 percent of the nitrate + nitrite for an overall contribution of 19 percent for the nitrogen species. Benthic release of ammonium contributed about 44 percent of the ammonium for an 18 percent overall contribution of nitrogen to the Inlet. The major sinks were primary production and the seaward flux of surface water to Puget Sound. The overall budget for the Inlet is essentially in balance.

Table 4.2   Nutrient budget for Budd Inlet--
total inlet

External (E) Internal (I) Source/Sink	SOURCES NH4-N (%) (lbs/day)	NO3+NO2-N (%) (lbs/day)	Total Inorg. N (%) (lbs/day)
FROM			
Puget Sound (E)	744 (20)	4927 (92)	5671 (63)
LOTT STP (E)	1303 (36)	415 (8)	1718 (19)
Benthic Release (I)	1600 (44)	----	1600 (18)
TO	SINKS		
Puget Sound (E)	441 (5)	2688 (26)	3130 (28)
Inner Inlet (E)	398 (5)	253 (2)	651 (6)
Primary Prod. (I)	(90) 7504	(72)	7504 (66)

Table 4.3 shows the budget for the nitrogen nutrients in the surface layer. The fluxes to the surface layer shown in Figure 4.5 are greater than the average loading from LOTT due to a nutrient-rich pocket of water which was advected through the upper boundary at station 7 during the ebb of occupations 9, 10 and 11 (see Figure 4.1). Nutrient fluxes into the upper layer before the nutrient-rich water arrived were about 400 lbs/day and 1,000 lbs/day for nitrate + nitrite and ammonium, respectively, which are similar to the measured LOTT loadings of 415 and 1303 lbs/day.

Table 4.3 Nutrient budget for Budd Inlet--
surface layer only

External (E) Internal (I) Source/Sink	SOURCES NH4-N (%) (lbs/day)	NO3+NO2-N (%) (lbs/day)	Total Inorg. N (%) (lbs/day)
FROM			
Vertical Flux (E)	320 (20)	1467 (78)	1787 (51)
LOTT STP (E)	1303 (80)	415 (22)	1718 (49)
TO	SINKS		
Puget Sound (E)	442 (6)	2688 (26)	3130 (29)
Primary Prod. (I)	(94)	7504 (74)	7504 (71)

These results indicate that the major sources of nitrogenous nutrients to Budd Inlet are Puget Sound, LOTT and benthic release, contributing approximately 60 percent, 20 percent and 20 percent, respectively. About 50 percent of the input to the surface layer in the box model was from vertical mixing with the other 50 percent contributed by LOTT.

Since the benthic nutrient release is linked to the SOD which is directly linked to nitrogen-limited primary production (see Section 4.2), a reduction in point source loadings from LOTT would also result in a decrease

in benthic release. Consequently, these two sources, which presently represent about 40 percent of the loading, could be substantially reduced by a reduction in the loading from LOTT.

Oxygen. The budget for oxygen was calculated using the fluxes from the box model shown in Figure 4.5 along with the SOD/benthic release and primary productivity measurements mentioned previously together with estimates of surface gas exchange. The budgets were determined for the whole Inlet (Table 4.4) and for the surface layer (Table 4.5). The major point source of dissolved oxygen to the Inlet during the May survey was Capitol Lake. The flux from the inner Inlet to the surface layer was assumed to contain the flux from Capitol Lake. Therefore, the source from the inner Inlet shown in Tables 4.4 and 4.5 was reduced to reflect the contribution from Capitol Lake.

The overall budget in Table 4.4 shows that the major fluxes of oxygen into and out of the Inlet are at the boundaries at the head (Inner Inlet) and the mouth (Puget Sound). These two boundaries account for over 90 percent of the oxygen interchange in the Inlet. The fluxes at the head are predominantly due to the transport of oxygen into the Inner Inlet from Puget Sound. The other two sources are primary production (15 percent) and Capitol Lake (3 percent), while the two other sinks are benthic SOD (6 percent) and surface exchange (3 percent).

The input and output fluxes at the head essentially cancel one another, so that there is no net transport of oxygen through that boundary except for what is introduced from Capitol Lake. The net flux at the mouth is out at the surface due to higher oxygen values in the surface layer as a result of photosynthesis. The net results show a net source of 17 thousand lbs/day which indicates that the Inlet is approximately in balance with respect to oxygen given the probable errors in these estimates.

Table 4.4 Oxygen budget for Budd Inlet--
total inlet

External (E) Internal (I) Source	Sources $D.O.$ (%) (10^3 lbs/day)	Sinks $D.O.$ (%) (10^3 lbs/day)	Net $D.O.$ (10^3 lbs/day)
Puget Sound (E)	314 (51)	358 (55)	-44
Inner Inlet (E) (w/o Capitol Lake)	197 (32)	194 (36)	3
Capitol Lake (E)	16 (3)	- - - -	16
Benthic SOD (I)	- - - -	33 (6)	-33
Primary Prod. (I)	90 (15)	- - - -	90
Surface Exchange (I)	- - - -	15 (3)	-15
Total	617	600	17

Table 4.5 Oxygen budget for Budd Inlet--
surface layer only

External (E) Internal (I) Source	Sources $D.O.$ (%) (10^3 lbs/day)	Sinks $D.O.$ (%) (10^3 lbs/day)	Net $D.O.$ (10^3 lbs/day)
Puget Sound (E)	- - - -	358 (96)	-358
Inner Inlet (E) (w/o Capitol Lake)	197 (54)	- - - -	197
Capitol Lake (E)	16 (4)	- - - -	16
Vertical Flux (I)	185 (32)	- - - -	185
Primary Prod. (I)	90 (10)	- - - -	90
Surface Exchange (I)	- - - -	15 (4)	-15
Total	455	373	115

The oxygen budget for the surface layer (Table 4.5) shows that the major input fluxes are from the inner Inlet and from vertical mixing. Primary production (10 percent) and Capitol Lake (4 percent) are the other two sources to the upper layer. By far the major output is the flux of the seaward flowing surface water to Puget Sound with diffusion out of the surface (surface exchange) representing only 4 percent of the total total output. There is an overall net gain in the surface layer of 115 thousand lbs/day due to primary productivity which is of similar magnitude to the internal source of 90 thousand lbs/day.

Overall results indicate the Inlet is in balance with respect to oxygen while the surface layer is gaining oxygen. Another important point brought out by this analysis is that the oxygen exchange within the Inlet is predominantly due to exchange with Puget Sound at the mouth. This implies that as the concentrations in Puget Sound change with the season, they will have an immediate effect on the overall concentration within the Inlet. This will consequently be an important consideration in the dynamic modeling.

4.2 DYNAMIC MODELING

Introduction

In choosing a dynamic model to be used in this study, it was necessary that a number of key factors could be accommodated by the model.

o   The model must account for the mixing/dispersion dynamics such as river flow, density currents and wind driven currents which control the advective processes. It must also include the wind and tidal mixing which control the diffusive processes. It must also be able to account for a constantly changing free surface due to the large tidal range within the Inlet.

o   The model must describe the dynamics of the nutrient/algae/DO system and be able to include loadings of BOD, DO and nutrients which may occur anywhere within the Inlet and which may vary with time.

o   The model must allow for sources and sinks at the surface and the bottom.

o   The model must be relatively simple and not cumbersome or too costly to be efficiently applied.

To satisfy these requirements, a laterally averaged two-dimensional finite-difference model developed by J. E. Edinger Associates was adapted for use in this study. This model includes all of the key factors and was preferable over vertically averaged two-dimensional models which would not give the vertically stratified estuarine flow.

The discussion of the model formulation, calibration and verification is presented in two sections. The first section deals with the physical processes of flow and circulation. The second section discusses the source, sink and reaction rates used for the eight interactive water quality constituents chosen to model the DO dynamics in Budd Inlet.

Physical Processes/Hydrodynamics

Model Formulation. The hydrodynamic model chosen for this study is a generalized hydrodynamics and transport model (GLVHT). The transport equations are solved in the longitudinal and vertical dimensions over time and include the transport of heat, salt and water quality constituents. The implicit finite difference solution technique permits the use of large and variable time steps so that either short- or long-term simulations may be performed. A more detailed explanation of the GLVHT model can be found in Appendix B, "Mathematic Basis of GLVHT".

Four types of data are required to apply the GLVHT model: the waterbody geometry; time-varying boundary condition data; source, sink and reaction rates for each of the constituents being simulated; and hydraulic and physical parameters. The initial conditions are derived from the verification data and can be either constant values throughout the finite-difference grid or vertically stratified. The other option is to make an initial run and save the results as the initial conditions for following simulations. For Budd Inlet, a combination of constant and stratified initial conditions for water quality constituents was adequate due to the large tidal exchange and fairly rapid mixing within the Inlet.

Developing the waterbody geometry for Budd Inlet involved dividing the inlet into longitudinal segments of length (Δx) and vertical layers of thickness (Δz) (Figure 4.8). The width of each cell thus formed is then taken as the area at that particular elevation divided by the length. Therefore, an average width is used such that the sum of each individual cell's area and volume reproduces the waterbody's elevation-area-volume curves. Outfall locations, tributaries as well as any other input sources can then be coupled into the resulting finite difference grid in both the longitudinal and vertical dimensions.

The time varying boundary condition data for Budd Inlet include meteorology data used for surface heat exchange, wind stress, evaporation and gas exchange computations, point source inflow rates and concentrations for each constituent to be modeled, and tide records and vertical profiles of temperature, salinity and constituent concentrations for open boundary applications. The tides were modeled using tidal constituent data derived from the 29 day analysis of Dofflemeyer Point in 1978 obtained from the Tidal Datums Section of the Tides and Water Branch of NOAA.

The third type of data required is source, sink and reaction rates for each of the modeled constituents. This data is discussed in <u>Biochemical Processes/Water Quality Module</u>. The fourth type of data are hydraulic and physical parameters such as the Chezy coefficient and horizontal dispersion coefficient.
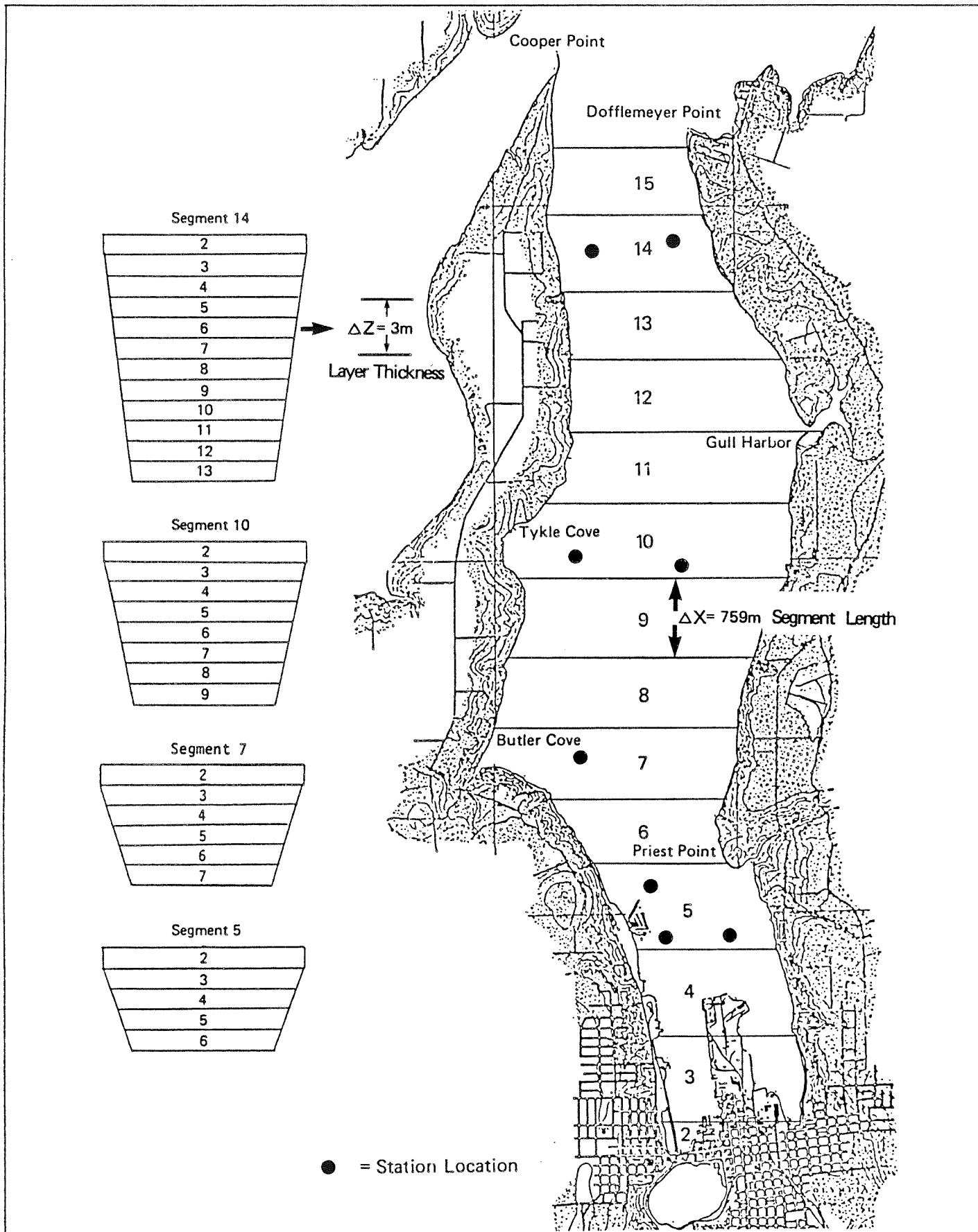
Figure 4.8   Segment locations, length (ΔX) and layer thickness (ΔZ) for
GLVHT hydrodynamic model of Budd Inlet.
(URS and J. Edinger & Associates)

The model generates snapshot grids of velocities and constituents and longitudinal profiles of surface elevations, and values through time of a particular parameter at a specific location.

Calibration. To calibrate the model, various coefficients must be developed with supporting data representative of the modeled system. The three major coefficients in the model which can affect mixing and transport are the vertical (K_v) and longitudinal (K_1) dispersion coefficients and the Chezy coefficient (C). The dispersive transport in an estuary is induced by the internal turbulence created by the tidal flows coupled with the bottom friction and surface wind stress. The longitudinal and vertical dispersion coefficients represent eddy diffusion, carrying away turbulent energy in the longitudinal and vertical directions respectively. The Chezy coefficient represents turbulent energy loss due to the frictional influence of the bottom.

We estimated the vertical dispersion coefficient (K_v) from the vertical diffusive exchange coefficient (E_v) determined in the box modeling (Section 4.1). The K_v was calculated as:

$$K_v = E_v (z_b - z_t)/\text{Area} \qquad (4.15)$$

where $z_b - z_t$ is the distance between the layers used in estimating E_v and Area is the horizontal cross-sectional area between the layers. The tidally averaged values are shown in Table 4.6.

Table 4.6   Estimates of K_v for the three box model segments of Budd Inlet

Section	E_v (m^3/sec)	Area (10^6 m^2)	$z_b - z_t$ (m)	K_v (10^{-6} m^2/sec)
Lower Inlet	3.23	3.17	1.25	1.27
Central Inlet	5.43	4.57	7.5	8.95
Upper Inlet	20.58	7.61	18.5	49.98

For comparison, molecular diffusivity of salt is about 1.5×10^{-9} m^2/sec, which is about 10,000 times smaller than these eddy diffusion coefficients. In the dynamic model K_v is a function of depth. The value of K_v was calibrated in the dynamic model to approximate the value of 10×10^{-6} m^2/sec in the Central Inlet at about 5 meters below the surface.

The longitudinal dispersion coefficient (K_1) is generally many orders of magnitude greater than the vertical coefficient (K_v), on the order of 1 to 1,000 m^2/sec (Bowie, 1985). Observed values in estuaries from dye experiments and numerical modeling range from 10 to 1500 m^2/sec (Fisher et al., 1979). Elliott (1976) estimated a ratio of K_1/K_v of about 10^6 in the Potomac Estuary. Using this factor, values were estimated of K_1 ranging from 2 to 100 m^2/sec. The calibration process revealed that values of K_1 of less than 10 m^2/sec yielded temperature and salinity distributions similar to measured values.

The Chezy coefficient relates the bottom stress to the velocity above the bottom. We can estimate a value for the coefficient from measurements of the frictional velocity (U_*) calculated from the relationship given by:

$$C = g^{1/2} (U/U_*) \qquad (4.16)$$

where g is the acceleration of gravity and U is the velocity above the bottom. We can use the Karman-Prandtl equation:

$$U_* = U \, k/\ln(z/z_0) \qquad (4.17)$$

to calculate the frictional velocity which when substituted into (4.18) yields:

$$C = g^{1/2} (\ln(z/z_0)/k) \qquad (4.18)$$

where z is the height above the bottom where U is measured, z_0 is the roughness length characterizing the surface roughness and k is Von Karmon's constant of 0.41. The roughness length is related to the roughness element height which in turn is related to the median grain size diameter of the surface sediments.

The bed roughness was determined using an iterative process calculating U_* and z_0 using the Karman-Prandtl equation and an empirical relationship between U_* and z_0. An initial value of $z_0 = .001$ cm was made and a Reynolds number calculation indicated smooth flow so that z_0 was calculated as $z_0 = \text{viscosity}/(9\ U_*)$. This new value for z_0 was substituted into the Karman-Prandtl equation and a new value of U_* determined. After three iterations, the values converged to yield values of z_0 between .002 and .004 cm for velocities of 10 and 20 cm/sec at one meter above bottom respectively. In all calculations we assumed a grain size of 7 phi (7.8×10^{-4} cm) and a viscosity of 1.25×10^{-2} cm^2/sec.

Based on this analysis using our estimated z_0 to be between .002 and .004 cm, we estimated C to be between 30 to 80 m$^{1/2}$/sec. This was the range we used in our calibration.

<u>Verification</u>. The first step in verification of the dynamic model for Budd Inlet involved comparing the predicted current speeds with those actually measured within the Inlet during the May 1985 intensive survey. During the September 1984 survey, a storm event occurred with strong westerly winds which created a strong cross-channel circulation (see Section 3.3). Therefore, the September comparison was not used in verification.

Since the Budd Inlet model is structured in two dimensions, the model predicts the average longitudinal current speed in each longitudinal segment and vertical layer (see Figure 4.8). The north-south component of measured current meter data was compared with that predicted by the model. Comparisons were accomplished by plotting predicted current speeds with measured current speeds. Figures 4.9-4.10 summarize the May 1985 comparisons. Positive values indicate a northerly current and negative values indicate a southerly current. Exact correlation between the predicted and observed current speeds is constrained due to the coarse vertical scale of the model and the fact that the model is laterally
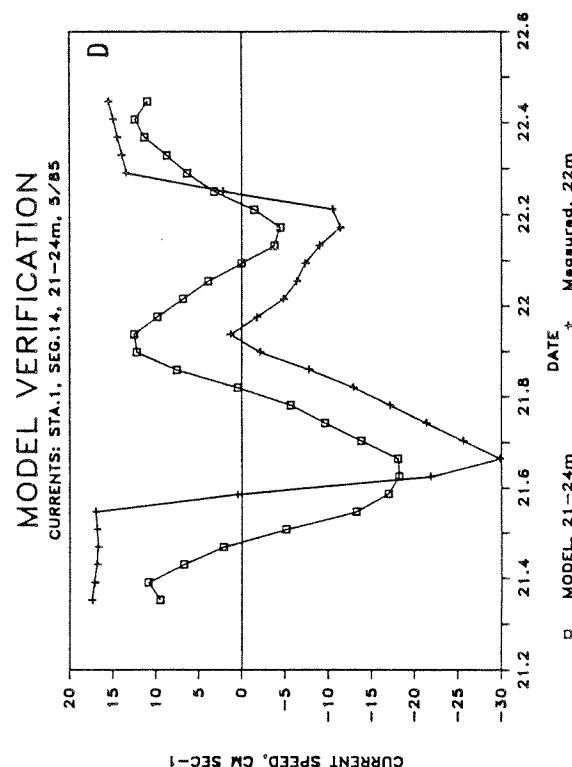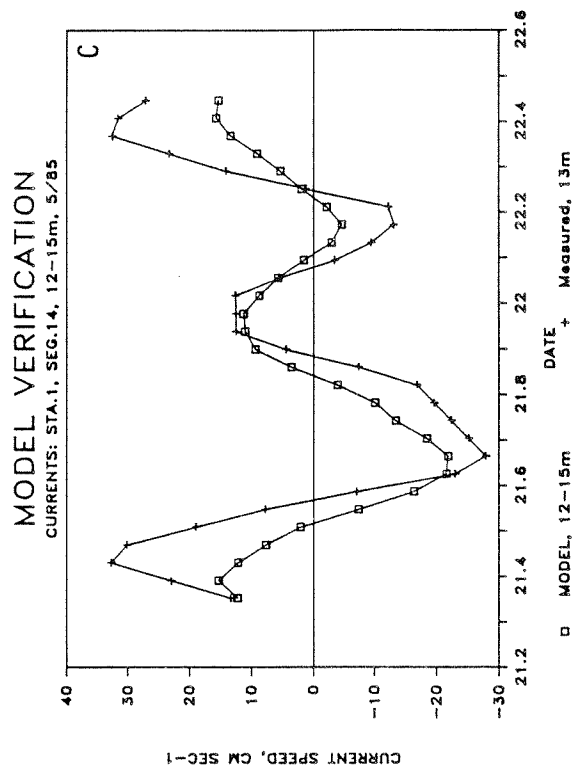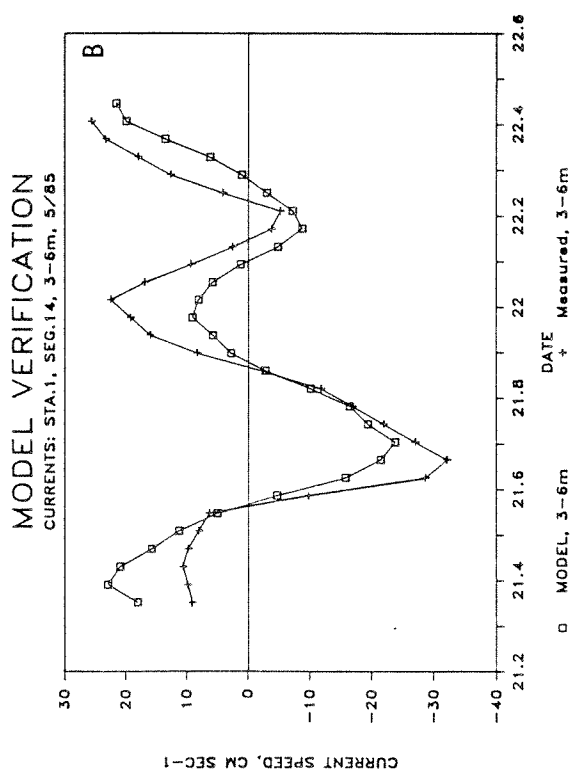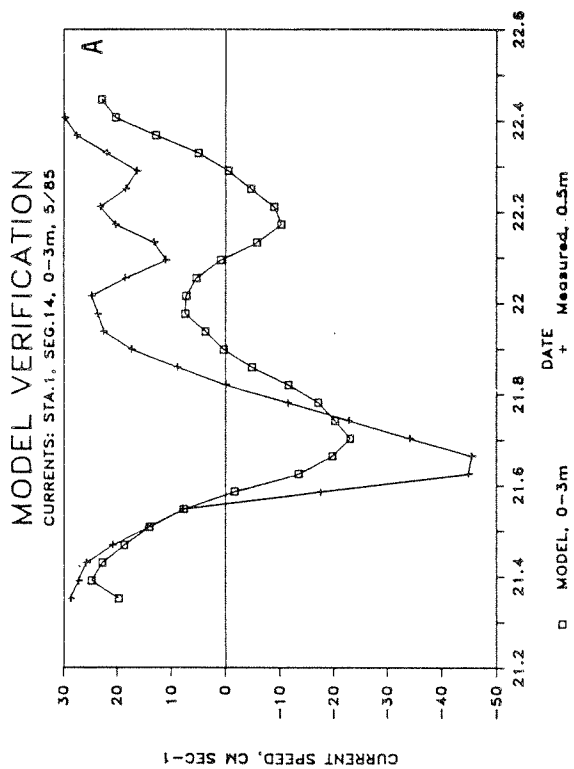
Figure 4.9   Predicted and observed current speeds at Station 1: 0 to 3 meters (A), 3 to 6 meters (B), 12 to 15 meters (C) and 21 to 24 meters (D) for the May 1985 Intensive Survey.
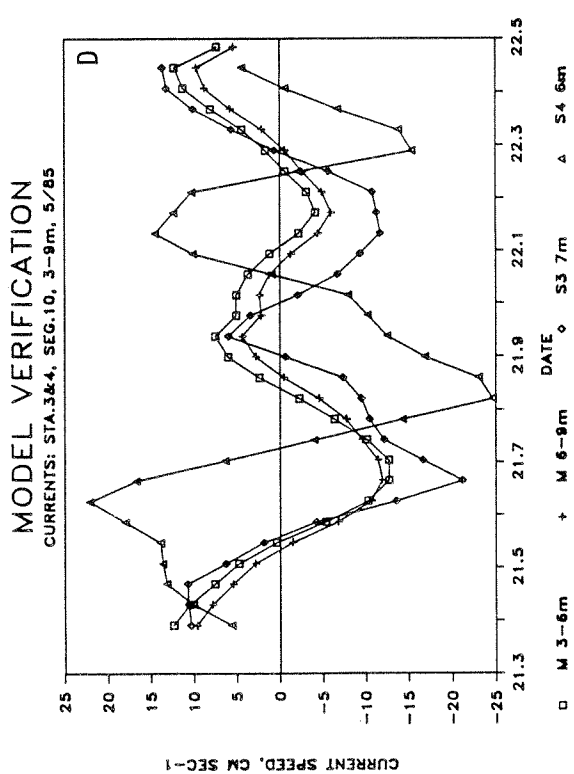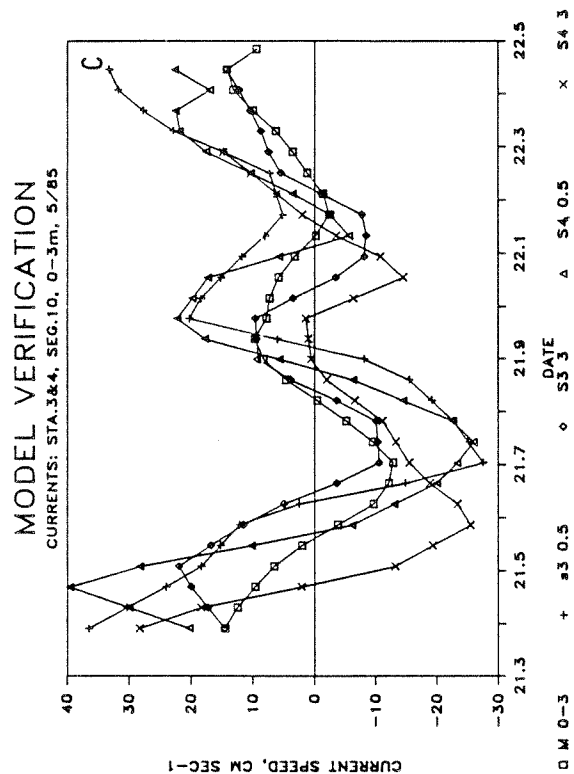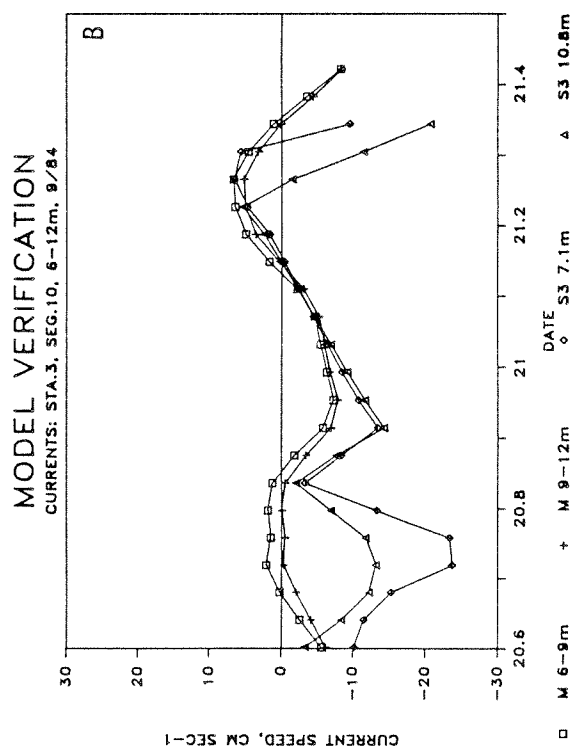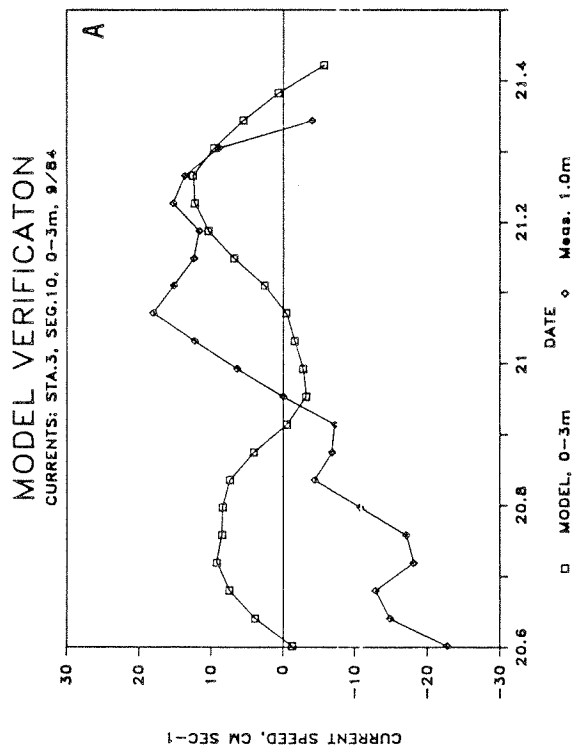
Figure 4.10 Predicted and observed current speeds at Station 3: 0 to 3 meters (A)
and 6 to 12 meters (B) for the September 1984 Intensive Survey and
Station 3 and 4: 0 to 3 meters (C) and 3 to 9 meters (D) for the
May 1985 Intensive Survey. M = model value, S3 = Station 3,
S4 = Station 4 observed values.

averaged. The model will tend to predict lower maximum current speeds for stations away from the shore since the model averages in the slower moving currents near the shoreline boundary. This artifact is generally more pronounced at higher velocities. Any other lateral circulation such as strong cross-channel wind driven currents or eddies would not be modeled accurately.

The comparisons also indicate that currents which were measured near the surface in the upper 1.5 meters were somewhat stronger than the model averaged value in the upper 3.0 meters indicating some stratification of flow in the upper three meters. Based on these comparisons the model is representative of the velocity distribution and overall circulation within the Inlet.

Biochemical Processes/Water Quality Module

Model Formulation. Eight (8) water quality constituents were used in the water quality module. They are: organic nitrogen (Org-N), ammonium (NH_4-N), nitrite (NO_2-N), nitrate (NO_3-N), Algae (Chl a), pheopigments, dissolved oxygen, and biochemical oxygen demand (BOD5). Three external source/sink terms: sediment oxygen demand (SOD), fecal pellets and atmospheric gas exchange reaeration were included. The major processes are shown in Figure 4.11 and discussed in the following section.

Biochemical processes are simulated within the water quality module using internal source/sink and reaction rate terms for each of the water quality constituents. Each constituent has reaction rates, settling velocities, and interactions with other constituents, which are incorporated into the source/sink and reaction rate term. These rate terms represent rate expressions of the form:

$$dC_1/dt = -K_1 C_1 + K_2 R_n (C_1 C_2 / a + BC_1) - K_3/z C_1 + \ldots \qquad (4.19)$$

Budd Inlet Water Quality Module

Schematic
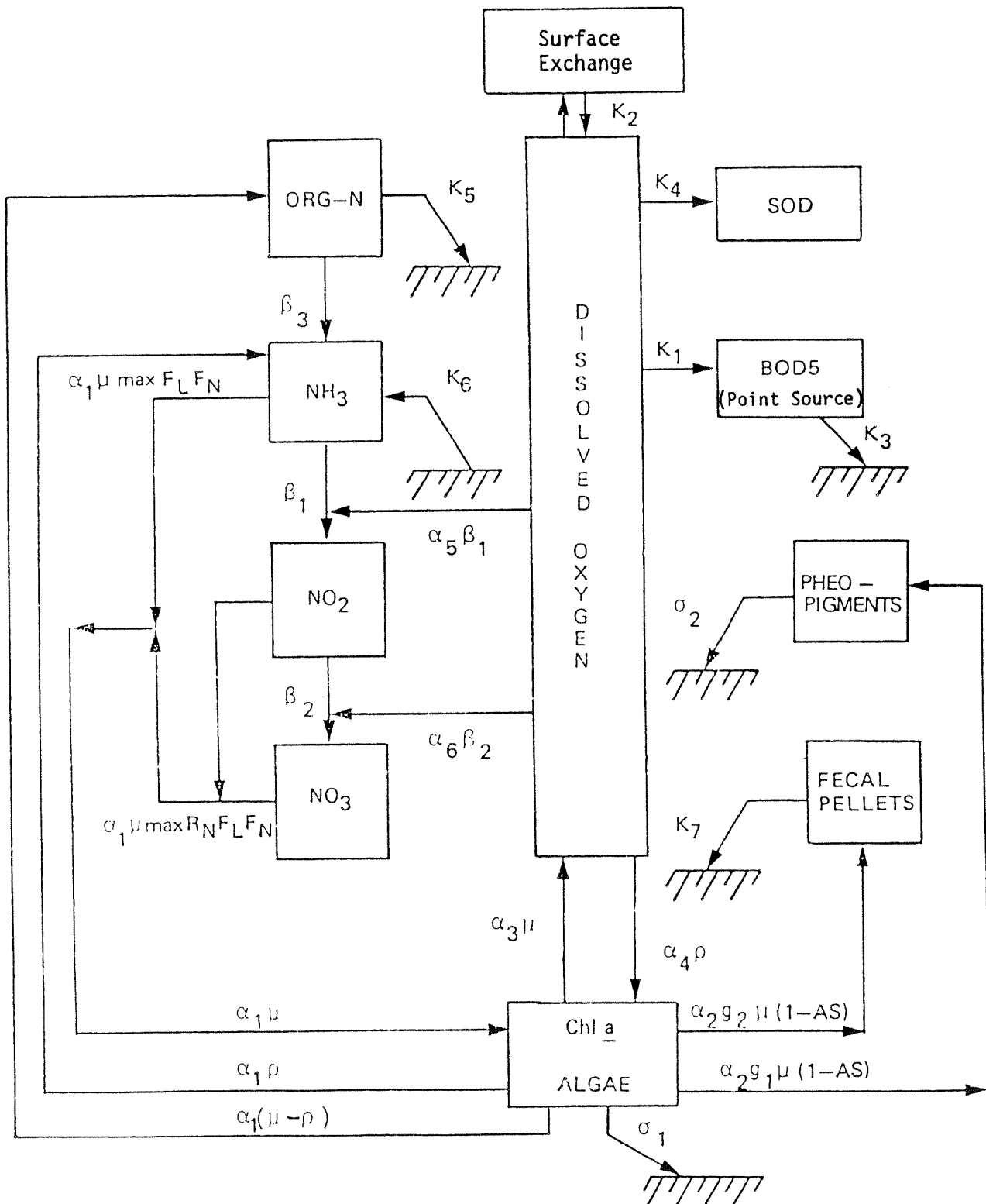
Figure 4.11 Schematic diagram of the water quality module utilized by the GLVHT hydrodynamic model of Budd Inlet.

where C_1 and C_2 are the concentrations of constituents 1 and 2 and the other terms represent rate coefficients (K_1, K_2), settling velocities (K_3), etc. Rate constants and coefficients used in the transfer of constituents from one pool to another are calculated prior to the evaluation of the overall rate term. Constituent concentrations and rate coefficients at each new time step are computed based on concentrations at the previous time step on each pass through the water quality module. This approach is valid for short computational time steps within which the biochemical processes can be assumed to change linearly with time. This eliminates having to use more lengthy and time consuming computational methods to simultaneously solve for each constituent concentration at each time step. This time savings allows for more efficient use of computer time. The specific formulations for each of the water quality constituent interactions are presented in the following discussion.

C_1: <u>Biochemical Oxygen Demand (BOD5-Point Source)</u> The BOD chosen to be modeled in the water quality module does not include BOD from algal production or any other internal source. The point source BOD is modeled using the 5-day first order rate expression from LOTT effluent BOD5 (Yake, 1981). The rate expression is:

$$dC_1/dt = -K_1 C_1 - (K_3/D) C_1 \quad (4.20)$$

where

K_1 = first order deoxygenation rate constant, 1/time

K_3 = settling rate of BOD, m/time

D = thickness of modeled layer, m

The deoxygenation rate constant varies with temperature through the empirical relation:

$$K_1(t) = K_1(20) \; CK_1^{(t-20)} \qquad (4.21)$$

where $K_1(20)$ is the rate constant at 20 degrees C and CK_1 is the temperature correction term. Table 4.7 lists the range of values, selected value, units, description and references for these constants and the other parameters used in the water quality module.

C_2: <u>Pheopigments</u> Pheopigment concentrations were modeled using the following rate expression:

$$dC_2 = (1-AS) \; \alpha_2 \; g_1 - (\sigma_2/D)C_2 \qquad (4.22)$$

where

AS = the assimilation efficiency of zooplankton

α_2 = ratio of pheopigments to chlorophyll

g_1 = grazing rate of microzooplankton, 1/time

σ_2 = the sinking rate of pheopigments, m/time

D = thickness of the bottom layer of the model, m

In this expression we are assuming that the major internal source of pheopigments is the grazing of phytopankton by microzooplankton. Welschmeyer and Lorenzen (1985) showed in their study of Dabob Bay, Washington that the concentration of pheopigments which can be measured from water samplers were due to the grazing of microzooplankton which produce fecal debris with relatively slow sinking rates. The grazing rate of microzooplankton was shown to be about half that of the fecal pellet-producing macrozooplankton which we will discuss later. The grazing rate g_1 is given by the expression:

$$g_1 = K_g \; (1.066)^{(t-20)} \; C_7 \qquad (4.23)$$

where K_g is the ingestion rate (1/time) along with its temperature function (Bowie et al., 1985). One minus the assimilation efficiency (As) is a

Table 4.7 Input parameters for the GLVHT
hydrodynamic model of Budd Inlet

WATER QUALITY MODEL
INPUT PARAMETERS

Input Parameter symbol	code name	Description	Units	Range of Value	Value used	References
α_0	ALPHA0	Ratio of oxygen to carbon during respiration	mg O/mg C	2.67	2.67	Bowie, et al., 1985
α_1	ALPHA1	Ratio of nitrogen to Chl a in algae	mg N/mg Chl a	6-19	12	O'Connor, 1981
α_2	ALPHA2	Ratio of Pheopigments to Chlorophyll a	mg Pheo/mg Chl a	.66	.66	Shuman and Lorenzen, 1975
α_3	ALPHA3	Oxygen production per unit of algal growth	mg O/mg Chl a	80-730	360	O'Connor, 1981
α_4	ALPHA4	Oxygen uptake per unit of aglae respired	mg O/mg Chl a	80-730	295	O'Connor, 1981
α_5	ALPHA5	Oxygen uptake per unit of NH3 oxidation	mg O/mg N	3.43	3.43	Bowie et al., 1985
α_6	ALPHA6	Oxygen uptake per unit of NO2 oxidation	mg O/mg N	1.14	1.14	Bowie et al., 1985
α_7	ALPHA7	Fraction of organic sediment loading which is readily metabolized	----	.2 - .5	0.5	Nixon, 1981

Table 4.7 (Continued)

WATER QUALITY MODEL
INPUT PARAMETERS

Input Parameter symbol	code name	Description	Units	Range of Value	Value used	References
μ_{max}	GROWMAX	Maximum specific growth rate of algae	1/day	0.2 - 5.0	4.3	Bowie et al., 1985
ρ	RESP	Algal respiration rate	1/day	.043 - .14	.043	Bowie et al., 1985
K_{gmax}	GRAZEMAX	Maximum zooplankton grazing rate	1/day	1.7	1.7	Winter et al., 1975
K_z	CKZOO	Michaelis-Menten constant for grazing	ug/L Chl $\underline{a}$	2.5	2.5	Winter et al., 1975
AS	AS	Assimilation efficiency of zooplankton grazing	----	.5 - .8	0.5	Bowie et al., 1985
β_1	CKNH3	Rate constant for oxidation of NH_3 to NO_2	1/day	.003 - .1	.02	Bowie et al., 1985
β_2	CKNO2	Rate constant for oxidation of NO_2 to NO_3	1/day	.09 - 10	.09	Bowie et al., 1985
β_3	CKORGN	Rate constant for oxidation of organic N to NH_3	1/day	.001 - .4	.001	Bowie et al., 1985
σ_1	ALGSET	Settling rate for algae	m/day	.1 - .8	.6	Welschmeyer and Lorenzen, 1985
σ_2	PHAEOSET	Settling rate for phaeopigments	m/day	1 - 12	2.2	Welschmeyer and Lorenzen, 1985

Table 4.7 (Continued)

WATER QUALITY MODEL
INPUT PARAMETERS

Input Parameter		Description	Units	Range of Value	Value used	References
symbol	code name					
K_1	CK1	Carbonaceous BOD decay rate	1/day	f(temp)	.2 (@ 20C)	Yake, 1981
K_2	CK2	Surface transfer rate	m/day	f(temp, wind speed)	0.9 (@ 20C, 10 mph)	Emerson, 1975 Broecker and Peng, 1974
K_3	CK3	Carbonaceous BOD sinking rate	1/day	0.1 - 8.6	1.0	Ozturgut and Lavelle, 1984
K_4	CK4	Sediment oxygen demand (SOD)	mg O/m^2/day	f(organic loading)		See text
K_5	CK5	Overall organic N sinking rate	1/day	$f(q_1, \sigma_2 K_7)$		See text
K_6	CK6	Ammonium remineralization from benthic SOD	mg N/m^2/day	$f(K_4)$		See text
K_7	CK7	Loss rate of fecal pellets to the sediments	mg C/m^2/day	$f(\mu, g_2, AS)$		See text
K_n	CKMM	Michaelis-Menten constant for NH3 and NO3	mg N/L	.0015 - .15	0.01	Bowie et al., 1985
R_n	RATIONO3	Ratio of max NO3 uptake rate to max NH3 uptake rate	----	f(NH3)	.075 (minimum)	Paasche and Kristiansen, 1982

4-34

fraction of ingested phytoplankton which are excreted. The ingestion rate is a function of the algal concentration (C_7) through a Michaelis-Menton type saturation feeding formulation:

$$K_g = K_{gmax} (C_7/(K_z + C_7)) \qquad (4.24)$$

where K_z is the half-saturation value of algal concentration. Since the zooplankton are not explicitly modeled, they are assumed to have a constant concentration of from 10 to 20 mg C/m^3 (Anderson et al., 1985; Winter et al., 1975) which is incorporated into the maximum ingestion rate K_{gmax} from Winter et al. (1975).

C_3: <u>Nitrate-N (NO_3-N)</u> The rate expression for modeling the nitrate concentration is given by:

$$dC_3/dt = \beta_2 C_4 - R_n \, \alpha_1 \, u_{max} \, F_L \, R_{NO3} \, (C_3/(K_n + C_3)) \, C_7 \qquad (4.25)$$

where

$\quad \alpha_1 \quad$ = ratio of nitrogen to chlorophyll in algae

$\quad \beta_2 \quad$ = rate constant for nitrite oxidation, 1/time

$\quad R_n \quad$ = ratio of maximum nitrate uptake rate to that of ammonium

$\quad u_{max}$ = maximum growth rate of phytoplankton, 1/time

$\quad F_L \quad$ = light limitation factor for phytoplankton growth

$\quad R_{NO3}$ = NO_3-N fraction of total NO_3-N + NO_2-N

$\quad K_n \quad$ = the Michaelis-Menten constant for nitrogen, ug/L

The change in concentration of nitrate is controlled by the internal source due to nitrite oxidation and the sink due to algal uptake. We have used a functional relationship, R_n, which we will call the ammonium inhibition factor, to model the inhibition of nitrate (and nitrite) uptake by ammonium which is a well established phenomenon for diatoms in marine waters (see Section 3.1). The inhibition factor will be described in the phytoplankton rate expression discussion.

4-35

To model nitrate and nitrite as independent species, we have assumed that nitrate and nitrite are each utilized in proportion to their fraction of the total concentration of these two species. The R_{NO3} ratio represents this fraction for nitrate.

C_4: __Nitrite (NO$_2$-N)__ The rate expression describing the change in nitrite concentration in the model is given by:

$$dC_4/dt = -\beta_2 C_4 + \beta_1 C_5 - R_n \alpha_1 u_{max} F_L R_{NO2} (C_4/(K_n + C_4)) C_7 \quad (4.26)$$

where the terms are the analogous to those for nitrate with the exception of the additional input from the oxidation of ammonium β_1.

C_5: __Ammonium (NH$_4$-N)__ The rate expression for ammonium used in the model is given by:

$$dC_5/dt = -\beta_1 C_5 + \beta_3 C_- - \alpha_1 u_{max} F_L (C_4/(K_n + C_4)) C_7 + \alpha_1 \rho C_7$$
$$+ (K_6)_{bottom} \quad (4.27)$$

where

β_3 = rate constant for organic nitrogen oxidation, 1/time

ρ = algal respiration rate, 1/time

K_6 = rate constant for sediment release, mg/m^2/time

The benthic release of ammonium (K_6) is directly related to the sediment oxygen demand (SOD). Figure 3.40 shows this relationship for a number of benthic release/SOD studies in various estuaries including our study in Budd Inlet (see Section 3.7). We have used the relationship in Figure 3.40 to derive the following expression for benthic ammonium release using the SOD rate K_4, which will be described later.

$$K_6 = .046 K_4 - .11 \quad (4.28)$$

This expression yields benthic ammonium release in units of mg NH$_4$-N/m^2/hr.

C_6: <u>Organic-N (ORG-N)</u> The rate expression for organic nitrogen is given by:

$$dC_6/dt = -\beta_3 C_6 + \alpha_1 C_7(u - \rho) - K_5 \qquad (4.29)$$

where K_5 is the combined loss due to sinking of all the organic nitrogen sources:

$$K_5 = \alpha_1 g_2 (1-AS) - (\alpha_1/\alpha_2)(\sigma_2/D) C_2 - (\sigma_1/D) C_7 \qquad (4.30)$$

The terms not already defined are:

α_2 = ratio of pheopigments to chlorophyll

g_2 = grazing rate of macrozooplankton, 1/time

σ_1 = sinking rate for algae, m/time

The other major loss other than sinking for organic nitrogen is the decomposition rate of β_3 to ammonium. The major internal source is the net production of organic matter in photosynthesis given by $(u - \rho)$.

C_7: <u>Phytoplankton (ALGAE)</u> The rate of change of phytoplankton with time, in units of chlorophyll <u>a</u>, is given by:

$$dC_7/dt = (u - \rho) C_7 - (g_1 + g_2) C_7 - (\sigma_1/D) C_7 \qquad (4.31)$$

In this expression the net growth rate $(u - \rho)$ is reduced by grazing $(g_1 + g_2)$ and sinking σ_1 of algal cells.

The growth rate is given by the expression:

$$u = u_{max} F_L (R_n (C_3 + C_4)/(K_n + C_3 + C_4) + C_5/(K_n + C_5)) \qquad (4.32)$$

where u_{max} is the maximum growth rate which varies with temperature given by:

$$u_{max} = K_p(20)(1.066)^{(t-20)} \qquad (4.33)$$

4-37

and $K_p(20)$ is the maximum growth rate at 20 degrees C. The light limitation function (F_L) is the most commonly used Steele (1965) formulation:

$$F_L = (I(z)/I_s) \, e^{(1-(I(z)/I_s))} \qquad (4.34)$$

where I_s is the saturation light intensity. The light at any depth $I(z)$ is defined by the Beer-Lambert law:

$$I(z) = I_0 \, e^{-\kappa z} \qquad (4.35)$$

where $I(z)$ is the light intensity at depth z below the surface, I_0 is the light intensity at the surface and   is the light extinction coefficient (1/m). The light extinction coefficient is given by the general equation:

$$\kappa = \kappa_0 + a_1 \, (\text{mg Chl } \underline{a}/\text{m}^2) \qquad (4.36)$$

where κ_0 is the light extinction coefficient for all absorption components other than phytoplankton which would include the seawater as well as other dissolved plus particulate material. The a_1 term (m/mg Chl $\underline{a}$) is the self-shading factor which accounts for the self-shading effects due to algal growth. Values for a_1 are generally in the range of .001 to .005 (Smith, 1981). We found that $\kappa_0 = 0.38$ and $a_1 = .005$ were the best fit to our chlorophyll and light extinction data based on our calibration of the phytoplankton sub-model which is discussed in a following section.

Nutrient growth limitation is modeled using both ammonium and the sum of nitrate plus nitrite since it is assumed that nitrate and nitrite are utilized equally in proportion to their concentration. This formulation for nutrient limitation (Paasche and Kristiansen, 1982), using the ammonium inhibition factor, R_n, (Figure 4.12) assumes that both ammonium and nitrate + nitrite are utilized simultaneously and that the maximum sustainable growth rate is the same on both substrates. Only at very low ammonium concentrations will the nitrate + nitrite be utilized in proportion to its share of the total dissolved nitrogen pool. This is in keeping with the

NO3-N:NH4-N Maximum Uptake Ratio
AS A FUNCTION OF NH4-N CONCENTRATION
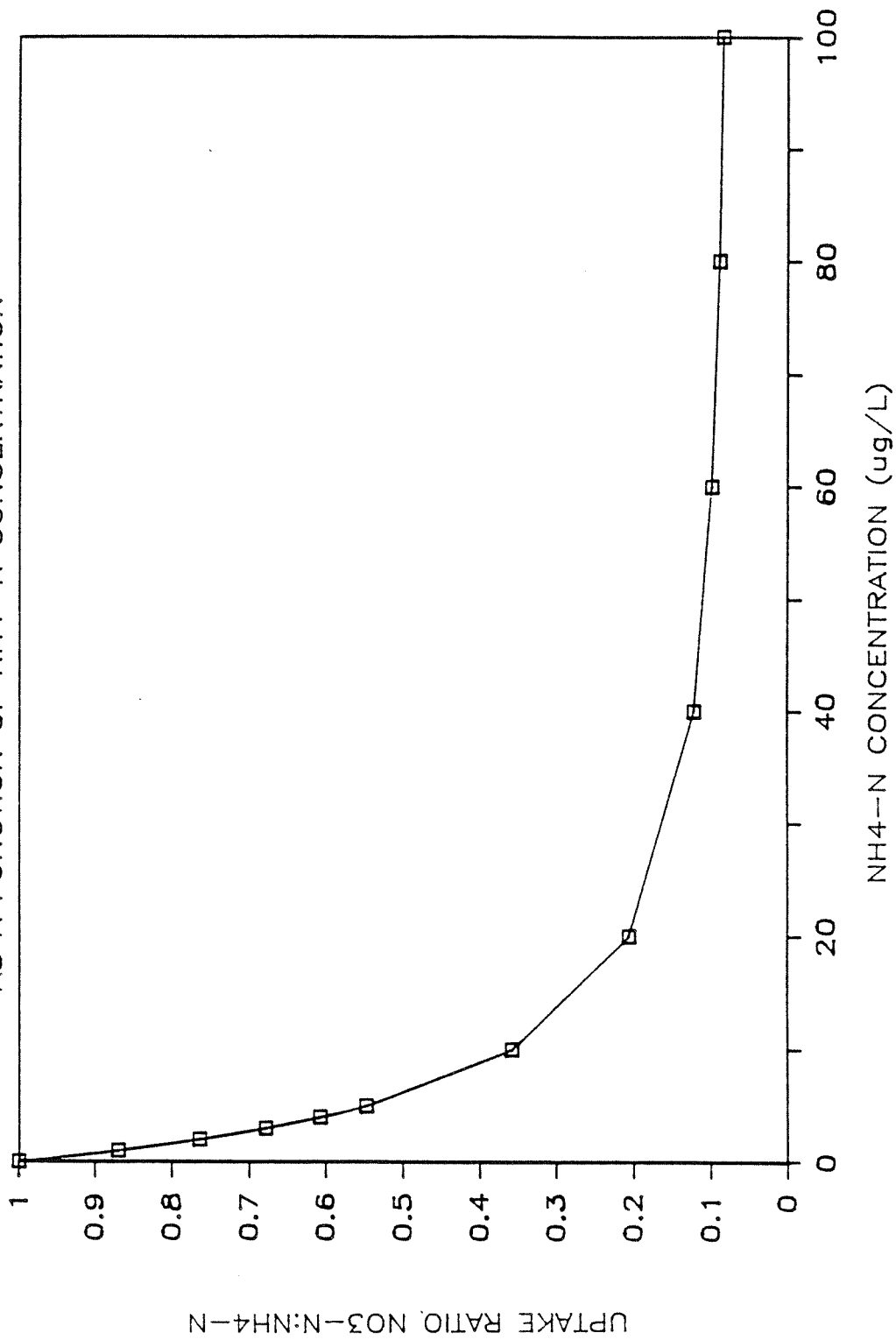
Figure 4.12   Relationship of nitrate to ammonium uptake as a function of ammonium concentration.   From Paasche and Kristiansen (1982).

observations of other researchers (McCarthy et al., 1975,1977; Paasche and Kristiansen, 1982). The inhibition factor is given by:

$$R_n = 0.925(1 + C_5/14)^{-2.2} + .075 \qquad (4.37)$$

which was fit to the data in Paasche and Kristiansen (1982).

C_8: <u>Dissolved Oxygen</u> The rate expression describing the change in dissolved oxygen with time is given by:

$$dC_8/dt = \alpha_3 u C_7 - \alpha_4 \rho C_7 - K_1 C_1 - \alpha_5 \beta_1 C_7 - \alpha_6 \beta_2 C_6$$

$$+ (K_2(C_s - C_8))_{surface} - (K_4)_{bottom} \qquad (4.38)$$

where

α_3 = ratio of oxygen produced per unit chlorophyll

α_4 = ratio of oxygen respired per unit chlorophyll consumed

α_5 = ratio of oxygen utilized per unit of NH_4-N oxidized

α_6 = ratio of oxygen utilized per unit of NO_2-N oxidized

K_2 = surface transfer rate, m/time

K_4 = sediment oxygen demand, $mg/m^2/time$

C_s = oxygen saturation concentration, g/m^3

The surface transfer rate, K_2, is derived from the classical stagnant boundary layer model. This model assumes that the rate limiting step in the transfer of gas between air and water is molecular diffusion through a hypothetical stagnant water film. The top of the stagnant film is assumed to have a gas concentration at equilibrium with the overlying air while the base of the stagnant layer is assumed to be the same concentration as that measured at the surface. The transfer rate is controlled by the thickness of the film (z_{film}) and the molecular diffusivity of the gas (D_{02}) and is given as:

$$K_2 = D_{02}/z_{film} \qquad (4.39)$$

The molecular diffusivity of oxygen is a function of temperature given by:

$$D_{O2} = e^{(-2326/T - 2.86)} \qquad (4.40)$$

where T is the temperature in kelvin (Broecker and Peng, 1974). The film thickness (z_{film}) is calculated from the empirical relation:

$$z_{film} = e^{(-.436\ WA + 7.21)} \qquad (4.41)$$

taken from a compilation of measurements in Emerson (1975). This expression relates the film thickness to the wind velocity, WA (m/sec) which decreases the thickness of the layer as the wind velocity increases.

The saturation concentration, C_s, is calculated from the following equation:

$$\ln C_s = -139.34411 + 1.575701X10^5/T - 6.642308X10^7/T^2 + 1.2438X10^{10}/T^3$$
$$- 8.621949X10^{11}/T^4 - (S/1.80655)\ (3.1929X10^{-2} - 1.9428X10^1/T$$
$$+ 3.8673X10^3/T^2) \qquad (4.52)$$

where S is the salinity (o/oo) and T the temperature is given in kelvin (Benson and Krause, 1984).

The sediment oxygen demand, K_4, is given by the following expression:

$$K_4 = \alpha_7(1000\ K_3\ C_1 + \alpha_4\ \sigma_1\ C_7 + (\sigma_4/\sigma_2)\ \sigma_2\ C_2$$

$$+ \alpha_4\ K_7\ (V_f\ (dt/z))) + \text{Background SOD} \qquad (4.43)$$

where:

$$K_7 = \text{Sum}_z(\ (1-AS)\ g_2\ C_7\ D) \qquad (4.44)$$

which is the depth integrated flux of fecal pellet production in the water column. The other terms not already defined are:

V_f = settling velocity of fecal pellets, m/time

α_7 = fraction of oxygen-demanding organic material which is readily metabolized

Since the SOD is an integral part of the dynamic model, the following section describes in more detail the approach and methodology used in its derivation.

Sediment oxygen demand (SOD). The overall approach we used in deriving equation 4.53 for SOD relied heavily on Pamatmat (1971). In this benchmark study, Pamatmat measured seasonal values of SOD at 23 stations throughout Puget Sound, including Budd Inlet in 1969 and 1970. His major conclusions were that the there was a seasonal cycle of oxygen consumption independent of seasonal temperature changes and that the temperature changes enhanced the seasonal cycle. He also concluded that the cycle was due to the seasonal phytoplankton blooms supplying organic matter to the sediments (Pamatmat and Banse, 1969). These findings lead us to believe that we could incorporate the SOD as a real-time dynamic part of the model using the settling rates of oxygen demanding organic material.

The major components we have used to represent the flux of oxygen demanding material are: algae, pheopigments, fecal pellets and BOD5. The first three components are a direct result of algal production in keeping with the findings of Pamatmat. The fourth component, BOD5, is considered a separate source of oxygen demand and is treated as an external source in the model.

The two major oxygen consuming processes which occur in the sediments are benthic respiration due to the benthic community living in and on the sediment, and chemical oxidation. A certain fraction of the organic matter reaching the sediments is not readily oxidizable and is utilized more slowly or not at all. Nixon (1981) showed that between one quarter and one half of all the organic matter loading to the sediments in coastal marine systems was readily oxidized. We have used this range of values in our modeling to represent the fraction of organic matter reaching the sediments which is quickly oxidized (α_7). The organic matter which is less readily oxidized is considered as the background SOD in equation 4.43. This value is taken

from SOD measurements in January (Pamatmat, 1971) when algal growth is at a minimum. At this time in Puget Sound, Pamatmat found that the total oxygen uptake was correlated with the organic carbon concentration in the sediments, indicating the utilization of the buried organic matter.

Besides the input of organic material, temperature also affects SOD. We have used the Van't Hoff form of the Arrhenius relationship:

$$SOD_t = SOD_{tr} (1.089)^{(t-t_r)} \qquad (4.55)$$

where:

SOD_t = sediment oxygen demand at ambient temperature, $mg/m^2/time$

SOD_{tr} = sediment oxygen demand at the reference temperature t_r, $mg/m^2/time$

t = temperature in degrees C

The temperature coefficient (1.089) was determined from the data in Pamatmat (1971) for Budd Inlet.

Wind Effects. Winds are an important input to the model since they effect vertical mixing and the exchange of oxygen through the surface. Wind speed and direction as well as the other meterological data, including air temperature, dew point and percent sky cover, were taken from data collected at the Olympia airport at four hour intervals. Model calculations between these time intervals use interpolated values for each time step.

The Olympia airport is located about eight miles south of the central portion of the Inlet. Consequently, we needed to correlate the wind speeds measured at the airport with the winds measured over the Inlet. The correlations for May and September are shown in Figure 4.13. The wind speeds over the Inlet were about 65 percent of those measured at Olympia airport at the same time. We therefore used a wind shading coefficient of 0.65 in estimating the winds over the Inlet from the data collected at the airport.

BUDD INLET VS OLYMPIA AIRPORT WINDS

September 1984 and May 1985

Intercept = 0.00
Slope = 0.65
R^2 = 0.71
n = 23

Inlet Winds (Knots)

Airport Winds (Knots)

□ SEPTEMBER 1984   +   MAY 1985
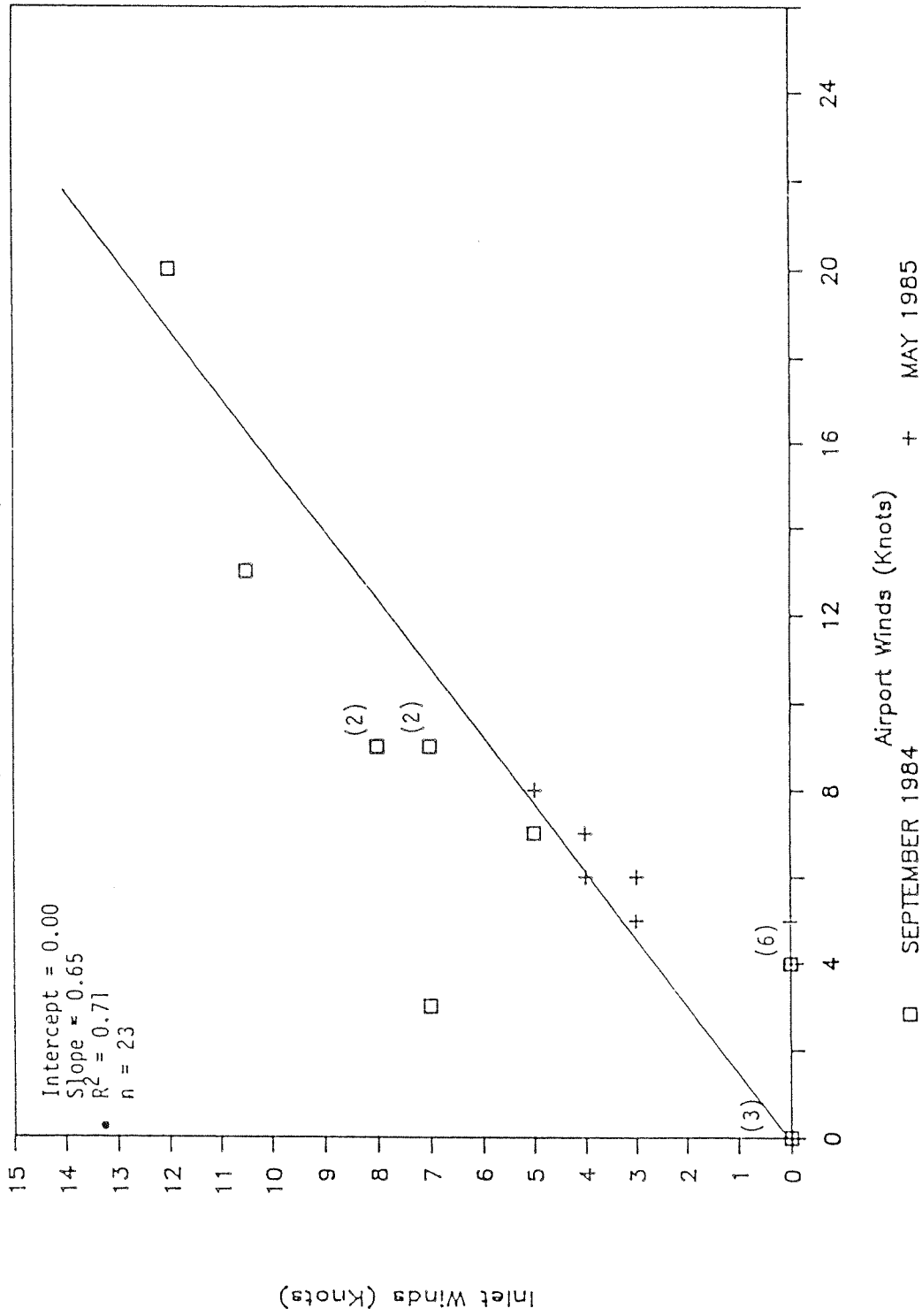
Figure 4.13   Correlation between winds measured on Budd Inlet and at the Olympia airport.

The wind direction is used in the model to determine the longitudinal component of the wind relative to the orientation of the Inlet. Wind direction during the September 1984 survey was generally from the WSW, while winds were generally from the NNE during the May 1985 survey. Wind direction at the airport agreed with the direction measured on the Inlet at the same time to within 30 degrees when wind speeds at the airport were at least 4 knots. Therefore, no correction was made for topographic channeling of the winds over the Inlet, although the Inlet did tend to "steer" the winds to a more north-south orientation.

External Sources. The major point sources used in the model were: Capitol Lake, LOTT outfall, Moxlie Creek and Ellis Creek. The loadings were determined from the source surveys (see Section 3.5) and included BOD, nitrate, nitrite, ammonium, organic nitrogen and dissolved oxygen. Since all of these sources are fresh water, they were allowed to flow into the surface layer of the model in their appropriate segment.

The source from Capitol Lake was special for a number of reasons. First, it is the major source of fresh water to the Inlet via the Deschutes River and therefore is the major driving force behind the estuarine circulation. Second, the outlet is controlled by a tide gate which will not allow discharge when the tidal height is greater than or equal to 14 feet. Third, it is a large source of BOD in part due to the algal production in the lake. Since the model can account for varying boundary conditions with time, we have incorporated the tide gate condition into the model. The algal production in the lake was assumed to act as a source of pheopigments in the model. Data from 1983 for Capitol Lake indicated that chlorophyll a concentrations at the tide gate ranged from 7 to 43 ug/L and averaged about 20 ug/L from April through August (Entranco, 1984). These chlorophyll levels are estimated to represent about half of the BOD loadings from Capitol Lake. The pheopigment loadings were not separated from the BOD loadings since they were not actually measured. Consequently, total organic loadings from Capitol Lake are overestimated.

The water leaving the outer boundary of the Inlet on the ebb tide was assumed to mix with water refluxed from Dana Passage before returning on the flood tide. We therefore maintained a realistic dynamic boundary condition throughout the simulation. The best estimate of the mixing or reflux coefficient from the URS Flushing Report (URS, 1986) was 0.6. Using this coefficient in the model implies that six out of every ten parts of water leaving the Inlet at the outer boundary are recycled into Budd Inlet and the remaining water is from Dana Passage. The data used to represent the refluxed water from Dana Passage was taken from our boundary Station 1 toward the end of a strong flood. This was assumed to best represent the water which had been vertically mixed over Dana Passage.

Preliminary Model Calibration

Since the water quality module includes many interactive parameters, we attempted to calibrate the major oxygen controlling factors independently as sub-models to streamline the time consuming calibration process. Measured inputs were used in a spreadsheet format to calculate the other parameters used to fit the calculated outputs to measured values. The two major internal processes which had the greatest influence over the oxygen distribution were identified in the box modeling as primary production and sediment oxygen demand. The calibration of these two processes is given below.

Phytoplankton sub-model. The net primary productivity measurements made during the September 1984 and the May 1985 were used to calibrate the phytoplankton sub-model section of the water quality module. The equations which were used to describe the primary productivity are the same as those shown in the phytoplankton (C_7) section of the water quality module (Equation 4.31 to 4.37). The only exception is that we did not include the grazing or the sinking terms since these are not an output of particulate carbon-14 in the incubation bottles used in the productivity measurements. The overall calibration uses three variables: the Michaellis-Menten constant, the maximum growth rate, and the C:Chl $\underline{a}$ ratio. Consequently, the estimates derived from the submodel for these variables are not unique but were chosen to best represent literature values.

The input values, calculated parameters, and output of the phytoplankton model for the September 1984 survey are shown in Table 4.8 and Table 4.9 for Stations 3 and 5 respectively. The nutrient concentrations shown for S collected the following day during the same tidal stage. Two formulations of the light extinction coefficient were also compared during the modeling runs. A measured extinction coefficient determined from the 1 or 10 percent light level measurements and a calculated coefficient using equation 4.35, which includes self-shading. The results are also shown graphically in Figures 4.14 which shows the comparison between the measured values for productivity and those calculated from the two types of light extinction coefficient. These tables include the chlorophyll $\underline{a}$ concentrations at station 1 since this is where they were incubated during the September survey. Tables 4.10 and 4.11 along with Figure 4.15 shows the results for the May 1985 survey for Stations 3 and 5 respectively.

Both stations 3 and 5 show a subsurface maximum in chlorophyll $\underline{a}$ and productivity for the September 1984 survey. This was due to the fact that the dominant phytoplankton found in the September survey were dinoflagellates (mainly $\underline{Gymnodinium}$ spp.). Dinoflagellates migrating vertically in response to light (Robinson and Brown, 1983) can position themselves in the water column to maximize growth, and assimilate nutrients for sustained growth at night. Dinoflagellates have a lower intrinsic growth rate than diatoms and can maintain their growth at lower nutrient concentrations with a higher N/Chl $\underline{a}$ uptake ratio, (Chan, 1978) and at a lower light saturation level (Robinson and Brown, 1983, Moshkina, 1961). These differences are reflected in the phytoplankton submodel.

$\underline{SOD \ sub\text{-}model}$. The sediment oxygen demand sub-model is based on equation 4.42 which describes the SOD for Budd Inlet. The results of the benthic lander studies conducted during the May survey were used to calibrate the input parameters such as settling rates and percent of readily oxidizable organic matter.

Table 4.8 Modeled and measured primary productivity for Station 3, September 18, 1984, in Budd Inlet

			Depth (m)		
Inputs	0	2	3.5	6	12
Conc. NO3+NO2 (umolar)	0.5	0.5	0.5	3.6	7.2
Conc. NH4 (umolar)	0.73	0.73	0.73	2	3.03
Ext coeff meas (k)	0.408	0.408	0.408	0.408	0.408
temp (C)	17.5	17.5	16	15	14.4
Mic/Ment (umolar)	0.6	0.6	0.6	0.6	0.6
Chl a Sta 01 (ug/L)	3.49	3.49	3.49	1.09	2.8
Chlorophyll (ug/L)	1.81	3.14	25.57	13.01	6.03
Growmax (1/day)	2.5	2.5	2.5	2.5	2.5
1% Light Level (m)	11.3	11.3	11.3	11.3	11.3

Calculated Parameters

	0	2	3.5	6	12
Integrated Chl a (mg/m^2)		5.965	19.349	46.324	80.719
Grow = f(t)	2.131	2.131	1.936	1.816	1.748
R(NO3:NH4)	0.352	0.352	0.352	0.158	0.118
R(N)	0.709	0.709	0.709	0.904	0.944
I (k measured)	211.000	93.393	50.680	18.297	1.587
R(I) (measured k)	0.711	0.389	0.228	0.087	0.008
Ext coeff (k)	0.400	0.430	0.497	0.632	0.804
I (k calculated)	211.000	89.318	37.087	4.769	0.014
R(I) (calc. k)	0.711	0.375	0.171	0.023	0.000

Outputs (C:Chl a = 112:1)

(using measured k)	0	2	3.5	6	12
ug Chl/L/day	1.787	1.700	7.375	1.719	0.072
mg C/m^3/day	200.168	190.346	825.959	192.565	8.013
mg C/m^2/day		390.514	762.229	1273.155	601.735
SUM mg C/m^2/day					3027.632

(using cal. k)	0	2	3.5	6	12
ug Chl/L/day	1.787	1.637	5.532	0.459	0.001
mg C/m^3/day	200.168	183.395	619.545	51.442	0.069
mg C/m^2/day		383.564	602.205	838.733	154.533
SUM mg C/m^2/day					1979.035

Measured Value

	0	2	3.5	6	12
mg C/m^3/day	203.250	198.370	422.400	135.740	15.620
mg C/m^2/day		401.620	465.578	697.675	454.080
SUM mg C/m^2/day					2018.953

Table 4.9 Modeled and measured primary productivity
for Station 5, September 18, 1984, in Budd Inlet

	Depth (m)			
	0	0.5	2	4.5
Inputs				
Conc. NO3+NO2 (umolar)	0.1	0.1	0.17	0.17
Conc. NH4 (umolar)	0.35	0.35	0.54	0.54
Ext coeff meas (k)	0.329	0.329	0.329	0.329
temp (C)	17.5	17.5	16	15
Mic/Ment (umolar)	0.9	0.9	0.9	0.9
Chl a Sta 01 (ug/L)	3.49	3.49	3.49	3.49
Chlorophyll (ug/L)	7.75	44.83	32.47	38.38
Growmax (1/day)	3	3	3	3
1% Light Level (m)	14	14	14	14
Calculated Parameters				
Integrated Chl a (mg/m^2)		1.745	6.98	15.705
Grow = f(t)	2.557	2.557	2.323	2.179
R(NO3:NH4)	0.553	0.553	0.433	0.433
R(N)	0.335	0.335	0.444	0.444
I (k measured)	211.000	179.001	109.290	48.023
R(I) (measured k)	0.711	0.639	0.443	0.218
Ext coeff (k)	0.400	0.462	0.483	0.560
I (k calculated)	211.000	167.456	80.345	16.993
R(I) (calc. k)	0.711	0.610	0.343	0.081
Outputs (C:Chl a = 112:1)				
(using measured k)				
ug Chl/L/day	4.344	22.592	13.637	7.427
mg C/m^3/day	217.181	1129.613	681.852	371.367
mg C/m^2/day		336.698	1358.599	1316.524
SUM mg C/m^2/day				3011.821
(using cal. k)				
ug Chl/L/day	4.344	21.583	10.567	2.781
mg C/m^3/day	217.181	1079.171	528.354	139.032
mg C/m^2/day		324.088	1205.644	834.233
SUM mg C/m^2/day				2363.966
Measured Value				
mg C/m^3/day	127.95	1039	481.36	350.53
mg C/m^2/day		291.7375	1140.27	1039.8625
SUM mg C/m^2/day				2471.870

PRIMARY PROD. VS. DEPTH FOR STA 3

SEPT. 1984 BUDD INLET

PRIMARY PROD. VS. DEPTH FOR STA 5

SEPT. 1984 BUDD INLET
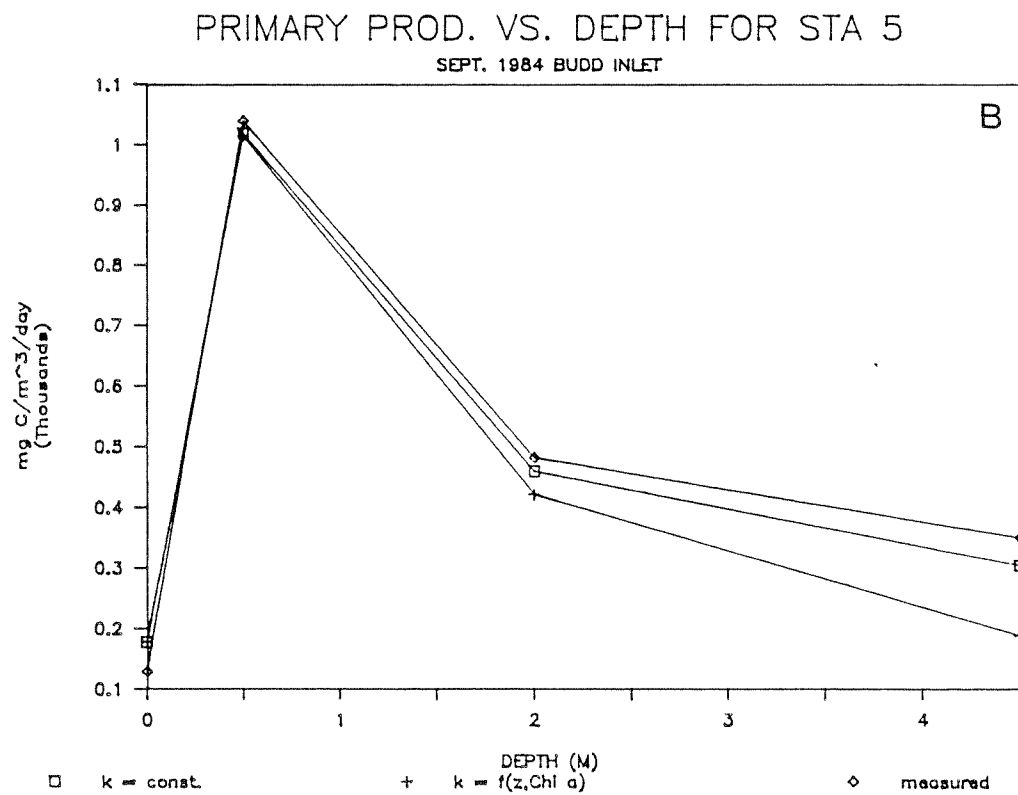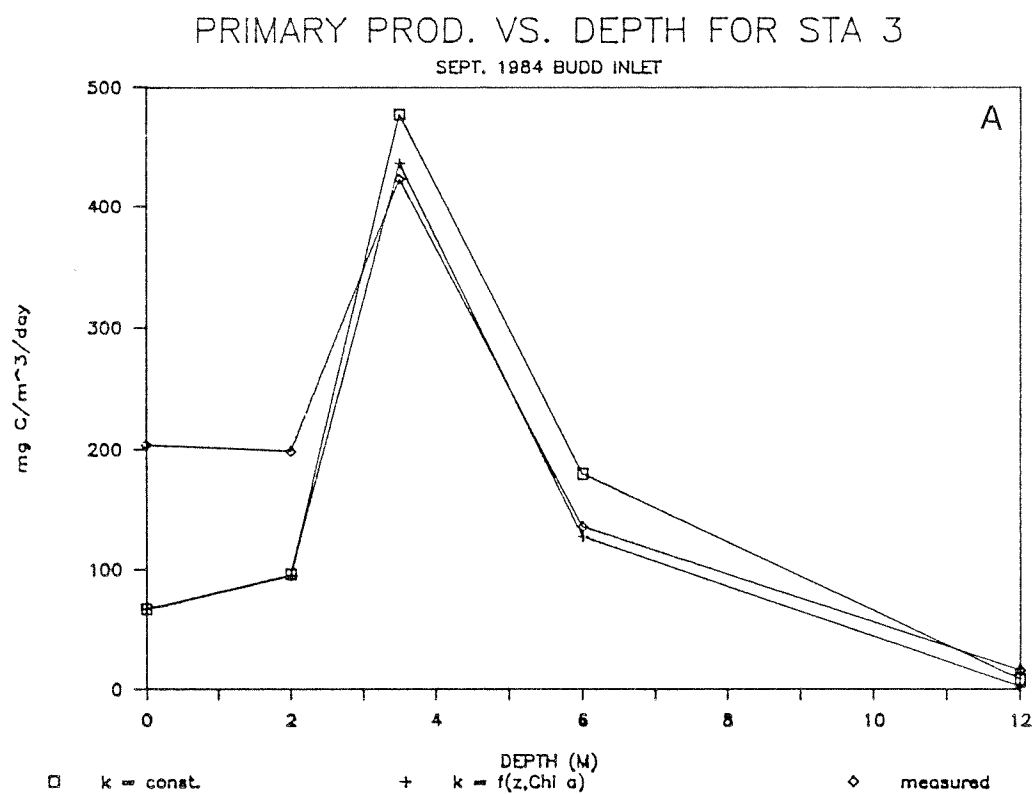
Figure 4.14   Primary production profile for (A) Station 3
and (B) Station 5, September 1984, Budd Inlet.

4-50

**Table 4.10   Modeled and measured primary productivity
for Station 3, May 20, 1985, in Budd Inlet**

	Depth (m)			
	0	2	4	7
Inputs				
Conc. NO3+NO2 (umolar)	0.49	0.45	4.2	7.95
Conc. NH4 (umolar)	0.28	0.37	0.55	1.33
Ext coeff meas (k)	0.576	0.576	0.576	0.576
temp (C)	14.9	11.4	10.6	10.4
Mic/Ment (umolar)	0.7	0.7	0.7	0.7
Chlorophyll (ug/L)	4.06	6.12	3.84	8.93
10% Light Level (m)	4	4	4	4
Growmax (1/day)	2.5	2.5	2.5	2.5
Calculated Parameters				
Integrated Chl a (mg/m^2)		10.18	20.14	39.295
Grow = f(t)	1.805	1.443	1.371	1.354
R(NO3:NH4)	0.612	0.538	0.428	0.219
R(N)	0.538	0.556	0.807	0.856
I (k measured)	211.000	66.724	21.100	3.752
R(I) (measured k)	0.711	0.292	0.100	0.018
Ext coeff (k)	0.400	0.451	0.501	0.596
I (k calculated)	211.000	85.632	28.476	3.243
R(I) (calc. k)	0.711	0.362	0.134	0.016
Outputs (C:Chl a = 112:1)				
(using measured k)				
ug Chl/L/day	2.576	1.320	0.392	0.175
mg C/m^3/day	115.927	59.396	17.643	7.892
mg C/m^2/day		175.323	77.039	38.303
SUM mg C/m^2/day				290.664
(using cal. k)				
ug Chl/L/day	2.576	1.637	0.522	0.152
mg C/m^3/day	115.927	73.651	23.493	6.828
mg C/m^2/day		189.578	97.144	45.482
SUM mg C/m^2/day				332.204
Measured Value				
mg C/m^3/day	113.120	72.330	12.600	13.890
mg C/m^2/day		185.450	84.930	39.735
SUM mg C/m^2/day				310.115

Table 4.11 Modeled and measured primary productivity
for Station 5, May 20, 1985, in Budd Inlet

	Depth (m)			
	0	2	4	7

Inputs

Conc. NO3+NO2 (umolar)	1.5	0.59	0.47	0.43
Conc. NH4 (umolar)	1.49	0.48	0.48	0.35
Ext coeff meas (k)	0.576	0.576	0.576	0.576
temp (C)	13.8	11.8	11	10.6
Mic/Ment (umolar)	0.5	0.5	0.5	0.5
Chlorophyll (ug/L)	3.8	3.84	3.58	4.43
10% Light Level (m)	4	4	4	4
Growmax (1/day)	2.8	2.8	2.8	2.8

Calculated Parameters

Integrated Chl a (mg/m^2)	1.884	7.64	15.06	25.0725
Grow = f(t)	0.199	1.658	1.575	1.535
R(NO3:NH4)	0.898	0.465	0.715	0.553
R(N)	211.000	0.742	21.100	0.667
I (k measured)	0.711	66.724	0.100	5.004
R(I) (measured k)	0.400	0.292	0.475	0.025
Ext coeff (k)	211.000	0.438	31.521	0.525
I (k calculated)	0.711	87.835	0.147	6.938
R(I) (calc. k)		0.370		0.034

Outputs (C:Chl a = 112:1)

(using measured k)

ug Chl/L/day	4.204	1.269	0.372	0.102
mg C/m^3/day	189.163	57.103	16.760	4.606
mg C/m^2/day		246.266	73.863	26.708
SUM mg C/m^2/day				346.837

(using cal. k)

ug Chl/L/day	4.204	1.608	0.546	0.141
mg C/m^3/day	189.163	72.339	24.568	6.364
mg C/m^2/day		261.502	96.907	38.665
SUM mg C/m^2/day				397.074

Measured Value

mg C/m^3/day	176.140	77.550	27.360	6.550
mg C/m^2/day		253.690	104.910	42.388
SUM mg C/m^2/day				400.988

PRIMARY PROD. VS. DEPTH FOR STA 3
MAY 1985 BUDD INLET

A

k — const.　　　　+　k — f(z,Chl a)　　　　◇　measured

PRIMARY PROD. VS. DEPTH FOR STA 5
MAY 1985 BUDD INLET

B

k — const.　　　　+　k — f(z,Chl a)　　　　◇　measured
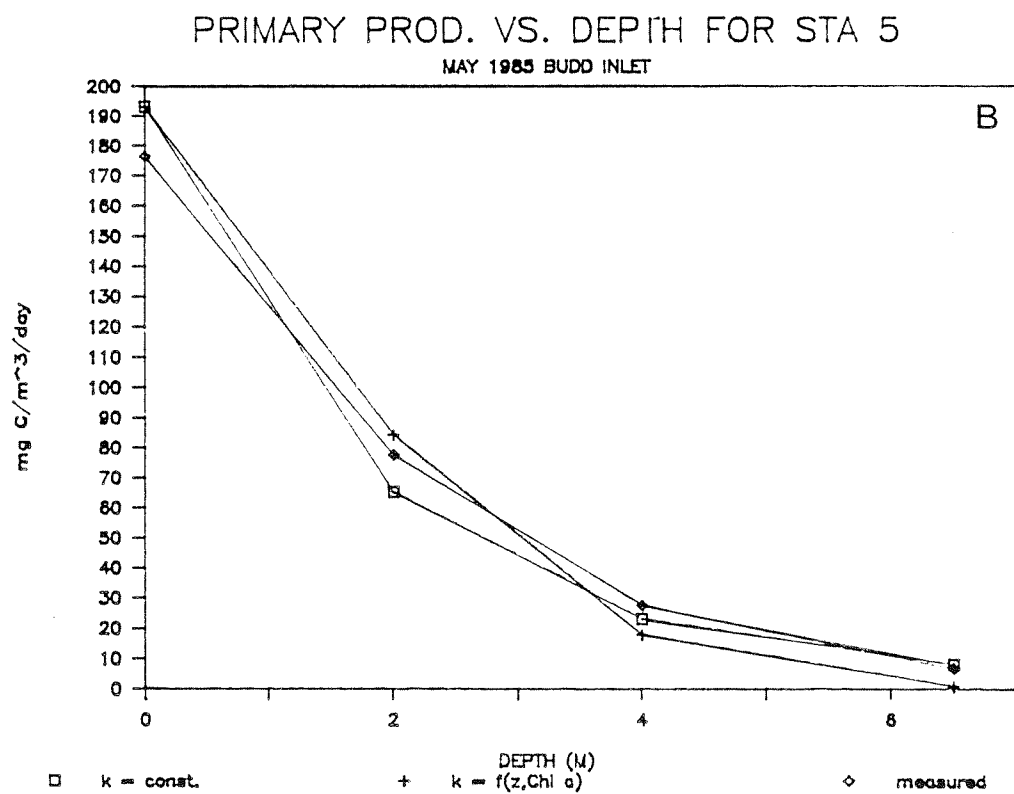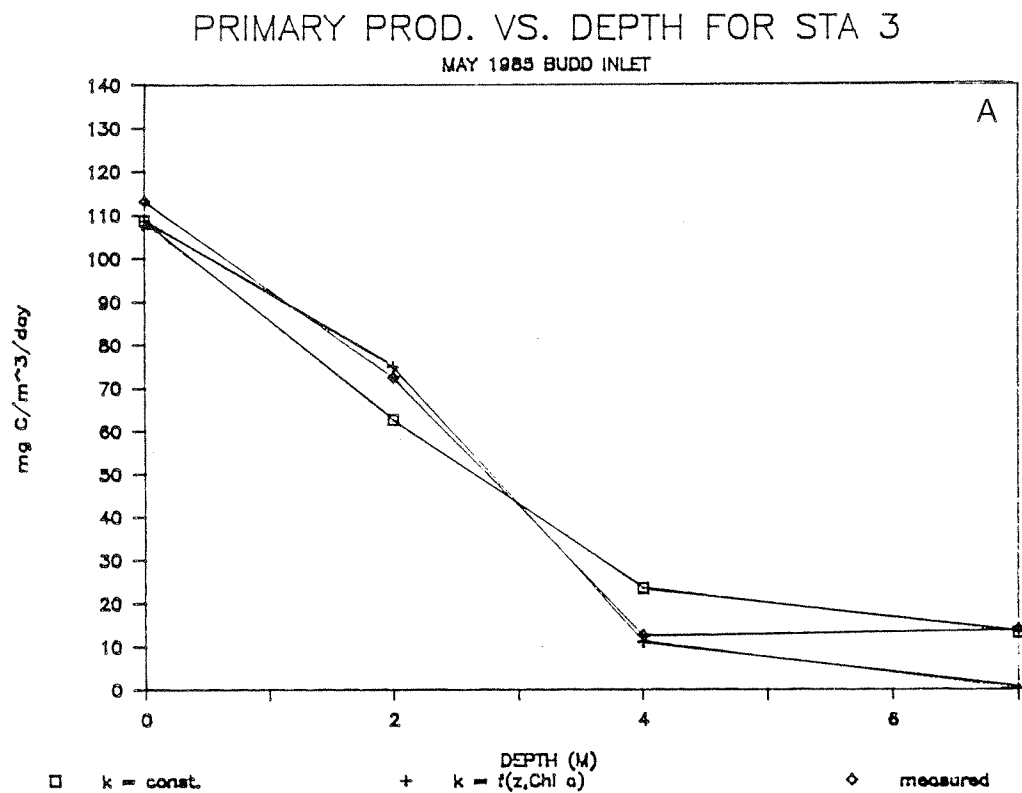
Figure 4.15　Primary productivity profile for (A) Station 3
and (B) Station 5, May 1985, Budd Inlet.

4-53

The best fit of the parameters to the measured data are shown in
Table 4.12. All concentrations listed in Table 4.12 represent an average
throughout the water column at each of the lander sites over the time period
of the May survey. The input parameters are labeled according to their
model designation. The only addition is the settling rate of fecal pellets
(FECSET) which was given as V_f in the water quality module. Since we did
not measure BOD5 at either of the lander sites, we have instead used
predicted concentrations from the dynamic model to estimate the average
concentration in the water column.

The results indicate that the major contribution to the oxidizable
organic matter reaching the sediments is the result of grazing by
zooplankton. The pheopigments and fecal pellets reaching the sediments
account for about 70 to 80 percent of SOD excluding the background. This is
due mainly to the higher settling rates for these materials. It is
important to note that the SOD related to the BOD5 is only a small fraction
of the total and that greater than 90 percent of the SOD is related to the
algal production in the water column. This is similar to the findings of
Kruger (1979) in his one-dimensional model of Budd Inlet. In that study he
concluded that BOD sources did not appear to appreciably lower dissolved
oxygen concentrations within the inlet, and that the DO sag in lower Budd
Inlet was due to a decaying phytoplankton bloom.

Final Calibration

May calibration. Final calibration of the dynamic water quality model
for May 1985 was initiated with the input values from the phytoplankton and
SOD sub-models. The final set of parameters used in the May simulation are
shown in Table 4.8. The only significant change made was an increase in the
maximum phytoplankton growth rate (GROWMAX) from 2.8 to 4.3 per day. This
was necessary to compensate for the somewhat coarse vertical scale in the
model geometry as mentioned above.

Done to make the Chlorophyll
levels observed equal the
predicted level.

Table 4.12 Modeled and measured sediment oxygen
demand (SOD) for Stations 3, 4, and 8,
in Budd Inlet

INPUT PARAMETERS

STATION 3&4 SIMULATION OF SOD
(mg O_2/m^2/min)

ALPHA2	0.66
ALPHAO	2.67
ALPHA4	133
ALPHA7	0.5
AS	0.5

BOD5	PHYTO	PHAEO	FECAL		TOTAL
0.01	0.12	0.33	0.18		0.91

K3	0.0035 m/min
SIGMA1	0.00035 m/min
SIGMA2	0.0022 m/min
FECSET	0.069 m/min
DEPTH	12 meters

BACKGROUND =   0.27   MEASURED = 0.69 - 1.08

C1   0.007 g/m^3
C2   1.48 mg/m^3
C7   5.32 mg/m^3

G2   0.00008 1/hr

INPUT PARAMETERS

STATION 8 SIMULATION OF SOD
(mg O_2/m^2/min)

ALPHA2	0.66
ALPHAO	2.67
ALPHA4	133
ALPHA7	0.5
AS	0.5

BOD5	PHYTO	PHAEO	FECAL		TOTAL
0.11	0.22	0.55	0.19		1.33

K3	0.0035 m/min
SIGMA1	0.00035 m/min
SIGMA2	0.0022 m/min
FECSET	0.069 m/min
DEPTH	7 meters

BACKGROUND =   0.27   MEASURED = 1.22

C1   0.06 g/m^3
C2   2.48 mg/m^3
C7   9.48 mg/m^3

G2   0.00008 1/hr

SOD = ALPHA7 (1000*K3*C1+ALPHA4*SIGMA1*C7 +(ALPHA4/ALPHA2)*SIGMA2*C2
+ALPHA4*FECSET*(1-AS)*G2*DEPTH) + BACKGROUND

The results of the calibration for the May survey are shown as vertical profiles in Figures 4.16-4.21 for the four segments (5, 7, 10, 14 in the model) which correspond to the May survey stations. Salinity and temperature as well as the four parameters related to phytoplankton growth (chlorophyll a, dissolved oxygen, ammonium and nitrate) were used in the calibration. The vertical profiles are taken from model predictions and field measurements at mid-afternoon on May 21 during low slack. There was no discernible "pulse" of ammonium from the LOTT treatment plant during this time. Note that the model profiles are usually deeper than the measured values at the stations since the model geometry includes the maximum depth in each segment.

Comparisons of the predicted profiles and observed data for salinity and temperature (Figures 4.16 and 4.17) suggest that the transport coefficients chosen are reasonable. The near-surface values for salinity and temperature are not expected to agree as well due to the coarse vertical scale and the horizontal averaging of the model. Consequently, overall agreement between predicted and observed values can be considered to be quite good.

The water quality constituents calibrated for segment 5 (Figure 4.8) are shown in Figure 4.18. The best agreement is between calculated and measured ammonium and chlorophyll values (station 8) with the oxygen measurements showing some scatter around the predicted value. The measured nitrate values show a decrease with depth rather than the increase predicted from the model. This would indicate a net sink for nitrate in the bottom waters. One possible explanation for this would be dentrification of the nitrate to ammonium. This process is generally considered to occur at significant rates only in oxygen depleted water. However, McCarthy et al. (1975) found rates of nitrate dentrification comparable to nitrification in well oxygenated waters using radioactively labeled nitrogen in Chesapeake Bay.
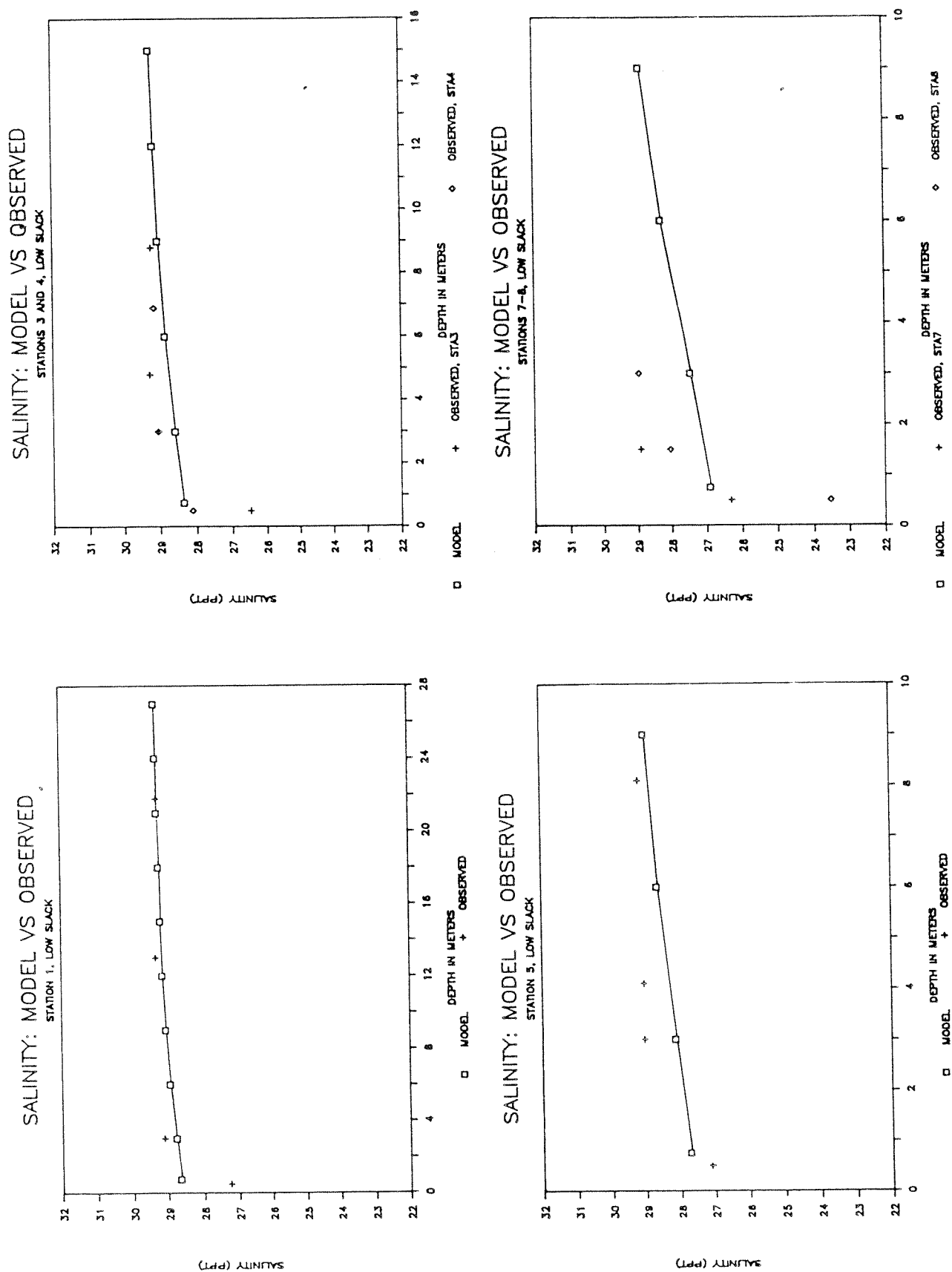
Figure 4.16 Comparison of modeled and observed salinity values.
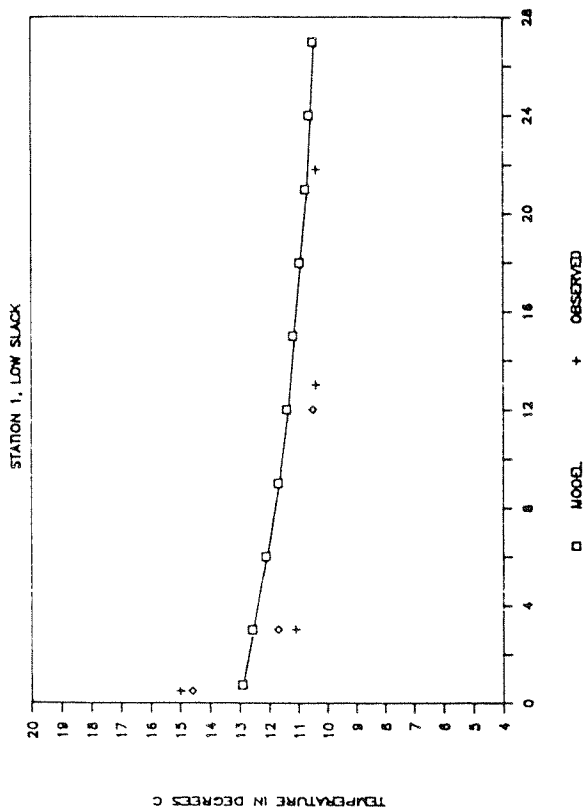
Figure 4.17 Comparison of modeled and observed temperature values.
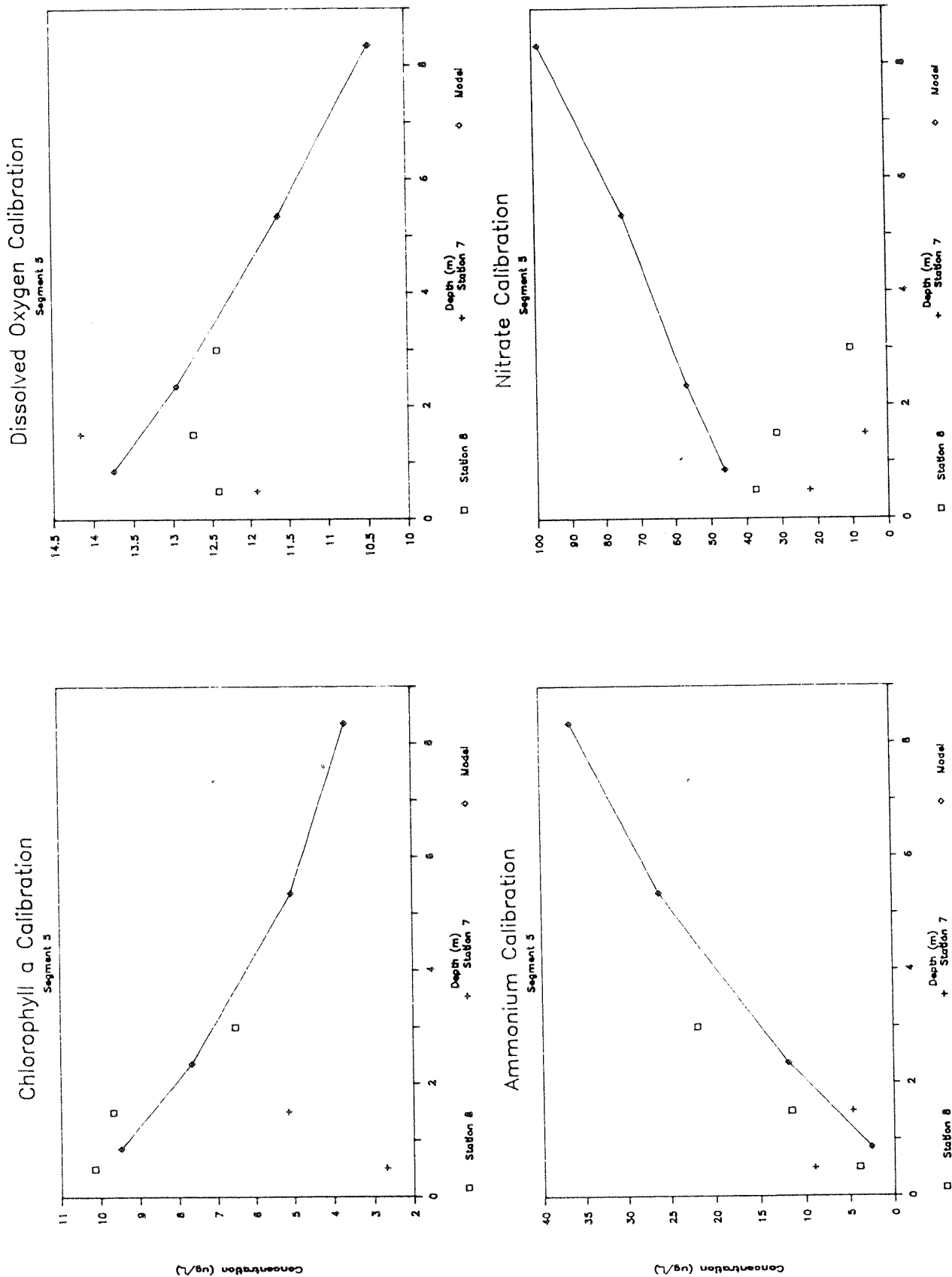
Figure 4.18   Model calibration results for Chl-a, dissolved oxygen, ammonium and nitrate concentrations at segment 5.

Calculated values for segment 7 and measured values at station 5 near Butler Cove (Figure 4.19) for dissolved oxygen and ammonium agree fairly well. Chlorophyll measurements are scattered about the predicted profile with the measured nitrate profile lower than predicted. Best agreement in segment 10 (Figure 4.20) is found for ammonium and dissolved oxygen with both stations 3 and 4. Chlorophyll measurements are again scattered around the predicted profile. The predicted nitrate profile more closely resembles the measured values for station 3, while station 4 measured values are low throughout the water column. Station 1 and segment 14 comparisons (Figure 4.21) agree fairly well for all of the four constituents. Again, the chlorophyll measurements are scattered and are lower in the surface than predicted by the model.

In general, the agreement between the observed and predicted values is good. The agreement between observed and predicted oxygen and ammonium concentrations were consistently quite good. Since the predicted oxygen and ammonium profiles are mainly controlled by the phytoplankton production and the LOTT ammonium discharge for the inner Inlet, the scatter of the measured phytoplankton chlorophyll values about the predicted values is not a serious concern. In fact, the integrated chlorophyll a graphs shown in Figure 4.23 for the four segments indicate very good agreement between the predicted and observed values. The measured nitrate values were in better agreement with the predicted values in the central and outer segments of the inlet where the flushing and replenishment of Budd Inlet water from the Sound would be enhanced. This leads us to believe that lateral circulation and other processes not accounted for by the model such as dentrification may influence nitrate concentrations in the inner portions of the inlet.

The results of the model calibration of the sediment oxygen demand (SOD) study conducted during the May survey (see section 3.7) are shown in Figure 4.23. The SOD measurements from the two side-by-side box core flux chambers at the Lander sites at station 8 (segment 5) and between stations 3 and 4 (segment 10) are shown in the figure along with the average predicted values for the two days of the survey from the dynamic model. Initial
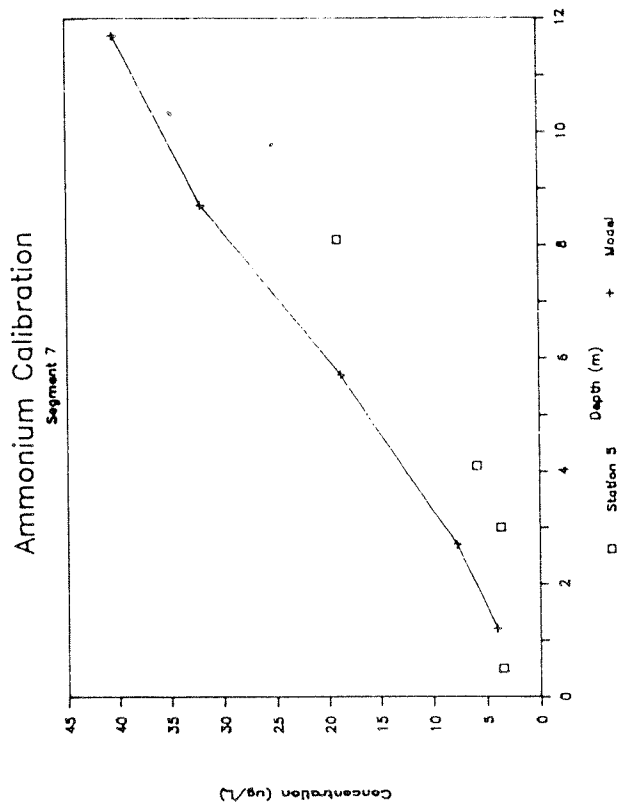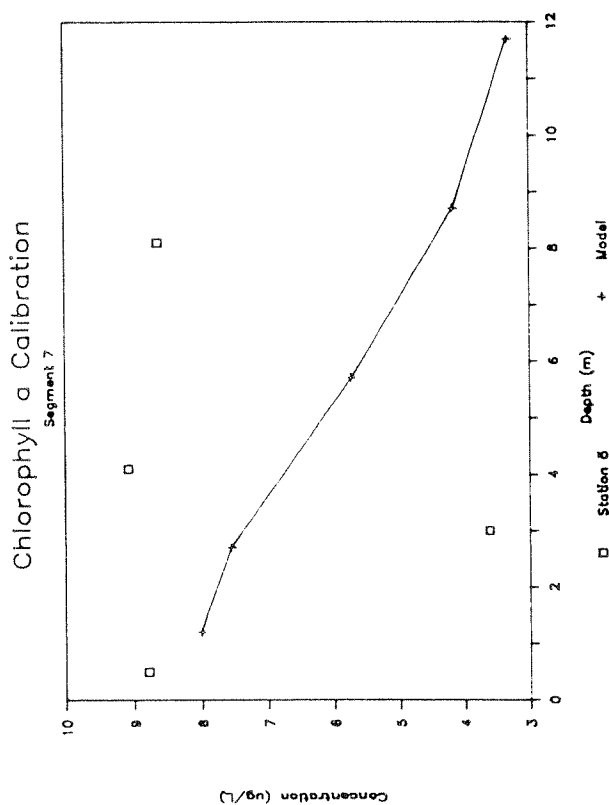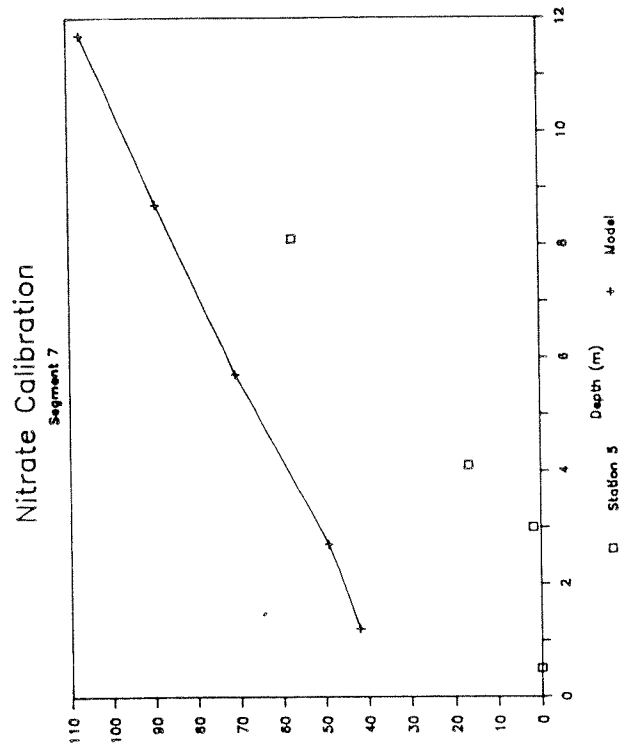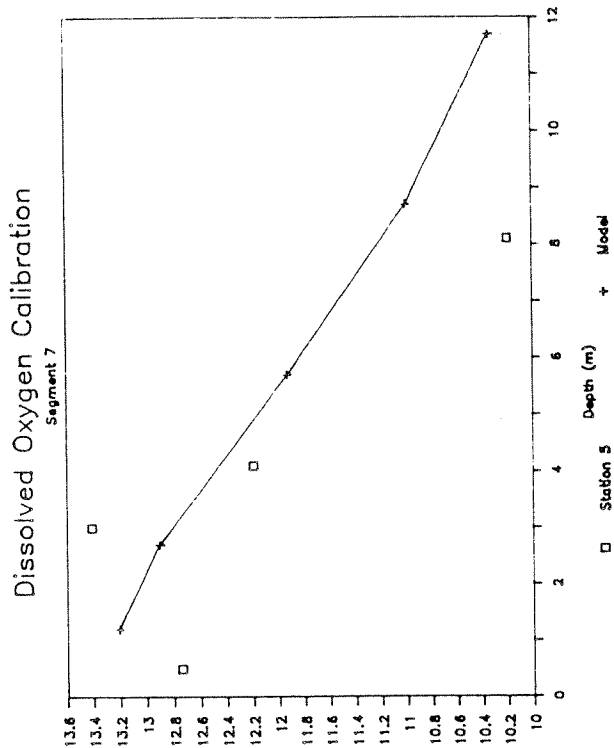
Figure 4.19 Model calibration results for Chl-a, dissolved oxygen, ammonium and nitrate concentrations at segment 7.
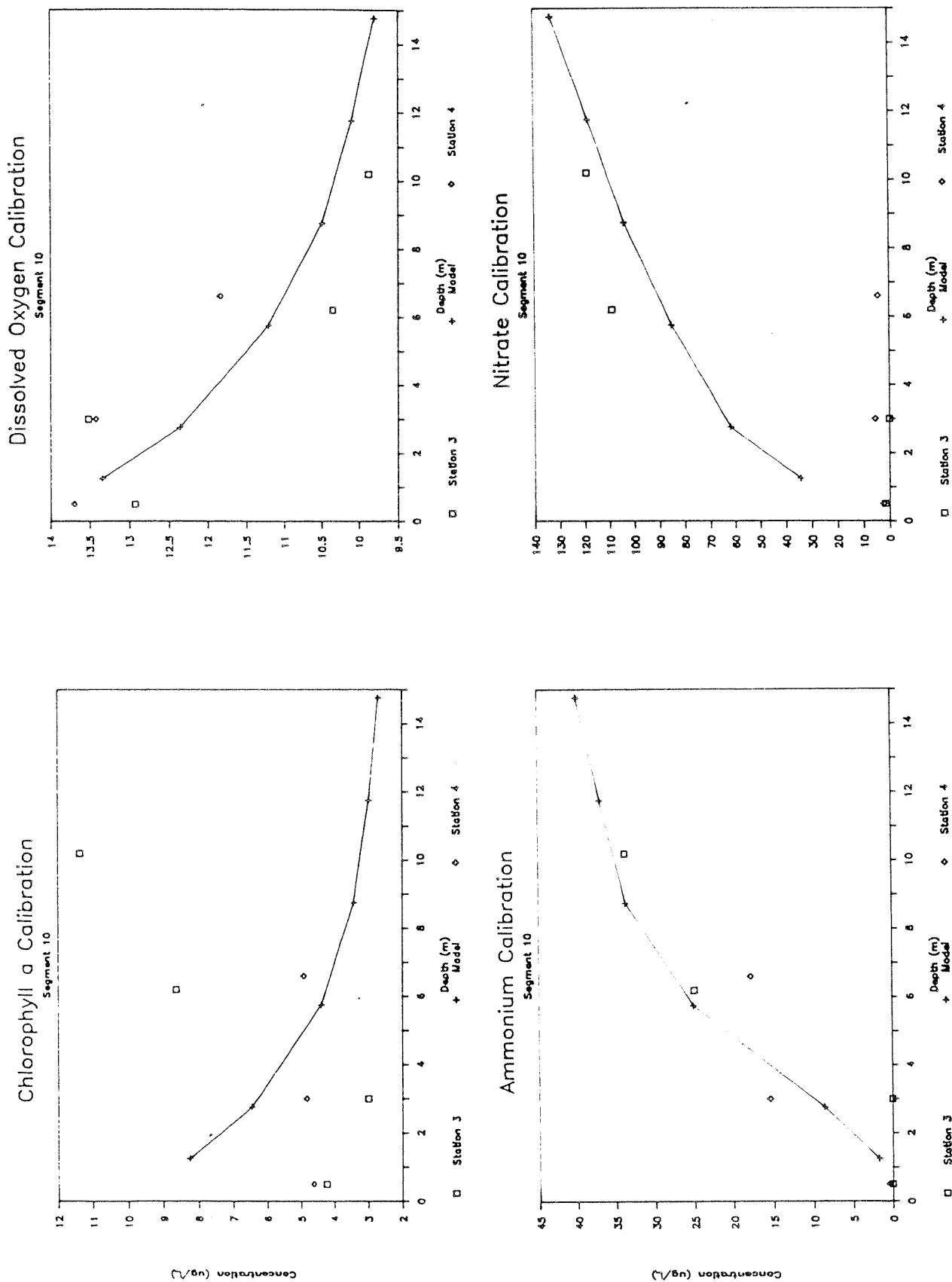
Figure 4.20 Model calibration results for Chl-a, dissolved oxygen, ammonium and nitrate concentrations at segment 10.
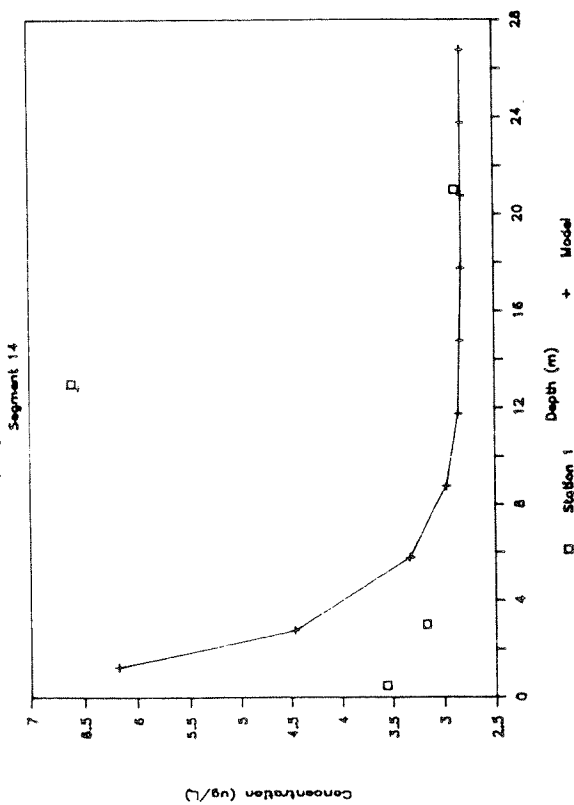
4-62
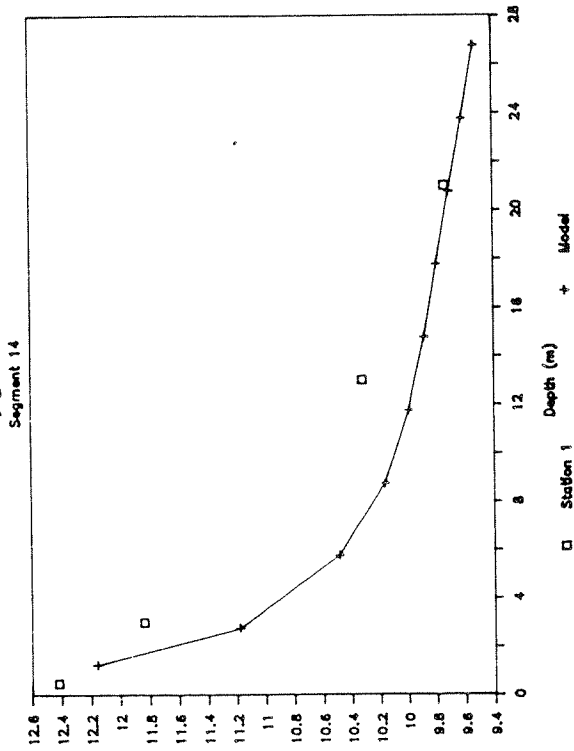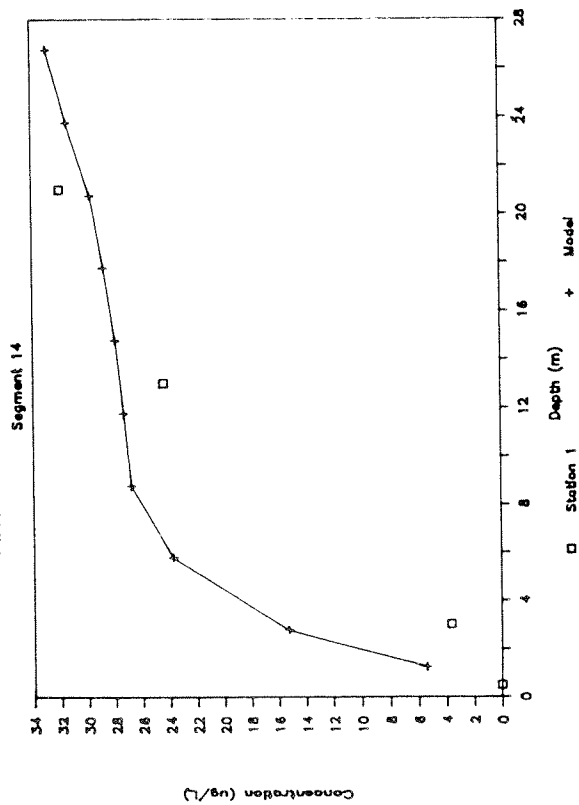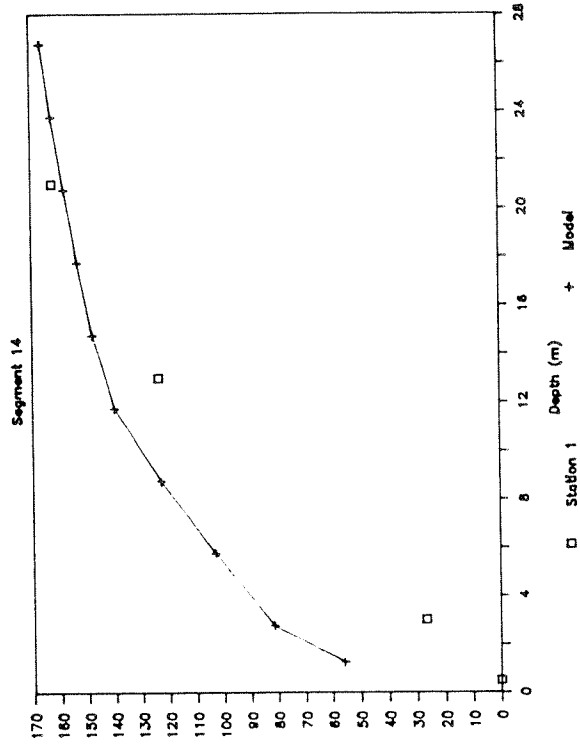
Figure 4.21 Model calibration results for Chl-a, dissolved oxygen, ammonium and nitrate concentrations at segment 14.
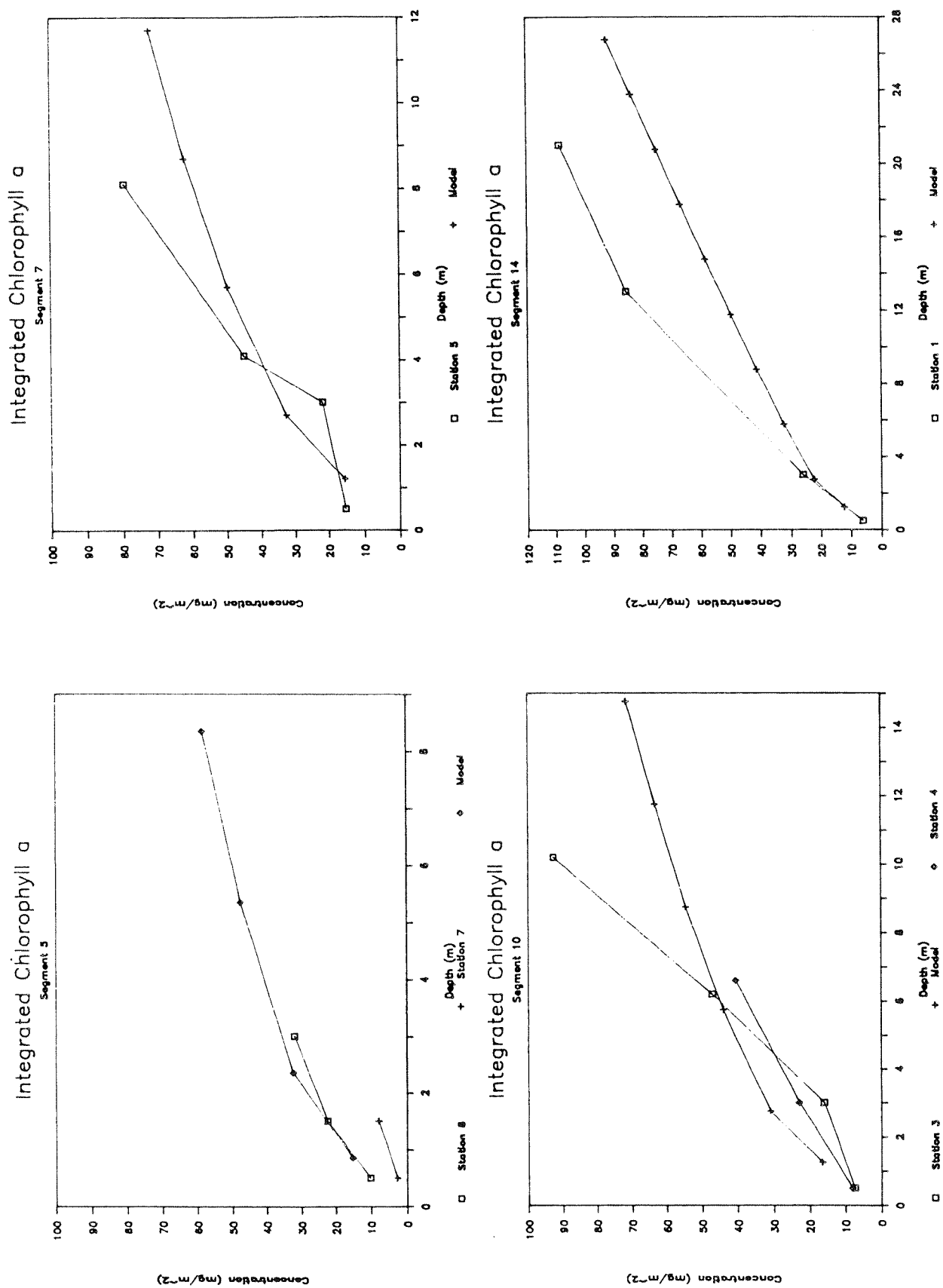
Figure 4.22 Comparison of modeled and measured integrated Chl a at segments 5, 7, 10 and 14.
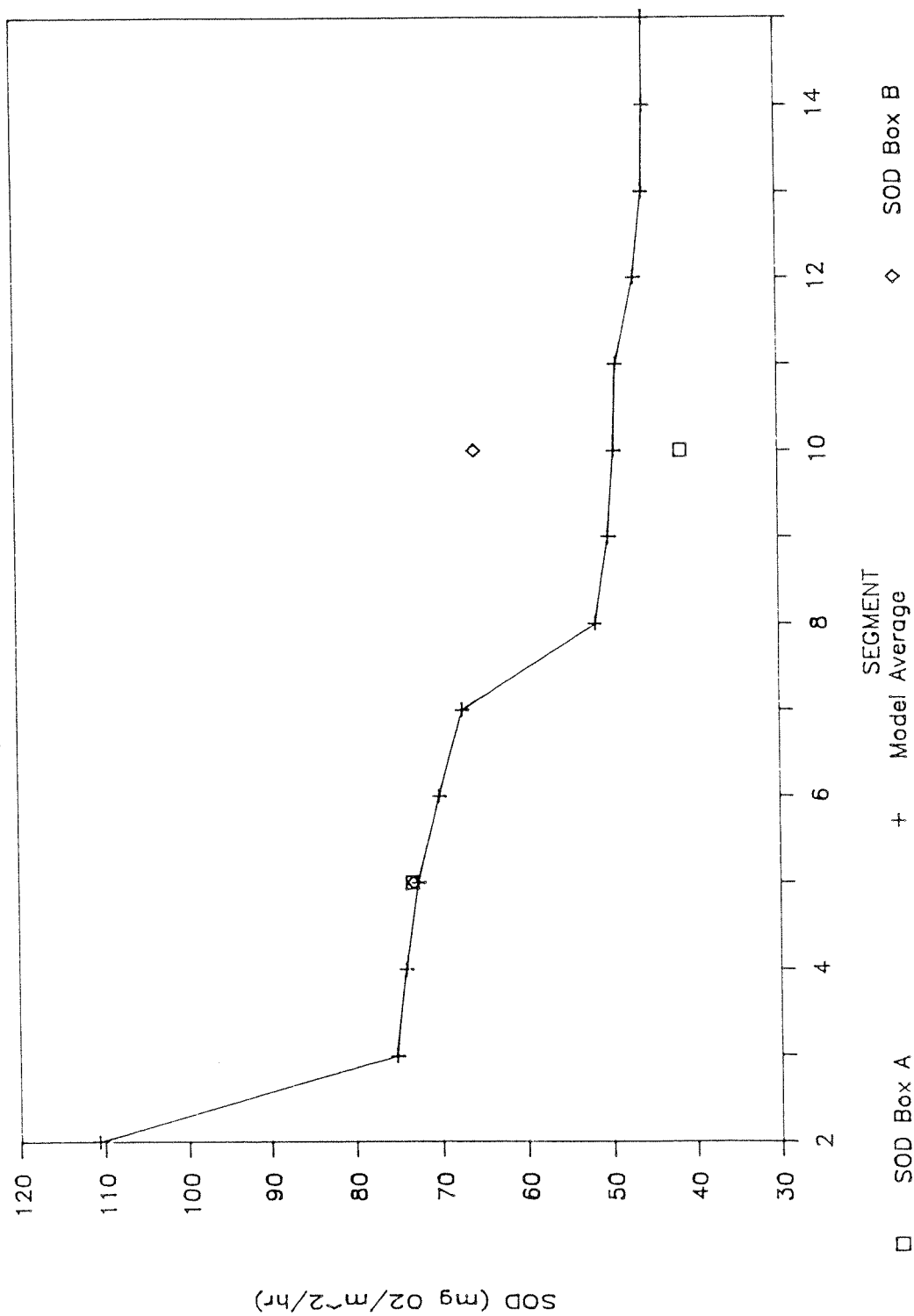
Figure 4.23 Model calibration results for sediment oxygen demand.

□ SOD Box A   + Model Average   ◇ SOD Box B

SEGMENT

values for settling velocities and other constants were taken from the SOD sub-model. The measured values bracket the predicted values in segment 10 and are almost identical in segment 4. The much higher SOD predicted for the head of the inlet in segment 2 is due to the large influx of BOD from Capitol Lake.

The benthic ammonium release (K_6) used in the dynamic model is taken from equation 4.27. The benthic ammonium release was applied to model segments 7-15 in the calibration runs. The other segments (2-6) were assumed to have no benthic ammonium release in accordance with what was observed at Lander site 1 near station 8 during the May survey. The rational for this being that the influence of the large BOD loading from Capitol Lake and the occasional LOTT discharge through the Fiddle Head storm sewer would yield a similar large number of benthic animals in these segments. During the calibration process when benthic release was maintained in segments 2-6, it was observed that there was only a slight increase in near-bottom ammonium concentrations due to the rapid vertical mixing in the inner inlet.

September calibration. The phytoplankton sub-model for the September 1984 survey, which was described previously, was used as the initial input to the dynamic model for September. The sinking rates taken from the May calibration were also used as initial input. These did not adequately simulate the measured values for most of the constituents. The following discussion outlines our attempts to calibrate the dynamic model for the September survey.

The oxygen and nutrient profiles from the September survey were the most difficult to reproduce even with unrealistically high phytoplankton growth rates of up to 8 per day. The main difficulty was in reproducing the profiles in the beginning of the survey before the storm event as shown for station 5 in Figure 4.24. This was the critical low dissolved oxygen period we wanted to simulate. At first it was thought that the low dissolved oxygen and high ammonium measurements in the bottom water were due to higher SOD and benthic ammonium release rates. However, calibration runs
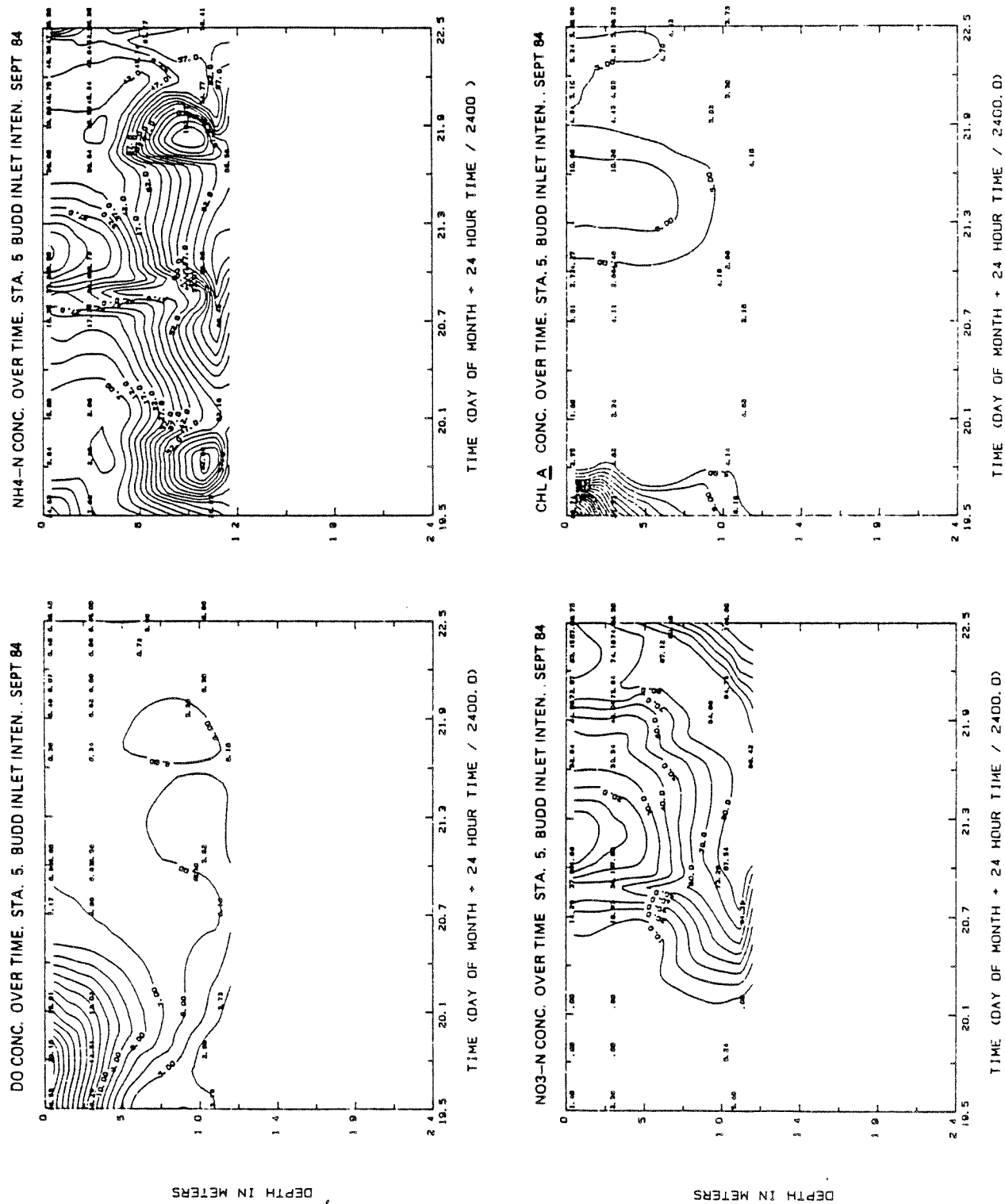
Figure 4.24 Contour plots of measured dissolved oxygen, ammonium, nitrate
            and chlorophyll a concentrations at Station 5, Budd Inlet, September 1984.

4-67

designed to maximize benthic oxygen demand and ammonium release with high growth, settling and grazing rates could not produce bottom oxygen values lower than about 5 mg/L. The vigorous vertical mixing would not allow such large vertical oxygen and nutrient gradients to be maintained.

Our final attempt at calibrating the dynamic model for September involved the revision of the water quality module to include algorithms which would simulate the phototaxic vertical migration of the dinoflagellates. It was believed that the active vertical migration of the dinoflagellates was the key process involved in maintaining the large vertical gradients of water quality constituents. Figure 4.25 shows the surface and near-bottom chlorophyll a concentrations over time for station 8 at the beginning of the September 1984 survey. The mirror image pattern of the figures clearly shows the vertical migration of the dinoflagellates at this station.

In effect the dinoflagellates are acting as a biological "pump" taking oxygen out of the bottom water and producing it in the surface water. As long as the pump, which is related to the vertical migration rate, is stronger than the vertical mixing, then large vertical gradients can be maintained.

The diel vertical migration will also couple with the two layered net longitudinal estuarine circulation within the inlet. This would tend to reduce the seaward displacement of the dinoflagellates and therefore reduce their flushing rate. The dispersion results for September also showed that material placed below the surface in the central and inner inlet were carried back toward the head of the inlet where it is detained. The net effect would be to create an accumulation mechanism for the dinoflagellates toward the head of the inlet.

In the model modifications, the phytoplankton were made to "swim" up at a certain threshold light intensity in response to an increase in the ambient light intensity. Once the phytoplankton reached their saturated light intensity they would stop. At night they would swim into the deeper

CHLOROPHYLL A NEAR BOTTOM
SEPTEMBER 1984

CHLOROPHYLL A IN SURFACE
SEPTEMBER 1984
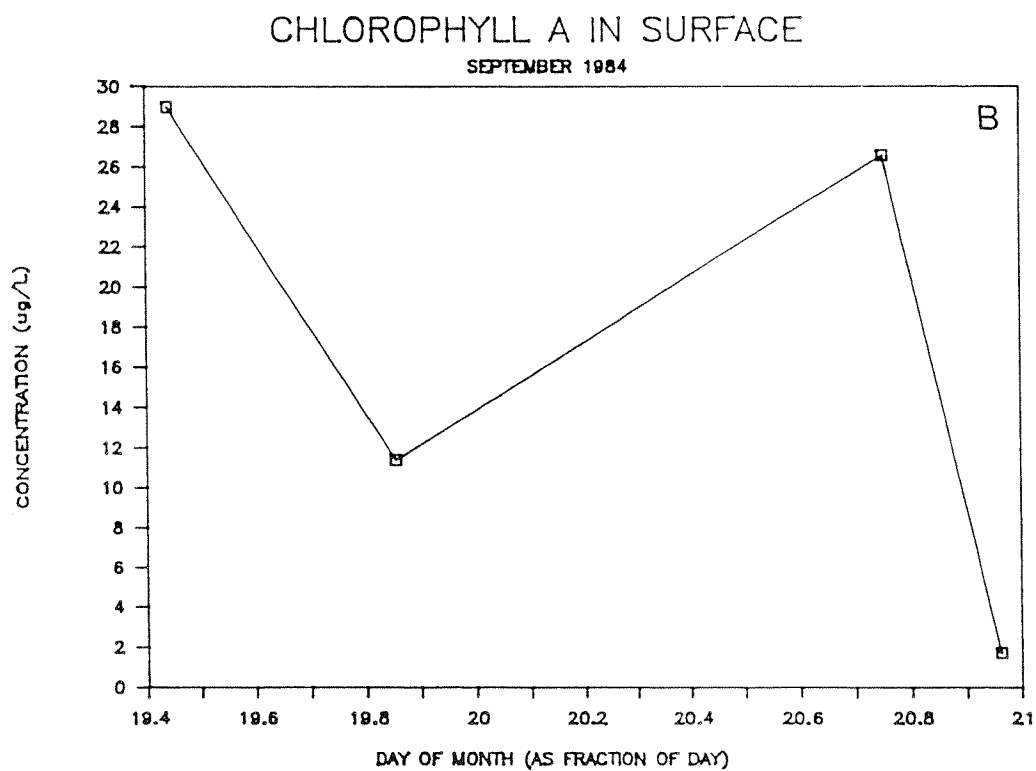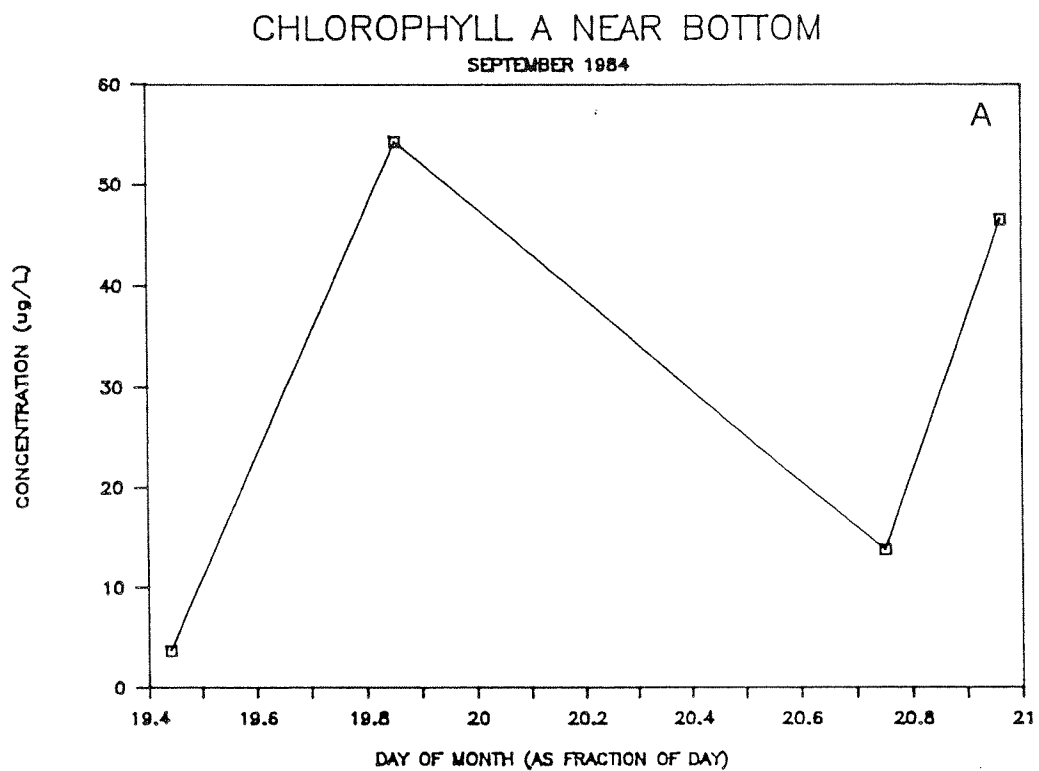
Figure 4.25   Temporal profiles of measured Chl a concentrations
(A) near bottom, and (B) in surface at station 8, September,
1984 showing vertical migration of dinoflagellates.

layers where they would continue to utilize the nitrogenous nutrients at a lower rate than during active photosynthesis. At the same time they would respire and release ammonium while depleting the oxygen.

This revised water quality module gave qualitative results which were very encouraging. We could achieve surface water dissolved oxygen levels of between 15 and 20 mg/L and bottom water values of less than 3 mg/L. Nitrate values were less than 2 ug/L throughout the water column in the inner inlet and ammonium values were higher by a factor of four in the bottom water. These results could not be obtained without the vertical migration along with the other physiological adaptations of the dinoflagellates. However, further refinements of the dinoflagellate model to make it more of a quantitative tool for water quality management for Budd Inlet were outside the scope of this project, and certainly could not be accomplished within the time frame of the project.

4.3 DYNAMIC MODELING RESULTS

The dynamic water quality model was used to investigate specific hydrodynamic characteristics of Budd Inlet. These include dilution, dispersion and flushing efficiency for various points throughout the Inlet. Because the conditions in September could not be simulated, the calibrated model for May was also used to determine the influence of alternative discharge sites and nutrient removal on phytoplankton growth, sediment oxygen demand and bottom water dissolved oxygen concentration.

Error dissipation of initial conditions in the numerical solution occurred in approximately 4,000 time steps. This transient period represents approximately the first two to three days in the month-long simulation figures shown in this section. No attempt was made to edit this transient state from the model output. Short-term simulations of dispersion were initiated following a five day initial equilibration period.

Flushing and Dilution

Flushing Efficiency. Flushing efficiency in this discussion is defined as the percent of a conservative tracer placed in the inlet at time zero remaining at a given later time. This is presented graphically as the percent remaining as a function of time. This was accomplished using the dynamic model by placing a given initial concentration (100 units/L) in a specific cell of the grid. The model would calculate the initial total mass based on the volume of the cell. This initial "slug" would then be dispersed and diluted as the model simulated the hydrodynamic transport within the inlet. At specified time intervals, the mass remaining in each cell would be calculated and summed over the whole grid. The ratio of the sum of the masses to the total initial mass would represent the fraction remaining in the inlet.

The tracer simulations were run using both the May and September flow and meterological conditions. We also wanted to determine the effect of refluxing or recycling a certain fraction of the water from Budd Inlet on the incoming flood tide. Two cases, 0 and 60 percent of the returning water being recycled Budd Inlet outer boundary water, were used.

Figure 4.26 shows the placement of the five test slugs in the model grid. These positions are coincident with the proposed alternative outfall alignments (LOTT, 1985) for the LOTT discharge (see Figure 4.40). Slugs 1 and 5 were placed at alignment E, slugs 2 and 4 were placed at alignment A, and slug 3 was placed in the outer inlet at alignment B.

Figures 4.27 and 4.28 show the results for September 1984 using a reflux coefficient of 0.0 and 0.6 respectively. There are three major observations which can be made from these data: 1) Flushing efficiency increases as you proceed towards the mouth of the inlet. The slug in the outer, middle and inner Inlet is 90 percent removed in about one, 14, and 20 days respectively. 2) Only a minor decrease in flushing efficiency is observed when the reflux coefficient is increased from 0 to 0.6. This decrease amounts to about one additional day to flush the inlet to the same extent. 3) The placement of the slugs in the water column made little
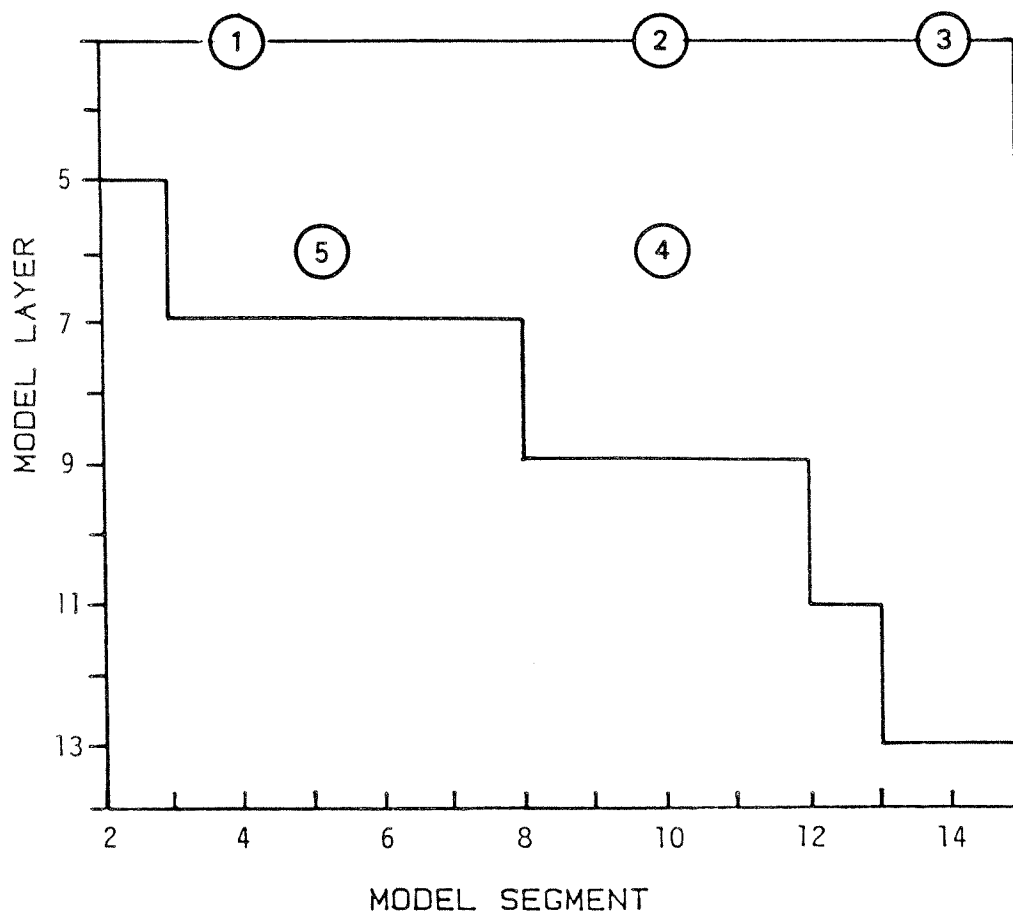
Figure 4.26 Location of the "slug" test placements referenced
in the model.
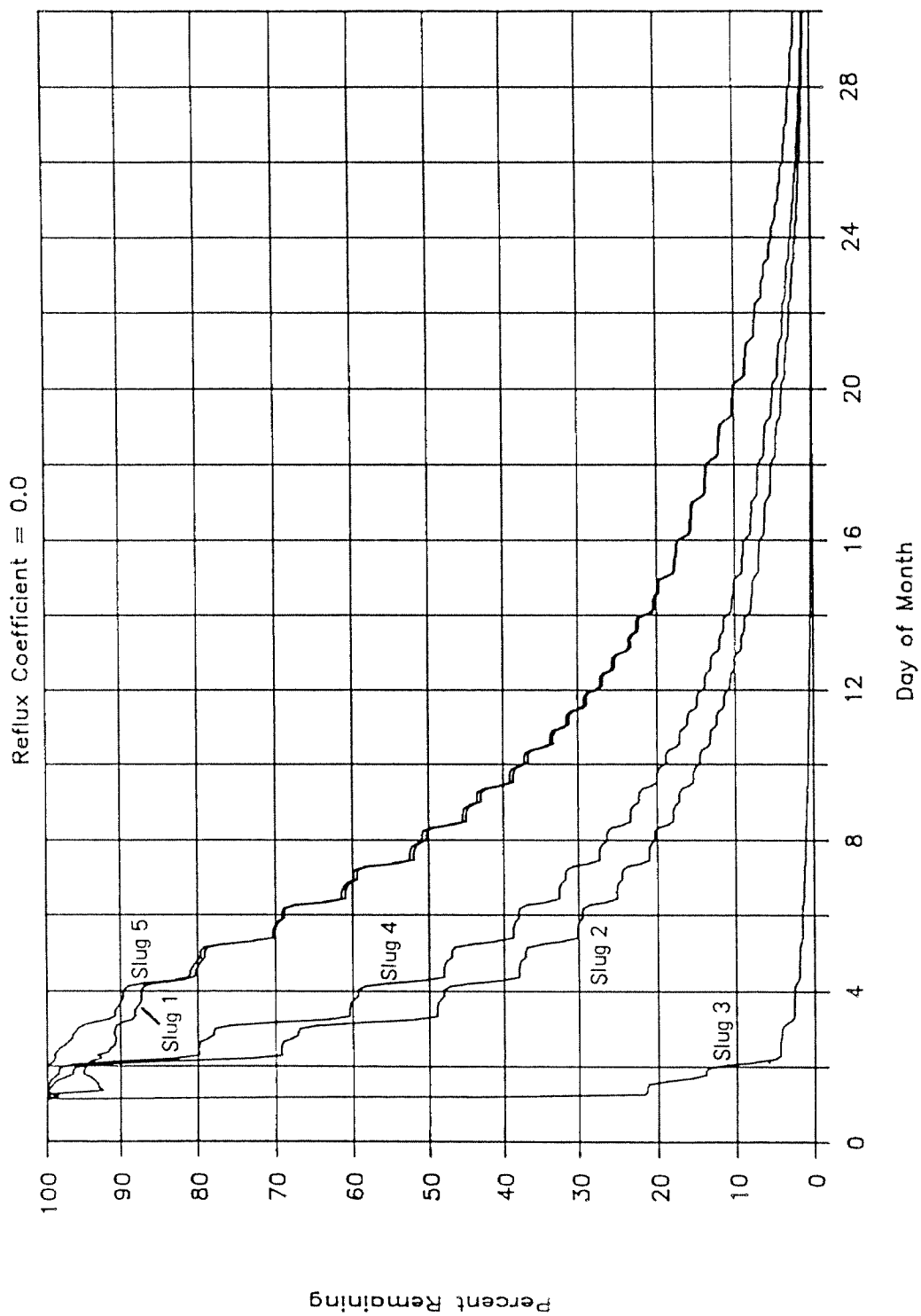
Figure 4.27 Flushing efficiency results from the "slug" test for Budd Inlet, September, 1984 (reflux coefficient = 0.0).
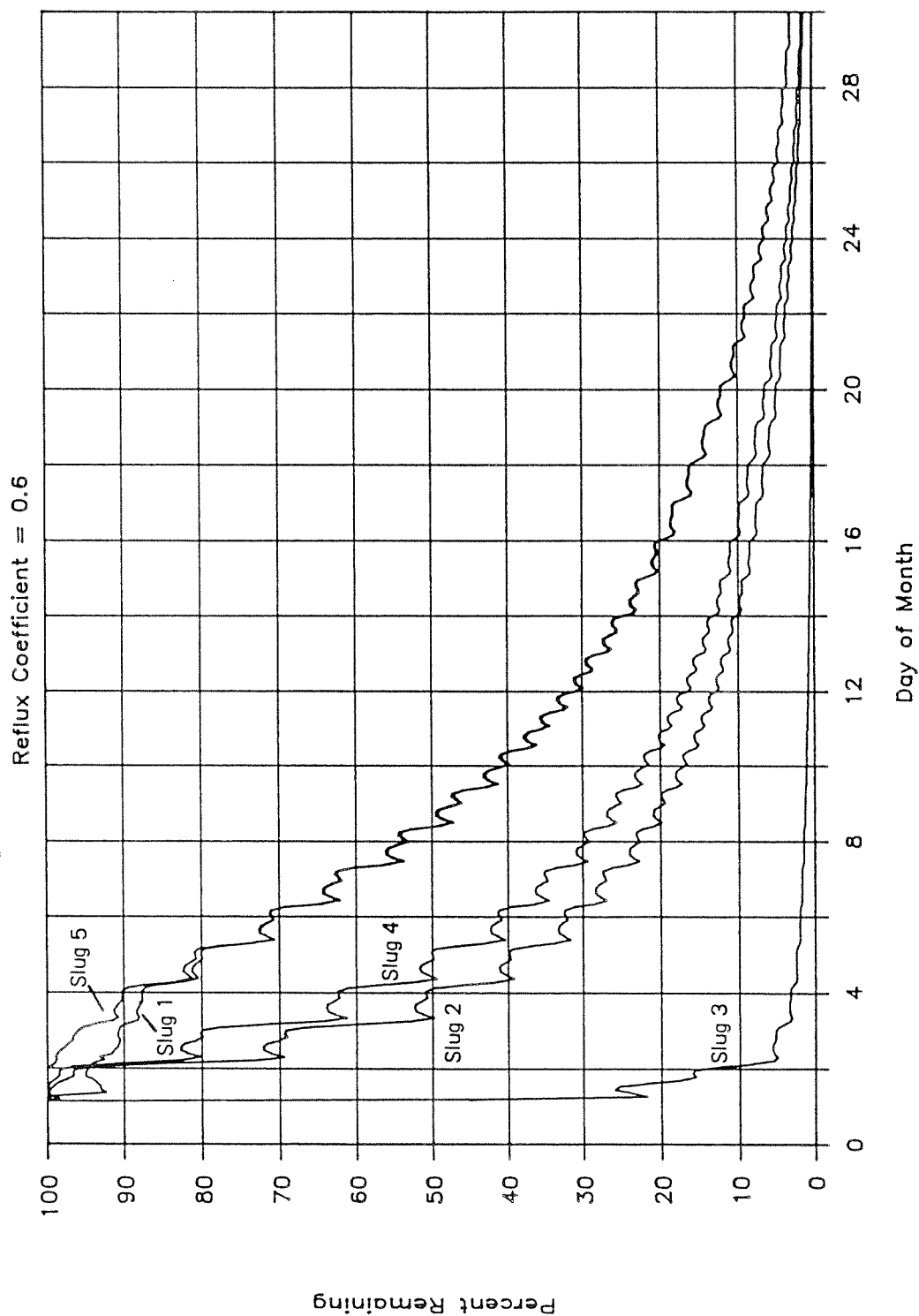
Figure 4.28 Flushing efficiency results from the "slug" test for Budd Inlet, September, 1984 (reflux coefficient = 0.6).

difference in the flushing efficiency because of the rapid vertical mixing. The central inlet showed slightly better flushing in the surface due in part to the increased estuarine circulation. The outer inlet surface water was by far the most efficiently flushed.

Figure 4.29 shows the comparison between the flushing efficiencies for May, 1985 and September, 1984 for two slug placements. The higher flow period during May is flushed more efficiently than the low flow period in September. The slug in the central inlet is 90 percent removed in about 5 days in May and 13 days in September. The inner inlet placement shows a much less dramatic difference with both May and September being flushed to the same extent within two to three days of each other.

In summary, we can say that the inner portion of Budd Inlet south of Priest Point is not very efficiently flushed regardless of season. The outer inlet, about a mile north of Gull Harbor, is very efficiently flushed regardless of season. The central portion of the inlet near Tykle Cove is more efficiently flushed during wet weather and high flow conditions.

Dilution and Dispersion. In order to investigate the dilution potential of each of the proposed outfall alignments, we ran month long simulations of a constant input of a conservative tracer into the surface layer at alignments E, A and B (Figure 4.39). We used the September, 1984 meterological conditions and source data for sources other than LOTT. The LOTT discharge rate used was taken to be the average dry weather design rate for the year 2010 of 24 mgd, as supplied by LOTT. The conservative tracer concentration was 16 mg/L which is the design concentration of ammonium, also supplied by LOTT. All runs were made with a reflux coefficient of 0.6.

The results of the three alignments are shown in Figures 4.30, 4.31, and 4.32 respectively. The average values over the month are shown on the figures and indicate that alignment B (Figure 4.32) in the outer inlet is about five times more diluted than alignment E (Figure 4.30) in the inner inlet. The central inlet (alignment A) falls in between, being about three times more dilute than alignment E in the inner inlet. The general rise in
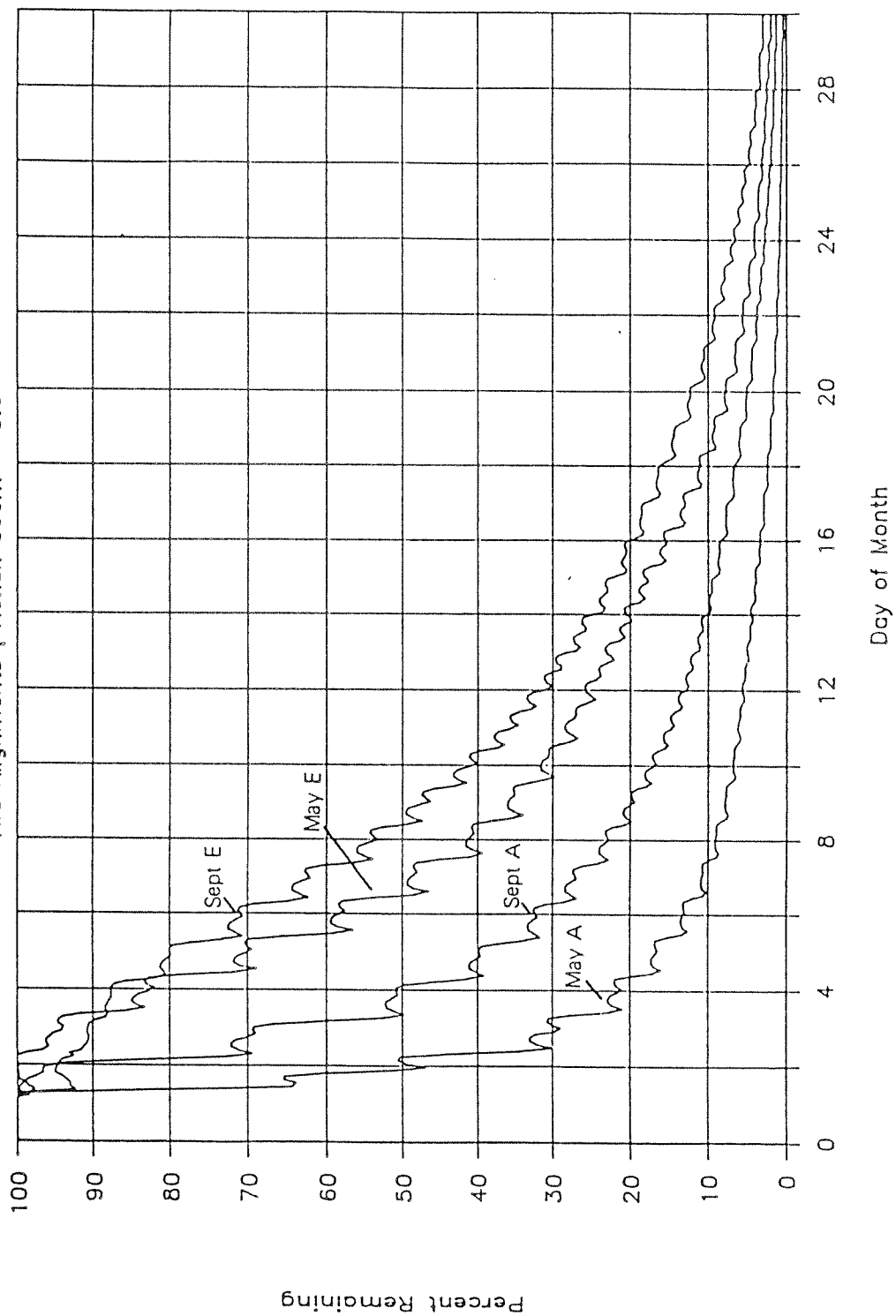
Figure 4.29 Flushing efficiency for alignment A and E, Budd Inlet, for May 1985 and September 1984 periods (reflux coefficient = 0.6).

Figure 4.30 Dilution of a conservative tracer with 24 mgd flow and initial concentration of 16,000 ug/L in the surface layer of alignment E, September 1984.

Conservative Tracer for Sept. 1984.
Alignrr Alignment A, Surface

AVG = 96 ug/L

Day of Month
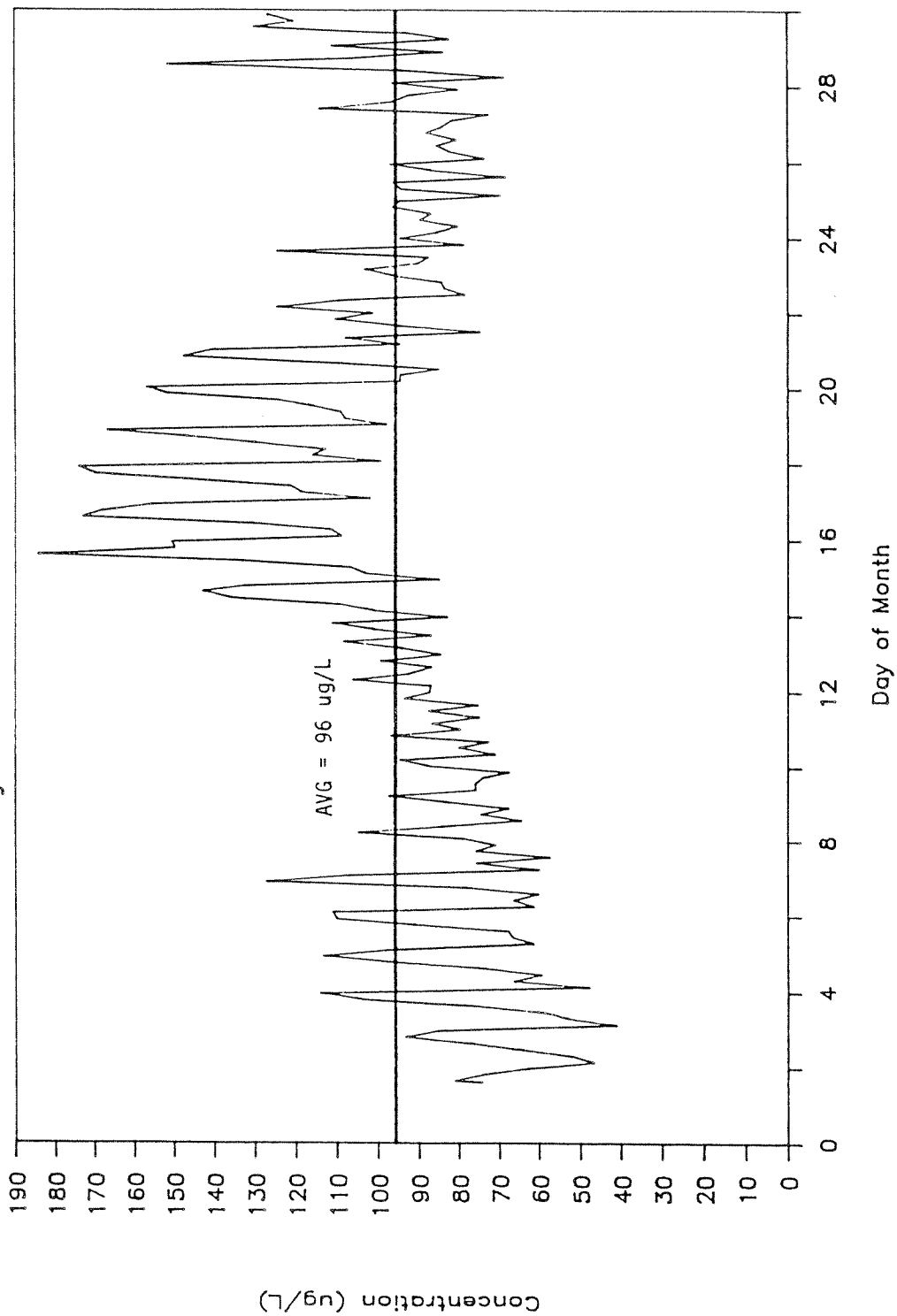
Concentration (ug/L)

Figure 4.31 Dilution of a conservative tracer with 24 mgd flow and initial
concentration of 16,000 ug/L in the surface layer of alignment A,
September 1984.
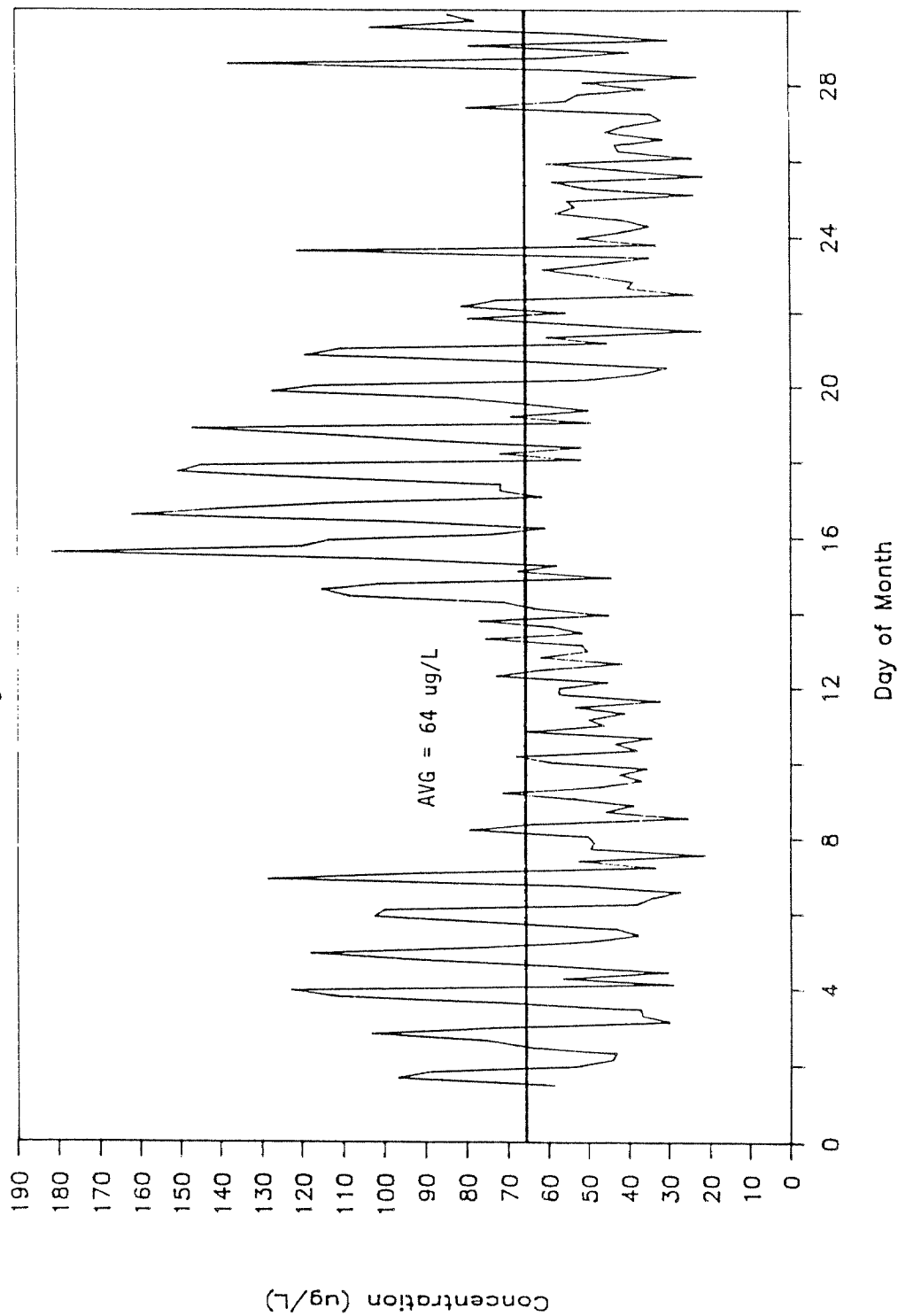
Figure 4.32 Dilution of a conservative tracer with 24 mgd flow and initial concentration of 16,000 ug/L in the surface of alignment B, September 1984.

the concentrations seen for alignments E and A starting about September 8 are due to an increase in the volume of the inlet which results from an increase in the mean tidal height (Figure 4.33(A)), coupled with decrease in the ebb between higher-high water and higher-low water (Figure 4.33(B)). These factors tend to decrease the ebb flow and allow more of the discharge to accumulate in the inner and central inlet where the flushing is less efficient.

The dispersion contour plots for slugs 1-3 (Figures 4.34-4.36) placed in the surface show an initial longitudinal and vertical dispersion pattern with the inner inlet showing more vigorous vertical mixing. The outer inlet (slug 3) is very rapidly dispersed and diluted with only minor amounts remaining after 24 hours. The central inlet placement (slug 2) showed that a portion of slug is mixed down into the landward return flow due to the estuarine circulation in the inlet. The inner inlet placement (slug 1) tends to show less longitudinal displacement due to the vertical mixing. In fact, the net circulation at the head actually moves the surface maximum towards the head of the inlet from segment four into segments two and three.

The sub-surface slug placements (Figures 4.37 and 4.38) show a consistent pattern of landward displacement with vertical mixing. The last time contoured at 63 hours shows the effect of the vertical circulation at the head of the inlet which tends to detain material in the surface of segments two, three and four.

Alternative Discharge Configurations

May scenarios. Three outfall alignments, four flow rates and two alternative nutrient removal scenarios for the LOTT discharge were supplied by LOTT and WDOE (Singleton, 1985) to be used as input to the dynamic model. The 24 million gallons per day (mgd) flow rate corresponds to the estimated average dry weather flow (ADWF) rates for the year 2010 using a factor of 0.71 to convert average wet weather flow rates to dry weather rates (Singleton, 1985). The 16.3 mgd flow rate corresponds to the presently
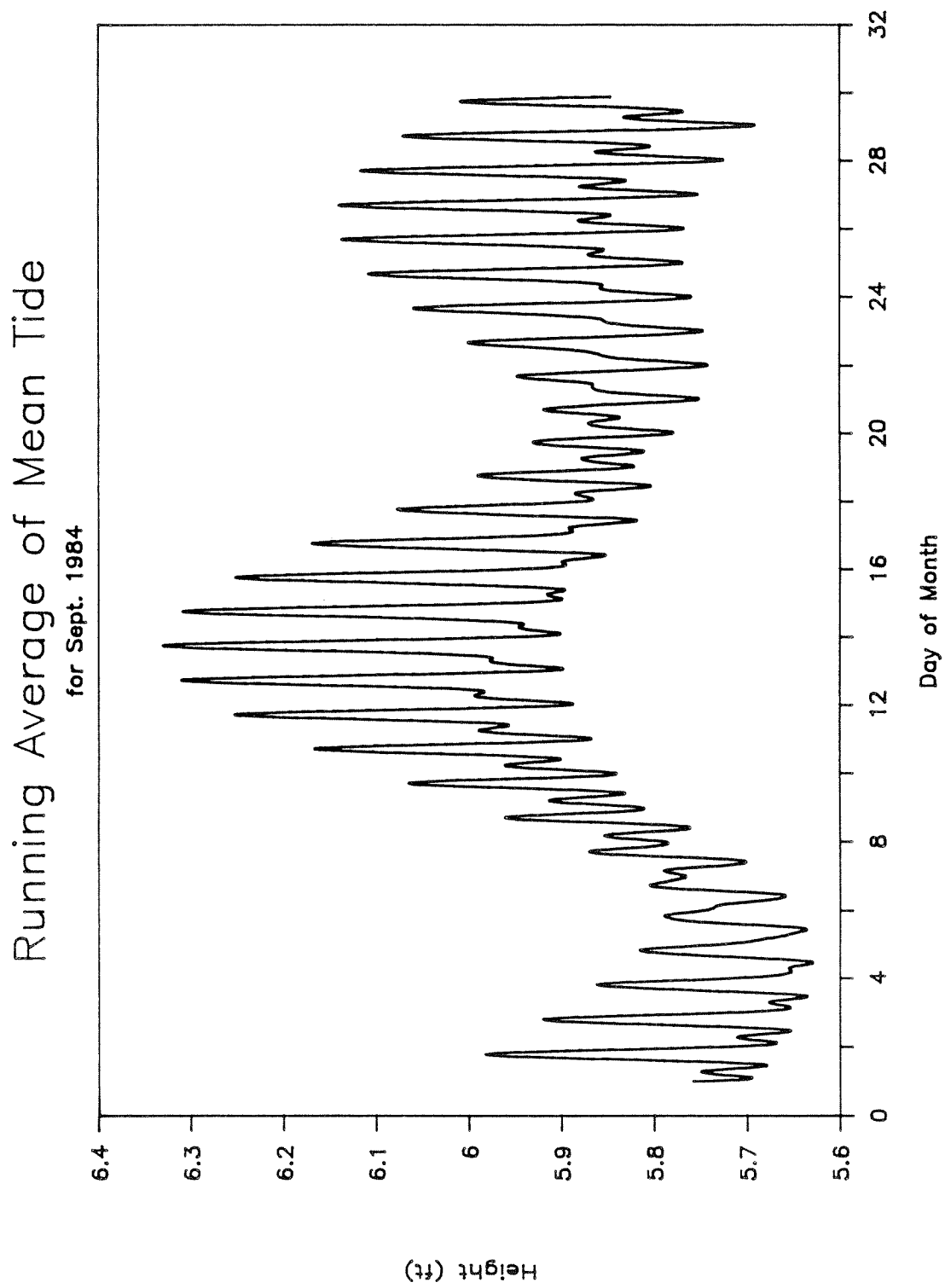
Figure 4.33A Mean tide based upon a running average over a 24 hour and 50 minute tidal cycle.

Figure 4.33B   September 1984 tidal range.
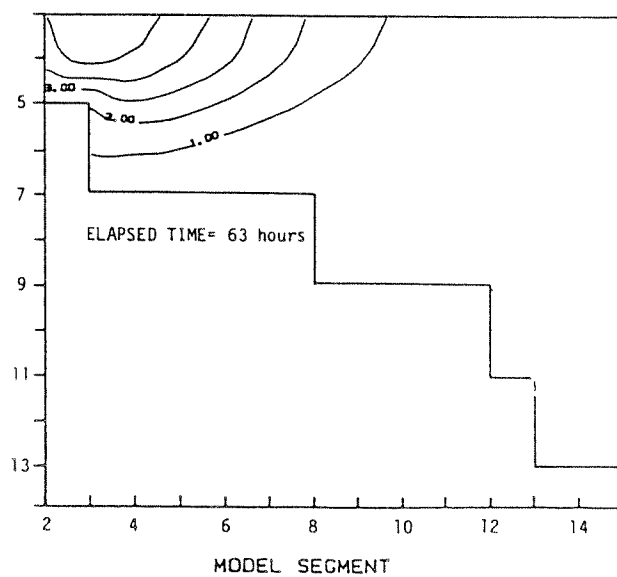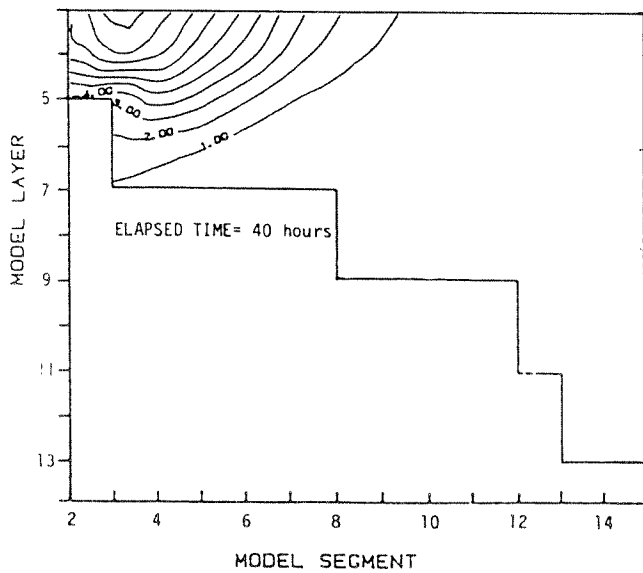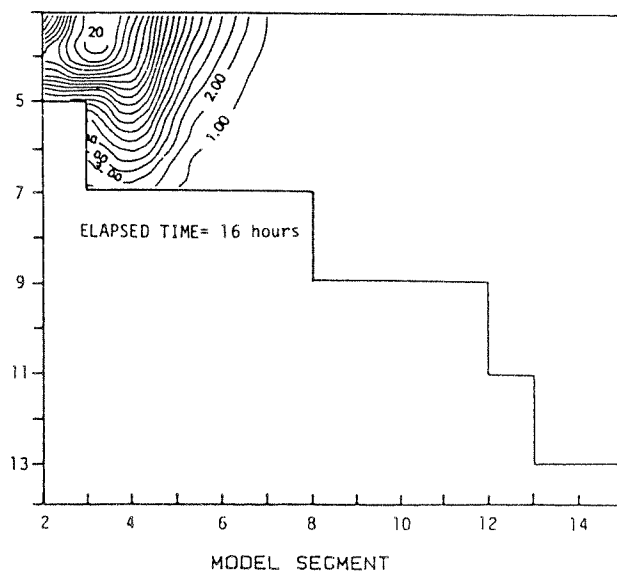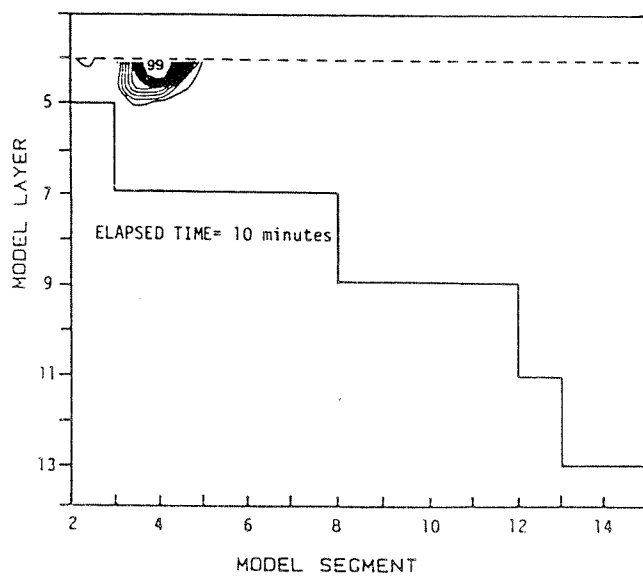
Figure 4.34 Modeled dispersion results for "slug" placement 1
for elapsed time of 10 minutes, 16, 40, and 63 hours.
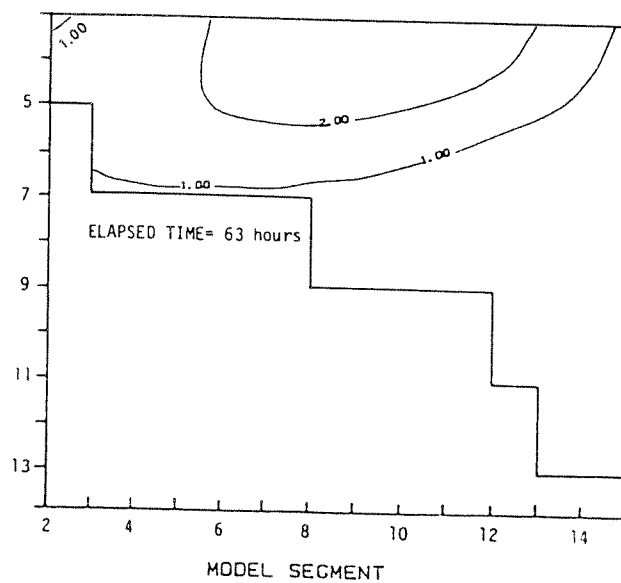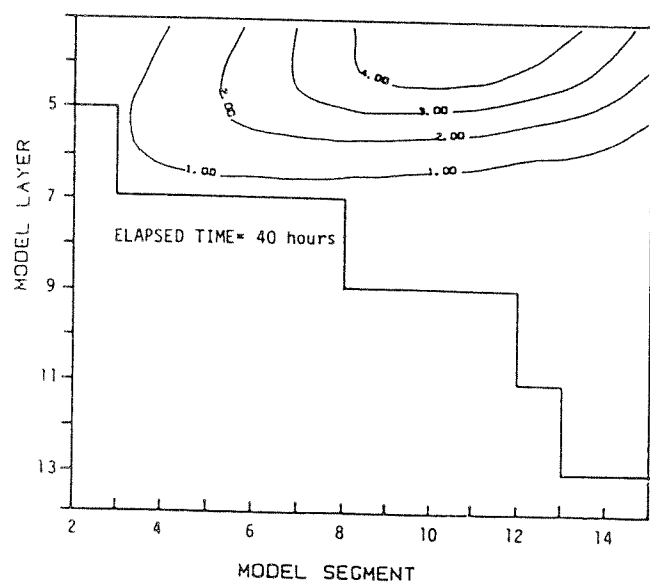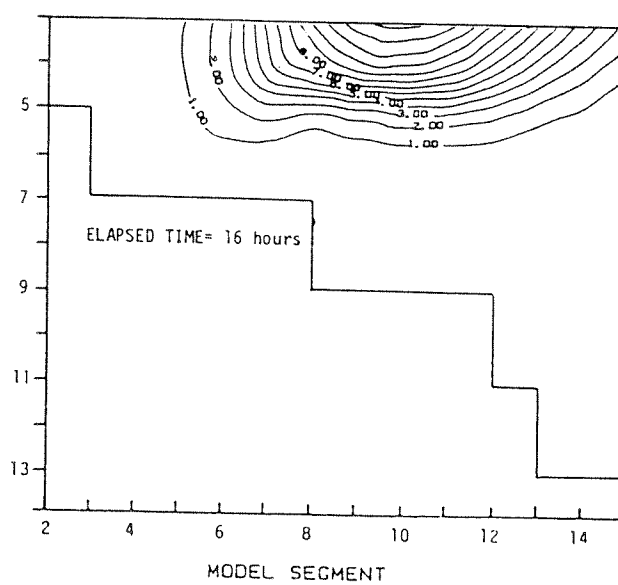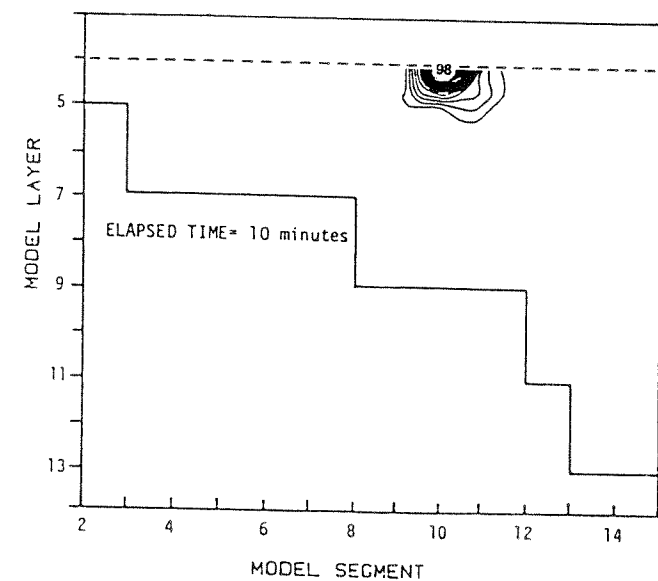
Figure 4.35 Modeled dispersion results for "slug" placement 2, for elapsed time of 10 minutes, 16, 40, and 63 hours.
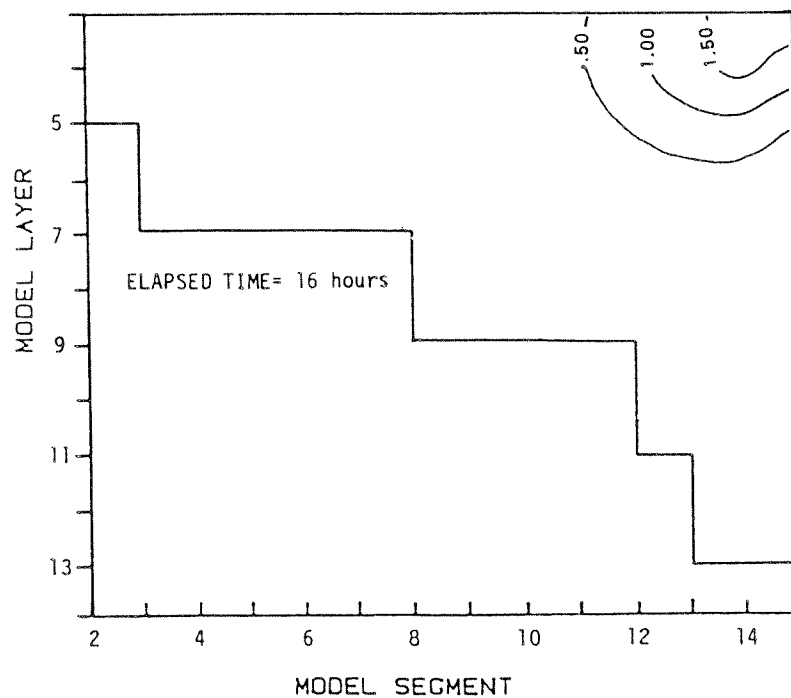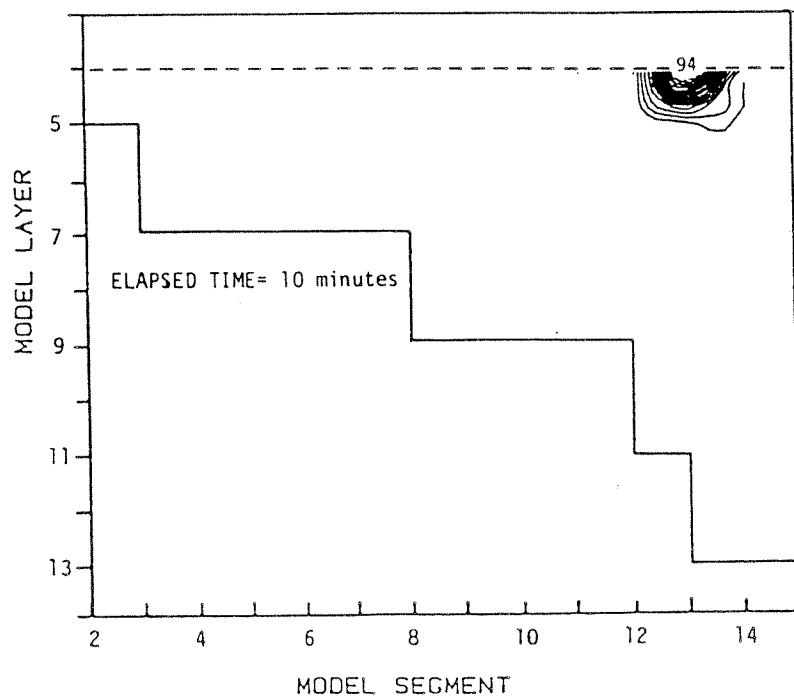
Figure 4.36 Modeled dispersion results for "slug" placement 3,
for elapsed time of 10 minutes, 16, 40, and 63 hours.
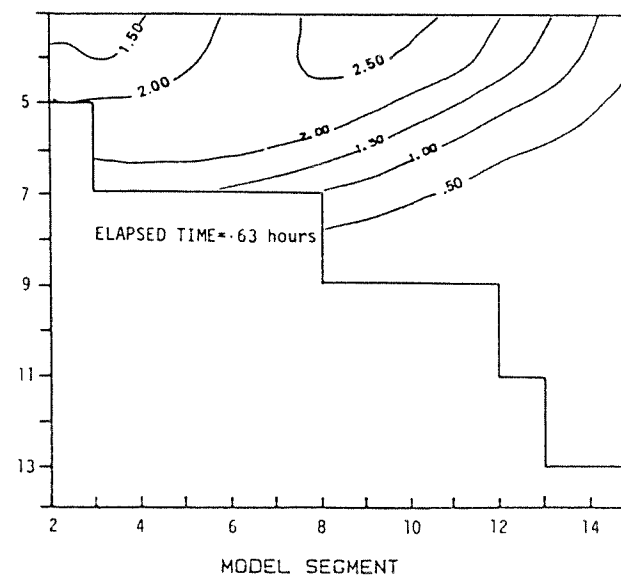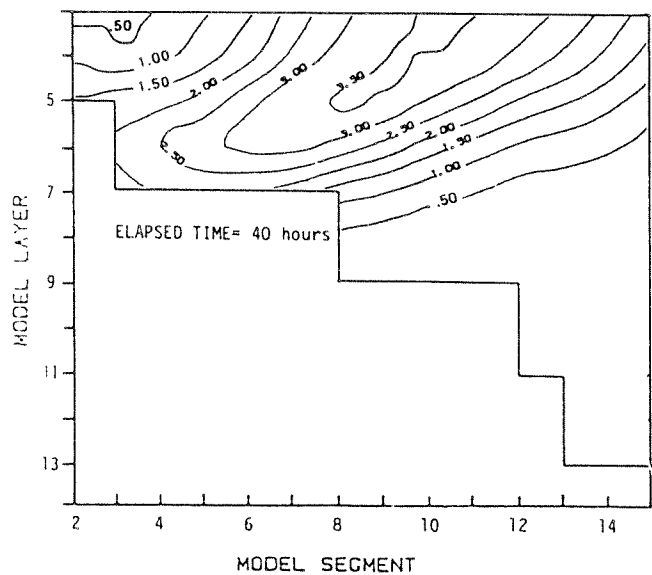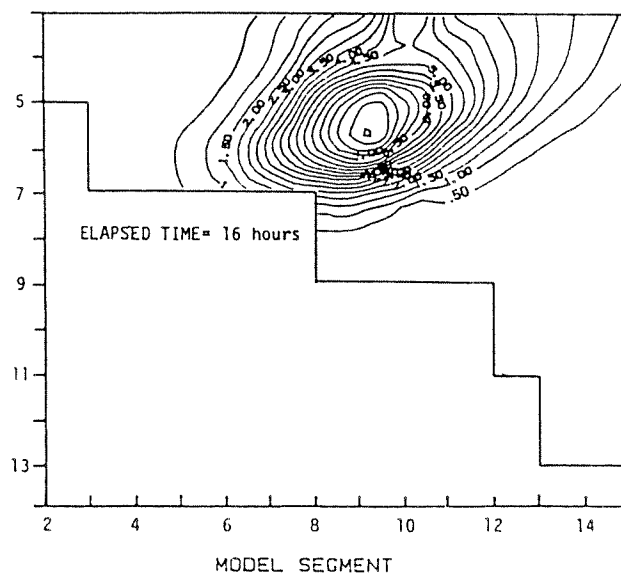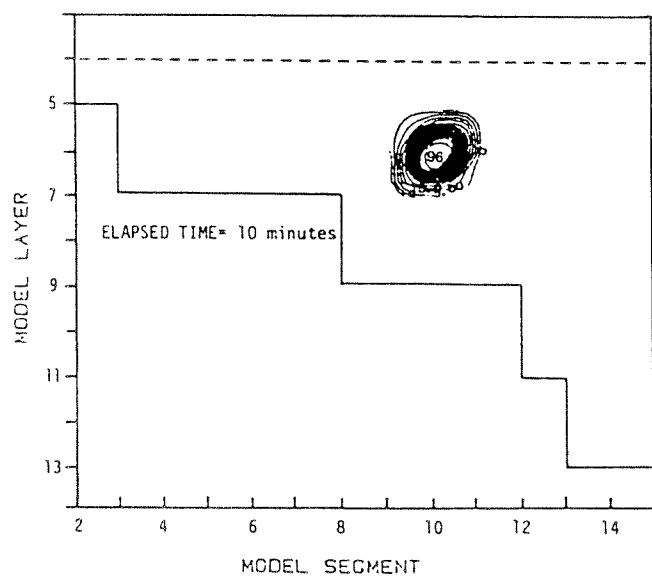
Figure 4.37 Modeled dispersion results for "slug" placement 4,
for elapsed time of 10 minutes, 16, 40, and 63 hours.
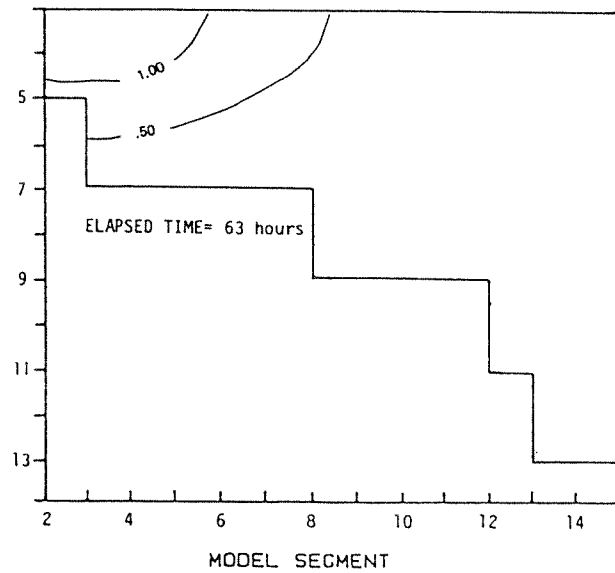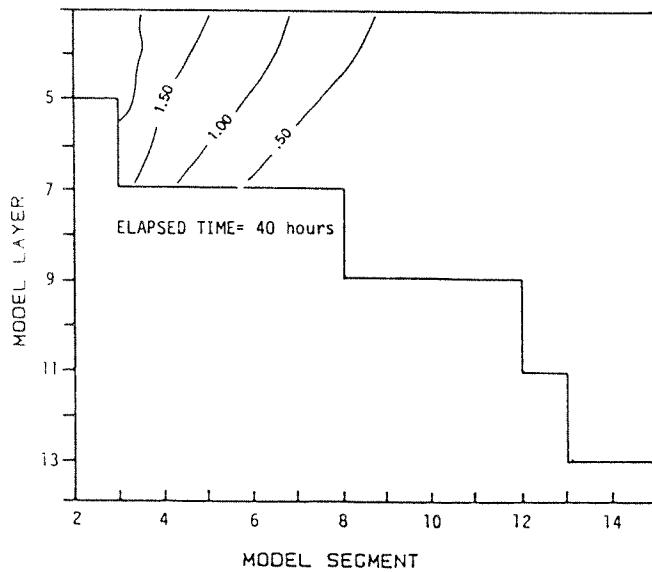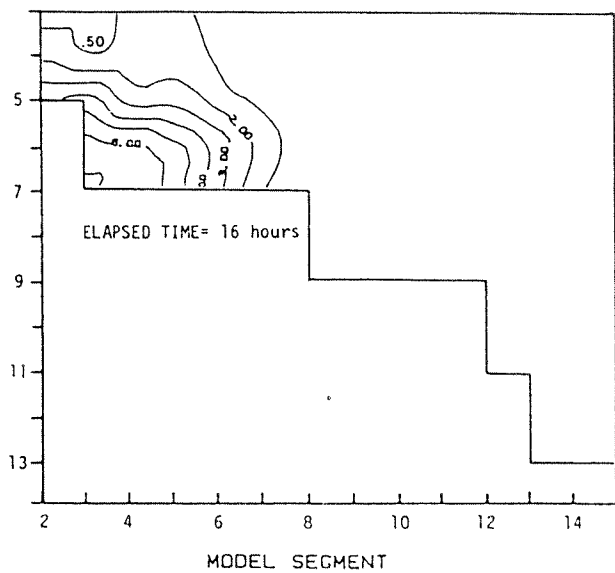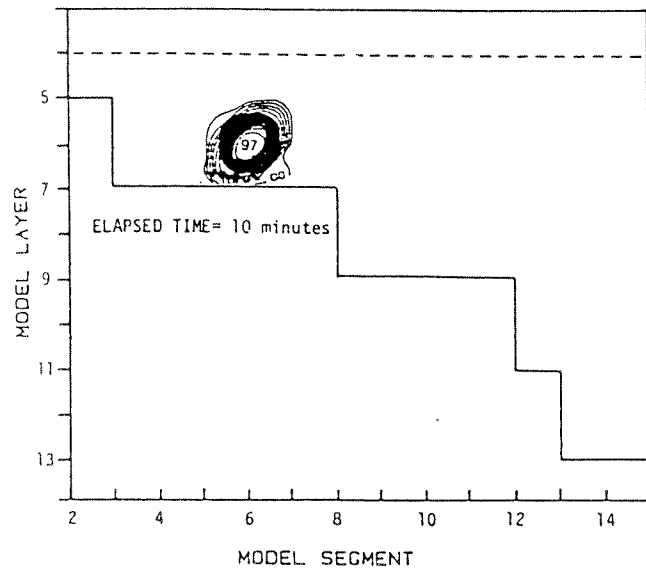
Figure 4.38 Modeled dispersion results for "slug" placement 5, for elapsed time of 10 minutes, 16, 40, and 63 hours.

permitted average wet weather flow (AWWF) rate. The 22 mgd flow rate represents the average wet weather flow design capacities for the LOTT treatment plant. A baseline scenario was added for alignment E which represents the existing conditions measured in May 1985 with a flow rate of 12.4 mgd. This accounted for a total of eight scenarios which are listed below.

Scenario	Alignment	AWWF	ADWF	Modeled Flow rate	Nutrient removal
1	E/Baseline	16.3	11.6	12.4 mgd	None
2	E	22.0	16.0	0.0 mgd	None
3	E	34.0	24.0	24.0 mgd	None
4	E	34.0	24.0	24.0 mgd	90% Removal
5	E	22.0	16.0	16.0 mgd	None
6	E	22.0	16.0	16.0 mgd	90% Removal
7	A	34.0	24.0	24.0 mgd	None
8	B	34.0	24.0	24.0 mgd	None

The outfall alignments (Figure 4.39) correspond to model segments 4, 10 and 14 for alignments E, A and B, respectively. Outfall alignment C was not simulated. This alignment was outside of the model grid and could not be treated as a simple boundary condition due to the complex circulation in this area (see Section 3.3).

The concentrations of nutrients, BOD, organic N and dissolved oxygen used in the scenarios are listed below. All constituents listed below are given in units of mg/L. Scenario 1 data, which we will call baseline, are taken from the May 1985 source survey.

LOTT Discharge Concentrations

Scenario	BOD	Nitrate-N	Nitrite-N	Ammonium-N	Org-N	D. O.
1	21	4.04	1.10	16.0	11.4	10.0
2	---	---	No Discharge	---	---	---
3	18	2.70	0.45	16.0	11.4	10.0
4	18	0.27	0.045	1.60	11.4	10.0
5	18	2.70	0.45	16.0	11.4	10.0
6	18	0.27	0.045	1.60	11.4	10.0
7	18	2.70	0.45	16.0	11.4	10.0
8	18	2.70	0.45	16.0	11.4	10.0

Figure 4.39
Alternative Outfall Alignments
and Diffuser Sites.
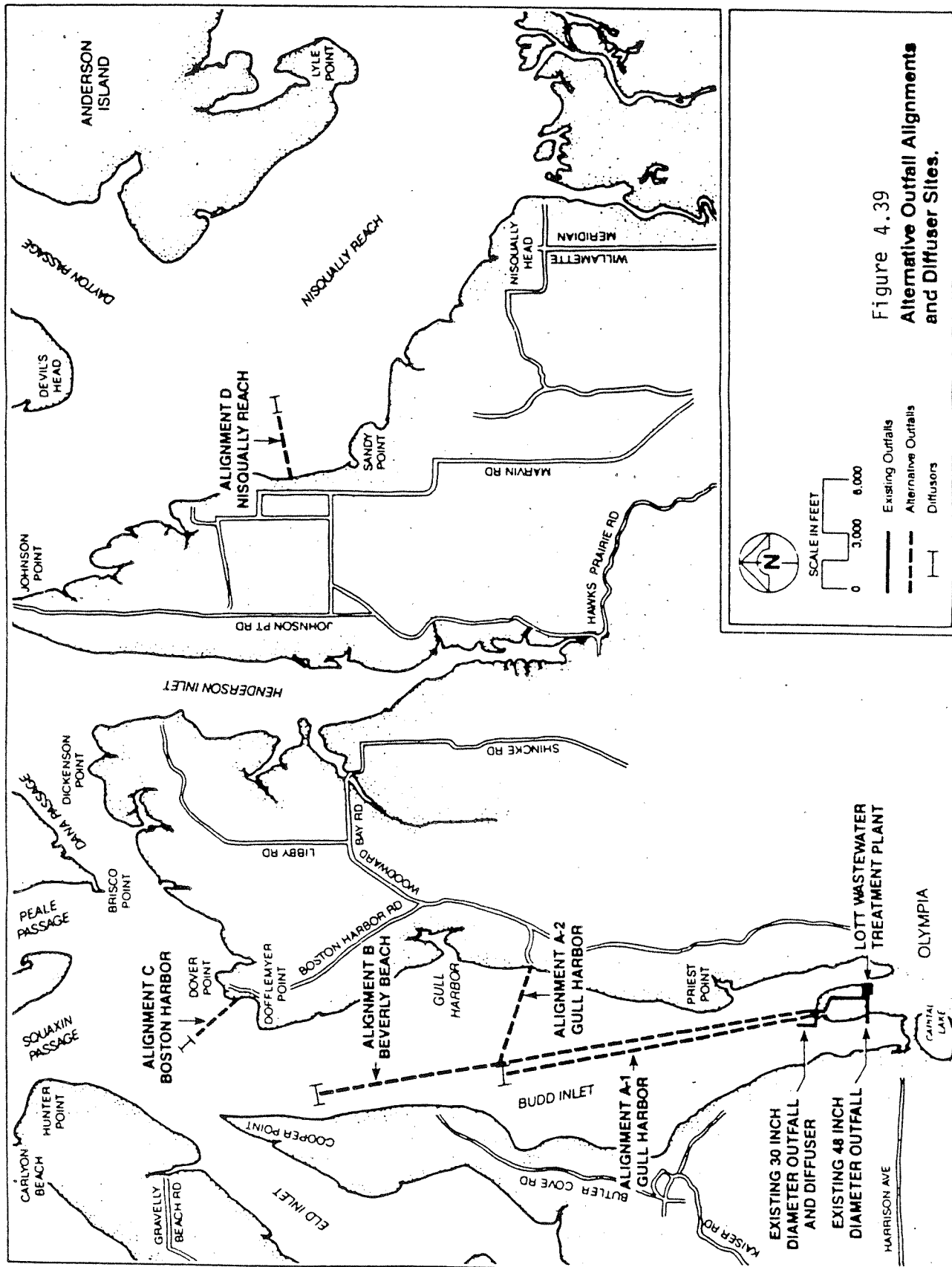
The three types of output from the model used in the analysis are integrated chlorophyll a, sediment oxygen demand and near-bottom dissolved oxygen concentration. These parameters were chosen to illustrate the effect of nutrient addition on algal growth and in turn on the SOD and bottom water oxygen levels. The output of these parameters is displayed both over time at each outfall placement, and at fixed time during bloom conditions over the length of the inlet.

Figure 4.40 compares the predicted integrated chlorophyll a for the alignment E scenarios (scenarios 1-6) for the month of May. These data show a bloom starting about May 15 which is clearly enhanced by the presence of the discharge. The no discharge scenario 2 shows peak values of about 100 mg Chl a/m^2 during the bloom, while the existing conditions shown in the baseline scenario show an increase to over 130 mg Chl a/m^2. The two scenarios with higher discharge rates show even higher levels of integrated chlorophyll a of 150 mg Chl a/m^2 or more which represent at leasts a 50 percent increase in algal growth. Finally, the two scenarios with 90 percent nutrient removal show peak bloom levels of between 100 and 110 mg Chl a/m^2.

A comparison of the integrated chlorophyll a for the three alternative alignments using the same discharge configuration is shown in Figure 4.41. These data indicate that the inner inlet alignment E shows the largest increase in chlorophyll levels during the bloom and the outer inlet alignment B shows the least. This would be expected based on our analysis of the dilution/dispersion and flushing potential of these alignments described previously.

The onset and duration of the bloom around May 15 was initiated by a few consecutive days of clear weather. This can be seen in Figure 4.42 which shows the chlorophyll a concentration in the surface at alignment E for scenario 3 along with the sky cover for the month. This is typical of spring diatom blooms in the main basin of Puget Sound (Winter et al.,1975). The strength of the bloom in Budd Inlet, however, is controlled by the

Chlorophyll – a

ALIGNMENT E, NO DISCHARGE

ALIGNMENT E, BASELINE

ALIGNMENT E, 16 MGD, 90% REMOVAL

ALIGNMENT E, 16 MGD, NO REMOVAL

ALIGNMENT E, 24 MGD, 90% REMOVAL

ALIGNMENT E, 24 MGD, NO REMOVAL
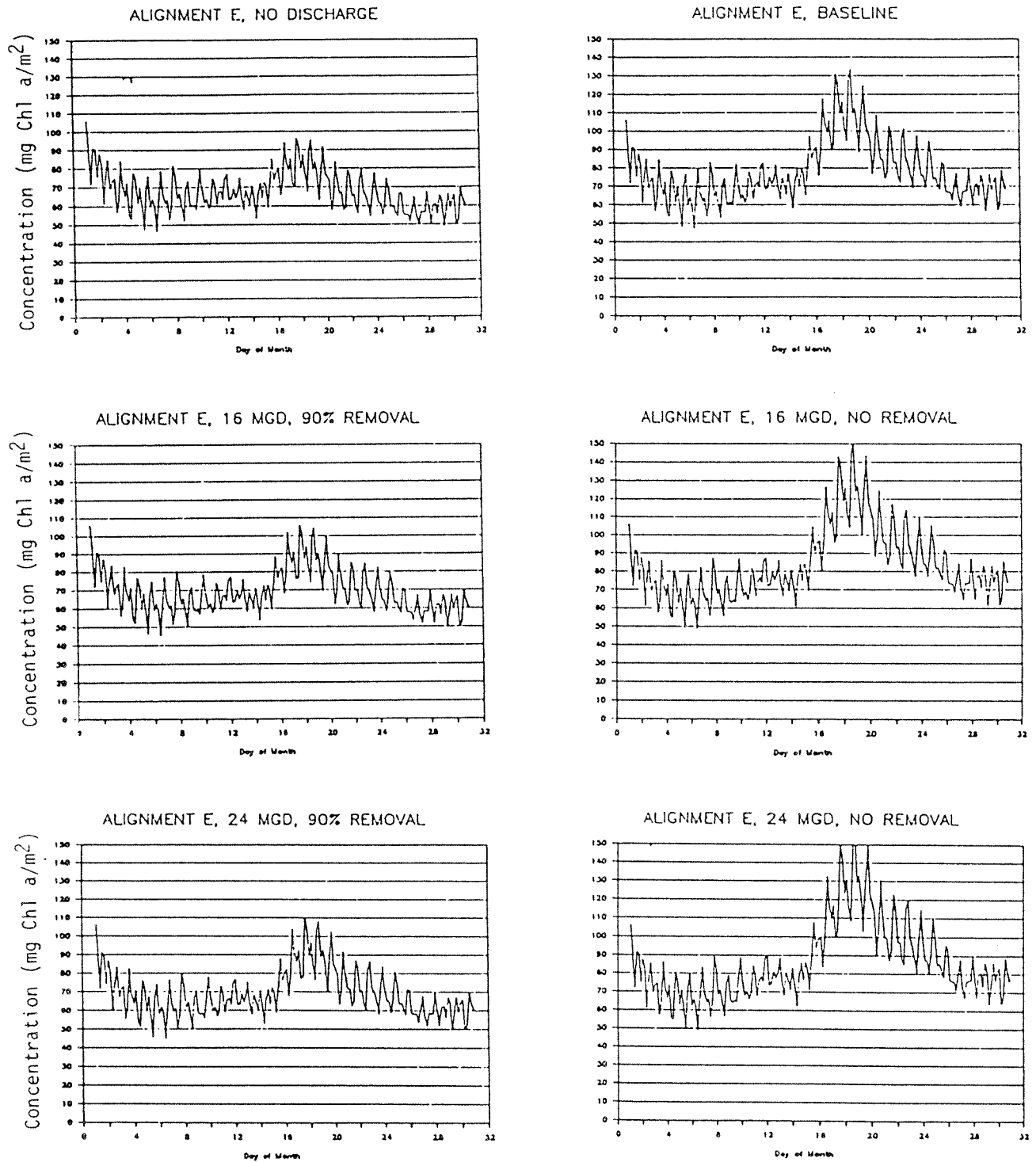
Figure 4.40 Modeled Chl-a results for alignment E scenarios, May 1985.

Chlorophyll – a

ALIGNMENT E, 24 MGD, NO REMOVAL

ALIGNMENT A, 24 MGD, NO REMOVAL

ALIGNMENT B, 24 MGD, NO REMOVAL
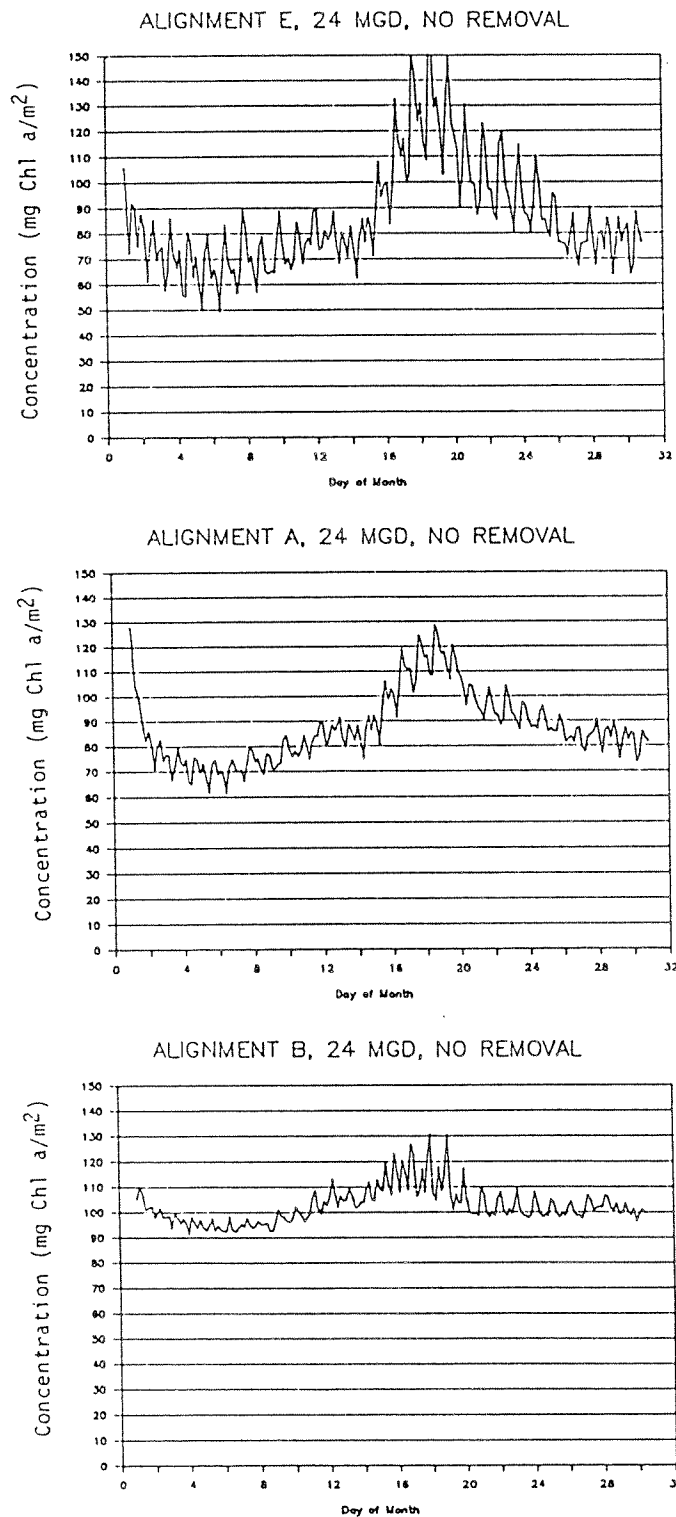
Figure 4.41 Modeled Chl a results for alignments E, A and B:
24 mgd, no removal, May 1985.
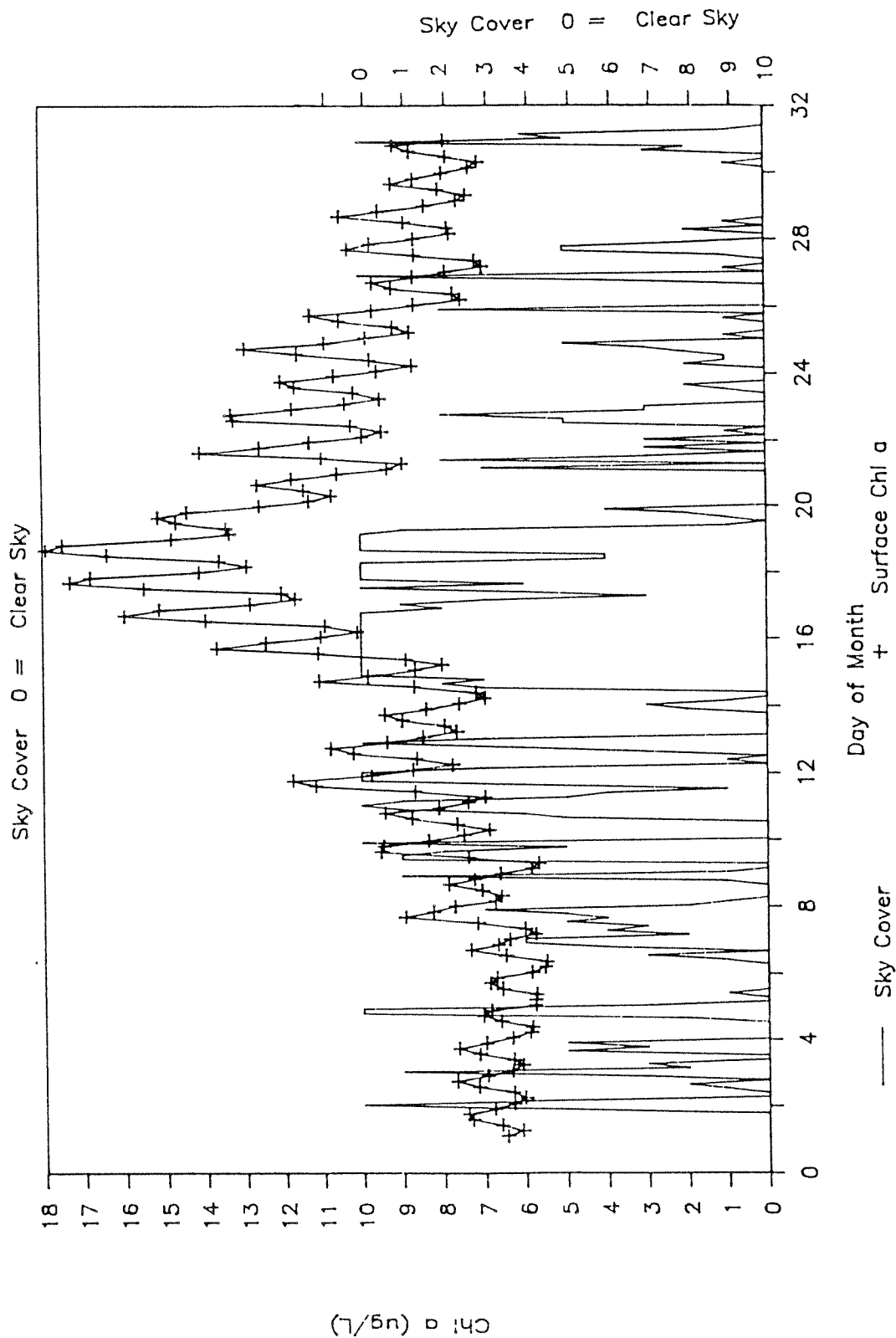
Figure 4.42 Modeled Chl a results and observed sky cover for May 1985.

amount, and by the location of the LOTT discharge in the inlet. This is
shown in Figure 4.43, which compares the integrated chlorophyll a throughout
the inlet at one time during the bloom for the alignment E configurations,
and Figure 4.44, which compares the three outfall alignment options. The
following table (Table 4.13) compares the sum of the predicted chlorophyll a
integrated over the water column in the inner inlet (segments 2-7), the
central inlet (segments 8-11) and the outer inlet (segments 12-15) for each
of the scenarios shown in Figures 4.43 and 4.44.

Table 4.13   Predicted integrated chlorophyll a for
portions of Budd Inlet by scenario
(units in mg Chl a/m^2)

Scenario	Inner inlet	Central inlet	Outer inlet
1	706	477	426
2	541	424	415
3	812	532	438
4	605	445	420
5	774	511	434
6	587	439	418
7	761	512	434
8	704	483	428

Figure 4.45 shows the comparative increase in the intensity of the May
bloom over the no discharge scenario 2 for all other scenarios for the
inner, central and outer inlet. These data indicate that next to discharge
elimination, nutrient removal is the next best option in order to
substantially reduce spring algal blooms. All scenarios without nutrient
removal show a 30 to 50 percent increase in the strength of the algal bloom
relative to the no discharge scenario for the inner inlet. Alignments A and
B (scenarios 7 and 8), even though they have the highest dilution potential,
are not significantly different from scenarios 5 and 1, respectively, of
alignment E.

The high algal production rates for alignments A and B is in part due
to the fact that phytoplankton uptake rate is faster than the flushing rate,

4-94
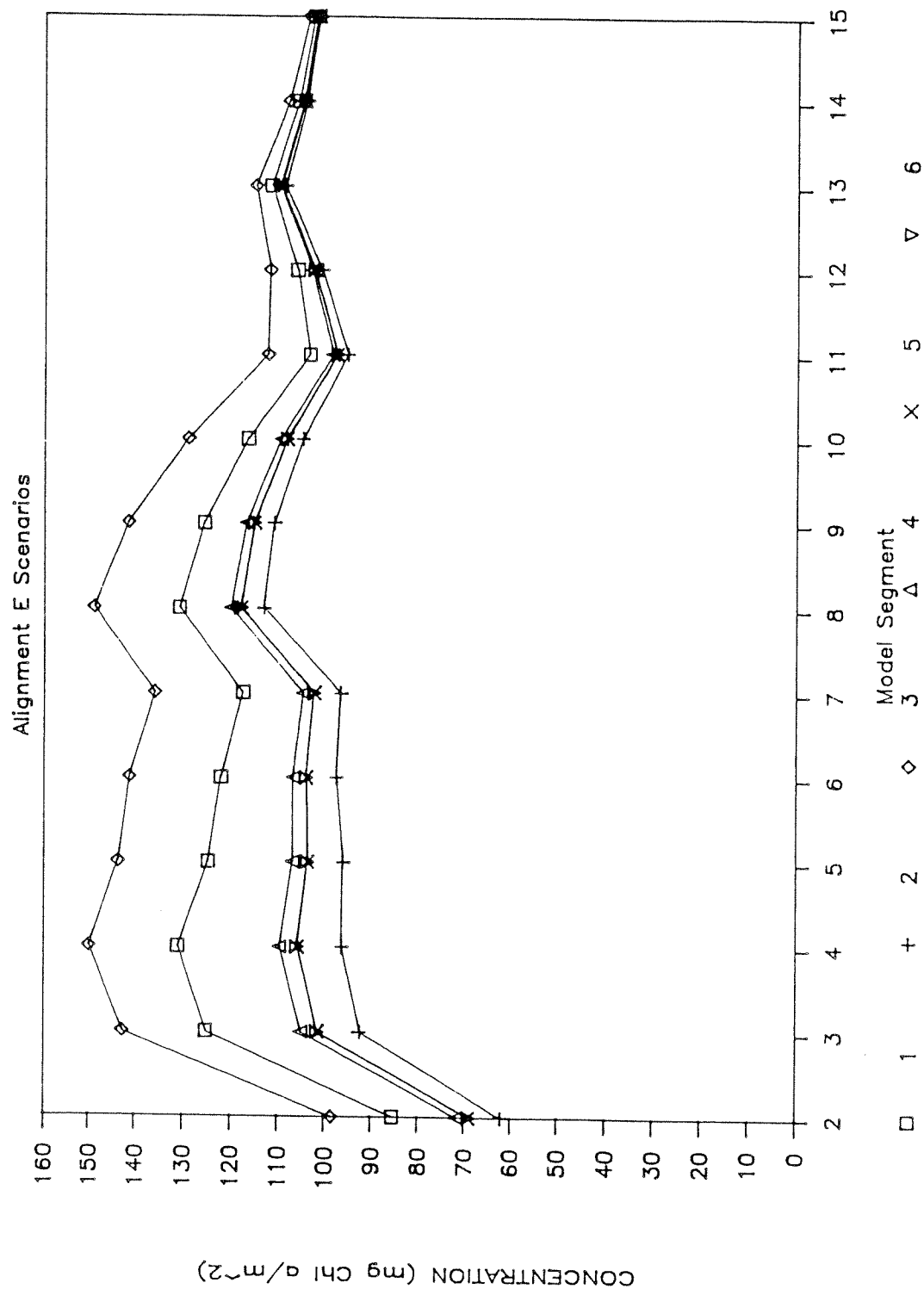
Figure 4.43 Predicted integrated Chl a for alignment E scenarios: May 1985
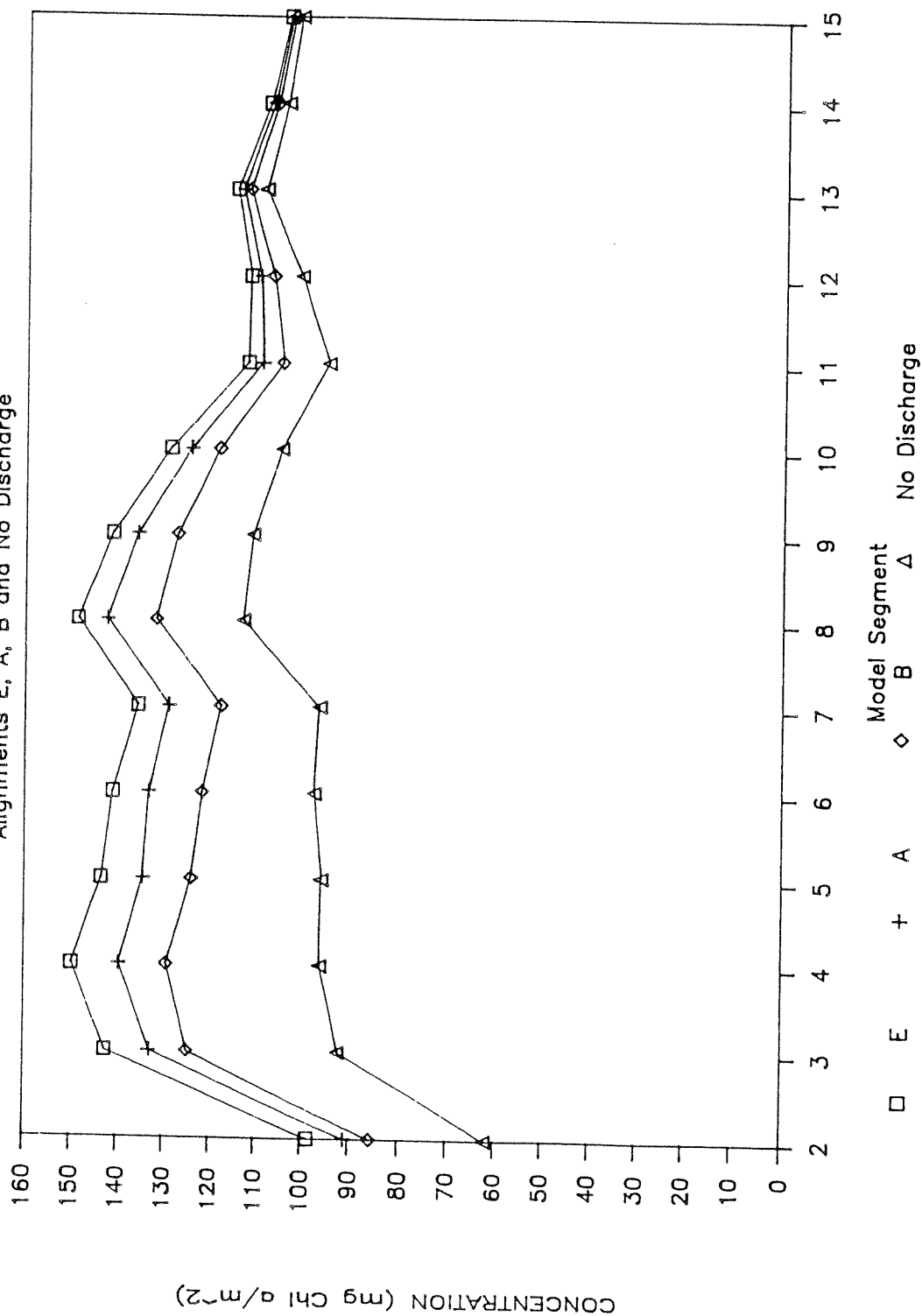
Figure 4.44 Predicted integrated Chl a for alignment E, A, B, and no discharge alternatives for May 1985.

Figure 4.45 Modeled May bloom enhancement as percent increase over no discharge alternative (scenario 2) for May 1935.

even for the outer inlet. It also is partly due to the estuarine circulation which will carry the sinking phytoplankton back into the inlet where a portion of them will be mixed or advected back into the surface layers. In addition, short-term recycling of ammonium due to algal respiration and excretion coupled with the estuarine circulation will tend to retard flushing of the nitrogenous nutrients.

The predicted sediment oxygen demand for the alignment E scenarios (Figure 4.46) follow the same pattern as the predicted integrated chlorophyll a values. This would be expected since the SOD is directly related to the algal production (section 4.2). Figure 4.47 compares the predicted SOD results at a fixed time during the bloom throughout the inlet for the E scenarios and Figure 4.48 shows the predicted values for scenarios 2,3,7 and 8. These data show that there is very little difference between the predicted SOD values for any of the scenarios for the central and outer inlet north of Butler Cove. The inner inlet segments show a maximum 15% increase in SOD for the high discharge scenario 3 over the no discharge scenario 2. The central and outer inlet outfall placements (alignments A and B) reflect the chlorophyll a results indicating similar SOD rates to alignment E scenarios 5 and 1.

Since the benthic ammonium release is directly proportional to the SOD, we might expect to see a similar increase in ammonium release for the higher discharge rates.

Figure 4.49 compares the predicted near-bottom dissolved oxygen concentrations for the alignment E scenarios. These predictions show an increase in dissolved oxygen related to an increase in algal growth. This is not unexpected based on our experience with the September calibration (section 4.2). What it indicates is that the vertical and horizontal mixing and transport processes can transfer oxygen produced near the surface to the bottom water in the inner inlet faster than it can be consumed by the sediment oxygen demand. This can also be seen in Figures 4.50 and 4.51 which show the longitudinal distribution of near-bottom dissolved oxygen for the alignment E scenarios and the three outfall alignments, respectively.

Sediment Oxygen Demand

ALIGNMENT E, NO DISCHARGE

ALIGNMENT E, BASELINE

ALIGNMENT E, 16 MGD, 90% REMOVAL

ALIGNMENT E, 16 MGD, NO REMOVAL

ALIGNMENT E, 24 MGD, 90% REMOVAL

ALIGNMENT E, 24 MGD, NO REMOVAL
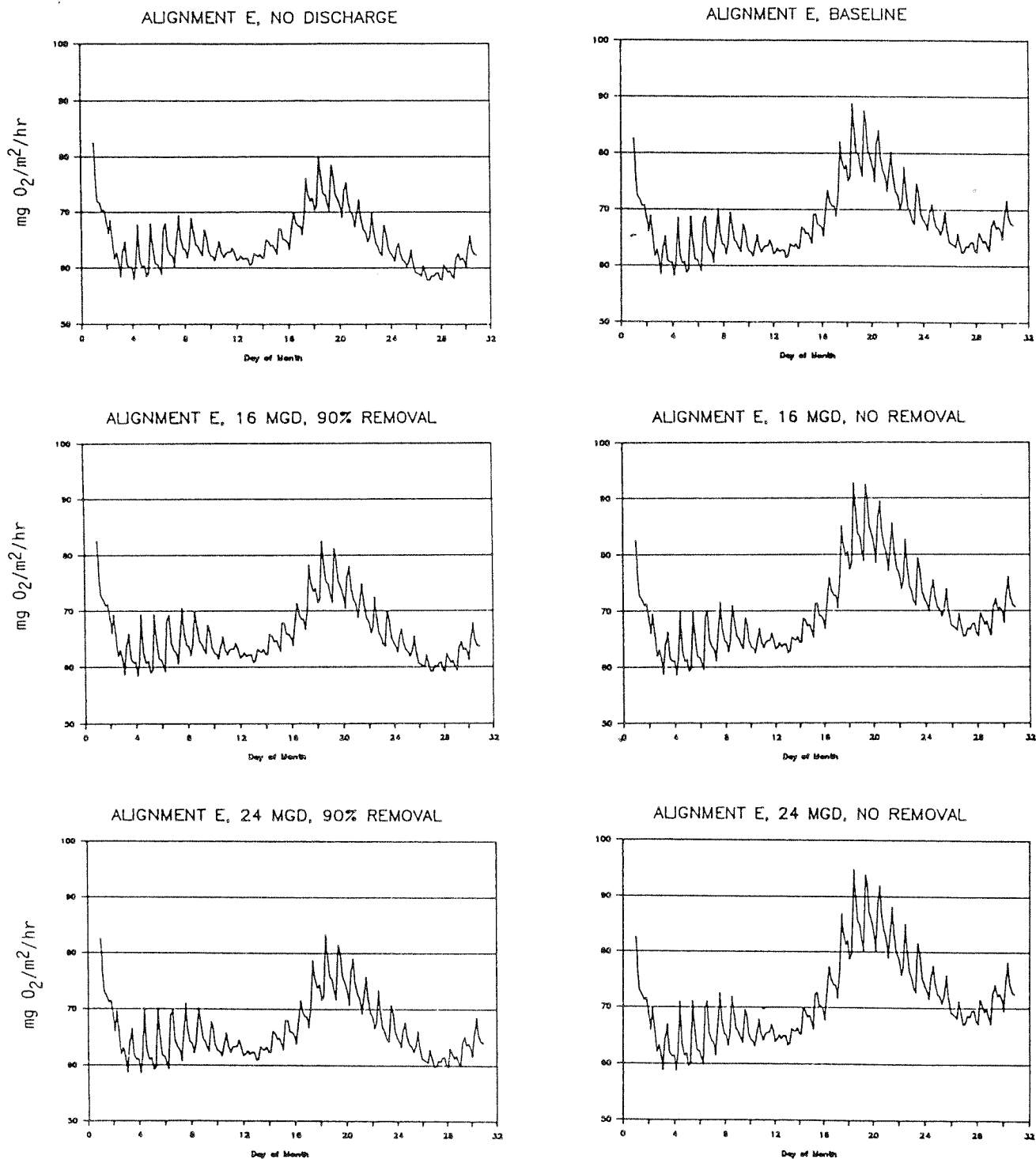
Figure 4.46 Modeled sediment oxygen demand over time for alignment E
scenarios: May 1985.

4-99
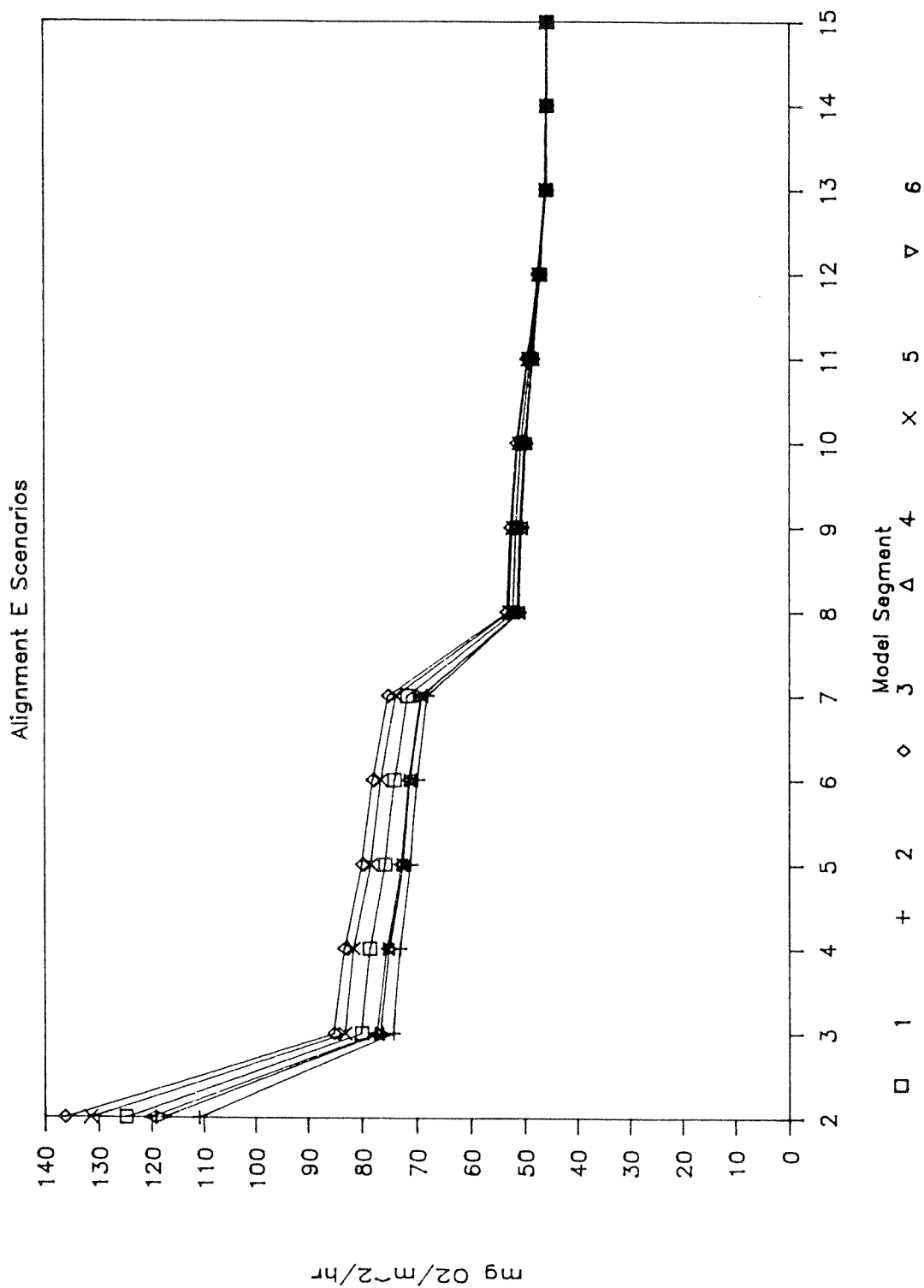
Figure 4.47 Modeled sediment oxygen demand during bloom along the Inlet for alignment E scenarios: May 1985.
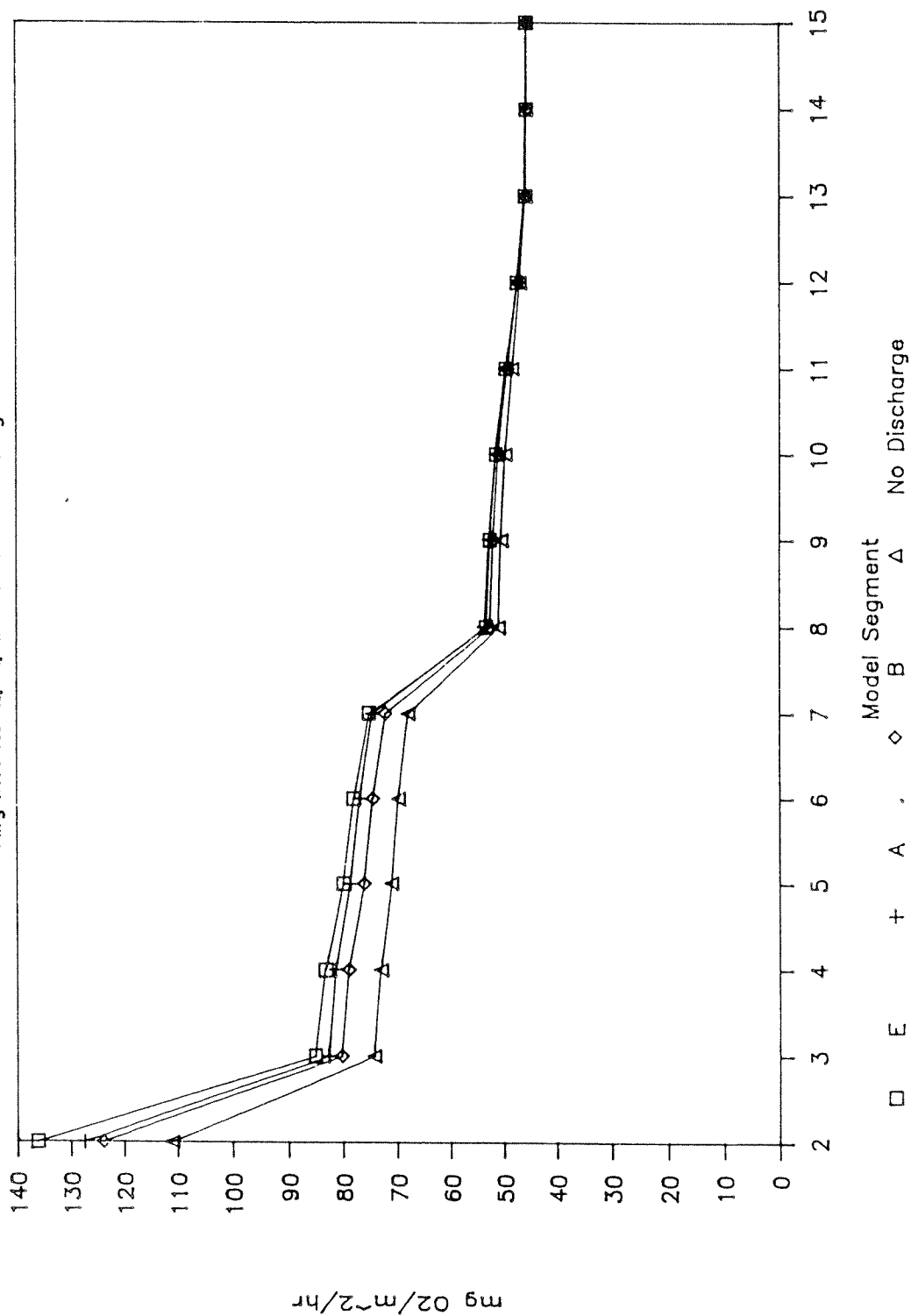
Figure 4.48 Modeled sediment oxygen demand during bloom along the Inlet for alignment E, A, B and no discharge alternative : May 1985.

Dissolved Oxygen
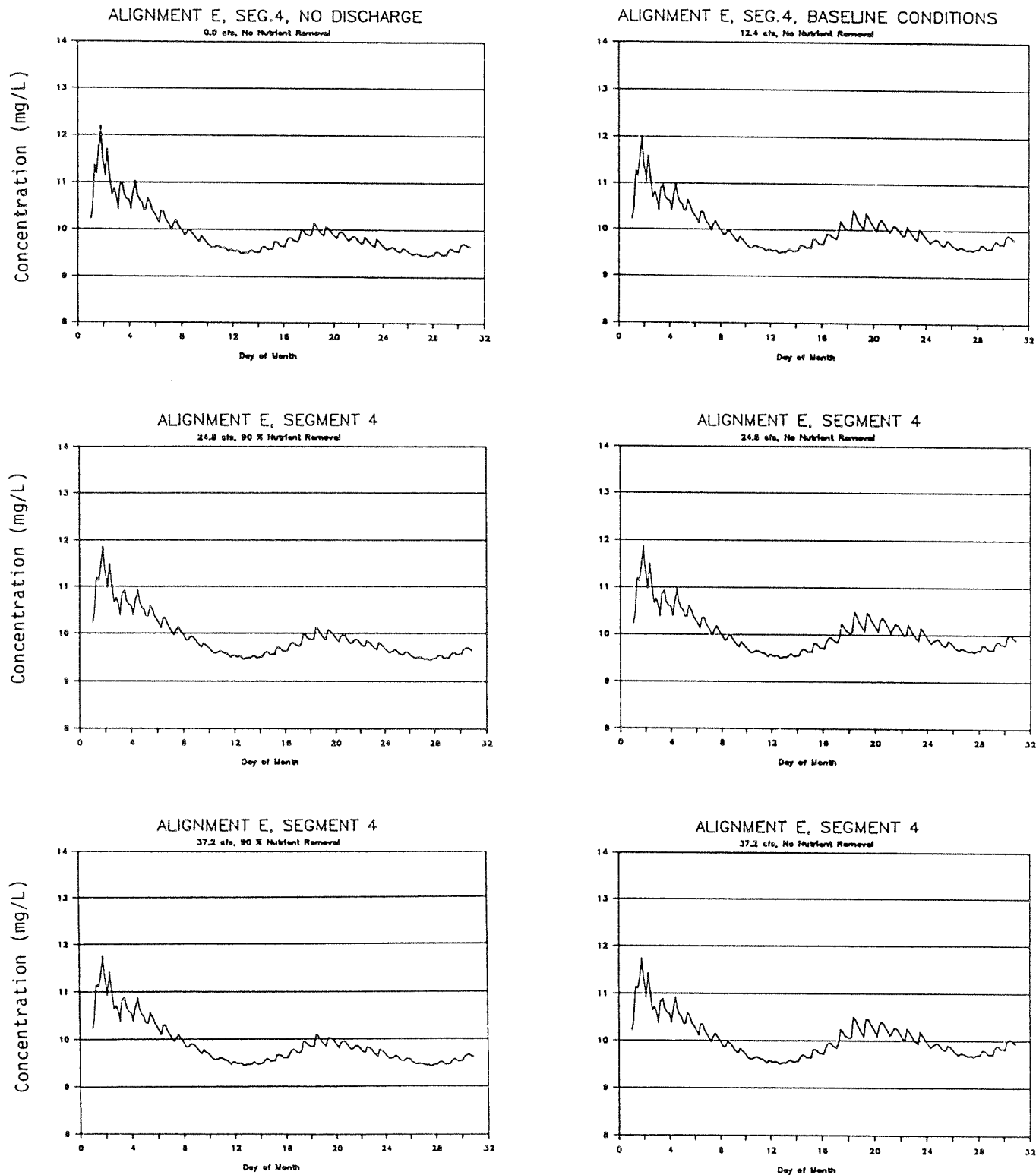
Figure 4.49   Modeled near bottom dissolved oxygen concentration over time for alignment E scenarios: May 1985.

Figure 4.50   Modeled near bottom dissolved oxygen concentration during bloom along the Inlet for alignment E scenarios: May 1985.

Figure 4.51 Modeled near bottom dissolved oxygen concentration during bloom along the Inlet for alignment E, A, B, and no discharge alternatives: May 1985.

<u>Dinoflagellate/low D.O. scenario</u>. Since we do not at present have a quantitative dynamic model of the dinoflagellate bloom in September, we will rely on our observations from the May scenarios along with our measurements in September to qualitatively discuss the effect of discharge alternatives on dinoflagellate blooms and the low dissolved oxygen problem in Budd Inlet.

Dinoflagellate blooms have been generally considered to be the final stage of a temporal succession of phytoplankton during the growing season. This succession begins in the spring with small-celled diatoms that have large surface/volume ratios and high growth rates, such as <u>Chaetoceros</u> spp., which were believed to be the dominant diatom present during our May 1985 survey (Andrea Copping, personal communication). This is followed by a period with a mixed community of diatoms containing more larger cell diatoms with higher sinking rates. As nutrients are depleted in the surface and light levels decrease following the summer solstice, migrating dinoflagellates with their ability to assimilate nutrients from the deeper water in the dark and to migrate back up in the water column to their optimum light level during the day, gain a competitive advantage over the diatoms (Epply and Harrison, 1975; Seliger et al., 1975). If stability in the water column is maintained and there is an ample supply of nutrients, monospecific blooms may occur (Robinson and Brown, 1983).

Since the occurrence of dinoflagellate blooms is part of the normal temporal succession of phytoplankton, the presence of dinoflagellate blooms in Budd Inlet is not as important to the low dissolved oxygen problem as are the strength and duration of the blooms. Based on our experience with the spring bloom in May, which showed 30 to 50 percent increase in the strength of algal bloom due to nutrient addition for any discharge configuration without nutrient removal, we can infer that a similar result would hold true for the dinoflagellate blooms.

The magnitude of the nutrient enhancement of the dinoflagellate bloom could in fact be greater than what we observed for the diatoms in May. The ability of the dinoflagellates to grow at lower light levels and to migrate to their optimum light level would indicate that, given the right

hydrodynamic conditions, they would rarely be light limited. Their ability to take up nutrients day and night implies that the magnitude of the bloom would be dependent on the supply of nutrients. This was not the case in May when the duration of the bloom was controlled by the number of consecutive sunny days. This scenario is supported by a recent study of the recurrent _Gymnodinium_ _sanguineum_ blooms observed during the fall in a coastal lagoon on Vancouver Island (Robinson and Brown, 1983). The authors concluded that the ultimate magnitude of each years bloom was regulated by the availability of nitrate supplied in runoff.

If we include in this scenario the lower flushing rates in the late summer and early fall, combined with the estuarine accumulation mechanism discussed in the previous section, we have the potential for a sustained dinoflagellate bloom enhanced by nutrient addition in Budd Inlet. The longer the bloom is sustained and the stronger it is, the larger the potential for oxygen depletion in the bottom waters, especially in the inner inlet. This agrees with the findings of Kruger for August of 1977 in Budd Inlet which, according to his WDOE report (Kruger, 1979), was the worst case on record for low DO in the inner inlet. The report further states that this low DO period coincided with an extensive dinoflagellate bloom throughout the inlet.

It is very probable that the duration of the dinoflagellate blooms in Budd Inlet are controlled by a combination of meterological and hydrodynamic conditions which disrupt the vertical migration of the dinoflagellates. This is what we observed in our September survey when strong vertical mixing and advection occurred due to heavy winds. This was also observed by Westley et al. (1973) in their September 1972 survey.

The bottom water oxygen depletion created by dinoflagellate blooms in the late summer and fall is aggravated by fact that the water from Puget Sound which flushes this inlet is on the average 2 mg/L lower in dissolved oxygen than in Spring. This lower D.O. water is brought into Puget Sound by coastal upwelling through the Straits of Juan de Fuca during the summer months when monthly winds prevail off the coast. This water migrates south

through Puget Sound and reaches Southern Puget Sound during the late summer. The bottom water temperature is also higher by three to four degrees in the late summer and fall which raises the SOD rates from 30 to 40 percent.

In summarizing the low D.O. scenario, we can say that even though conditions exist in the late summer and fall which contribute to lower dissolved oxygen values in the bottom water, these conditions alone cannot account for the observed vertical profiles of dissolved oxygen in the inlet. Only the active vertical migration of dinoflagellates under bloom conditions, coupled with their high respiratory rates, can produce the observed vertical gradients. The evidence strongly suggests that a reduction in nutrient addition will result in a reduction in the magnitude of the dinoflagellate bloom, and consequently a reduction in the magnitude of the oxygen depletion.

CHAPTER 5. CONCLUSIONS AND RECOMMENDATIONS

5.1 CONCLUSIONS

The following summarizes major conclusions derived from the results of this study related to the dynamics, nutrient supply, and estuarine ecology of Budd Inlet. The focus of these conclusions is directed toward the low dissolved oxygen problem in the inlet.

Circulation

o   Budd Inlet can be classified as a stratified, partially mixed estuary with a distinct two-layered flow.

o   Current meter studies indicate that the inner and central inlet are generally subject to lateral and eddy-like circulation except during strong ebb and flood tides.

o   During sustained periods of strong east-west winds, sustained cross-channel flows are developed in Budd Inlet.

o   Currents near the mouth of the inlet are nearly always oriented north-south on the ebb and flood tides with a short period of rotation in between.

o   On weak ebbs, a clockwise circulation occurs in the inner Inlet.

Point Source Survey

o   The results of the five month point source survey indicated that the LOTT treatment plant contributed about 75 percent of the nitrate, 95 percent of the nitrite, and 95 percent of the ammonium from the measured sources.

o   Capitol Lake accounted for between 60 and 80 percent of the BOD
     loading to Budd Inlet and 90 percent of the dissolved oxygen.
     Major sources of fecal coliforms were Moxlie Creek, Capitol Lake,
     and the LOTT treatment plant.

Bacteriological Survey

o   Moxlie creek was found to be the major source of fecal coliform
     bacteria loading to Budd Inlet during the two detailed surveys.
     It was found to contribute 95 percent of the loadings in April
     1985 and 90 percent of the loadings in September 1985.

o   Moxlie Creek appeared to be receiving additional inputs of fecal
     coliform bacteria between its upper reaches and its point of
     discharge into Budd Inlet.

Limiting Nutrient

o   Analysis of historical data and data from two intensive surveys
     indicate that nitrogen is the limiting nutrient in Budd Inlet.

o   During the spring and summer when diatoms predominate, ammonium
     will be preferred over nitrate.

o   During the late summer and early fall when dinoflagellates
     predominate, there is no ammonium preference.

Sediment Oxygen Demand

o   Higher rates of sediment oxygen demand were measured in the inner
     inlet than in the central inlet. Ammonium release was not
     observed in the inner inlet site due to enhanced bioturbation.

o   The benthic release of ammonium in the central inlet was related
     to the sediment oxygen demand and followed the same trend as in
     other coastal marine estuaries and bays.

o   Greater than 90 percent of the sediment oxygen demand is related to the algal production in the water column, less than 10 percent in related to BOD sources. About 70 to 80 percent of the sediment oxygen demand is the direct result of grazing and excretion by zooplankton.

Nutrient Budgets

o   A two-dimensional box model for Budd Inlet developed for the May survey showed that the major sources of nitrogenous nutrients to Budd Inlet are Puget Sound, LOTT, and benthic release, each contributing approximately 60, 20, and 20 percent, respectively. The budget for the surface layer (upper 3 meters) indicates that LOTT supplies about half and vertical mixing of Puget Sound water supplies the other half of the nitrogenous nutrients to the surface layer.

o   The breakdown by component for the whole inlet revealed that Puget Sound supplies 20 percent of the ammonium and 92 percent of the nitrate + nitrite; LOTT supplies about 36 percent of the ammonium and 8 percent of the nitrate + nitrite; and benthic release supplies about 44 percent of the ammonium. The budget for the surface layer (upper 3 meters) indicates that LOTT supplies about 80 percent of the ammonium and 22 percent of the nitrate + nitrite and vertical mixing of Puget Sound water supplies about 20 percent of the ammonium and 78 percent of the nitrate + nitrite to the surface.

o   A similar budget for oxygen revealed that oxygen exchange within the Inlet is predominantly due to the exchange with Puget Sound.

Flushing, Dispersion and Dilution

o   Modeling of the flushing efficiency of Budd Inlet indicated that

the inner portion of Budd Inlet south of Priest Point is not very
efficiently flushed regardless of season.

o   The outer inlet is very efficiently flushed regardless of flow
      conditions, while the central inlet is more efficiently flushed
      during high flow conditions.

o   Modeling results suggested that there is only a minor decrease in
      the flushing efficiency when the amount of Budd Inlet water being
      recycled on the incoming flood was increased from 0 to 60 percent.

o   Modeling shows the influence of estuarine circulation in
      transporting outgoing surface material back toward the head of the
      inlet. Upon reaching the head, some of the material became
      detained due to enhanced vertical circulation.

o   The dilution modeling showed that with a constant input of a
      conservative tracer, the outer inlet was about 5 times more dilute
      than the inner inlet, and 3 times more dilute than the central
      inlet.

Modeling the Dissolved Oxygen System

o   Dynamic modeling results for May indicated that spring diatom
      blooms are initiated and sustained by periods of clear weather
      and are enhanced by at least 30 percent in the inner portions of
      Budd Inlet by the existing nutrient loadings from the LOTT
      treatment plant.

o   Computer simulations of alternative discharge configurations
      indicate that next to complete discharge elimination, nutrient
      removal is the next best option in order to substantially reduce
      spring algal blooms. All scenarios without nutrient removal,
      regardless of placement within the inlet, show a 30 to 50 percent

increase in the strength of the algal bloom relative to the no
discharge scenario for the inner portions of the inlet.

o   The strength of the bloom enhancement is controlled by the
    location of the LOTT discharge in the Inlet, with the inner Inlet
    placement showing the greatest enhancement.

o   Predicted sediment oxygen demand for the May model runs are
    directly related to algal production. All scenarios without
    nutrient removal, including existing conditions and estimated
    average dry weather flow for the year 2010, yield a 10 to 15
    percent increase in SOD in the inner inlet over the no discharge
    scenario.

o   Predicted bottom water dissolved oxygen results from the May model
    runs show increased oxygen levels with increased algal production
    in the water column. This indicates that horizontal and vertical
    mixing and transport can transfer photosynthically produced oxygen
    into the bottom water faster than it can be consumed by the
    sediment oxygen demand.

o   During the late summer and early fall, dinoflagellate blooms occur
    in Budd Inlet. Based on the computer modeling and analysis of the
    intensive survey data from September, 1984, the high respiration
    rates, coupled with the diel vertical migration of the
    dinoflagellates, were the probable cause of the low dissolved
    oxygen conditions in the bottom waters.

o   In effect the dinoflagellates are acting as a biological "pump"
    taking oxygen out of the bottom water at night and producing it in
    the surface water during the day. As long as the pump (vertical
    migration rate) is stronger than the vertical mixing, large
    vertical oxygen gradients can be maintained.

o   Other conditions which exist in the late summer and fall such as decreased flushing, lower Puget Sound dissolved oxygen concentrations and increased sediment oxygen demand contribute to the low dissolved oxygen problem. However, these conditions alone, without the vertical migration and physiology of the dinoflagellates, cannot account for the observed vertical dissolved oxygen gradients.

o   Based on the available data, it would appear that the severity of the dissolved oxygen depletion is related to strength and duration of the dinoflagellate bloom.

o   From our analysis of the modeling results and the existing data, we would conclude that the dinoflagellate blooms have the potential of being enhanced at least as much as the diatom blooms (30-50 percent) in the inner Inlet for all scenarios without nutrient removal from the LOTT treatment plant.

5.2 RECOMMENDATIONS

LOTT Discharge Configuration

The probable cause of the low dissolved oxygen conditions in the late summer and early fall in Budd Inlet is the presence and persistence of dinoflagellate blooms. When bloom conditions prevail, there is strong evidence which suggests that the magnitude of the blooms are dependent on the supply of nitrogenous nutrients. Although we do not, at this time, have a quantitative dinoflagellate model for Budd Inlet, we can infer from our qualitative modeling results and our diatom model for May that the magnitude of the dinoflagellate bloom in the inner inlet could be enhanced from 30 to 50 percent by discharge configurations without nutrient removal regardless of outfall placement in the inlet. State water quality standards allow natural dissolved oxygen levels to be degraded by up to only 0.2 mg/L by man-caused activities, regardless of the water classification. Therefore we feel that nutrient removal should be implemented as soon as practicable in order to attempt to meet the State water quality standards.

We have ranked the eight alternative alignment scenarios modeled in ascending order of potential for enhancement of dinoflagellate blooms and subsequent oxygen depletion. Of course the top ranking option is the elimination of the discharge from the inlet. This is followed by the two nutrient removal scenarios. We have separated the first three scenarios from the remaining five to indicate the large gap between the nutrient removal options and all other discharge configurations. Nutrient removal during the growing season from April through October should strongly be considered.

Table 5.1
Ranking of Alternative Alignment Scenarios

Rank	Scenario	Alignment	AWWF	ADWF	Modeled Flow Rate	Nutrient Removal	
1	2	E	22.0	16.0	0.0 mgd	None	no LOTT
2	6	E	22.0	16.0	16.0 mgd	90% Removal	
3	4	E	34.0	24.0	24.0 mgd	90% Removal	Not an option
4	8	B	34.0	24.0	24.0 mgd	None	
5	1	E/Baseline	16.3	11.6	12.4 mgd	None	
6	7	A	34.0	24.0	24.0 mgd	None	
7	5	E	22.0	16.0	16.0 mgd	None	
8	3	E	34.0	24.0	24.0 mgd	None	

Under the recommendations of WDOE, we believe an algal bloom enhancement of 10 percent or less as the result of nutrient addition from the LOTT treatment plant is acceptable. The following recommendations would achieve this acceptable level and would minimize the potential magnitude of oxygen depletion in the late summer and early fall due to dinoflagellate blooms in Budd Inlet.

o   For the present outfall location, maintain the permitted flow rate of 16.3 mgd (AWWF) and establish nutrient removal of at least

90 percent using best available technology. This could be accomplished on a seasonal basis from April through October.

o For _any_ _outfall_ _location_ within the Inlet or any increase in permitted flow up to 22 mgd (AWWF), establish nutrient removal of at least 90 percent using best available technology. This could be accomplished on a seasonal basis from April through October.

Further Studies

Budd Inlet is nearly an ideal area in which to study estuarine processes including estuarine ecology. The relocation or alteration of the present LOTT discharge offers a rare opportunity to study its effects on the inlet with implications toward other estuaries or embayments. The following recommended studies would aid in our understanding and predictive capabilities for determining the controlling factors and effects of dinoflagellate blooms in Budd Inlet.

Further refinement and final verification of a "dynamic dinoflagellate model" for Budd Inlet would be necessary to have a more quantitative tool for water quality management in Budd Inlet. This could then be applied to other embayments in Puget Sound which may suffer dinoflagellate blooms and/or oxygen depletion. Further refinement of the model geometry to accommodate one meter rather than three meter thick vertical layers could improve model results.

Yearly surveys should be conducted of the inner and central Budd Inlet on a weekly or biweekly basis during the summer and early fall to monitor stratification, nutrients, DO, chlorophyll and phytoplankton species composition. This would be done before and after any change in discharge configuration by LOTT. This study would go a long way towards understanding the impacts of nutrient loadings on dinoflagellate blooms in the inlet. This would also have implications toward other effects associated with dinoflagellate blooms such as paralytic shellfish poisoning and mortality in larval and adult oysters, clams and shrimp, as well as juvenile salmon.

A more detailed study of sediment oxygen demand and benthic nutrient release in the inner inlet before and after any change in discharge configuration should be conducted. This could be accompanied by benthic invertebrate studies to determine the extent of enhanced bioturbation due to larger numbers of burrowing benthic animals.

A detailed bacteriological survey during a storm event would be valuable since the two bacteriological surveys conducted were taken during dry weather periods. Moxlie Creek and its tributaries should be investigated more thoroughly. It was found to be the major source of fecal coliform bacteria loading to Budd Inlet during the surveys.

REFERENCES

Anderson, J., A. Copping, T. Jagielo, J. Postel, W. Peterson, B. Dumbauld, G. Heron, R. Hood and M. Strom. 1985. Renton sewage treatment plant. Project: Seahurst Baseline Study. Volume III. METRO. 316 pp.

Benson, B.B., and D. Krause, Jr. 1984. The concentration and isotopic fractionation of oxygen dissolved in freshwater and seawater in equilibrium with the atmosphere. Limnol. and Oceanogr.

Bernhardt, J. and B. Yake. 1981. LOTT Phase II Receiving Water Considerations. Memorandum to Frank Monahan, State of Washington, Department of Ecology. June 22, 1983.

Bowie, G.L., W.B. Mills, D.B. Porcella, C.L. Campbell, J.R. Pagenkopf, G.L. Rupp, K.M. Johnson, P.W.H. Chan, S.A. Gherini, and C.E. Chamberlin. 1985. Rates, constants, and kinetics formulations in surface water quality modeling, for Environmental Research Laboratory. U.S. Environmental Protection Agency. Athens, GA. EPA-600/3-85/040. 455 pp.

Broecker, W.S. and T.H. Peng. 1974. Gas exchange rates between air and sea. Tellus 26:21-35.

Callender, E., and D.E. Hammond. 1982. Nutrient exchange across the sediment-water interface in the Potomac River estuary. Estuarine, Coastal and Shelf Science. 15:395-413.

CH_2M Hill. 1978. Water quality in Capitol Lake, Olympia, Washington. Prepared for: State of Washington, Department of Ecology and General Administration.

Cokelet, E.D., and R.J. Stewart. 1985. The exchange of waters in fjords: The efflux/reflux theory of advective reaches separated by mixing zones. J. of Geophysical Res. 90:7287-7306.

Collias, E.E. 1970. Index to physical and chemical oceanographic data of Puget Sound and its approaches, 1932-1966. University of Washington, Department of Oceanography Special Report No. 43. 823 pp.

Copping, A. 1985. Personal communication.

Cox, J.M., C.C. Ebbesmeyer, C.A. Coomes, J.M. Helseth, and L.R. Hinchey. 1984. Synthesis of current measurements in Puget Sound, Washington. Volume 1 - Index to current measurements made in Puget Sound from 1908-1980, with daily and record averages for selected measurements. NOAA Technical Memorandum NOS OMS 3. 38 pp.

Dugdale, R.C. and J.J. Goering. 1967. Uptake of new and regenerated forms of nitrogen in primary productivity. Limnol. and Oceanogr. 12:196-206.

Elliott, A.J. 1976. Estimates of Advection and Diffusion in the Potomac Estuary. J. Environ. Sci. Health - Environ Sci. Eng. A11 (2):131-152.

Emerson, S. 1975. Gas exchange rates in small Canadian Shield lakes. Limnol. and Oceanogr.

Eppley, R.W., and W.G. Harrison. 1975. Physiological ecology of Gonyaulax polyedra, a red water dinoflagellate of southern California. In: Proceedings of the first international conference on toxic dinoflagellate blooms. (V.R. LoCicero ed.) Massachusetts Science and Technology Foundation, Wakefield, MA. pp. 11-22.

Entranco. 1984. Water quality in Capitol Lake, Olympia, Washington. Prepared for: State of Washington, Department of General Administration.

Fischer, H.B., E.J. List, C.Y. Koh, J. Imberger, and N.H. Brooks. 1979. Mixing in Inland and Coastal waters. Academic Press. San Francisco, California.

Fisher, T.R., P.R. Carlson, and R.T. Barber. 1982. Sediment nutrient regeneration in three North Carolina estuaries. Estuarine, Coastal and Shelf Science. 14:101-116.

Fisher, T.R., P.R. Carlson, and R.T. Barber. 1982. Carbon and nitrogen primary productivity in three North Carolina estuaries. Estuarine, Coastal and Shelf Science. 15:621-644.

Goldman, J.C. and J.J. McCarthy. 1978. Steady state growth and ammonium uptake of a fast growing marine diatom. Limnol. and Oceanogr. 23:695-703.

Kendra, W. and T. Determan. 1985. Effects of three small sewage treatment plants on Budd Inlet receiving waters. Memorandum to Tom Eaton, State of Washington, Department of Ecology. November 6, 1985.

Koike, I., A. Hattori, M. Takahashi, and J.J. Goering. 1982. The use of enclosed experimental ecosystems to study nitrogen dynamics in coastal waters. In: Marine Mescosms. (G.D. Grice and M.R. Reeve, eds.). Springer-Verlog, New York. pp. 291-303.

Kruger, D.M. 1979. Effects of point source discharges and other inputs on water quality in Budd Inlet, Washington. State of Washington, Department of Ecology, DOE 79-11, 77 ppp.

LOTT. 1985. Letter to Lynn Singleton from Parametrix, Inc. PMX 11-1577-03.

McCarthy, J.J., W.R. Taylor, and J.L. Taft. 1975. The dynamics of nitrogen and phosphorus cycling in the open waters of the Cheasapeake Bay. In: Marine Chemistry in the Coastal Environment (Church, T.M., ed.). American Chemical Society. Washington, D.C. pp. 664-681.

McCarthy, J.J. 1977. Nitrogenous nutrition of the plankton in the Chesapeake Bay. I. Nutrient availability and phytoplankton preferences. Limnol. and Oceanogr. 22:996-1011.

McCarthy, J.J. 1980. Nitrogen. In: The Physical Ecology of Phytoplankton. (I. Morris, ed.). University of California Press, Berkeley.

Moshkina, L.V. 1961. Photosynthesis by dinoflagellatae of the Black Sea. (English translation.) Plant Physiol. 8:129-132.

Nixon, S.W.. 1981. Remineralization and nutrient cycling in coastal marine ecosystems. In: Estuaries and Nutrients. (B.J. Neilson and L.E. Cronin, eds.). Humana Press. Clifton, New Jersey.

O'Connor, D.J. 1981. Modeling of eutrophication in estuaries. In: Estuaries and Nutrients. (B.J. Neilson and L.E. Cronin, eds.). Humana Press. Clifton, New Jersey.

Officer, C.B. 1981. Box models revisited. In: Estuarine and Wetland Processes (Hamilton, P. & Macdonald, K.B., eds.). Plenum Press, New York. pp. 65-114.

Olcay, N. 1959. Oceanographic conditions near the head of Southern Puget Sound August 1957 through September 1958. University of Washington, Department of Oceanography Master's Thesis.

Ozturgut, E., J.W. Lavelle. 1984. New method of wet density and settling velocity determination for wastewater effluent. Environ. Sci. Technol., 18(12):947-952.

Paasche, E. and S. Kristiansen. 1982. Nitrogen nutrition of the phytoplankton in the Oslofjord. Estuarine, Coastal and Shelf Science 14:237-240.

Pamatmat, M.M. 1968. Ecology and metabolism of a benthic community on an intertidal sandflat. Int. Revue ges. Hydrobiol. 53: 211-298.

Pamatmat, M.M., and D. Fenton. 1968. An instrument for measuring subtidal benthic metabolism in situ. Limnol. and Oceanogr. 13:537-540.

Pamatmat, M.M., and K. Banse. 1969. Oxygen consumption by the seabed. II. In situ measurements to a depth of 180m. Limnol. Oceanogr. 14:250-259.

Pamatmat, M.M. 1971. Oxygen consumption by the seabed. IV. Shipboard and laboratory experiments. Limnol. and Oceanogr. 16:536-550.

Parsons, T.R., M. Takahashi. 1973. Biological oceanograhic processes. Pergamon Press Ltd.

Parsons, T.R., M.Yoshiaki, and C.M. Lalli. 1984. A manual of chemical and biological methods for seawater analysis. Pergramon Press Ltd. 173 pp.

Pearson, C.A. 1981. Guide to R2D2 - Rapid Retrieval Data Display. NOAA Technical Memorandum ERL PMEL-29. Pacific Marine Environmental Laboratory, Seattle, Washington. 148 pp.

Pritchard, D.W. 1969. Dispersion and flushing of pollutants in estuaries. J.Hydraulics Div. Amer. Soc. Civil. Eng. 95, No. HY1, Proc. Paper 6344, pp. 115-125.

Pritchard, D.W. 1967. What is an estuary: physical viewpoint. In: Estuaries, Amer. Assoc. Adv. Sci. Publ. (G. Lauff, ed.), 83. pp. 3-5.

Redfield, A.C. 1958. The biological control of chemical factors in the environment. Am. Scientist. 46:205-221.

Robinson, M.G. and L.N. Brown. 1983. A recurrent red tide in a British Columbia coastal lagoon. Can. J. Fish. Aquat. Sci. 40:2135-2143.

Seliger, H.H., M.E. Loftus, and D.V. Subba Rao. 1975. Dinoflagellate accumalations in Chesapeake Bay. In: Proceedings of the first international conference on toxic dinoflagellate blooms. (V.R. LoCiero, ed.). Massachusetts Science and Technology Foundation, Wakefield, MA. pp. 2135-2143.

Shuman, F.R. and C.J. Lorenzen. 1975. Quantitative degradation of chlorophyll by a marine herbivore. Limnol. and Oceanogr. 20:580-586.

Singleton, L. 1985. Letter to Charlie Tang dated December 19, 1985.

Smith, S.V. 1984. Phosphorous versus nitrogen limitation in the marine environment. Limnol. and Oceanogr. 29:1149-1160.

Smith, W.O., Jr. 1982. The relative importance of chlorophyll, dissolved and particulate material, and seawater to the vertical extinction of light. Estuarine, Coastal and Shelf Science. 15:459-465.

Standard methods for the examination of water and wastewater. 1976. 14th Edition. American Public Health Association.

Strickland, J.D.H., and T.R. Parsons. 1972. A practical handbook of seawater analysis. Fisheries Research Board of Canada. Bulletin 167. 2nd Edition. Ottawa, Canada. 310 pp.

Taft, J.L., A.J. Elliott, and W.R. Taylor. 1978. Box model analysis of Chesapeake Bay ammonium and nitrate fluxes. In: Estuarine Interactions. (M.L. Wiley, ed.). Academic Press, New York. pp. 115-130.

Taylor, M.M. 1984. The Henderson/Eld Water Quality Study. Prepared by Thurston County Health Department for State of Washington, Department of Ecology.

URS Corporation. 1985. Discharge zone classification system. Southern Puget Sound water quality assessment study. Prepared for Washington Department of Ecology.

URS Corporation. 1986. Circulation and flushing in South Puget Sound. Southern Puget Sound water quality assessment study. Prepared for Washington Department of Ecology.

Washington State Department of Ecology. 1980. Water quality standards for waters of the State of Washington in Laws and Regulations, Water Pollution. Olympia, WA. pp. 1-11.

Welschmeyer, N.A., and C.J. Lorenzen. 1985. Chlorophyll budgets: Zooplankton grazing and phytoplankton growth in a temperate fjord and the Central Pacific Gyres. Limnol. and Oceanogr. 30(1):1-25

Westley, R.E., E. Finn, M.I. Carr, M.A. Tarr, A.J. Scholz, L. Goodwin, R.W. Sternberg, and E.E. Collins. 1973. Evaluation of effects of channel maintenance dredging and disposal on the marine environment in Southern Puget Sound, Washington. State of Washington, Department of Fisheries. 308 pp.

Whitledge, T.E. 1981. Automated nutrient analysis in seawater. Oceanographic Sciences Division, Brookhaven National Laboratory. Upton, N.Y.

Winter, D.F., K. Banse, and G.C. Anderson. 1975. The dynamics of phytoplankton blooms in Puget Sound, a fjord in the Northwestern United States. Marine Biology, 29:139-176.

Yake, B. 1981. Interpretation of June 3, 1981, Budd Inlet data with particular respect to oxygen depletion. Memorandum to John Bernhardt, State of Washington, Department of Ecology. June 6, 1981.

APPENDIX A.   QA/QC SUMMARY

A Quality Control/Quality Assurance (QA/QC) program was established by URS to ensure field collection and analytical quality and integrity of the data collected during the Budd Inlet intensive surveys. One out of every twenty samples was collected in triplicate during both intensive surveys for dissolved oxygen, algal nutrients, chlorophyll A, pheopigments and BOD-5. The samples were collected, preserved and handled in the field in a consistent manner and analyzed in the laboratory in the same fashion as non-triplicate samples. Analysis of the triplicate samples provided useful information concerning overall field and laboratory precision.

The laboratory QA/QC results were organized in table format and the following statistical calculations were performed upon each triplicate set: sample mean, standard deviation (SD), coefficient of variation (% CV), 95 percent confidence interval (95% CI) and percent standard error (% SE). The coefficient of variation expresses the standard deviation as a percentage of the mean, while the percent standard error expresses the 95 percent confidence interval as a percentage of the mean. These are indicators of the relative precision of the data.

Tables of the triplicate data and statistics for each intensive survey are presented in Tables A.1 and A.2.   A summary of the statistical results, given as mean values of the standard deviation, coeffecient of variation and percent standard error, are shown in Table A.3. This table also presents reported detection limits and laboratory analytical precision. Any triplicate set containing values at or below the analytical detection limit was not utilized in the mean calculation, since they give rise to unrealistically large relative precision values.

The statistical summaries (Table A.3) show that the standard deviation of the analytical methods in comparison to the overall procedures (which would include sampling and handling) are within a factor of about two to three of one another. The standard deviations are similar

A-1

between the May and September surveys. The relative precision statistics for the nutrients were higher for the May survey than the September survey due to lower mean values of the nutrients in May. This was also true for the chlorophyll $\underline{a}$ measurements, although some of the scatter in the May chlorophyll data was probably due to the presence of a large centric diatom (<u>Coscinodiscus</u> <u>sp.</u>) which create non-homogeneity in the samples. In conclusion, we find the field and analytical methods and results acceptable for this study and within acceptable levels given the scope and goals of the study. All analytical laboratories utilized by URS provided consistent and defendable data and cooperated fully with our quality assurance/quality control program.

Overall, the QA/QC program maintained excellent sample integrity and quality. For the approximately 2,100 samples collected during the two intensive surveys, less than a dozen of the samples were either lost, broken, mislabled or otherwise could not be used. The comparable variability of analytical and sample results indicates a consistent and high quality data set from the two intensive surveys.

Table A.1 QA/QC statistical summary for the September 1984 intensive survey.

BUDD INLET INTENSIVE SURVEY
SEPTEMBER 1984
QA/QC STATISTICAL SUMMARY

Station and Depth	DO Code	DO (mg/L)	Nutrient Code	PO4-P (ug/L)	SIO4-Si (mg/L)	NO3-N (ug/L)	NO2-N (ug/L)	NH3-N (ug/L)	TotN TotP Code	TOTAL N (ug/L)	TOTAL P (ug/L)	Chl Phaeo Code	CHLORO (ug/L)	PHAEO (ug/L)	BOD 5 Code	BOD (mg/L)
0106 8m															23	2.0
															34	1.0
															30	2.0
Mean																1.67
SD (n-1)																0.58
% CV																34.64
95% CI n=2																1.43
% SE																86.05
0112 15m															60	3.0
															55	1.0
															36	1.0
Mean																1.67
SD (n-1)																1.15
% CV																69.28
95% CI n=2																2.87
% SE																172.10
0119 .5m															27	2.0
															48	2.0
															52	2.0
Mean																2.00
SD (n-1)																0.00
% CV																0.00
95% CI n=2																0.00
% SE																0.00

Table A.1 Continued.

BUDD INLET INTENSIVE SURVEY
SEPTEMBER 1984
QA/QC STATISTICAL SUMMARY

Station and Depth	DO Code	DO (mg/L)	Nutrient Code	PO4-P (ug/L)	SIO4-Si (mg/L)	NO3-N (ug/L)	NO2-N (ug/L)	NH3-N (ug/L)	TotN TotP Code	TOTAL N (ug/L)	TOTAL P (ug/L)	Chl Phaeo Code	CHLORO (ug/L)	PHAEO (ug/L)	BOD 5 Code	BOD (mg/L)
0139 8a			148	68.14	1.53	131.10	7.00	21.29	NP 20	333.50	66.90	2	4.33	0.32		
			147	68.14	1.52	131.52	7.28	22.13	NP 21	381.54	70.93	3	4.21	0.78		
			150	68.76	1.52	131.80	7.00	21.29	NP 22	338.12	66.59	4	4.28	0.82		
Mean				68.35	1.52	131.48	7.10	21.57		351.05	68.14		4.27	0.64		
SD (n-1)				0.36	0.01	0.35	0.16	0.49		26.50	2.42		0.06	0.28		
% CV				0.52	0.38	0.27	2.28	2.25		7.55	3.55		1.41	43.41		
95% CI n=2				0.89	0.01	0.88	0.40	1.21		65.84	6.01		0.15	0.69		
% SE				1.30	0.95	0.67	5.66	5.59		18.75	8.82		3.50	107.84		
0307 .5a	457	15.50														
	459	15.90														
	464	16.02														
Mean		15.807														
SD (n-1)		0.27														
% CV		1.70														
95% CI n=2		0.67														
% SE		4.23														
0307 3a			296	51.42	1.55	17.65	1.68	2.52	NP 366	307.03	70.00	3	7.6	1.76		
			301	52.97	1.55	17.79	1.68	2.80	NP 372	329.44	73.41	8	7.42	1.85		
			302	52.97	1.56	17.79	1.68	2.66	NP 373	320.47	69.69	9	7.2	1.7		
Mean				52.45	1.55	17.74	1.68	2.66		318.98	71.03		7.41	1.77		
SD (n-1)				0.89	.00	0.08	0.00	0.14		11.28	2.06		0.20	0.08		
% CV				1.70	0.19	0.46	0.00	5.26		3.54	2.90		2.70	4.27		
95% CI n=2				2.22	0.01	0.20	0.00	0.35		28.02	5.12		0.50	0.19		
% SE				4.23	0.48	1.13	0.00	13.07		8.78	7.21		6.72	10.80		

Table A.1 Continued.

Station and Depth	DO Code	DO (mg/L)	Nutrient Code	PO4-P (ug/L)	SIO4-Si (mg/L)	NO3-N (ug/L)	NO2-N (ug/L)	NH3-N (ug/L)	TotN TotP Code	TOTAL N (ug/L)	TOTAL P (ug/L)	Chl Phaeo Code	CHLORO (ug/L)	PHAEO (ug/L)	BOD 5 Code	BOD (mg/L)
0346.5a			172	66.59	1.70	45.66	2.38	16.53	NP 44	349.89	79.29	5	5.39	1.52		
			173	67.52	1.71	43.84	2.38	21.99	NP 45	337.98	78.67	6	5.32	0.87		
			174	66.28	1.70	42.86	2.24	16.67	NP 46	329.58	78.98	1	5.49	0.92		
Mean SD (n-1)				66.80 0.64	1.70 0.01	44.12 1.42	2.33 0.08	18.40 3.11		339.15 10.21	78.98 0.31		5.40 0.09	1.10 0.36		
% CV				0.97	0.30	3.22	3.46	16.93		3.01	0.39		1.58	32.78		
95% CI n=2 % SE				1.60 2.40	0.01 0.75	3.53 8.00	0.20 8.60	7.74 42.05		25.35 7.47	0.77 0.97		0.21 3.93	0.90 81.43		
0453 3a	387	6.61														
	388	6.54														
	389	6.69														
Mean SD (n-1)		6.613 0.07														
% CV		1.09														
95% CI n=2 % SE		0.18 2.71														
0453 8a			10	73.41	1.94	45.66	4.48	36.84	NP 220	401.85	102.83	4	11.4	0.58		
			11	66.28	1.72	28.43	4.20	19.61	NP 221	335.74	96.84	5	10.48	1.3		
			12	70.00	2.01	31.38	4.62	28.29	NP 222	454.38	114.91	6	10.66	1.2		
Mean SD (n-1)				69.90 3.56	1.89 0.15	35.16 9.22	4.44 0.21	28.25 8.61		397.32 59.45	104.79 9.29		10.85 0.49	1.03 0.39		
% CV				5.10	8.13	26.21	4.82	30.50		14.96	8.87		4.50	37.99		
95% CI n=2 % SE				8.85 12.66	0.38 20.20	22.89 65.11	0.53 11.98	21.40 75.75		147.67 37.17	23.09 22.03		1.21 11.17	0.97 94.37		

A-5

Table A.1 Continued

Station and Death	DO Code	DO (mg/L)	Nutrient Code	PO4-P (ug/L)	SIO4-Si (mg/L)	NO3-N (ug/L)	NO2-N (ug/L)	NH3-N (ug/L)	TotN TotP Code	TOTAL N (ug/L)	TOTAL P (ug/L)	Chl Phaeo Code	CHLORO (ug/L)	PHAEO (ug/L)	BOD 5 Code	BOD (ug/L)
0515 .5a	210	14.98														
	209	15.17														
	208	14.86														
Mean		15.002														
SD (n-1)		0.15														
% CV		1.02														
95% CI n=2		0.38														
% SE		2.55														
0515 3a												8	2.3	0.69		
												9	2.25	0.87		
												10	2.47	0.88		
Mean													2.34	0.61		
SD (n-1)													0.12	0.11		
% CV													4.93	13.15		
95% CI n=2													0.19	0.27		
% SE													8.31	32.66		
0515 11a			271	74.65	1.86	0.42	1.12	52.10	NP 399	362.07	92.61					
			270	74.65	1.86	1.26	0.28	52.10	NP 400	339.52	90.13					
			269	74.65	1.86	1.26	0.28	52.10	NP 401	350.87	91.68					
Mean				74.65	1.86	0.98	0.56	52.10		350.82	91.48					
SD (n-1)				0.00	.00	0.49	0.49	.00		11.28	1.25					
% CV				0.00	0.13	49.49	66.60	.00		3.21	1.37					
95% CI n=2				0.00	0.01	1.21	1.21	.00		28.01	3.11					
% SE				0.00	0.32	122.93	215.12	.00		7.98	3.40					

Table A.1 Continued.

Station and Depth	DO Code	DO (mg/L)	Nutrient Code	PO4-P (ug/L)	SIO4-Si (mg/L)	NO3-N (ug/L)	NO2-N (ug/L)	NH3-N (ug/L)	TotN TotP Code	TOTAL N (ug/L)	TOTAL P (ug/L)	Chl Phaeo Code	CHLORD (ug/L)	PHAEO (ug/L)	BOD 5 Code	BOD (mg/L)
0560 .5m			32	70.93	1.89	65.69	3.92	45.52	NP 242	355.21	91.68	5	4.87	0.56		
			33	72.79	1.88	67.51	4.90	48.32	NP 243	310.25	83.94	6	5.94	0.66		
			34	73.41	1.89	88.07	4.62	48.32	NP 244	321.31	83.94	1	5.16	1.45		
Mean				72.38	1.89	67.09	4.48	47.39		328.92	86.52		5.32	0.89		
SD (n-1)				1.29	.00	1.24	0.51	1.62		23.43	4.47		0.55	0.49		
% CV				1.78	0.23	1.86	11.27	3.41		7.12	5.17		10.40	54.78		
95% CI n=2				3.20	0.01	3.09	1.25	4.02		58.19	11.11		1.37	1.21		
% SE				4.43	0.58	4.61	27.99	8.48		17.69	12.84		25.82	136.07		
0560 3m	413	6.50														
	414	6.45														
	415	6.40														
Mean		6.448														
SD (n-1)		0.05														
% CV		0.74														
95% CI n=2		0.12														
% SE		1.85														
0767 1.5m			64	96.64	1.96	54.07	3.92	92.30	NP 273	459.58	65.97	3	7.45	0.94		
			62	97.88	1.97	54.63	4.20	99.45	NP 271	460.68	68.45	4	8.23	0.95		
			61	97.57	1.97	52.24	4.48	86.70	NP 270	494.30	68.76	1	8.15	1.02		
Mean				97.36	1.97	53.65	4.20	92.82		471.19	67.73		7.94	0.97		
SD (n-1)				0.64	0.01	1.24	0.28	6.39		20.04	1.53		0.43	0.04		
% CV				0.66	0.27	2.32	6.67	6.88		4.25	2.26		5.40	4.49		
95% CI n=2				1.60	0.01	3.09	0.70	15.87		49.79	3.80		1.07	0.11		
% SE				1.65	0.67	5.76	16.56	17.10		10.57	5.60		13.42	11.16		

Table A.1 Continued.

Station and Depth	DO Code	DO (mg/L)	Nutrient Code	PO4-P (ug/L)	SIO4-Si (mg/L)	NO3-N (ug/L)	NO2-N (ug/L)	NH3-N (ug/L)	TotN TotP Code	TOTAL N (ug/L)	TOTAL P (ug/L)	Chl Phaeo Code	CHLORO (ug/L)	PHAEO (ug/L)	BOD 5 Code	BOD (mg/L)
0767 4.5a	438	5.49														
	439	5.52														
	440	5.57														
Mean		5.525														
SD (n-1)		0.04														
% CV		0.73														
95% CI n=2		0.10														
% SE		1.81														
0824 0.5a			200	112.13	2.24	3.64	6.86	81.66	NP 141	1104.85	111.51	2	25.28	3		
			201	109.65	2.24	3.50	7.00	88.10	NP 142	944.89	113.67	5	26.94	1.19		
			202	106.55	2.24	3.08	7.42	88.24	NP 143	1006.80	113.36	6	27.49	3.56		
Mean				109.44	2.24	3.41	7.10	86.00		1018.85	112.85		26.57	2.58		
SD (n-1)				2.79	.00	0.29	0.29	3.76		80.66	1.17		1.15	1.24		
% CV				2.55	0.09	8.55	4.11	4.37		7.92	1.04		4.33	47.95		
95% CI n=2				6.94	0.01	0.72	0.72	9.34		200.35	2.91		2.86	3.08		
% SE				6.34	0.22	21.25	10.21	10.86		19.66	2.58		10.76	119.11		
0824 4.5a	283	4.37														
	284	5.01														
	285	7.02														
Mean		5.466														
SD (n-1)		1.39														
% CV		25.36														
95% CI n=2		3.44														
% SE		62.98														

Table A.1 Continued.

BUDD INLET INTENSIVE SURVEY
SEPTEMBER 1984
QA/QC STATISTICAL SUMMARY

Station and Depth	DO Code	DO (mg/L)	Nutrient Code	PO4-P (ug/L)	SIO4-Si (mg/L)	NO3-N (ug/L)	NO2-N (ug/L)	NH3-N (ug/L)	TotN TotP Code	TOTAL N (ug/L)	TOTAL P (ug/L)	Chl Phaeo Code	CHLORO (ug/L)	PHAEO (ug/L)	BOD 5 Code	BOD (mg/L)
0830 1.5a	231	11.82														
	233	11.68														
	234	12.30														
Mean		11.936														
SD (n-1)		0.33														
% CV		2.74														
95% CI n=2		0.81														
% SE		6.80														
0830 3.5a			223	97.88	2.01	1.23	1.12	58.59	NP 164	1384.42	117.39	11	46.4	5.77		
			224	97.26	1.99	0.28	0.98	55.61	NP 165	1246.32	119.87	6	44.46	6.11		
			225	89.51	2.00	0.00	0.98	46.64	NP 166			9	48.71	7.26		
Mean				94.88	2.00	0.51	1.03	52.95		1315.37	118.63		46.52	6.38		
SD (n-1)				4.66	0.01	0.66	0.08	5.48		97.66	1.75		2.13	0.78		
% CV				4.91	0.53	128.89	7.87	10.35		7.42	1.48		4.57	12.24		
95% CI n=2*				11.57	0.03	1.64	0.20	13.61		877.34	15.74		5.29	1.94		
% SE				12.20	1.31	320.15	19.56	25.71		66.70	13.27		11.36	30.40		

* n=1 for Total N and P

A-9

Table A.2 QA/QC statistical summary for the May 1985 intensive survey.

BUDD-INLET INTENSIVE SURVEY
MAY 1985
QA/QC STATISTICAL SUMMARY

Station and Depth	DO Code	DO (mg/L)	Nutrient Code	PO4-P (ug/L)	SIO4-Si (mg/L)	NO3-N (ug/L)	NO2-N (ug/L)	NH3-N (ug/L)	TotN TotP Code	TOTAL N (ug/L)	TOTAL P (ug/L)	Chl Phaeo Code	CHLORO (ug/L)	PHAEO (ug/L)	BOD 5 Code	BOD 5 (mg/L)
1A05 0.5m	A229	10.29														
	237	10.99														
	233	10.62														
MEAN		10.63														
SD (n-1)		0.35														
% CV		3.31														
95% CI (n=2)		0.87														
% SE		8.22														
1A05 3.0m			Q36	41.50	1.25	95.25	3.78	12.33	NP393	314.31	48.32	17	4.465	0.795		
			Q13	43.36	1.24	95.25	3.78	14.29	NP394	297.64	48.32	18	2.705	0.583		
			Q14	44.60	1.24	96.65	3.64	9.52	NP395	299.32	46.15	19	6.015	3.051		
MEAN				43.16	1.25	95.71	3.74	12.05		303.76	47.60		4.395	1.476		
SD (n-1)				1.56	0.01	0.81	0.08	2.39		9.18	1.25		1.656	1.368		
% CV				3.61	0.41	0.84	2.17	19.87		3.02	2.63		37.682	92.649		
95% CI (n=2)				3.87	0.01	2.01	0.20	5.95		22.79	3.11		4.114	3.398		
% SE				8.97	1.02	2.10	5.38	49.36		7.50	6.53		93.601	230.141		
1A05 13.0m															1A05.13	1.00
															1A05.13.1	1.00
															1A05.13.2	2.00
MEAN																1.33
SD (n-1)																0.58
% CV																43.30
95% CI (n=2)																1.43
% SE																107.56

Table A.2 Continued.

Station and Depth	DO Code	DO (mg/L)	Nutrient Code	PO4-P (ug/L)	SIO4-Si (mg/L)	NO3-N (ug/L)	NO2-N (ug/L)	NH3-N (ug/L)	TotN TotP Code	TOTAL N (ug/L)	TOTAL P (ug/L)	Chl Phaeo Code	CHLORO (ug/L)	PHAEO (ug/L)	BOD 5 Code	BOD (mg/L)
1A06 0.5m			0580	45.53	1.32	130.54	4.34	13.31	NF17	363.33	50.18	22	1.917	0.713		
			0584	45.22	1.28	130.12	3.92	14.99	NP21	491.92	53.27	23	3.454	0.696		
			0585	46.15	1.28	132.22	4.76	22.69	NP22	465.16	50.49	24	3.152	0.883		
MEAN				45.63	1.29	130.96	4.34	16.99		440.14	51.31		2.841	0.759		
SD (n-1)				0.47	0.02	1.11	0.42	5.00		67.85	1.71		0.814	0.091		
% CV				1.04	1.70	0.85	9.68	29.44		15.41	3.32		28.663	11.955		
95% CI (n=2)				1.18	0.05	2.76	1.04	12.43		168.53	4.24		2.023	0.225		
% SE				2.58	4.22	2.11	24.04	73.14		38.29	8.26		71.200	29.695		
1A06 25.7m	162	9.86														
	164	10.37														
	160	9.86														
MEAN		10.03														
SD (n-1)		0.30														
% CV		2.95														
95% CI (n=2)		0.73														
% SE		7.32														
1A08 0.5m	A24	10.48														
	A23	10.46														
	A22	10.53														
MEAN		10.49														
SD (n-1)		0.03														
% CV		0.32														
95% CI (n=2)		0.68														
% SE		0.79														

Table A.2 Continued.

BUDD INLET INTENSIVE SURVEY
MAY 1985
QA/QC STATISTICAL SUMMARY

Station and Depth	DO Code	DO (mg/L)	Nutrient Code	PO4-P (ug/L)	SIO4-Si (mg/L)	NO3-N (ug/L)	NO2-N (ug/L)	NH3-N (ug/L)	TotN TotP Code	TOTAL N (ug/L)	TOTAL P (ug/L)	Chl Phaeo Code	CHLORO (ug/L)	PHAEO (ug/L)	BOD 5 Code	BOD (mg/L)
1A08 3.0m			0623	50.18	1.13	112.75	4.06	31.09	NP59	580.44	48.01	33	3.493	0.698		
			0624	46.15	1.13	113.31	4.06	30.67	NP60	562.37	46.46	34	3.222	0.724		
			0626	44.60	1.12	113.87	4.06	33.90	NP61	517.13	51.42	35	3.020	0.818		
MEAN				46.98	1.13	113.31	4.06	31.89		553.31	48.63		3.278	0.747		
SD (n-1)				2.88	.00	0.56	.00	1.75		32.61	2.54		0.240	0.063		
% CV				6.13	0.09	0.49	.00	5.49		5.89	5.21		7.306	8.455		
95% CI (n=2)				7.15	.00	1.39	.00	4.35		81.01	6.30		0.595	0.157		
% SE				15.22	0.22	1.23	.00	13.64		14.64	12.95		18.147	21.002		
3A07 0.5m	368	14.06														
	367	13.42														
	366	13.81														
MEAN		13.76														
SD (n-1)		0.32														
% CV		2.34														
95% CI (n=2)		0.80														
% SE		5.81														
3A07 3.0m			0603	32.82	1.04	16.25	1.96	13.45	NP39	708.88	47.08	83	3.848	0.676		
			0604	29.43	1.03	10.93	1.96	6.30	NP40	534.22	47.08	84	5.978	1.368		
			0605	32.63	1.04	16.73	2.10	8.40	NP41	527.07	44.91	85	4.649	1.064		
MEAN				31.70	1.04	12.65	2.01	9.38		590.06	46.35		4.825	1.056		
SD (n-1)				1.97	0.01	3.11	0.08	3.67		102.97	1.25		1.076	0.347		
% CV				6.21	0.54	24.61	4.03	39.12		17.45	2.70		22.297	33.480		
95% CI (n=2)				4.89	0.01	7.74	0.20	9.12		255.77	3.11		2.672	0.862		
% SE				15.42	1.34	61.14	10.01	97.18		43.35	6.71		55.387	83.163		

A-12

Table A.2 Continued.

BUDD INLET INTENSIVE SURVEY
MAY 1985
QA/QC STATISTICAL SUMMARY

Station and Depth	DO Code	DO (mg/L)	Nutrient Code	PO4-P (ug/L)	SIO4-Si (mg/L)	NO3-N (ug/L)	NO2-N (ug/L)	NH3-N (ug/L)	TotN TotP Code	TOTAL N (ug/L)	TOTAL P (ug/L)	Chl Phaeo Code	CHLORO (ug/L)	PHAEO (ug/L)	BOD 5 Code	BOD (mg/L)
3A10 0.5m	A188	12.95														
	A187	12.91														
	A186	13.02														
MEAN		12.93														
SD (n-1)		0.09														
% CV		0.69														
95% CI (n=2)		0.22														
% SE		1.71														
3A10 3.0m			Q403	31.59	1.11	65.97	2.94	3.36	NP244	319.21	52.35	97	3.966	0.703		
			Q404	23.54	1.11	62.05	2.80	14.43	NP245	310.11	47.70	98	3.362	0.674		
			Q405	36.55	1.10	64.99	2.94	6.72	NP246	265.29	44.29	99	4.686	1.144		
MEAN				30.56	1.11	64.34	2.89	8.17		298.20	48.11		4.005	0.840		
SD (n-1)				6.57	0.01	2.04	0.08	5.67		28.57	4.04		0.663	0.263		
% CV				21.48	0.69	3.17	2.79	69.43		9.68	8.40		16.552	31.343		
95% CI (n=2)				16.31	0.02	5.07	0.20	14.09		71.71	10.04		1.647	0.654		
% SE				53.37	1.70	7.88	6.94	172.46		24.05	20.87		41.115	77.855		
4A09 0.5m	A112	12.22														
	A111	12.14														
	A110	12.11														
MEAN		12.16														
SD (n-1)		0.06														
% CV		0.47														
95% CI (n=2)		0.14														
% SE		1.18														

Table A.2 Continued.

Station and Depth	DO Code	DO (mg/L)	Nutrient Code	PO4-P (ug/L)	SIO4-Si (mg/L)	NO3-N (ug/L)	NO2-N (ug/L)	NH3-N (ug/L)	TotN TotP Code	TOTAL N (ug/L)	TOTAL P (ug/L)	Chl Phaeo Code	CHLORO (ug/L)	PHAEO (ug/L)	BOD 5 Code	BOD (mg/L)
4A09 3.0m			Q383	31.28	0.93	0.42	0.70	2.52	NP224	283.64	50.49	134	3.911	0.899		
			Q384	29.73	0.92	0.28	0.98	2.66	NP225	266.27	48.32	135	4.649	0.948		
			Q385	27.57	0.89	0.56	0.84	3.92	NP226	279.99	47.70	136	4.760	1.012		
MEAN				29.53	0.91	0.42	0.84	3.03		276.63	48.84		4.440	0.953		
SD (n-1)				1.87	0.02	0.14	0.14	0.77		9.16	1.46		0.461	0.057		
% CV				6.32	2.37	33.33	16.67	25.42		3.31	3.00		10.394	5.946		
95% CI (n=2)				4.64	0.05	0.35	0.35	1.92		22.75	3.64		1.146	0.141		
% SE				15.71	5.90	82.80	41.40	63.14		8.22	7.45		25.818	14.770		
4A11 0.5m	A30	12.94														
	C34	12.69														
	B29	12.50														
MEAN		12.71														
SD (n-1)		0.22														
% CV		1.77														
95% CI (n=2)		0.56														
% SE		4.39														
4A11 3.0m			Q424	31.28	0.91	0.00	3.36	8.54	NP265	229.29	48.63	140	4.539	1.700		
			Q425	32.52	0.95	0.70	2.38	7.84	NP266	236.29	48.94	141	3.985	0.766		
			Q426	29.43	0.94	3.64	2.38	16.53	NP267	246.80	46.46	142	3.139	0.565		
MEAN				31.08	0.93	1.45	2.71	10.97		237.46	48.01		3.888	1.010		
SD (n-1)				1.56	0.02	1.93	0.57	4.82		8.81	1.35		0.705	0.606		
% CV				5.02	2.06	133.51	20.90	43.97		3.71	2.81		18.136	59.947		
95% CI (n=2)				3.87	0.05	4.80	1.41	11.98		21.89	3.35		1.751	1.504		
% SE				12.46	5.12	331.64	51.93	109.22		9.22	6.99		45.049	148.909		

Table A.2 Continued.

Station and Depth	DO Code	DO (mg/L)	Nutrient Code	PO4-P (ug/L)	SIO4-Si (mg/L)	NO3-N (ug/L)	NO2-N (ug/L)	NH3-N (ug/L)	TotN TotP Code	TOTAL N (ug/L)	TOTAL P (ug/L)	Chl Phaeo Code	CHLORO (ug/L)	PHAEO (ug/L)	BOD 5 Code	BOD (mg/L)
5A12 0.5m	339	13.09														
	A343	13.14														
	551	13.02														
MEAN		13.08														
SD (n-1)		0.06														
% CV		0.43														
95% CI (n=2)		0.14														
% SE		1.07														
5A12 3.0m			Q129	24.78	1.06	15.55	2.10	6.16	NP149	230.13	37.48	193	2.942	0.845		
			Q128	24.78	1.08	14.99	2.10	5.74	NP150	239.65	39.03	194	2.193	0.722		
			Q127	24.47	1.08	14.99	2.10	4.06	NP151	247.22	37.48	195	3.060	0.716		
MEAN				24.68	1.07	15.17	2.10	5.32		239.00	37.99		2.732	0.761		
SD (n-1)				0.18	0.01	0.32	ERR	1.11		8.56	0.89		0.470	0.073		
% CV				0.72	0.98	2.13	ERR	20.89		3.58	2.35		17.213	9.567		
95% CI (n=2)				0.44	0.03	0.80	ERR	2.76		21.27	2.22		1.168	0.181		
% SE				1.80	2.44	5.30	ERR	51.88		8.90	5.85		42.758	23.765		
5A13 3.0m			Q109	27.26	1.11	14.71	2.66	7.84	NP169	343.44	53.58	199	6.937	2.158		
			Q106	27.26	1.15	15.83	2.80	10.75	NP170	327.34	51.42	200	5.857	2.062		
			Q107	33.14	1.16	15.27	2.80	7.14	NP171	378.46	55.13	201	7.085	2.214		
MEAN				29.22	1.14	15.27	2.75	8.45		349.75	53.38		6.630	2.145		
SD (n-1)				3.40	0.02	0.56	0.08	1.69		26.14	1.87		0.665	0.077		
% CV				11.63	2.00	3.67	2.94	20.05		7.47	3.50		10.025	3.584		
95% CI (n=2)				8.44	0.06	1.39	0.20	4.21		64.93	4.64		1.651	0.191		
% SE				28.89	4.97	9.12	7.29	49.80		18.56	8.69		24.902	8.904		

Table A.2 Continued.

Station and Depth	DO Code	DO (mg/L)	Nutrient Code	PO4-P (ug/L)	SIO4-Si (mg/L)	NO3-N (ug/L)	NO2-N (ug/L)	NH3-N (ug/L)	TotN TotP Code	TOTAL N (ug/L)	TOTAL P (ug/L)	Chl Phaeo Code	CHLORO (ug/L)	PHAEO (ug/L)	BOD 5 Code	BOD (mg/L)
8A02 0.5m	B196	12.19														
	A268	12.11														
	A195	12.45														
MEAN		12.25														
SD (n-1)		0.18														
% CV		1.43														
95% CI (n=2)		0.44														
% SE		3.56														
8A02 1.5m			Q38	61.64	2.55	28.57	14.71	27.31	NP116	373.28	86.73	243	8.303	2.221		
			Q39	64.43	2.01	15.55	8.54	28.01	NP115	415.44	92.30	244	10.443	2.792		
			Q40	61.95	1.67	11.49	5.88	24.79	NP114	456.62	95.40	245	11.697	2.732		
MEAN				62.67	2.09	18.54	9.71	26.71		415.11	91.43		10.148	2.582		
SD (n-1)				1.53	0.44	8.93	4.53	1.69		41.67	4.39		1.716	0.314		
% CV				2.44	21.25	48.16	46.61	6.34		10.04	4.80		16.912	12.154		
95% CI (n=2)				3.80	1.10	22.18	11.24	4.21		103.51	10.92		4.263	0.779		
% SE				6.06	52.78	119.64	115.78	15.76		24.94	11.93		42.009	30.191		
8A03 0.5m	A284	12.35														
	A283	12.42														
	A282	12.46														
MEAN		12.41														
SD (n-1)		0.06														
% CV		0.45														
95% CI (n=2)		0.14														
% SE		1.12														

Table A.2 Continued.

BUDD INLET INTENSIVE SURVEY
MAY 1985
QA/QC STATISTICAL SUMMARY

Station and Depth	DO Code	DO (mg/L)	Nutrient Code	PO4-P (ug/L)	SIO4-Si (mg/L)	NO3-N (ug/L)	NO2-N (ug/L)	NH3-N (ug/L)	TotN TotP Code	TOTAL N (ug/L)	TOTAL P (ug/L)	Chl Phaeo Code	CHLORO (ug/L)	PHAEO (ug/L)	BOD 5 Code	BOD (mg/L)
BAO3 1.5m			Q48	62.57	2.73	30.25	13.45	21.29	NP369	371.04	86.42	248	9.595	2.096		
			Q25	61.95	2.94	31.80	13.73	17.93	NP370	355.21	83.63	249	10.074	1.732		
			Q26	50.40	2.94	32.08	13.45	19.05	NP371	336.86	81.77	250	9.373	1.676		
MEAN				61.64	2.87	31.38	13.54	19.42		354.37	83.94		9.681	1.835		
SD (n-1)				1.12	0.12	0.98	0.16	1.71		17.10	2.34		0.358	0.228		
% CV				1.81	4.24	3.12	1.19	8.81		4.83	2.79		3.701	12.430		
95% CI (n=2)				2.77	0.30	2.44	0.40	4.25		42.49	5.81		0.890	0.566		
% SE				4.50	10.54	7.76	2.97	21.89		11.99	6.92		9.193	30.876		

Table A.3 Comparison of mean SD's, mean CV's and mean SE's between the September 1984 and May 1985 intensive surveys.

BUDD INLET INTENSIVE SURVEY

QA/QC STATISTICAL SUMMARY

PARAMETER	D.O.	PO4-P	SiO4-Si	NO3-N	NO2-N	NH3-N	TOTAL N	TOTAL P	CHLORO	PHAEO	BOD-5
Analytical Detection Limits	0.080	1.55	0.006	1.40	0.28	2.10	1.40	1.55	0.05	0.05	1.00
Analytical Precision											
% C.V.	0.43	2.00	1.00	0.60	2.00	6.00	4.00	4.00	No Data	No Data	No Data
S.D.	No Data	0.62	0.006	0.840	0.28	0.840	No Data	4.00	No Data	No Data	No Data
Triplicate Data Analysis September, 1984											
Mean of S.D.'s	0.33	1.65	0.021	1.67	0.23	3.29	37.83	2.69	0.59	0.42	0.58
Mean of % C.V.'s	4.77	2.02	1.14	6.13	5.06	8.68	6.55	3.00	4.42	27.90	34.64
Mean of % S.E.'s	11.85	5.02	2.83	15.22	12.57	22.07	16.01	7.93	10.55	69.29	86.05
Number of Samples	7	9	9	7	8	9	9	9	9	9	3
Triplicate Data Analysis May, 1985											
Mean of S.D.'s	0.17	2.10	0.060	2.05	0.56	2.75	32.08	2.10	0.80	0.32	0.06
Mean of % C.V.'s	1.42	6.04	3.30	9.67	9.73	26.26	7.67	3.77	17.17	25.59	43.30
Mean of % S.E.'s	3.52	15.00	8.20	24.03	24.16	65.22	19.05	9.38	42.57	63.57	107.56
Number of Samples	10	11	11	7	10	7	11	11	11	11	1

APPENDIX B

MATHEMATICAL BASIS OF GLVHT

Reprinted from Document No. 84-18-R

J. E. Edinger Associates, Inc.

37 West Avenue Wayne, Pennsylvania   19087-3226

30 June 1986

2. LATERALLY AVERAGED WATERBODY DYNAMICS

The laterally averaged equations of fluid motion can be derived from the three-dimensional equations of fluid motion as illustrated in Edinger and Buchak (1980b). There are six unknowns and six equations including: (1) the free water surface elevation, η; (2) the pressure, P; (3) the horizontal velocity, U; (4) the vertical velocity, W; (5) the constituent, C; and (6) the density, ρ. The six equations are: (1) the free surface wave equation; (2) the hydrostatic pressure; (3) horizontal momentum; (4) continuity; (5) consitutuent transport; and (6) an equation of state relating density and constituents including temperature and salinity.

2.1 The Basic Relationships

The laterally averaged equations of fluid motion and transport are the horizontal momentum balance:

$$\partial UB/\partial t + \partial UUB/\partial x + \partial WUB/\partial z = -1/\rho \, \partial BP/\partial x$$

$$+ \partial/\partial x(BA_x \partial U/\partial x) + B\partial\tau_z/\partial z \tag{2-1}$$

where B is the waterbody width as a function of x and z; and U and W are the laterally averaged horizontal and vertical velocity components. The vertical equation of motion reduces to the hydrostatic approximation:

$$\partial P/\partial z = \rho g \tag{2-2}$$

The equation of continuity becomes:

$$\partial UB/\partial x + \partial WB/\partial z = qB \tag{2-3}$$

where q is the side or tributary inflow per $\Delta x \Delta z B$ volume. Vertically integrated continuity gives the free water surface relationship of:

$$\partial \bar{B}\eta/\partial t = \partial/\partial x \int_{\eta}^{h} UBdz - \int_{\eta}^{h} qBdz \qquad (2\text{-}4)$$

where $\bar{B}$ is the time and spatially varying surface width and η is the free water surface elevation. The constituent transport becomes:

$$\partial BC/\partial t + \partial UBC/\partial x + \partial WBC/\partial z - \partial/\partial x(BD_x \partial C/\partial x)$$

$$- \partial(BD_z \partial C/\partial z)/\partial z = Cq\,B \qquad (2\text{-}5)$$

where Cq is the tributary source flux per $\Delta x \Delta z B$ volume, and

$$\rho = R(C) \qquad (2\text{-}6)$$

is the equation of state. Each constituent such as temperature, salinity, suspended sediment or dissolved oxygen has a balance as in Equation 2-5 with specific source and sink terms. The equation of state includes each constituent such as temperature and salinity that has a significant effect on density.

Equations 2-1 to 2-6 constitute six equations to be solved for the six unknowns of U, P, W, η, C and ρ. Lateral averaging eliminates the lateral momentum balance, the lateral velocity component and the Coriolis acceleration. The computational problem is reduced to six equations in six unknowns and, most important, to two coordinate directions. The reduction to two coordinate directions is the main feature that reduces computational time and storage over the three-dimensional case.

The laterally averaged horizontal pressure gradient in the horizontal momentum balance is the density driving force. It can be expanded to:

$$\partial(BP/\partial x) = B(\partial P/\partial x) + P(\partial B/\partial x) \qquad (2\text{-}7)$$

The second term, $P\partial B/\partial x$, represents the static force of the fluid on the x projection of the lateral boundary which in turn is cancelled by the force

of the boundary on the fluid. Thus, B P/ x represents the internal fluid horizontal pressure gradient. The horizontal pressure gradient is evaluated from Equation 2-2 to give:

$$B(\partial P/\partial x) = - gB\partial\eta/\partial x + gB\int_{\eta}^{z} 1/\rho \ (\partial\rho/\partial x)dx \tag{2-8}$$

at any depth z. The horizontal pressure gradient is divided into the two components of the surface slope and the vertical integral of the horizontal density gradient. The first term is known as the barotropic gradient and the second as the baroclinic gradient. The horizontal density gradient is the major driving force for the density circulation exhibited in many waterbodies.

2.2 The Free Surface Wave Equation

The basic characteristics of the longitudinal and vertical free water surface hydrodynamics can be examined through evaluation of the water surface relationship, Equation 2-4. The vertical integral of the horizontal flow required in Equation 2-4 can be determined from the algebraic forward time difference of the local acceleration of horizontal momentum in Equation 2-1. Formulation of the forward time difference of UB is the first step in evaluating the numerical equations. It gives:

$$U'B' = UB - B\Delta t/\rho \ \partial P/\partial x + F_x \Delta t \tag{2-9}$$

where Fx is:

$$F_x = \partial/\partial x(BA_x\partial U/\partial x) - \partial(UUB)/\partial x - \partial(WUB)/\partial z + \partial(B\tau_x)/\partial z \tag{2-10}$$

The vertical integrals of the various terms in Equations 2-9 and 2-10 can be further evaluated for insertion into the vertical integral of the flow required in the free water surface balance, Equation 2-4.

The vertical integral of the horizontal pressure gradient can be evaluated from Equation 2-8 to give:

B-3

$$1/\rho \int_\eta^h (B\partial P/\partial x)dx =$$

$$-\partial \eta/\partial x \; g\int_\eta^h Bdz + g/\rho \; h \; [B\int_\eta^z (\partial\rho/\partial x)dz] \; dz \qquad (2-11)$$

The first term on the right-hand side results from the fact that $\partial\eta/\partial x$ is a function only of x and is constant over z. The integral of width, B, over depth is the total cross-sectional area across which the surface slope contribution to the horizontal pressure gradients acts. The second term is the force due to the horizontal density gradient.

The vertical integral of the horizontal shear stress can be expanded from the derivations of $B\tau_x/\partial z$ to give:

$$\int_\eta^h (B\partial\tau_x/\partial z)dz = B_h \; \tau_h - B_\eta\tau_\eta - \int_\eta^h \tau_x(\partial B/\partial z)dz \qquad (2-12)$$

The first term is the bottom shear evaluated at z=h and can be evaluated from bottom velocity friction relationships. The surface shear, $B_\eta\tau_\eta$ is the surface wind shear component parallel to the x axis. The third term is the wall or bottom shear due to the horizontal projection of the sloping sides of the waterbody ($\partial B/\partial z$). It is evaluated as bottom shear over the projected width ∂B at each elevation. The internal velocity shear cancels out of the vertical integration.

Collecting the various terms of Equation 2-9 into Equation 2-4 gives the surface elevation equation of:

$$\bar{B}\eta/\partial t - g\Delta t(\partial/\partial x) \; (\partial\eta/\partial x\int_\eta^h Bdz) = \partial/\partial x\int_\eta^h U B \; dz$$

$$- g\Delta t/\rho \; \partial/\partial x\int_\eta^h [B \int_\eta^z (\partial\rho/\partial x)dz] \; dz$$

$$+ \partial/\partial x \; [B_h \; \tau_h - \bar{B}\tau_\eta - \int_\eta^h \tau_x(\partial B/\partial z)dz] \; \Delta t$$

$$+ \partial/\partial x \; (\int_\eta^h F_x dz)\Delta t + (\int_\eta^h qB \; dz) \; \Delta t \qquad (2-13)$$

With the η or surface coordinate terms collected on the left-hand side, Equation 2-13 is the water surface equation of the integrated waterbody. Equation 2-13 is, therefore, a numerical form of the frictionally dampened long wave equation for an irregular geometry, stratified waterbody.

2.3 The Numerical Solution

The numerical procedure for solving for the six unknowns on each time step is to compute first the water surface elevations from Equation 2-13 and to obtain the horizontal velocity components from Equation 2-9. The vertical velocity component is found from continuity, Equation 2-3, and the constituent distribution from the constituent balance, Equation 2-5. The water surface elevation equation essentially results from the simultaneous algebraic substitution and solution of horizontal momentum, Equation 2-1, and vertically integrated continuity, Equation 2-4, giving U and η simultaneously. This substitution makes the solution spatially implicit in η and U at the same time level through Equation 2-13 and eliminates the Courant gravity wave speed criterion that $\Delta x/\Delta t > \sqrt{gH_{max}}$ which leads to short computational Δt in deep waterbodies.

With the laterally averaged equations of motion expressed in an algebraic form, it is necessary to devise a finite difference coding for numerical computations. The coding not only includes the finite difference form of the equations but also the logic and algorithms needed to carry out the computations. These procedures are discussed in Chapter 4.

The variables are located on a physical space and computational grid as shown in Figure 2-1. It is called a space staggered grid since certain variables are at one location and the remainder displaced $\Delta x/2$ or $\Delta z/2$. There is a rational basis for choosing the grid locations which can be seen by using imaginary control volumes about a point.

The constituent concentration C is surrounded by a cell that has the U and W at the boundaries. Therefore, the U and W can transport C into and out of this cell with no spatial averaging to determine the change in C over time. Similarly, the W is computed for the same volume using the U's.

The velocity, U, is surrounded by a cell with the water surface elevations, η, and densities known at either end. U is computed from horizontal gradients of the surface slope and density with no spatial averaging of the primary variables. Advection of momentum into and out of the cell does require spatial averaging to determine the fluxes at the ends of the cell, but the variable U being computed remains centered.

For purposes of finite differencing, the variables are referenced to the computational point (I,K) using the space-staggered scheme shown in Figure 2-1. The velocity components, U(I,K) and W(I,K), the internal shear stresses, τ_b(I,K-1/2) and τ_b(I,K+1/2) are placed at the boundaries of an imaginary cell surrounding the (I,K) point. The variables Z(I), P(I,K) ρ(I,K) and C(I,K) are placed at the center of the cell. The dispersion coefficients Ax(I,K), Dx(I,K), Az(I,K) and Dz(I,K) are defined at the cell boundaries.

The geometry is specified as in Figure 2-1 by a cell width B(I,K), cell thickness H(I,K) and cell length Δx. The average cross-sectional area between two cells (I,K) and (I+1,K) is defined as:

$$BHR(I,K) = 1/2[B(I,K)\ H(I,K) + B(I+1,K)\ H(I+1,K)] \tag{2-14}$$

Each cell has a tributary or side inflow Q(I,K) and a tributary influx of constituent HNC(I,K,JC).

The I,K computational points or cells are arrayed in a grid as shown in Figure 2-2. The segments I=1 and I=IMAX are boundary columns with the U(1,K) and the U(IMAXM1,K) as specified boundary velocities. The
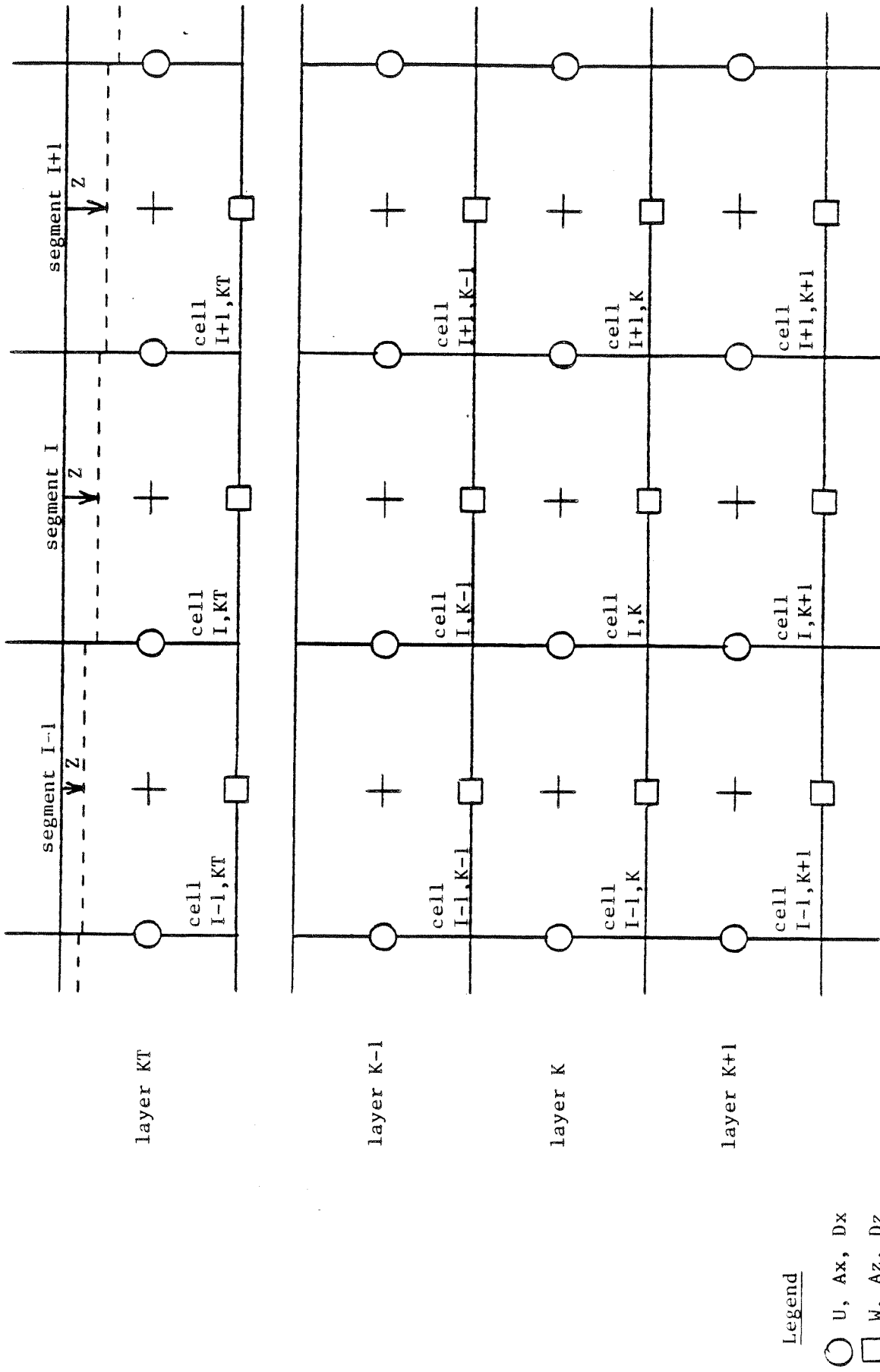
Figure 2-1. Location Convention for Variables on Finite Difference Grid

segment I-1

segment I

segment I+1

Z

Z

Z

cell I-1,KT

cell I,KT

cell I+1,KT

cell I-1,K-1

cell I,K-1

cell I+1,K-1

cell I-1,K

cell I,K

cell I+1,K

cell I-1,K+1

cell I,K+1

cell I+1,K+1

layer KT

layer K-1

layer K

layer K+1

Legend

○ U, Ax, Dx

□ W, Az, Dz

+ all other variables,
   e.g. C and ρ

computational region extends from K=KT downward to K=KB where KT is the time-varying top layer index computed on each time step and KB is the index of the bottom cell for each I segment. The deviation of the free water surface, Z, is computed as positive downward from the top of the KT layer.

2.4 The Surface Wave Equation

The numerical form of the surface wave equation, Equation 2-13, can be written in terms of the spatial grid and its definitions given in Figure 2-2. The momentum functions from the wave equation can be written in finite difference form as:

$$F(I,K) = - gBHR(I,K)/\rho \int_Z^{zk} (\partial\rho/\partial x)dZ - \partial/\partial x(U^2Bh) - (u_b w_b b)_{k+1/2}$$

$$+ (u_b w_b b)_{k-1/2} + \partial/\partial x[BhAx(\partial U/\partial x)] - (\tau_z b)_{k+1/2} + (\tau_z b)_{k-1/2} \quad (2-15)$$

where, when computing Z'(I) the terms in F(I,K) are evaluated from parameters available at time step N. The terms making up F(I,K) are respectively the density gradient component of the horizontal pressure gradient; the gradient of horizontally advected momentum; the vertical advection of momentum out of the K layer; the vertical advection of momentum into the K layer; the horizontal dispersion of momentum; the horizontal shear stress on the bottom of the K layer and the horizontal shear stress on the top of the K layer.

The surface wave equation can be written in time-forward, spatially implicit tridiagonal form as:

$$A(I)Z'(I-1) + V(I)Z'(I) + C(I)Z'(I+1) = D(I) \quad (2-16)$$

where the tridiagonal matrix coefficients, A(I), V(I), C(I) include the reservoir geometry summed over a cross section as:
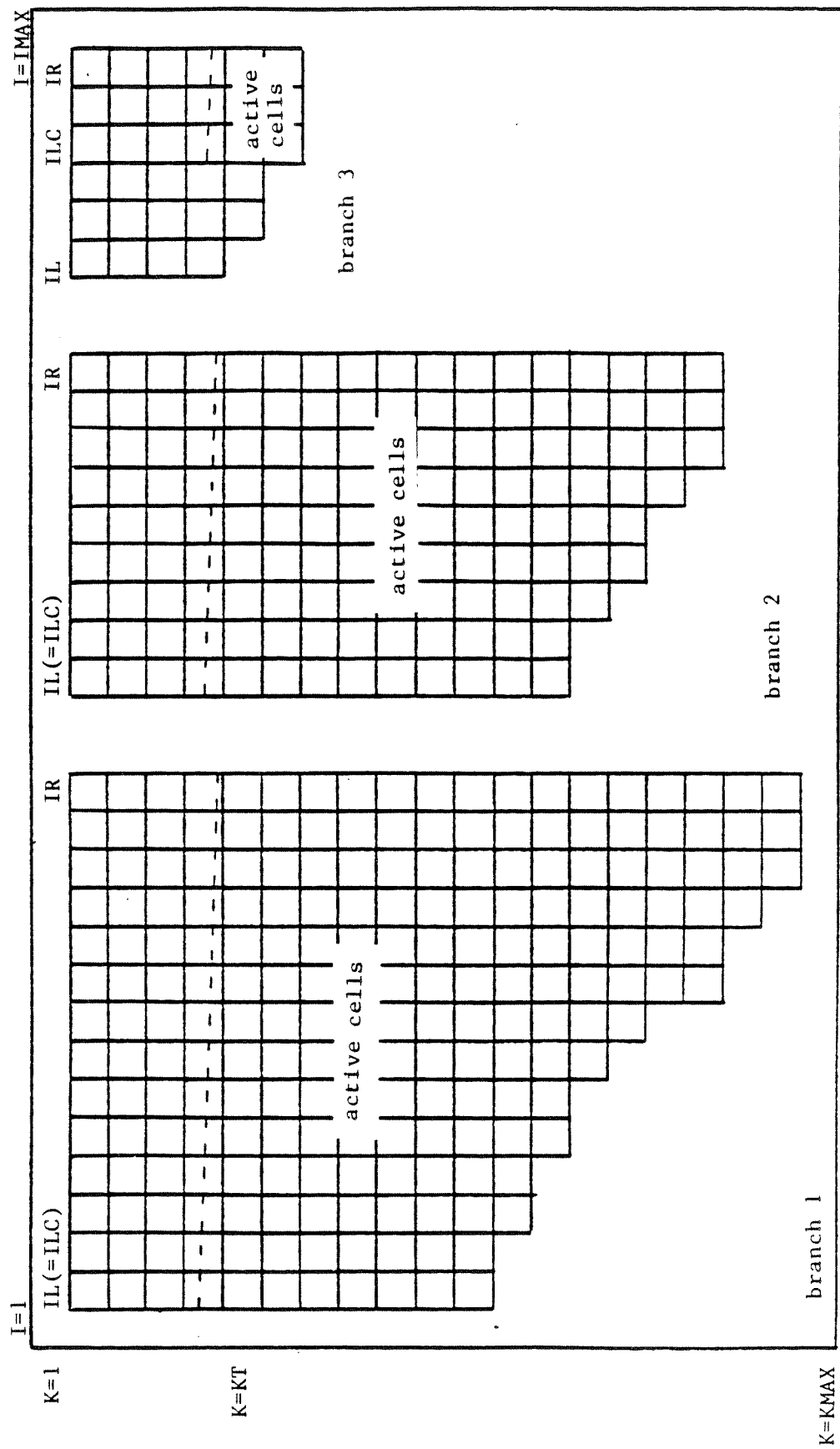
Figure 2-2. Grid Representation of Three-Branch Case

$$A(I) = -g(\Delta t^2/\Delta x) \sum_k BHR(I-1,K) \tag{2-16a}$$

$$V(I) = B(I,KT) + g(\Delta t^2/\Delta x) \left[\sum_k BHR(I-1,K) + \sum_k BHR(I,K)\right] \tag{2-16b}$$

$$C(I) = - g(\Delta t^2/\Delta x) \sum_k BHR(I,K) \tag{2-16c}$$

The A(I) geometry is the cross-sectional area between the I-1 and I segments and the C(I) geometry is the cross-sectional area between the I and I+1 segments. The geometry in V(I) is the sum of the two cross sections. The tridiagonal coefficient, D(I), includes the overall dynamics, inflows and outflows as:

$$D(I) = B(I,KT)Z(I) + \Delta t^2 \sum_k F(I,K) - F(I-1,K]$$

$$- \Delta t \sum_k [U(I,K)BHR(I,K) - U(I-1,K)BHR(I-1,K)] - \Delta t \sum_k Q'(I,K) \tag{2-16d}$$

Equation 2.16 is solved using the Thomas tridiagonal algorithm.

The surface deviation, Equation 2-16, results from substitution of the vertically integrated momentum balance into the vertically integrated continuity balance. The terms of the momentum balance taken forward in time are the local temporal acceleration and the surface slope. Substitution of these terms into the vertically integrated continuity is analogous to algebraically cross differentiating the vertically integrated continuity and momentum balances to arrive at the classical surface-long wave equation and finite differencing the latter implicitly forward in time. Thus, Equation 2-16 is the implicit finite difference form of the frictionally dampened long wave equation.

Equation 2-16 applies throughout the grid that represents the water body, including boundary regions where there is zero flux. To incorporate flow type boundary conditions, D(I) is modified by subtracting the net

inflow at the boundary. This method avoids the use of the applied boundary velocity, U, computed as:

$$U(I-1,K) = QIN(JB)/BHR(I-1,K)$$

or

$$U(I,K) = QOUT(J)/BHR(I,K)$$

where I=ILC (upstream segment number) in the first expression and I=IR (downstream segment number) in the second and QIN(JB) and QOUT(J) are the inflow and outflow, respectively. These applied velocities are derived variables and their use in the long wave equation leads to accumulating errors which the direct use of QOUT(J) and QIN(JB) avoids.

Head type boundary conditions are incorporated into the solution by using the off-diagonal coefficients A(ILC) and C(IR) with the applied boundary elevations at the upstream and downstream ends, respectively, of the active finite difference grid. Since these terms are ordinarily ignored by the Thomas algorithm, they are subtracted from the right-hand side expression, D(I), to be considered in the solution for Z(I). There are two cases in which the head type boundary conditions are used. These are open water boundaries, for which the external head, or elevation, is known from an observation record and the boundaries of branches, where the applied head is generated by the solution to the surface wave equation in a joining branch. The first case is the common estuary case. The second case is represented by multi-stemmed lakes, reservoirs or estuaries, canals and cuts and deltas. In applications to these geometries, the numerical solution is applied to each branch in turn with the internal boundary conditions permitting the joining of the branches to form the waterbody.

2.5 Evaluation of F(I,K) Terms

The forcing function in the wave equation, F(I,K) in Equation 2-15, must be evaluated before the water surface elevations are computed at the

new time step. All of the terms in F(I,K) are therefore evaluated for variables computed from the past time step. The new time step data entering the wave equation are the boundary inflows, outflows and tide heights. Many of the terms entering the F(I,K) including the longitudinal and vertical advection of momentum, the longitudinal dispersion of momentum and the horizontal shears also enter the horizontal momentum balance for the computation of U(I,K) and are therefore evaluated as separate arrays.

The contribution of the horizontal density gradient to horizontal momentum is an integral over depth from a fixed reference surface of the horizontal density gradient. It applies at the I to I+1 boundary or where U(I,K) is located, and the gradient is therefore computed as [RHO(I+1,K)-RHO(I,K)]/Δx at each level and then summed vertically to the K-th layer. The space staggered grid allows using the array of RHO(I,K) directly in the computation with no spatial averaging.

The horizontal advection of momentum is computed around the transport of the quantity U(I,K) BHR(I,K) by velocities at I+1/2 and I-1/2 which are found by spatial averaging. Upwind differencing is used to evalute the horizontal advection of momentum terms:

```
ARR=∅.
UR=(U(I+1,K)+U(I,K))/2.
IF(UR.GT.∅.) ARR=1.
AL=∅.
UL=(U(I,K)+U(I-1,K))/2.
IF(UL.GT.∅.) AL=1.
ADMX(I,K)=(BH2(I+1,K)*UR*(ARR*U(I,K)+(1.-ARR)
*U(I+1,K))-BH2(I,K)*UL*(AL*U(I-1,K)
+1(1.-AL)*U(I,K)))/DLX(JB)
```

The horizontal advection of momentum as centered about I,K uses results from each of the neighboring grid points.

The vertical advection of horizontal momentum is similarly evaluated using upwind differencing for the transport of the cell centered quantity:

```
AB=Ø.
WB=(W(I+1,K)+W(I,K))/2.
IF(WB.GT.Ø.) AB=1.
ADMZ(I,K)=(BR(I,K)+BR(I,K+1))
*WB*(AB*U(I,K)+(1.-AB)*U(I,K+1))/2.
```

The horizontal shears are evaluated at the cell upper and lower interfaces based on the velocity gradient relationships of:

```
ST(I,K)=ST(I,K)+AZ(I,K-1)*Ø.5*(BR(I,K-1)
+BR(I,K))*(U(I,K-1)
-U(I,K))/H2(I,K)
```

and

```
SB(I,K)=ST(I,K+1)+GC2
*(BR(I,K)
-BR(I,K+1))*U(I,K)*ABS(U(I,K))
```

where ST(I,K) initially consists of the vertical attenuation of wind shear. The AZ(I,K) is evaluated at the top and bottom interface. Evaluation of Az is as a function of density gradients and wind shear is discussed in Chapter 3 as an auxiliary function.

The vertical integral of the horizontal density gradient is computed at the location of the U(I,K) velocity component. It is computed using the vertical integration of pressure as:

```
P(I,K)=P(I,K-1)+RHO(I,K)*G*H2(I,K)
```

and

```
HPG(I,K)=0.5*DLXR*BR(I,K)*(H2(I+1,K)
*(P(I+1,K-1)+P(I+1,K))-H2(I,K)*(P(I,K-1)+P(I,K)))
```

to form HPG(I,K). The second integral is formed when compiling the tridiagonal coefficients in Equation 2.16d.

2.6 Computation of Horizontal Velocity and Vertical Velocity

The horizontal velocity component is computed from Equation 2-9. The pressure and horizontal pressure gradients are computed immediately after the surface displacements are obtained from the wave equation. The horizontal velocity component is then computed from the horizontal pressure gradient and the advection of momentum and shear components developed for the wave equation.

The horizontal velocity equation is:

```
U(I,K)=(BHR2(I,K)*U(I,K)+DLT*(-ADMX(I,K)
-ADMZ(I,K)+ADMZ(I,K-1)-HPG(I,K)+DM(I,K)+ST(I,K)-SB(I,K)))
/BHR1(I,K)
```

where the horizontal pressure gradient, HPG(I,K), is updated for the new Z(I). Many of the other terms were previously evaluated when determining F(I,K).

The vertical velocity components are computed from Equation 2-3 by integrating continuity from the bottom upward as:

```
WT1=W(I,K+1)*BB(I,K+1)
WT2=((BHR1(I,K+1)*U(I,K+1))-(BHR1(I-1,K+1)
*U(I-1,K+1)))/DLX(JB)-Q(I,K+1)/DLX(JB)
W(I,K)=(WT1+WT2)
/BB(I,K)
```

where:

    BB(I,K) = (B(I,K) + B(I,K+1))/2

and Q(I,K) is the lateral inflow and outflow to cell I,K.

    The top cell W(I,KT) is computed separately from the surface change
in elevation to maintain continuity in the surface layers and to correct
for truncation errors accummulated from summing over the whole water
column. W(I,KT) is used in the transport computation.

2.7 Constituent Transport

    The constituent transport relationship is solved for N constituents
with values of C(I,K,N) in the adjacent cell formulation of:

    T1(I,K)=(TCC(I,K)*T2(I,K)+TCL(I,K)*T2(I-1,K)
    +TCR(I,K)*T2(I+1,K)+TCT(I,K)*T2(I,K-1)
    +TCB(I,K)*T2(I,K+1)+HNT(I,K)/DLX(JB))
    *DLT/BH1(I,K)

where the coefficients are determined from the general form of the
transport equation. They are solved once during a time step and applied
across all constituents. The transport coefficients are:

    TCR(I,K)=DLX1*BHR1(I,K)
    *(-(1.-US(I,K))*U(I,K)+DX(I,K)/DLX(JB))

    TCL(I+1,K)=TCR(I,K)+DLX1*BHR1(I,K)*U(I,K)

    TCB(I,K)=-W(I,K)*BB(I,K)*1.-WS(I,K))
    +DZ(I,K)*2.*BB(I,K)
    /(H2(I,K)+H2(I,K+1))

    TCT(I,K+1)=TCB(I,K)+W(I,K)*BB(I,K)

```
TCC(I,K)=BH2(I,K)/DLT
+DLX1*BHR2(I-1,K)
*((1.-US(I-1,K))*U(I-1,K)-DX(I-1,K)/DLX(JB))
*DLX1*BHR2(I,K)
*(-US(I,K)*U(I,K)-DX(I,K)/DLX(JB))
-W(I,K)*BB(I,K)*WS(I,K)
+W(I,K-1)*BB(I,K-1)*(1.-WS(I,K-1))
-DZ(I,K)*2.*BB(I,K)/(H2(I,K)+H2(I,K+1))
-DZ(I,K-1)*2.*BB(I,K-1)/(H2(I,K-1)+H2(I,K))
```

The source and sink term for each constituent, HNC(I,K,JC), includes reaction kinetics and interactions between constituents. It is evaluated in a separate part of the program.

3. AUXILIARY FUNCTIONS

Auxiliary functions are relationships that describe processes which are independent of the computational scheme of the GLVHT model and that can be changed or revised as knowledge advances or to suit individual users or situations. The auxiliary functions include the descriptions of the turbulent dispersion processes, the constituent reactions and interactions, heat budget and ice relationships. Often the auxiliary functions depend on a number of the six basic variables used in the model formulation and their definitions in relation to the computational grid. The turbulent vertical mixing processes depend on vertical density gradients and velocity shear and can be computed from the model densities and velocities. An example of changing an auxiliary function to suit a different case is changing the vertical mixing schemes from turbulent processes to laminar processes when applying the model to experimental flumes where laminar flow dominates. These changes can be made without changing the basic variable definitions or the computational process.

Certain auxiliary relationships have been developed for use with longitudinal vertical hydrodynamics as a result of necessity and of applications. These include the wind shear and vertical mixing rela tionships, surface ice formation, and methods for inclusion of constituent reactions and interactions.

3.1 Wind Shear and Mixing

In two-dimensional longitudinal-vertical models, wind shear enters the longitudinal momentum balance through the vertical transport of horizontal momentum written for the time averaged, instantaneous velocity as $\partial<wu>/\partial z$. The instantaneous horizontal and vertical velocity can be written as:

$$u = U + u' + u'' \tag{3-1a}$$

$$w = W + w' + w'' \tag{3-1b}$$

where U and W are the time averaged, mean velocity components, u′ and w′ are the turbulent velocity fluctuations about the mean generated by velocity shear, and u″ and w″ are the velocity components of wind waves propagated downward from the water surface. The time mean of the instantaneous velocity product becomes:

$$<uw> = UW + <u'w'> + <u"w">$$ (3-2)

The turbulent transport is related to the mean velocity as:

$$<u'w'> = - Az \, \partial U/\partial z$$ (3-3)

where Az is the vertical eddy viscosity. The shear due to wind waves can be evaluated from the vertical decay of wind wave velocities given for simple sinusoidal waves as:

$$u" = A\sigma e^{-kz} \, Sin(kx - \sigma t)$$ (3-4a)

$$w" = A\sigma e^{-kz} \, Sin(kx - \sigma t + \phi)$$ (3-4b)

for which k=2π/L where L=wave length; σ=ck where σ is the wave frequency (2π/T where T=wave period) and c=wave speed; and φ is the phase shift between vertical and horizontal components. Averaged over time, the shear due to the velocity fluctuations becomes:

$$<u"w"> = \tau_{wx} \, e^{-2kz}$$ (3-5)

where τ_{wx} is the surface shear due to wind along the x-axis of the model. The horizontal shear becomes:

$$\tau_x = - Az \, \partial U/\partial z + \tau_{wx} \, e^{-2kz}$$ (3-6)

Thus, the wind shear decays with depth and generates horizontal velocities directly through the horizontal momentum balance and the momentum is dissipated through the vertical eddy viscosity.

3.2 Vertical Eddy Viscosity and Wind Shear

The vertical eddy viscosity for longitudinal-vertical dynamics can be formulated by analogy to the three-dimensional case:

$$A_z = k(l^2/2) \, [(\partial U/\partial z)^2 + (\partial V/\partial z)^2]^{1/2} \, \text{Exp}(-CR_i) \qquad (3-7)$$

where k is the von Karman constant, l is the vertical length scale taken as z for finite differences, and R_i is the local Richardson number.

In a longitudinal-vertical model, the lateral velocity, V and its gradient $\partial V/\partial z$ is due to the lateral component of wind wave motion and average laterally to zero, but not necessarily the square $(\partial V/\partial z)^2$. It is assumed that the cross wind shear τ_{wy} generates lateral wave components v" such that $<w"v">=\tau_{wy} \, e^{-2kz}$. Further let

$$A_z^2 (\partial V/\partial z)^2 = \tau_{wy} \, e^{-2kz}]^2 \qquad (3-8)$$

giving for the cross wind shear:

$$(\partial V/\partial z)^2 = [\tau_{wy} \, e^{-2kx}/A_z]^2 \qquad (3-9)$$

Thus, the eddy viscosity with cross wind shear becomes:

$$A_z = k(l^2/2) \, [(\partial U/\partial z)^2 + (\tau_{wy} \, e^{-2kz}/A_z)^2]^{1/2} \, \text{Exp}(-CR_i) \qquad (3-10)$$

In numerical form, A_z can be iterated from Equation 3-10 by using an old time step value to evaluate the cross wind shear contribution.

One obvious limitation on A_z is that it should not be less than the molecular kinematic viscosity for water. For implicit finite differences there is also the limit that $A_z < \Delta z^2/\Delta t$. It is intuitively obvious that A_z should be allowed to increase with Δz or the coarseness of the vertical detail.

The decrease in the maximum value of Az with Δt is not so obvious. However, as Δt is increased, the Torrence limit $\Delta t < \Delta x/U$ is approached which says that more of the momentum or constituent mass of a computational cell is displaced by advection over a time step Δt as Δt increases and there is less momentum or constituent mass that can be transported out of the cell by turbulent transport. If the Torrence condition were satisfied perfectly for each cell on each time step, then mass, momentum, and constituent would be translated directly from one cell to the next on each time step. Thus, the increase in the maximum value of Az with Δt limits numerical dispersion resulting from a lagged transport of mass, momentum or constituent.

The above formulation of wind shear in horizontal momentum and evaluation of Az leads to wind driven surface currents that are three percent to ten percent of the surface wind velocity with the higher values appearing at higher wind speeds. This is in accordance with the few attempts to relate wind speed and surface current velocity from field data that appear in the literature. With the formulation, the surface current does not reach abnormal values as it does for the case of wind shear applied only to the surface and as the thickness of the surface layer decreases. The depth of the wind driven surface layer increases with wind speed and the mass transport due to wind appears to be insensitive to the finite difference layer thickness.

The Quabbin application of the GLVHT model with three interconnected arms showed the importance of wind shading geographically over each arm as well as the importance of variable fetch as it affects the wind wave decay. In this case, there were significant differences in temperature profiles between the three arms at a given time that were attributable to wind effects that the degree of wind shading could be identified.

The need to identify the geographical distribution of wind shading, fetch, and angle of an arm segment axis relative to the wind leads to great flexibility in characterizing wind conditions on real waterbodies. Presently, wind speed and direction as a function of time are known at

best for one or two stations in reservoir research studies, and at worst in the usual applied case from a distant airport anemometer. More effort is required to characterize the variability of wind speed, direction and resulting wind waves throughout geometrically complex reservoirs before fixed rules can be established for assigning wind shading and fetch to reservoir segments. In the interim, it is possible to proceed to new case applications using the experience of past applications.

The wind wave formulation is presently based on the significant wave height and period. It is obvious that there is a whole spectrum of wind wave components, u" and v" (Equations 3-4a and 3-4b) and hence a whole spectrum of wind wave decay rates that produce a spectrum of wind shears. It is presently not known if the major portion of the wind shear is propagated by the waves making up the significant wave height and period portion of the wind wave spectrum. The present formulation provides the basis for further theoretical investigations.

3.3 Surface Heat Exchange

Surface heat exchange can be formulated as a term-by-term process using the explicit adjacent cell transport computation as long as the integration time step is shorter than the time step of the meteorological data. The surface heat exchange processes depending on water surface temperatures are computed at previous time step data and are therefore lagged from the transport processes by the integration time step.

The term-by-term surface heat exchange is computed as:

$$Hn = (Hs+Ha-Hsr-Har) - (Hbr+He+Hc) \tag{3-11}$$

where:

Hn = the net rate of heat exchange across the water surface, $w\ m^{-2}$
Hs = incident short wave solar radiation
Ha = incident long wave radiation

Hsr = reflected short wave solar radiation

Har = reflected long wave radiation

Hbr = back radiation from the water surface

He = evaporative heat loss

Hc = heat condition

The first group of terms in Equation 3-1 are incoming energy. The short wave solar radiation is either measured directly or computed from sun angle relationships and cloud cover. The long wave atmospheric radiation is computed from air temperature and cloud cover or air vapor pressure using Brunts formula. The right-hand terms are all water surface temperature dependent.

The water surface back radiation is computed as:

$$Hbr = \sigma(Ts+273)^4 \qquad (3\text{-}12)$$

where Ts is the water surface temperature. Like the remaining terms it is computed for each surface layer cell on each iteration time step.

The evaporation is computed as:

$$He = f(W)(es-ea) \qquad (3\text{-}13)$$

where f(W) is an evaporative wind speed function and es and ea are the saturation vapor pressure at the water surface temperature and the atmospheric vapor pressure respectively. The latter depends on air temperature and dew point temperature or relative humidity. The surface vapor pressure is computed from the surface temperature for each surface cell on each iteration.

The surface heat conduction is computed as:

$$Hc = Cf(W)(Ts-Ta) \qquad (3\text{-}14)$$

where C is the Bowen ratio constant and Ta is air temperature.

Short wave solar radiation penetrates the surface and decays exponentially with depth according to Bears Law as:

$$Hs(z) = Hs\ Exp(-\alpha z)/(1+\beta) \tag{3-15}$$

where Hs is the short wave radiation reaching the surface. It is removed successively from the bottom of the top cell in the computations and passed into the top of the next lower cell.

Aside from the problems of measuring meteorological data relative to a large waterbody and especially the problem of translating climatological data from distant weather stations, the most uncertain parameter in the surface heat exchange computations is the evaporative wind speed function f(W). Various formulations of f(W) have been examined in Edinger, et al. (1974) as f(W) has been applied to numerous situations. Unlike the use of wind speed in wind shear relations as discussed in Section 3.1, the evaporative wind speed is thought to be a "ventilation speed" rather than a vector velocity. The different formulations result from the empirical determination of f(W) for different size and shape waterbodies with data from different locations and averaged over different periods of time.

3.4 Ice Cover Relationships

The onset and loss of ice cover as well as ice thickness play an important role in the heat transport of waterbodies in northern climates. At high latitudes, the ice cover might remain until late spring or early summer and prevent warming due to absorption of short wave solar radiation.

The ice model is based on the processes which include an ice cover with ice-to-air heat exchange, conduction through the ice thickness and conduction between the underlying water and a "melt temperature" layer on

the bottom of the ice (Ashton, 1979). The overall heat balance for the water to ice-to-air system is:

$$\rho i L \Delta h / \Delta t = hai(Ti-Te) - hwi(T-Tm) \qquad (3-16)$$

where:

ρi = density of ice

L = latent heat of ice

$\Delta h / \Delta t$ = change in ice thickness, h, with time

hai = ice-to-air coefficient of surface heat exchange

Ti = ice temperature

Te = equilibrium temperature of ice-to-air heat exchange

hwi = coefficient of water-to-ice heat exchange through the melt layer

T = water temperature below ice

Tm = melt temperature ($0°C$)

The ice-to-air coefficient of surface heat exchange, hai, and its equilibrium temperature, Te, are computed the same as for water surface heat exchange in Edinger, et al. (1974) because the heat balance of the thin ice surface water layer is the same as the net rate of surface heat exchange discussed in Section 3.2. The coefficient of water-to-ice exchange, hwi, depends on the turbulence and water movement under the ice and their effect on the melt layer thickness. It is known to be a function of water velocity for rivers and streams but must be empirically adjusted for reservoirs.

The ice temperature in the overall ice heat balance is computed from equating the rate of surface heat transfer between the ice and the air to the rate of heat conduction through the ice as:

$$hai(Ti-Te) = -ki(Ti-Tm)/h \qquad (3-17)$$

where ki is the molecular heat conductivity of ice. When solved for the ice temperature, Ti, and inserted in the overall ice heat balance, the ice thickness relationship becomes:

$$\rho i L \Delta h/\Delta t = (Tm-Te)/(h/ki+1/hia) - hwi(T-Tm) \qquad (3-18)$$

from which the ice cover thickness can be computed for each longitudinal surface segment of the GLVHT model. Heat from the water to the ice transferred by the last term is removed in the water temperature transport computations.

The main variations with the onset of ice cover and its seasonal growth and melting over the area of the waterbody, depend on the relative locations and temperatures of inflows and outflows that affect the underlying water temperature and the variations of evaporative wind over the ice surface and the effects of water movement on the ice-to-water exchange coefficient. Often ice will form in reservoir branches before forming in the main pool and remain there longer due to the above effects.

3.5 Constituent Reactions and Interactions

The constituent transport relationships described in Chapter 2 have been designed to efficiently compute the transport of any number of constituents with their unit volume reaction and interaction rates expressed in the source and sink term HC(I,K,N). The evaluation of the source and sink term can be performed directly in the program as is done for surface heat exchange because it is used so frequently or can be written for interacting constituents in a separate subroutine.

Constituent reactions and interactions have been developed in many different forms. These range from the simple dissolved oxygen, nutrient, biochemical oxygen demand relationships to breaking the nutrient con stituents into as many separate components as possible. The biologist tends to have many components for specific algae, fish forms and food chain interactions with simple chemistry while the chemical limnologist

tends toward detailed description of the physiochemical processes with limited biology. The scheme of the transport computations has been designed to accommodate any of the numerous rate reaction interaction chemical and biological models.

As described in Chapter 5, the constituent transport has been used to represent simple tracers of various inflows through a waterbody. They have been applied to the study of the movement of the diverted Connecticut River water through Quabbin Reservoir and the changes in the movement of inflows of Nanika River into Morice Lake in the Kemano diversion studies.

The GLVHT model has been used for transport and interaction of the bicarbonate balance in Lakes Powell and Mead including surface exchange, production and uptake of carbon dioxide and epilimnetic production of carbon dioxide due to biochemical oxidation. Ammonia and nitrogen transport and reactions were included in the Dillon Reservoir analysis. Fish egg and larvae life cycles have been coupled with hydrodynamically generated transport coefficients on Patuxent Estuary.

The reaction and interaction models can be assembled as subroutines in terms of unit volume descriptions. These subroutines can be called into the main program, or as in the case of the Patuxent study, the hydrodynamic and transport model can be used to generate transport coefficients between aggregate segments of the waterbody from the detailed grid. The latter method has the advantage that the hydrodynamic computations need to be made only a few times and that the time scale and space scale of the transport coefficients can be chosen to be compatible with the chemical and biochemical computations.

3.6 Inflow and Outflow Boundary Conditions

Inflows and outflows are specified either as lateral flows normal to the longitudinal-vertical plane or as velocities at the longitudinal boundaries. The boundary velocities are usually computed from the inflows and outflows and contribute to horizontal momentum fluxes. The vertical

distribution of velocities must be specified as a boundary condition. Associated with the velocity distributions is the constituent distribution which may influence horizontal density gradients and momentum.

Lacking specific velocity distribution data, the simplest velocity inflow boundary distribution is a uniform velocity computed from the inflow rate and cross section. The uniform velocity distribution is usually redistributed by the hydrodynamic computations themselves over the cross section within one or two-model segment lengths of the inflow location. This is the normally encountered inflow velocity case for shallow tail waters.

Deeper upstream segments and significant density anomalies of the inflow relative to the main waterbody can result in distorted inflow velocity profiles. A uniform distribution of a dense inflow can cause artifically large density flows in the tailwater and reverse circulation and inflow mixing as the flow becomes established. Such flows may require redistribution over the cross section with more of the flow near the bottom layers for denser flows and more near the top for lighter flows to give a more realistic inflow profile. Outflows from reservoirs are usually from ports that are within a layer or two in thickness. Tests have shown that single layer outflows produce up-reservoir velocity withdrawal envelopes similar to those found in selective withdrawal schemes. It has not been necessary to use any selective withdrawal scheme to represent withdrawals from an outflow except in the case of a deep intake that extended through many layers. Additional testing of withdrawal computations is required.

BIBLIOGRAPHY

Ashton, G. D. 1979. Suppression of River Ice by Thermal Effluents. CRREL Report 79-30, U. S. Army Corps of Engineers, Cold Regions Research and Engineering Laboratory, Hanover, New Hampshire.

Edinger, J. E. and E. M. Buchak. 1980b. Numerical Hydrodynamics of Estuaries in Estuarine and Wetland Processes with Emphasis on Modeling, (P. Hamilton and K. B. Macdonald, eds.). Plenum Press, New York, New York, pp. 115-146.

Edinger, J. E., D. K. Brady and J. C. Geyer. 1974. Heat Exchange and Transport in the Environment. Report No. 14, prepared for Electric Power Research Institute, Cooling Water Discharge Research Project (RP-49), EPRI Publication No. 74-049-00-3, Palo Alto, California. November.